STUDY OF DOWNLINK PD-NOMA FOR ENHANCED SPECTRUM AND ENERGY EFFICIENT SYSTEM WITH INTERFERENCE MANAGEMENT THROUGH NOMA CLUSTERING

A thesis submitted towards partial fulfilment of the requirements for the degree of

MASTER OF ENGINEERING

in

ELECTRONICS AND TELECOMMUNICATION ENGINEERING

Submitted by

DONA CHAKRABORTY

University Roll No.: 002210702006

Examination Roll No.: M4ETC24004

Registration No.: 163532 of 2022-2023

Under the guidance of

PROF. ITI SAHA MISRA

DEPARTMENT OF ELECTRONICS AND TELECOMMUNICATION ENGINEERING

JADAVPUR UNIVERSITY

KOLKATA - 700032

FACULTY OF ENGINEERING AND TECHNOLOGY

JADAVPUR UNIVERSITY

KOLKATA - 700032

MAY 2024

FACULTY OF ENGINEERING AND TECHNOLOGY

JADAVPUR UNIVERSITY, KOLKATA

CERTIFICATE OF RECOMMENDATION

This is to certify that the dissertation entitled "**STUDY OF DOWNLINK PD-NOMA FOR ENHANCED SPECTRUM AND ENERGY EFFICIENT SYSTEM WITH INTERFERENCE MANAGEMENT THROUGH NOMA CLUSTERING**" has been carried out by **DONA CHAKRABORTY (University Registration No.: 163532 of 2022-2023, University Roll No.: 002210702006)** under the guidance and supervision of **PROF. ITI SAHA MISRA** and be accepted in partial fulfilment of the requirements for the degree of **Master of Engineering** in **Electronics and Telecommunication Engineering**. The research results presented in the thesis have not been included in any other paper submitted for any degree to any other University or Institute.

Prof. Iti Saha Misra

(Thesis Supervisor)

Department of Electronics and Telecommunication Engineering

Jadavpur University

Kolkata- 700032

Prof. Manotosh Biswas

(Head of the Department)

Department of Electronics and Telecommunication Engineering

Jadavpur University

Kolkata- 700032

Prof. Dipak Laha

(DEAN of Faculty of Engineering and Technology)

Department of Electronics and Telecommunication Engineering

Jadavpur University

Kolkata- 700032

FACULTY OF ENGINEERING AND TECHNOLOGY

JADAVPUR UNIVERSITY, KOLKATA

CERTIFICATE OF APPROVAL*

The foregoing thesis is hereby approved as a creditable study of an engineering subject, carried out and presented in a manner satisfactory to warrant its acceptance as a prerequisite to the degree for which it has been submitted. It is understood that by this approval the undersigned do not necessarily endorse or approve any statement made, opinion expressed, or conclusion drawn therein but approve the thesis only for the purpose for which it has been submitted.

_____ _____

Signature of the Examiner Signature of the Supervisor

* Only in case the thesis is approved.

FACULTY OF ENGINEERING AND TECHNOLOGY

JADAVPUR UNIVERSITY, KOLKATA

DECLARATION OF ORIGINAL AND COMPLIANCE OF ACADEMIC THESIS

I hereby declare that this thesis titled "**STUDY OF DOWNLINK PD-NOMA FOR ENHANCED SPECTRUM AND ENERGY EFFICIENT SYSTEM WITH INTERFERENCE MANAGEMENT THROUGH NOMA CLUSTERING**" contains literature survey and original research work by the undersigned candidate, as part of her degree of Master of Technology in Electronics and Telecommunication Engineering.

All information has been obtained and presented in accordance with academic rules and ethical conduct.

I also declare that, as required by these rules and conduct, I have fully cited and referenced all materials and results that are not original to this work.

Name: **DONA CHAKRABORTY**

Examination Roll No.: **M4ETC24004**

University Roll No.: **002210702006**

Thesis Title: **STUDY OF DOWNLINK PD-NOMA FOR ENHANCED SPECTRUM AND ENERGY EFFICIENT SYSTEM WITH INTERFERENCE MANAGEMENT THROUGH NOMA CLUSTERING**

_____

Signature of the candidate with date

FACULTY OF ENGINEERING AND TECHNOLOGY

JADAVPUR UNIVERSITY, KOLKATA

ACKNOWLEDGEMENT

I take this opportunity to express my sincere thanks and deepest sense of gratitude to **Prof. Iti Saha Misra**, Department of Electronics and Telecommunication Engineering, Jadavpur University who has supervised this thesis. The thesis would have never been completed without her able guidance, constant vigil, careful supervision, and inspiration at all stages of the work. Her words always inspire me and bring me to a higher level of thinking. I am privileged to witness her enthusiastic and dedicated interest towards advanced research that motivates me and enriches my growth as a student and a researcher.

I would also like to thank the entire Department of Electronics and Telecommunication Engineering for giving me the opportunity to work on this thesis. I am also grateful to my friends and seniors, who found time from their busy schedule to help me finish my thesis. I convey my heartfelt thanks to **Sreya Ghosh, Sukanta Behera, Suman Paria**, **Nahali Sen** and **Abhishek Guha** for their constructive advice to improve my thesis.

I also deeply acknowledge the support from DST, Govt. of India for this work in the form of FIST Project on "Broadband Wireless Communication" in the Department of ETCE, Jadavpur University.

I would like to conclude by thanking and conveying my regards to my parents and elder brother. Without their constant support it was impossible for me to finish my work.

Dona Chakraborty
University Roll No.: **002210702006**
Examination Roll No.: **M4ETC24004**
Date:
Place: **Dept. of Electronics and Telecommunication Engineering,**
Jadavpur University, Kolkata: 700032.

ABSTRACT

With the advancement of wireless communication systems, the demand for higher data rates is increasing exponentially. Non-Orthogonal Multiple Access (NOMA) is expected to play an important role in 5G networks. In contrast to conventional Orthogonal multiple access schemes, NOMA allows different users to efficiently share the same resources (i.e., time, frequency, and code) at different power levels so that the user with lower channel gain is served with a higher power and vice versa. As a result, it increases the system performance compared to traditional orthogonal multiple access techniques.

In this thesis work, we have analyzed the performance of different users Power Domain NOMA (PD-NOMA) system in a Downlink scenario in terms of Sum Capacity, Spectral Efficiency, Energy Efficiency, and total Interference. We have analyzed the system performance with and without employing SVD precoding technique, under different power allocation schemes (Fixed Power Allocation and Dynamic Power Allocation) and different modulation techniques. As we increase the number of users in the system, we observe that NOMA technique suffers from increased interference among the users sharing the same resources. NOMA Clustering technique can resolve the problem by grouping users into clusters. As a result, interference among users in a cluster decreases and system performance improves. Here we have discussed 3 types of clustering. We have analyzed the performance of NOMA Clustering system employing SVD precoding technique, under different power allocation schemes (Fixed Power Allocation and Dynamic Power Allocation) and different modulation techniques and compare the performance of PD-NOMA Clustering system with the performance of PD-NOMA system in a downlink scenario. We have performed these experiments using a transceiver board named WARP V3 in 2.4GHz band and MATLAB software.

	Contents	
Chapter No.	**Title of the Topic**	**Page No.**
	Chapter 1 (Introduction)	**1-10**
1.1	Background of Wireless Communication	1
1.2	Multiple Access Technique	1
1.2.1	OMA Technique	2
1.2.1.1	FDMA	2
1.2.1.2	TDMA	3
1.2.1.3	CDMA	3
1.2.1.4	OFDMA	4
1.3	History: Different Multiple Access Techniques from 1G to 4G	5
1.4	Drawbacks of OMA technique	6
1.5	NOMA Technique	7
1.5.1	Drawbacks of NOMA Technique	7
1.6	Merits of NOMA Clustering over NOMA technique	8
1.7	Motivation	9
1.7.1	Objective of the thesis	10
1.8	Organization of the thesis	10
1.9	Summary of the chapter	10
	Chapter 2 (Literature Survey)	**11-15**
	Chapter 3 (Fundamental Concept of NOMA)	**16-37**
3.1	Basics of NOMA	16
3.1.1	Superposition Coding (SC)	18
3.1.2	Successive Interference Cancellation (SIC)	18
3.2	System Model Description	19
3.3	Precoding Technique	22
3.3.1	Processing Flow of Precoding	22
3.3.2	Singular Value Decomposition (SVD) precoding	23
3.4	Mathematical Model of PD-NOMA system	24
3.5	Power Allocation strategy	26
3.5.1	Derivation of Dynamic Power Allocation coefficients	27
3.6	Digital Modulation Techniques	31
3.6.1	Binary Phase Shift Keying (BPSK)	31
3.6.2	Quadrature Phase Shift Keying (QPSK)	32
3.6.3	Quadrature Amplitude Modulation (QAM)	34
3.7	Performance Analysis Parameters	35
3.7.1	Sum Capacity	35
3.7.2	Spectral Efficiency	35
3.7.3	Energy Efficiency	35

3.7.4	Total Interference	36
3.7.5	Constellation Diagram	37
3.8	Summary of the chapter	37
	Chapter 4 (Concept of NOMA Clustering Technique)	**38-47**
4.1	Basics of NOMA Clustering	38
4.2	System Model Description	39
4.3	Summary of the chapter	47
	Chapter 5 (WARP Hardware Setup)	**48-76**
5.1	Description of WARP V3 board	48
5.1.1	Hardware components of WARP V3 Board	49
5.1.2	Integration of WARP Hardware with WARPLab Framework	50
5.2	Transmitter Receiver Block Diagram	51
5.2.1	CFO, Phase Error and SFO	53
5.3	Components required to perform the experiments	53
5.3.1	Experimental setup and steps for performing the experiments	54
5.3.2	Steps required for performing the Experiments	54
5.4	Experimental Results	58
5.5	Summary of the chapter	76
	Chapter 6 (Simulation and hardware-based Results)	**77-111**
	Chapter 7 (Conclusion and Future Scope)	**112-114**
7.1	Conclusion	112
7.2	Future Scopes	113
	References	**115-122**

List of Tables

Table No.	Title of Table	Page No.
1.1	Tabular representation of different generations of wireless communication	6
5.1	Parameters for (2x2) PD-NOMA	55
5.2	Parameters for (1x2) PD-NOMA	56
5.3	Parameters for (1x3) PD-NOMA	57

List of Figures

Fig No.	Title of Figure	Page No.
1.1	Pictorial representation of FDMA	2
1.2	Pictorial representation of TDMA	3
1.3	Pictorial representation of CDMA	4
1.4	Pictorial representation of FDM Vs OFDM	4
1.5	Pictorial representation of different Multiple Access schemes	5
3.1	Graphical representation between OMA and NOMA	16
3.2	Block diagram of the conventional PD-NOMA system	17
3.3	Pictorial representation of Code domain NOMA	17
3.4	Transmitter implementing Superposition coding (SC)	18
3.5	Pictorial representation of Successive Interference Cancellation process	19
3.6	Illustration of Downlink 1x2 SIMO PD-NOMA system	19
3.7	Illustration of Downlink 1x3 SIMO PD-NOMA system	20
3.8	Illustration of Downlink 2x2 MIMO PD-NOMA system	21
3.9	Block diagram of BPSK Transmitter side	32
3.10	BPSK modulated waveform	32
3.11	Block diagram of BPSK Receiver side	32
3.12	Block diagram of QPSK Transmitter side	33
3.13	QPSK modulated waveform	33
3.14	Block diagram of QPSK Receiver side	34
3.15	Constellation Diagram of BPSK, QPSK and 16 QAM modulation technique	37
4.1	Illustration of Downlink 1x3 PD-NOMA system model with NN Clustering	39
4.2	Illustration of Downlink 1x3 PD-NOMA system model with NF Clustering	40
4.3	Illustration of Downlink 1x3 PD-NOMA system model with FF Clustering	41
4.4	Illustration of Downlink 1x4 PD-NOMA system model with NN Clustering	42
4.5	Illustration of Downlink 1x4 PD-NOMA system model with NF Clustering	43
4.6	Illustration of Downlink 1x8 PD-NOMA system model with NN Clustering	44
4.7	Illustration of Downlink 1x8 PD-NOMA system model with NF Clustering	45
4.8	Illustration of Downlink 1x16 PD-NOMA system model with NN Clustering	46
4.9	Illustration of Downlink 1x16 PD-NOMA system model with NF Clustering	47
5.1	Hardware diagram of WARP	48
5.2	Figure of WARP V3 board	50
5.3	Experimental setup using WARP	51
5.4	Transmitter Receiver Block diagram	51
5.5	Experimental setup for (2x2) PD-NOMA system	54
5.6	Constellation Diagram of (2x2) NOMA for BPSK modulation without Precoding employing FPA	58
5.7	Constellation Diagram of (2x2) NOMA for QPSK modulation without Precoding employing FPA	58
5.8	Constellation Diagram of (2x2) NOMA for Adaptive modulation	58

	without Precoding employing FPA	
5.9	Constellation Diagram of (2x2) NOMA for 16 QAM modulation without Precoding employing FPA	58
5.10	Constellation Diagram of (2x2) NOMA for 64 QAM modulation without Precoding employing FPA	58
5.11	Constellation Diagram of (2x2) NOMA for BPSK modulation with SVD Precoding employing FPA	59
5.12	Constellation Diagram of (2x2) NOMA for QPSK modulation with SVD Precoding employing FPA	59
5.13	Constellation Diagram of (2x2) NOMA for Adaptive modulation with SVD Precoding employing FPA	59
5.14	Constellation Diagram of (2x2) NOMA for 16 QAM modulation with SVD Precoding employing FPA	59
5.15	Constellation Diagram of (2x2) NOMA for 64 QAM modulation with SVD Precoding employing FPA	59
5.16	Constellation Diagram of (2x2) NOMA for BPSK modulation with SVD Precoding employing DPA	60
5.17	Constellation Diagram of (2x2) NOMA for QPSK modulation with SVD Precoding employing DPA	60
5.18	Constellation Diagram of (2x2) NOMA for Adaptive modulation with SVD Precoding employing DPA	60
5.19	Constellation Diagram of (2x2) NOMA for 16 QAM modulation with SVD Precoding employing DPA	60
5.20	Constellation Diagram of (2x2) NOMA for 64 QAM modulation with SVD Precoding employing DPA	60
5.21	Constellation Diagram of (1x2) NOMA for BPSK modulation without Precoding employing FPA	62
5.22	Constellation Diagram of (1x2) NOMA for QPSK modulation without Precoding employing FPA	62
5.23	Constellation Diagram of (1x2) NOMA for Adaptive modulation without Precoding employing FPA	62
5.24	Constellation Diagram of (1x2) NOMA for 16 QAM modulation without Precoding employing FPA	62
5.25	Constellation Diagram of (1x2) NOMA for 64 QAM modulation without Precoding employing FPA	62
5.26	Constellation Diagram of (1x2) NOMA for BPSK modulation with SVD Precoding employing FPA	63
5.27	Constellation Diagram of (1x2) NOMA for QPSK modulation with SVD Precoding employing FPA	63
5.28	Constellation Diagram of (1x2) NOMA for Adaptive modulation with SVD Precoding employing FPA	63
5.29	Constellation Diagram of (1x2) NOMA for 16 QAM modulation with SVD Precoding employing FPA	63
5.30	Constellation Diagram of (1x2) NOMA for 64 QAM modulation with SVD Precoding employing FPA	63
5.31	Constellation Diagram of (1x2) NOMA for BPSK modulation with SVD Precoding employing DPA	64
5.32	Constellation Diagram of (1x2) NOMA for QPSK modulation with SVD Precoding employing DPA	64
5.33	Constellation Diagram of (1x2) NOMA for Adaptive modulation with SVD Precoding employing DPA	64
5.34	Constellation Diagram of (1x2) NOMA for 16 QAM modulation with SVD Precoding employing DPA	64
5.35	Constellation Diagram of (1x2) NOMA for 64 QAM modulation	64

	with SVD Precoding employing DPA	
5.36	Constellation Diagram of (1x3) NOMA for BPSK modulation without Precoding employing FPA	66
5.37	Constellation Diagram of (1x3) NOMA for QPSK modulation without Precoding employing FPA	66
5.38	Constellation Diagram of (1x3) NOMA for Adaptive modulation without Precoding employing FPA	66
5.39	Constellation Diagram of (1x3) NOMA for 16 QAM modulation without Precoding employing FPA	66
5.40	Constellation Diagram of (1x3) NOMA for 64 QAM modulation without Precoding employing FPA	66
5.41	Constellation Diagram of (1x3) NOMA for BPSK modulation with SVD Precoding employing FPA	67
5.42	Constellation Diagram of (1x3) NOMA for QPSK modulation with SVD Precoding employing FPA	67
5.43	Constellation Diagram of (1x3) NOMA for Adaptive modulation with SVD Precoding employing FPA	67
5.44	Constellation Diagram of (1x3) NOMA for 16 QAM modulation with SVD Precoding employing FPA	67
5.45	Constellation Diagram of (1x3) NOMA for 64 QAM modulation with SVD Precoding employing FPA	67
5.46	Constellation Diagram of (1x3) NOMA for BPSK modulation with SVD Precoding employing DPA	68
5.47	Constellation Diagram of (1x3) NOMA for QPSK modulation with SVD Precoding employing DPA	68
5.48	Constellation Diagram of (1x3) NOMA for Adaptive modulation with SVD Precoding employing DPA	68
5.49	Constellation Diagram of (1x3) NOMA for 16 QAM modulation with SVD Precoding employing DPA	68
5.50	Constellation Diagram of (1x3) NOMA for 64 QAM modulation with SVD Precoding employing DPA	68
5.51	Constellation Diagram of (1x3) NN NOMA Cluster for BPSK modulation employing FPA	70
5.52	Constellation Diagram of (1x3) NN NOMA Cluster for QPSK modulation employing FPA	70
5.53	Constellation Diagram of (1x3) NN NOMA Cluster for Adaptive modulation employing FPA	70
5.54	Constellation Diagram of (1x3) NN NOMA Cluster for 16 QAM modulation employing FPA	70
5.55	Constellation Diagram of (1x3) NN NOMA Cluster for 64 QAM modulation employing FPA	70
5.56	Constellation Diagram of (1x3) NF NOMA Cluster for BPSK modulation employing FPA	71
5.57	Constellation Diagram of (1x3) NF NOMA Cluster for QPSK modulation employing FPA	71
5.58	Constellation Diagram of (1x3) NF NOMA Cluster for Adaptive modulation employing FPA	71
5.59	Constellation Diagram of (1x3) NF NOMA Cluster for 16 QAM modulation employing FPA	71
5.60	Constellation Diagram of (1x3) NF NOMA Cluster for 64 QAM modulation employing FPA	71
5.61	Constellation Diagram of (1x3) FF NOMA Cluster for BPSK modulation employing FPA	72
5.62	Constellation Diagram of (1x3) FF NOMA Cluster for QPSK	72

	modulation employing FPA	
5.63	Constellation Diagram of (1x3) FF NOMA Cluster for Adaptive modulation employing FPA	72
5.64	Constellation Diagram of (1x3) FF NOMA Cluster for 16 QAM modulation employing FPA	72
5.65	Constellation Diagram of (1x3) FF NOMA Cluster for 64 QAM modulation employing FPA	72
5.66	Constellation Diagram of (1x3) NN NOMA Cluster for BPSK modulation employing DPA	73
5.67	Constellation Diagram of (1x3) NN NOMA Cluster for QPSK modulation employing DPA	73
5.68	Constellation Diagram of (1x3) NN NOMA Cluster for Adaptive modulation employing DPA	73
5.69	Constellation Diagram of (1x3) NN NOMA Cluster for 16 QAM modulation employing DPA	73
5.70	Constellation Diagram of (1x3) NN NOMA Cluster for 64 QAM modulation employing DPA	73
5.71	Constellation Diagram of (1x3) NF NOMA Cluster for BPSK modulation employing DPA	74
5.72	Constellation Diagram of (1x3) NF NOMA Cluster for QPSK modulation employing DPA	74
5.73	Constellation Diagram of (1x3) NF NOMA Cluster for Adaptive modulation employing DPA	74
5.74	Constellation Diagram of (1x3) NF NOMA Cluster for 16 QAM modulation employing DPA	74
5.75	Constellation Diagram of (1x3) NF NOMA Cluster for 64 QAM modulation employing DPA	74
5.76	Constellation Diagram of (1x3) FF NOMA Cluster for BPSK modulation employing DPA	75
5.77	Constellation Diagram of (1x3) FF NOMA Cluster for QPSK modulation employing DPA	75
5.78	Constellation Diagram of (1x3) FF NOMA Cluster for Adaptive modulation employing DPA	75
5.79	Constellation Diagram of (1x3) FF NOMA Cluster for 16 QAM modulation employing DPA	75
5.80	Constellation Diagram of (1x3) FF NOMA Cluster for 64 QAM modulation employing DPA	75
6.1	Comparison of Sum Capacity of (2x2) PD-NOMA system for BPSK modulation	77
6.2	Comparison of Spectral Efficiency of (2x2) PD-NOMA system for BPSK modulation	77
6.3	Comparison of Energy Efficiency of (2x2) PD-NOMA system for BPSK modulation	78
6.4	Comparison of total Interference of (2x2) PD-NOMA system for BPSK modulation	78
6.5	Comparison of Sum Capacity of (2x2) PD-NOMA system for QPSK modulation	78
6.6	Comparison of Spectral Efficiency of (2x2) PD-NOMA system for QPSK modulation	78
6.7	Comparison of Energy Efficiency of (2x2) PD-NOMA system for QPSK modulation	78
6.8	Comparison of total Interference of (2x2) PD-NOMA system for QPSK modulation	78
6.9	Comparison of Sum Capacity of (2x2) PD-NOMA system for	79

	Adaptive modulation	
6.10	Comparison of Spectral Efficiency of (2x2) PD-NOMA system for Adaptive modulation	79
6.11	Comparison of Energy Efficiency of (2x2) PD-NOMA system for Adaptive modulation	79
6.12	Comparison of total Interference of (2x2) PD-NOMA system for Adaptive modulation	79
6.13	Comparison of Sum Capacity of (2x2) PD-NOMA system for 16 QAM modulation	79
6.14	Comparison of Spectral Efficiency of (2x2) PD-NOMA system for 16 QAM modulation	79
6.15	Comparison of Energy Efficiency of (2x2) PD-NOMA system for 16 QAM modulation	80
6.16	Comparison of total Interference of (2x2) PD-NOMA system for 16 QAM modulation	80
6.17	Comparison of Sum Capacity of (2x2) PD-NOMA system for 64 QAM modulation	80
6.18	Comparison of Spectral Efficiency of (2x2) PD-NOMA system for 64 QAM modulation	80
6.19	Comparison of Energy Efficiency of (2x2) PD-NOMA system for 64 QAM modulation	80
6.20	Comparison of total Interference of (2x2) PD-NOMA system for 64 QAM modulation	80
6.21	Comparison of Sum Capacity of different users SIMO-NOMA system for BPSK modulation	82
6.22	Comparison of Spectral Efficiency of different users SIMO-NOMA system for BPSK modulation	82
6.23	Comparison of Energy Efficiency of different users SIMO-NOMA system for BPSK modulation	82
6.24	Comparison of total Interference of different users SIMO-NOMA system for BPSK modulation	83
6.25	Comparison of Sum Capacity of different users SIMO-NOMA system for QPSK modulation	83
6.26	Comparison of Spectral Efficiency of different users SIMO-NOMA system for QPSK modulation	83
6.27	Comparison of Energy Efficiency of different users SIMO-NOMA system for QPSK modulation	84
6.28	Comparison of total Interference of different users SIMO-NOMA system for QPSK modulation	84
6.29	Comparison of Sum Capacity of different users SIMO-NOMA system for Adaptive modulation	84
6.30	Comparison of Spectral Efficiency of different users SIMO-NOMA system for Adaptive modulation	85
6.31	Comparison of Energy Efficiency of different users SIMO-NOMA system for Adaptive modulation	85
6.32	Comparison of total Interference of different users SIMO-NOMA system for Adaptive modulation	85
6.33	Comparison of Sum Capacity of different users SIMO-NOMA system for 16 QAM modulation	86
6.34	Comparison of Spectral Efficiency of different users SIMO-NOMA system for 16 QAM modulation	86
6.35	Comparison of Energy Efficiency of different users SIMO-NOMA system for 16 QAM modulation	86
6.36	Comparison of total Interference of different users SIMO-NOMA	87

	system for 16 QAM modulation	
6.37	Comparison of Sum Capacity of different users SIMO-NOMA system for 64 QAM modulation	87
6.38	Comparison of Spectral Efficiency of different users SIMO-NOMA system for 64 QAM modulation	87
6.39	Comparison of Energy Efficiency of different users SIMO-NOMA system for 64 QAM modulation	88
6.40	Comparison of total Interference of different users SIMO-NOMA system for 64 QAM modulation	88
6.41	Comparison of Sum Capacity of 1x3 NOMA with NOMA Clustering system for BPSK modulation	90
6.42	Comparison of Spectral Efficiency of 1x3 NOMA with NOMA Clustering system for BPSK modulation	90
6.43	Comparison of Energy Efficiency of 1x3 NOMA with NOMA Clustering system for BPSK modulation	91
6.44	Comparison of total Interference of 1x3 NOMA with NOMA Clustering system for BPSK modulation	91
6.45	Comparison of Sum Capacity of 1x3 NOMA with NOMA Clustering system for QPSK modulation	91
6.46	Comparison of Spectral Efficiency of 1x3 NOMA with NOMA Clustering system for QPSK modulation	92
6.47	Comparison of Energy Efficiency of 1x3 NOMA with NOMA Clustering system for QPSK modulation	92
6.48	Comparison of total Interference of 1x3 NOMA with NOMA Clustering system for QPSK modulation	92
6.49	Comparison of Sum Capacity of 1x3 NOMA with NOMA Clustering system for Adaptive modulation	93
6.50	Comparison of Spectral Efficiency of 1x3 NOMA with NOMA Clustering system for Adaptive modulation	93
6.51	Comparison of Energy Efficiency of 1x3 NOMA with NOMA Clustering system for Adaptive modulation	93
6.52	Comparison of total Interference of 1x3 NOMA with NOMA Clustering system for Adaptive modulation	94
6.53	Comparison of Sum Capacity of 1x3 NOMA with NOMA Clustering system for 16 QAM modulation	94
6.54	Comparison of Spectral Efficiency of 1x3 NOMA with NOMA Clustering system for 16 QAM modulation	94
6.55	Comparison of Energy Efficiency of 1x3 NOMA with NOMA Clustering system for 16 QAM modulation	95
6.56	Comparison of total Interference of 1x3 NOMA with NOMA Clustering system for 16 QAM modulation	95
6.57	Comparison of Sum Capacity of 1x3 NOMA with NOMA Clustering system for 64 QAM modulation	95
6.58	Comparison of Spectral Efficiency of 1x3 NOMA with NOMA Clustering system for 64 QAM modulation	96
6.59	Comparison of Energy Efficiency of 1x3 NOMA with NOMA Clustering system for 64 QAM modulation	96
6.60	Comparison of total Interference of 1x3 NOMA with NOMA Clustering system for 64 QAM modulation	96
6.61	Comparison of Sum Capacity of 1x8 NOMA Cluster with different of users in each cluster for BPSK modulation	98
6.62	Comparison of Spectral Efficiency of 1x8 NOMA Cluster with different number of users in each cluster for BPSK modulation	98
6.63	Comparison of Energy Efficiency of 1x8 NOMA Cluster with	98

	different number of users in each cluster for QPSK modulation	
6.64	Comparison of Spectral total Interference of 1x8 NOMA Cluster with different number of users in each cluster for QPSK modulation	98
6.65	Comparison of Sum Capacity of 1x8 NOMA Cluster with different number of users in each cluster for QPSK modulation	99
6.66	Comparison of Spectral Efficiency of 1x8 NOMA Cluster with different number of users in each cluster for QPSK modulation	99
6.67	Comparison of Energy Efficiency of 1x8 NOMA Cluster with differ number of users in each cluster for QPSK modulation	99
6.68	Comparison of total Interference of 1x8 NOMA Cluster with different number of users in each cluster for QPSK modulation	99
6.69	Comparison between Sum Capacity performed by Simulation and WARP V3 board of different users PD-NOMA with and without Clustering for BPSK modulation	100
6.70	Comparison between Sum Capacity performed by Simulation of different users PD-NOMA with and without Clustering for BPSK modulation	100
6.71	Comparison between Spectral Efficiency performed by Simulation and WARP V3 board of different users PD-NOMA with and without Clustering for BPSK modulation	101
6.72	Comparison between Spectral Efficiency performed by Simulation of different users PD-NOMA with and without Clustering for BPSK modulation	101
6.73	Comparison between Sum Capacity performed by Simulation and WARP V3 board of different users PD-NOMA with and without Clustering for QPSK modulation	102
6.74	Comparison between Sum Capacity performed by Simulation of different users PD-NOMA with and without Clustering for QPSK modulation	102
6.75	Comparison between Spectral Efficiency performed by Simulation and WARP V3 board of different users PD-NOMA with and without Clustering for QPSK modulation	103
6.76	Comparison between Spectral Efficiency performed by Simulation of PD-NOMA different users PD-NOMA with and without Clustering for QPSK modulation	103
6.77	Comparison between Sum Capacity performed by Simulation and WARP V3 board of different users PD-NOMA with and without Clustering for Adaptive modulation	104
6.78	Comparison between Sum Capacity performed by Simulation of different users PD-NOMA with and without Clustering for Adaptive modulation	104
6.79	Comparison between Spectral Efficiency performed by Simulation and WARP V3 board of different users PD-NOMA with and without Clustering for Adaptive modulation	105
6.80	Comparison between Spectral Efficiency performed by Simulation of different users PD-NOMA with and without Clustering for Adaptive modulation	105
6.81	Comparison between Sum Capacity performed by Simulation and WARP V3 board of different users PD-NOMA with and without Clustering for 16 QAM modulation	106
6.82	Comparison between Sum Capacity performed by Simulation of different users PD-NOMA with and without Clustering for 16 QAM modulation	106
6.83	Comparison between Spectral Efficiency performed by Simulation and WARP V3 board of different users PD-NOMA with and	107

	without Clustering for 16 QAM modulation	
6.84	Comparison between Spectral Efficiency performed by Simulation of different users PD-NOMA with and without Clustering for 16 QAM modulation	107
6.85	Comparison between Sum Capacity performed by Simulation and WARP V3 board of different users PD-NOMA with and without Clustering for 64 QAM modulation	108
6.86	Comparison between Sum Capacity performed by Simulation of different users PD-NOMA with and without Clustering for 64 QAM modulation	108
6.87	Comparison between Spectral Efficiency performed by Simulation and WARP V3 board of different users PD-NOMA with and without Clustering for 64 QAM modulation	109
6.88	Comparison between Spectral Efficiency performed by Simulation of different users PD-NOMA with and without Clustering for 64 QAM modulation	109

Chapter-1

Introduction:

1.1 Background of Wireless Communication:

Wireless communication refers to the use of wireless signals to transfer data between two or more devices without the use of wires or other physical connections. It is the most active and quickly expanding sector in the communication industry. Data is transferred from the transmitter to the receiver in a communication system. The transmission distance while employing wireless communication might range from a few meters to thousands of kilometres. Using mobile phones, it provides the freedom and flexibility to communicate even when moving around at a noticeably high throughput [1]. Compared to wired communication, wireless communication has simpler infrastructure and is less expensive to set up. Some of the most common wireless communication systems in our day-to-day life are Wi-Fi, Cell phones, Global Positioning System (GPS), headset, satellite television, etc. With the increasing demand for wireless services, efficient utilization of the available frequency spectrum, time slots, or code space is essential to accommodate a large number of users simultaneously. So, the ability of wireless communication system, to provide communication service between multiple users simultaneously over a single channel by using channelization techniques based on time, frequency or code is known as multiple access. The concept of multiple access technique is explained below in details.

1.2 Multiple Access Technique:

Multiple Access Technique refers to the method or scheme used in communication systems to enable multiple users or devices to share the same communication channel simultaneously. Multiple access techniques are used to allow a large number of mobile users to share the allocated spectrum in the most efficient manner. Basically, it is a technique where a single channel is accessed by multiple users for effective use of bandwidth between the users. So, this technique is crucial in scenarios where multiple users need to share a common communication medium efficiently. There is a slight difference between multiplexing and multiple access technique. Multiplexing is a method of combining multiple signals into a single signal that can be transmitted over a shared medium while multiple access allows multiple signals to share the same communication channel. A channel or bandwidth is defined as the physical or wireless medium through which multiple users are connected to each other. This channel is used for transfer of data between different users and is used to establish

a connection between different users [2]. For different users to send or transfer data to the network on a limited bandwidth simultaneously, multiple access technique is used.

The Multiple access technique is categorized into two parts.

i) Orthogonal Multiple Access (OMA) Technique,

ii) Non-Orthogonal Multiple Access (NOMA) Technique.

1.2.1 OMA Technique:

Orthogonal Multiple Access (OMA) is a multiple access technique that utilizes orthogonal resources to allow multiple users to simultaneously share the same frequency band, time, or code without interfering with each other [3]. The term "orthogonal" implies that the signals associated with different users are mathematically orthogonal, which means they are independent and do not interfere with each other when combined.

Some widely used OMA techniques are:

a. Frequency Division Multiple Access (FDMA),

b. Time Division Multiple Access (TDMA),

c. Code Division Multiple Access (CDMA),

d. Orthogonal Frequency Division Multiple Access (OFDMA).

1.2.1.1 FDMA:

Frequency Division Multiple Access (FDMA) is a multiple access technique which enables multiple users to share the same communication channel simultaneously. FDMA achieves this by dividing the total frequency bandwidth into smaller sub-bands, and each user is allocated a unique frequency band for communication [3]. Guard bands are used between each frequency band to prevent interference between the sub-bands. An example of FDMA is Analog FM (Frequency Modulation) radio broadcasting. In this technique different radio stations are allocated different frequency bands (channels) on the FM dial. Each station broadcasts its signal on its assigned frequency band, and listeners can tune into the specific frequency to receive the desired station.

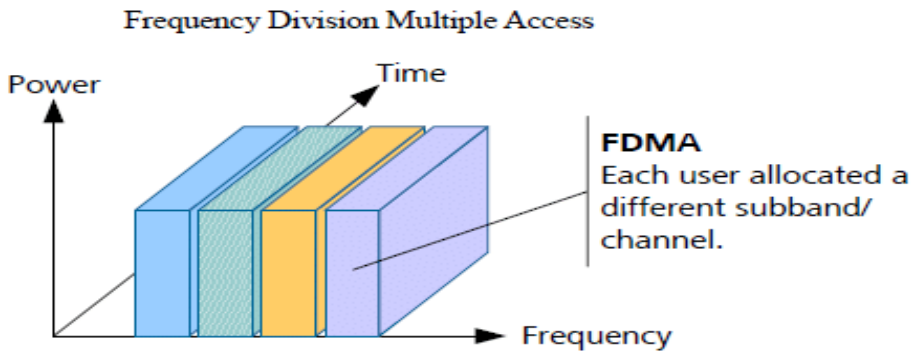


Fig 1.1: Pictorial representation of FDMA [4]

1.2.1.2 TDMA:

Time Division Multiple Access (TDMA) is a channel access method used in telecommunications to allow multiple users to share the same frequency channel by dividing the signal into different non-overlapping time slots [5]. TDMA is widely used in various communication systems, including cellular networks and satellite communication. In simplest term, TDMA enables multiple users to share the same frequency by dividing each cellular channel into different time slots. In effect, a single frequency supports multiple and simultaneous data channels. So, with a two-time slot TDMA, two users can share the same frequency. With a three-time slot TDMA, three users can share the same frequency and so on.

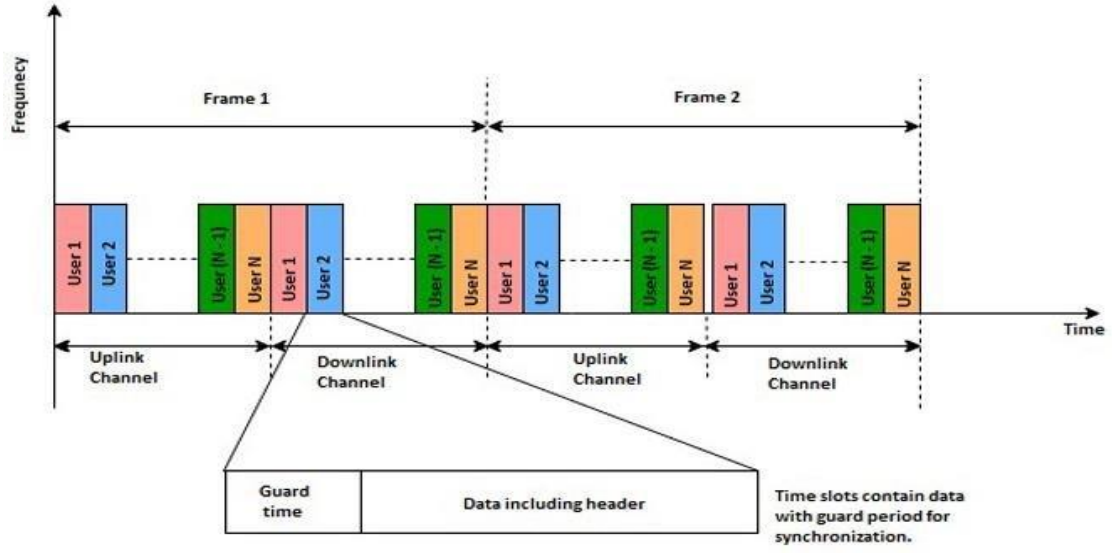


Fig 1.2: Pictorial representation of TDMA [6]

1.2.1.3 CDMA:

Code Division Multiple Access (CDMA) is another channel access method used in telecommunications, particularly in mobile communication systems. CDMA allows multiple users to share the same frequency band simultaneously by assigning a unique code to each user to distinguish each user's data signal from other users' data signals. This coding technique enables multiple signals to coexist without interfering with each other. Each user in a CDMA system is assigned a unique code, referred to as a spreading code [7]. These codes are orthogonal to each other, meaning they have a low correlation with each other. In this system, multiple users can transmit and receive data simultaneously on the same frequency band. This is possible because the unique codes assigned to each user allow their signals to be distinguished at the receiving end. At the receiving end, the system uses the corresponding code to retrieve the original signal. The receiver correlates the received signal with the known spreading code to extract the desired information. This technique is based on spread spectrum [2].

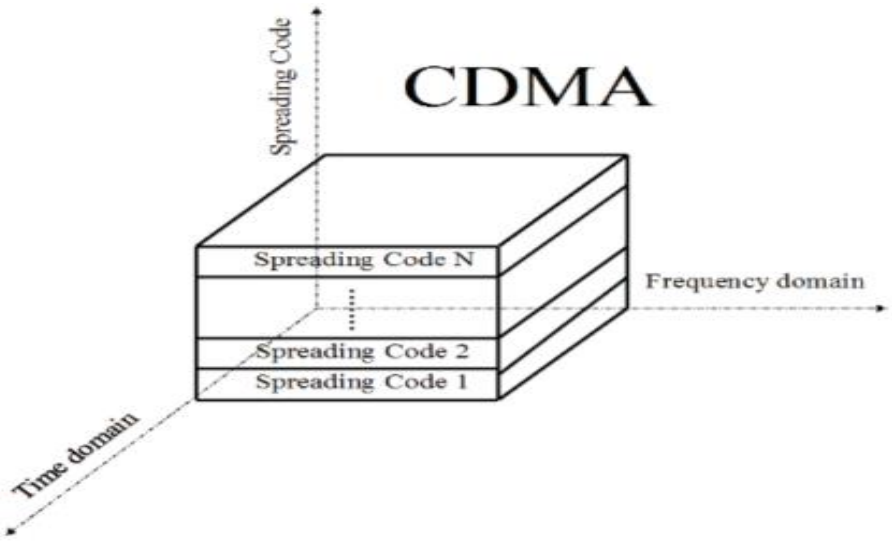


Fig 1.3: Pictorial representation of CDMA [8]

1.2.1.4 OFDMA:

OFDMA builds upon the principles of OFDM. OFDM is a digital data transmission method where available band is divided into large number of closely spaced frequency bands. These frequency bands are called Subcarriers. Input signal is split into multiple parallel streams and each stream is assigned with each separate subcarriers and by adding all the modulated subcarriers together, the output OFDM signal is created [9]. FDM suffers from Intersymbol Interference (ISI) due to the lack of orthogonality between different frequency bands. On the other hand, OFDM uses closely spaced narrow band subcarriers, which are orthogonal to each other. So, symbols in one subcarrier will not interfere with other symbols in other subcarriers. A Cyclic Prefix is a technique used in OFDM system to reduce the effect of multipath fading, ISI effect on the signal. It is a copy of the last few samples of the input symbol that is added to the beginning of the symbol. OFDMA is commonly used in various wireless communication standards, including 4G LTE (Long-Term Evolution), WiMAX (Worldwide Interoperability for Microwave Access).

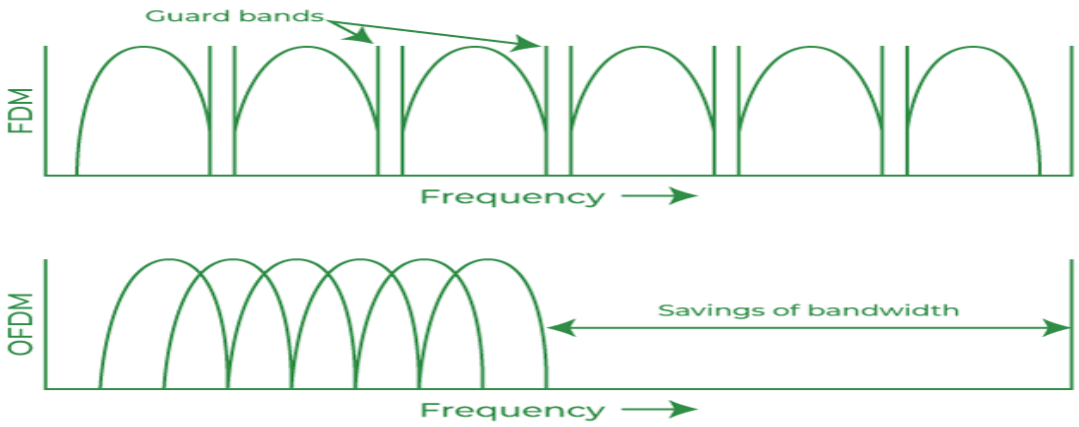


Fig 1.4: Pictorial representation of FDM Vs OFDM [10]

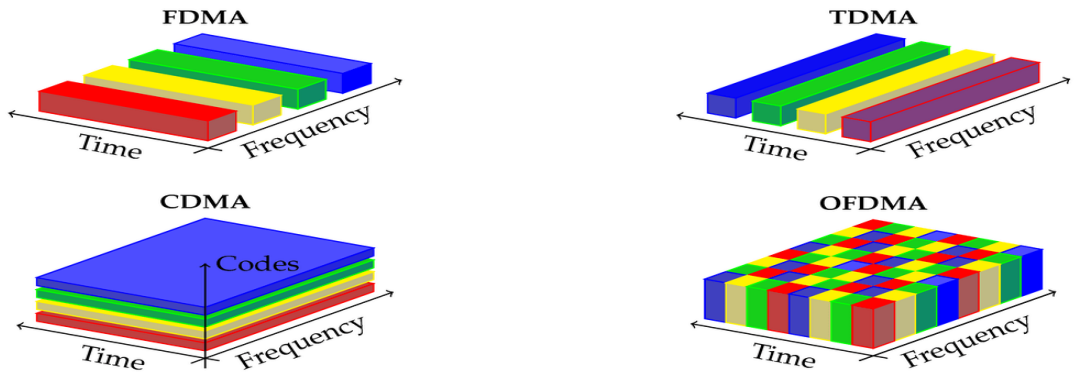


Fig 1.5: Pictorial representation of different Multiple Access schemes [11]

1.3 History: Different Multiple Access Techniques from 1G to 4G

- **1G** - First Generation 1G, or first generation, refers to the earliest wireless communication technologies. These networks were based on analog signals and provided basic voice and text messaging capabilities. 1G networks were introduced in the 1980s and were the first step towards the development of wireless communication networks. The first commercially available 1G network was launched in Japan in 1979 by NTT (Nippon Telegraph and Telephone). The network used an analog modulation technique known as **Frequency division multiple access (FDMA)** and provided voice-only services [12].
- **2G** - Second Generation 2G, or second generation, represents a significant advancement in wireless communication technology. These networks were based on digital signals and offered improved voice and data capabilities, including the ability to send and receive text messages [13]. The first 2G network was launched in Finland in 1991 by Radiolina. The network used a digital modulation technique known as **Time division multiple access (TDMA)** and allowed multiple users to share a single frequency band. This allowed for greater network capacity and improved call quality. 2G networks also enabled the development of mobile data services, such as mobile web browsing and email.
- **2.5G** - 2.5G or GPRS (General Packet Radio Service) is a stepping stone between 2G and 3G technology that was introduced in 2001. It comprises an extension of 2G for packet switched data transmissions. Packet-switched networks move data in small blocks or packets [13]. In the late 1990s, another digital modulation technique, known as code division multiple access (CDMA), was introduced. CDMA offered greater network capacity and improved call quality over TDMA. 2.5G is based on the multiple access technique **CDMA**.
- **3G** - Third Generation 3G, or third generation, represents another major advancement in wireless communication technology. These networks offered significant improvements in data speed and capacity, enabling more advanced mobile applications such as video streaming and online

gaming. The first 3G network was launched in Japan in 2001 by NTT DoCoMo. The network used a digital modulation technique known as **Wideband code division multiple access (WCDMA)** and offered data speeds of up to 384 kbps. Other 3G technologies, such as CDMA2000 and Enhanced Data rates for GSM Evolution (EDGE), were also introduced, offering even higher data speeds and capacity [13].

- **4G** - Fourth Generation 4G, or fourth generation networks are based on a technology known as Long-Term Evolution (LTE) and offer higher data speeds and capacity than 3G networks. The first 4G network was launched in Sweden in 2009 by TeliaSonera. The network used LTE technology and offered data speeds of up to 100 Mbps. 4G networks enable the development of even more advanced mobile applications, such as virtual and augmented reality, and enable new use cases such as the Internet of Things (IoT). Advanced version of FDMA used in the implementation of 4G is **OFDMA** [14].

Table 1.1: Tabular representation of different generations of wireless communication

Features	1G	2G	2.5G	3G	4G
Duration	1970-1980	1980-1990	1990-1999	2004-2005	2011
Data Rate	2kbps	9.6kbps	384kbps	2Mbps	1Gbps
Standards	AMPS, TACS, NTT etc	GSM	GPRS, EDGE	CDMA2000, WCDMA	LTE, Wi-Fi, WiMax
Services	Analogue Voice	Digital voice, messages	High speed Packet Data	Integrated Higher quality audio, video, and data	Mobile multimedia, dynamic information access
Multiple Access Technique	FDMA	FDMA, TDMA	CDMA	CDMA	OFDMA

1.4 Drawbacks of OMA technique:

OMA technique has some disadvantages. Some drawbacks of OMA technique are:

a) **Limited Capacity:** OMA systems may experience limited capacity, especially in scenarios with a large number of users. This limitation arises because each user requires a separate orthogonal resource, and the available orthogonal resources are finite.

b) **Interference:** In OMA, users are assigned separate orthogonal resources to avoid interference between them. However, in practical scenarios, perfect orthogonality may not be achievable due

to various factors such as channel imperfections, synchronization errors, and multipath fading. Interference between users can degrade the system's performance.

c) **Synchronization requirement:** OMA systems often require precise synchronization among users to maintain orthogonality. Achieving and maintaining this synchronization can be challenging, especially in dynamic and mobile environments.

d) **Scalability Issue:** As the number of users increases, the management and allocation of orthogonal resources become more complex. Scalability can be a concern in OMA systems, particularly in scenarios with a large number of devices.

1.5 NOMA Technique:

The increasing number of devices and high data speed requirements are putting OMA technique into a challenge. To overcome these challenges a new multiple access technology was introduced, which is **Non-Orthogonal Multiple Access technology (NOMA)**. In recent times, for fifth generation (5G) cellular networks, NOMA schemes have gained considerable interest [15].

In the **NOMA** protocol, one resource block (RB) serves more than one user, and one user can use more than one RB to improve their data rate. The users' signal is multiplexed at the transmitter side using Superposition Coding (SC) and demultiplexed at the receiver side using the Successive Interference Cancellation (SIC) technique. The usage of SC enhances the sum rate, user fairness, and scheduling flexibility. On the other hand, the inter-user interference created by SC multiplexing can be eliminated by SIC. NOMA is broadly classified into power-domain NOMA (PD-NOMA) and code-domain NOMA (CD-NOMA). In PD-NOMA, multiple users are served opportunistically as per the channel conditions from a common orthogonal RB. On the other hand, in CD-NOMA, the code spreading sequences are used to serve different users [16].

Though NOMA is a powerful multiple access technique, it faces several challenges that NOMA Clustering aims to address.

1.5.1 Drawbacks of NOMA Technique:

i. **Interference management:** As the number of user increases, managing interference and resource allocation becomes more challenging. Clustering groups users with similar channel conditions together, allowing interference to be managed more effectively within each cluster. This improves overall system performance and helps to achieve simultaneous transmission and reception.

ii. **Fairness enhancement:** In NOMA, users with stronger channel condition can dominate the resources, potentially leading to unfair resource allocation. Clustering helps to ensure fairness

enhancement by grouping users with similar channel conditions, which allows for more equitable distribution of resources within each cluster.

iii. **Heterogeneous Network environment:** In heterogeneous networks, users have diverse channel condition, Quality of Service (QoS) requirements and service types. Clustering allows for efficient management of different user types within the network, adapting resource allocation to their specific needs. NOMA Clustering enables load balancing among users in heterogeneous network. It allows users to be distributed evenly among different clusters, reducing congestion and improving network performance.

iv. **System Capacity:** NOMA clustering helps to enhance the system capacity by efficiently utilizing the available resources. Traditional multiple access schemes allocate orthogonal resources to users, which can lead to underutilization of the available bandwidth. By allowing multiple users to share the same time-frequency resource, NOMA clustering enables more efficient resource utilization and can support a larger number of users compared to orthogonal multiple access schemes. This leads to increased system capacity and improved scalability.

v. **Accommodating large number of users:** With the proliferation of wireless devices, accommodating a large number of users within limited spectrum resources is a critical requirement. NOMA Clustering's ability to support multiple users in the same time-frequency resources while maintaining QoS helps to address the challenges of scalability in wireless networks.

vi. **Latency reduction:** NOMA Clustering can contribute to lower latency compared to traditional techniques. The use of SIC decoding at receiver allows efficient separation of user signals, reducing the overall transmission delay and improving real time communication performance.

vii. **Energy efficiency:** NOMA Clustering's ability to optimize resource allocation can lead to improved energy efficiency. By allocating resources more judiciously, the system can reduce unnecessary power consumption while maintaining desired communication qualities.

1.6 Merits of NOMA Clustering over NOMA technique:

Non-Orthogonal Multiple Access (NOMA) has shown promise in improving spectral efficiency and enhancing the capacity of wireless communication systems. However, it also faces several challenges that NOMA Clustering aims to address. NOMA clustering is a technique used in NOMA systems to group users into clusters or clusters into superclusters. The goal of NOMA clustering is to enhance the system performance by optimizing the allocation of resources and managing interference among users. Within each cluster, power domain NOMA or code domain NOMA techniques are employed to allocate power levels or assign different codes to individual users, enabling simultaneous transmission and reception. Users within the same cluster share the same time-

frequency resources but are separated by assigning different power levels or codes to achieve signal separation at the receiver side.

The clustering process in NOMA aims to maximize the overall system capacity, spectral efficiency. NOMA clustering can be done based on channel conditions, required Quality of Services etc.

1.7 Motivation:

With the growing demand for high-speed data services, limited spectrum resources have led to the conventional approach of Orthogonal multiple access being ineffective in ensuring the desired quality of service. NOMA technique is required to address the challenges as there is a need to improve spectral efficiency to accommodate more users and applications within the limited available spectrum resource. NOMA allows multiple users to share the same resources simultaneously, thereby increasing spectral efficiency compared to traditional orthogonal multiple access techniques. So, NOMA is a promising technique for enhancing the performance of wireless communication systems, especially in scenarios with high user density and limited spectrum resources.

On the other hand, traditional NOMA technique suffers from increased interference among the users sharing the same resources, especially when the users have significantly different channel conditions. NOMA typically relies on successive interference cancellation (SIC) techniques at the receiver to decode signals from multiple users sharing the same resources. However, in scenarios with strong interference, the performance of SIC may degrade, leading to errors in decoding. NOMA Clustering addresses this issue by grouping users into clusters with similar channel conditions, thereby reducing the interference within each cluster and improving overall system performance. NOMA Clustering also improves the sum capacity of the system compared to conventional NOMA. By clustering users with similar channel conditions together and allocating resources optimally within each cluster, NOMA Clustering can serve higher sum capacity. Spectral efficiency is also enhanced in NOMA Clustering due to the better utilization of available frequency resources. By dynamically adjusting power allocation based on users' channel conditions within each cluster, NOMA Clustering maximizes spectral efficiency, allowing more data to be transmitted over the same bandwidth.

So, NOMA Clustering offers significant advantages over traditional NOMA techniques in terms of sum capacity and spectral efficiency, making it a promising solution for enhancing the performance of wireless communication systems in terms of data throughput and bandwidth utilization.

1.7.1 Objective of the thesis:

The most popular NOMA scheme is Power-domain NOMA (PD-NOMA). In this thesis we have analysed the performances in terms of Sum Capacity, Spectral Efficiency, Energy Efficiency, and total Interference of different users downlink PD-NOMA system with downlink PD-NOMA Clustering system with and without precoding under different power allocation schemes for different modulation techniques using MATLAB software and a transceiver board named as WARP V3. WARP comprises of the FPGA module and WARPLab framework. This WARPLab framework is used to combine the MATLAB software with the WARP board. WARP board can operate in two frequency bands: 2.4 GHz and 5 GHz. We have performed the experiments using the transceiver board at 2.4 GHz band. Experimentally we have observed that Downlink PD-NOMA Clustering system has higher Sum Capacity, Spectral Efficiency compared to Downlink PD-NOMA system.

1.8 Organization of the thesis:

- **Chapter 2** provides the Literature Survey on PD-NOMA and PD-NOMA Clustering system that have been performed by different researchers previously.
- **Chapter 3** provides the fundamental concept of NOMA system in details, along with concept of Precoding, different power allocation schemes, different Digital modulation techniques and performance analysis parameters that have been used in our work.
- **Chapter 4** provides the concept of PD-NOMA Clustering system and different NOMA Clustering system that have been analysed in our work.
- **Chapter 5** provides the detail description of the transceiver board, WARP V3 that has been used to perform the experiments, details of experimental setup and steps those are required to perform the experiments.
- **Chapter 6** provides an extensive analysis of performances, with respect to Sum Capacity, Spectral Efficiency, Energy Efficiency, and total amount of Interference of different users downlink PD-NOMA system with downlink PD-NOMA Clustering system with and without precoding for different Power Allocation strategies and different modulation techniques.
- **Chapter 7** gives a brief conclusion from this work and different future scopes of the research.

1.9 Summary of the chapter:

This chapter helps us to understand the background of the various OMA techniques as well as their drawbacks. The NOMA technique was created to address such drawbacks of OMA techniques. We also gain an understanding of the fundamentals of NOMA and NOMA Clustering technique from this chapter, along with the reasons behind the necessity of these 2 techniques.

Chapter-2

Literature Survey

Khairat et al., 2022 [17] have analysed the performance between OMA and NOMA technique. At the output it was observed that NOMA outperforms OMA. In paper **[18]** authors have worked on Power-Domain NOMA. They have surveyed on progress of NOMA system based on capacity analysis, power allocation strategies, and User fairness. In this paper they have also discussed how NOMA performs when it is integrated with various wireless communication techniques, such as cooperative communications, multiple-input multiple-output, beamforming, space–time coding, and network coding among others. **Reddy et al., 2021 [19]** have analysed different variants in NOMA and compared NOMA with OMA. The challenges for implementing NOMA commercially have also been addressed elaborately in this paper. Authors of **[20-23]** have analysed the performance of Downlink Power Domain NOMA (PD-NOMA) system in terms of Bit Error Rate (BER) under various channel conditions for different number of users. **Pavithra et al., 2022 [24]** compared the bit error rate, channel capacity, and outage probability with different users between OMA and PD-NOMA system using fixed power allocation scheme considering Rayleigh fading channel between the transmitter and receiver with AWGN noise. From the output result it is observed that PD-NOMA outperforms OMA. **Saraswat et al., 2020 [25]** have studied rate optimization Techniques when the Power Domain-NOMA scheme is joint with MIMO. The optimization methods used to maximize the promising rates. Authors have compared the performance of OMA and PD-NOMA system with respect to User throughputs, Ergodic Capacity etc. At the output it is observed that NOMA performs better than OMA system. **Ismail et al., 2020 [26]** have reviewed and analysed resource allocation problem for PD-NOMA in 5G networks and discussed the proposed solutions. **Hassan et al., 2021 [27]** have combined non-orthogonal multiple access (NOMA) with cognitive radio (CR) to maximize spectrum efficiency and performance of the system. **Chandrasekhar et al., 2022 [28]** have evaluated the performance of 2 users Multi-Input Multi-Output Non-Orthogonal Multiple Access (MIMO NOMA) for next generation wireless Communication systems in terms of Bit Error Rate (BER), Outage Probability, Channel Capacity considering Rayleigh fading channel between transmitter and receiver and compared these parameters with OMA technique. **Srivastava et al., 2022 [29]** proposed a constellation-based approach for Power Allocation (PA) in a two-user uplink PD-NOMA system. This approach suggested the optimal PA coefficients range for a two-user uplink PD-NOMA system. In this approach both the user symbols can be decoded simultaneously, without using the SIC process. The absence of SIC in such system offered a significant improvement in the error performance of the

system. The main aim of the central idea was to counter the imperfect SIC and associated anomalies by employing a constellation-based approach for user detection, instead of the conventional SIC approach and at the output it is observed that the formulated approach overcame SIC-related anomalies at the receiver. **Chauhan et al., 2023 [30]** determined the power allocation constraint (PAC) for a K -user power domain non-orthogonal multiple access (PD-NOMA) system, where each user employs an identical M− ary phase-shift keying modulation scheme. The angular periphery method was used to derive the PAC that determines the range of the power allocation factor to ensure reliable error performance. Further, analytical expressions for the bit error rate (BER), average BER, and diversity order of K− user PD-NOMA were derived under Nakagami- m fading channel with the help of order statistics for a generalized value of M. **Raju et al., 2023 [31]** have evaluated the energy efficiency and spectral efficiency of NOMA and compare it with other networks to demonstrate its superior performance. **Dadi et al., 2023 [32]** have analysed the performance of NOMA-MIMO scheme for 5G as a function of SNR and data rate achievement.

Kim et al., 2015 [33] proposed a novel user clustering algorithm for non-orthogonal multiple access (NOMA) considering the channel correlation between users and the channel gain. **Ali et al., 2016 [34]** proposed a low-complexity user clustering and power allocation scheme in downlink and uplink NOMA systems. In this work, users are clustered in groups according to the difference in their channel's gain in order to enhance the sum throughput of the system. This clustering scheme relies on selecting a feasible number of clusters, i.e., decides the number of clusters and the number of users per cluster. Once the number of users in a cluster is decided, then user grouping is performed. In each group, the power coefficients of the users are optimized by Lagrange multipliers. **Ding et al., 2016 [35]** compared the impact of user clustering on system performance under two different power allocation strategies: NOMA with fixed power allocation (F-NOMA) and cognitive radio inspired NOMA (CR-NOMA) and compared the performance of NOMA system with OMA system. In the simulation it was observed that F-NOMA can offer a larger sum rate than OMA, and the performance gain of F-NOMA over conventional MA can be further enlarged by selecting users whose channel conditions are more distinctive. For CR-NOMA, the quality of service (QoS) for users with the poorer channel condition can be guaranteed since the transmit power allocated to other users is constrained by the concept of cognitive radio networks. Because of this constraint, CR-NOMA exhibits different behavior compared to F-NOMA. For example, for the user with the best channel condition, CR-NOMA prefers to pair it with the user with the second-best channel condition, whereas the user with the worst channel condition is preferred by F-NOMA. **Zhang et al., 2018 [36]** proposed two user pairing algorithms based on neighborhood search methods, specifically the hill climbing and simulated annealing in Downlink NOMA network. Users are divided into multiple 2-user clusters. In

each cluster, the two users share the same transmit source, like time slot and spectrum, and the base station (BS) distributes the total transmit power to them. The goal of the user pairing is to divide N users into multiple clusters and find the pairing policy that leads to the largest sum throughput. In the simulation it was observed that combined with power allocation schemes, this algorithm can achieve a near-optimal sum throughput as well as low complexity compared with exhaustive search. **You et al., 2020 [37]** proposed a user clustering scheme in a hybrid downlink NOMA system based on a genetic algorithm (GA). The objective of the algorithm was to maximize the system total throughput under minimum rate constraints. In this algorithm there is no limit on the number of users in each cluster. Simulation results showed that the proposed scheme can significantly reduce computational complexity and have a better performance compared with schemes based on the other heuristic algorithms and random user clustering with greedy strategy. At the end of the paper researchers compared the performance of the proposed user clustering scheme with the random user clustering based on greedy strategy. **Zhu et al., 2019 [38]** proposed an optimal user clustering scheme of the even user scenario in a NOMA network. They first prove the optimality in the scenarios where there are only 2 and 4 users, and then extend the results to the cases with any even number of users. **Chen et al., 2021 [39]** proposed an algorithm for user clustering and power allocation to maximize the energy efficiency under maximal transmission power, minimum data transmission rate requirement and SIC requirement. At the end of the paper researchers collected the energy efficiency performance of 2-user, 3-user, and 4-user NOMA systems and compared them with orthogonal frequency division multiple access (OFDMA) based systems. **Ren et al., 2019 [40]** proposed an unsupervised machine learning based user clustering methods, including expectation maximization (EM) based method for the fixed user scenario, and an online EM (OLEM) based method for the dynamic user scenario to maximize the sum rate in a NOMA system. In the simulation researchers proposed that OLEM based user clustering method can reach the same or better performance compared to the complete EM-based method in dynamic scenario. **Tai et al., 2022 [41]** proposed a Clustering model using the method of pairing of two users and three users together and combine the threshold Signal-to-noise ratio (SNR) levels to decide on two or three pairings to ensure the Quality of services (QoS) for users. Researchers used K- means algorithm to form the Cluster. **Mouni et al., 2022 [42]** proposed an adaptive multi-user clustering and power allocation algorithms for downlink NOMA systems. This proposed algorithm uses minimum signal-to-interference-plus-noise ratio difference criterion between two successive NOMA users in a NOMA cluster to achieve higher rates than an equivalent orthogonal multiple access system. At the output researchers found that higher user data rates were achieved. **Sun et al., 2020 [43]** worked on the power consumption and user pairing of multi-input single-output non-orthogonal multiple access (MISO-NOMA) system. **Chakraborti et al., 2022 [44]** worked on

power allocation in user clustering in a NOMA system to improve network sum data rate. The enhancement of user data rate was achieved by grouping users by K-means algorithm based on channel quality indicator and signal to noise ratio. At the output result it was observed that the sum data rate was increased with the increase of clusters for poor channel condition in the proposed power distribution scheme. **Rezwan et al., 2020 [45]** proposed a reinforcement learning-based power allocation algorithm with a simple and efficient user clustering technique. They have used a Q-learning algorithm among all reinforcement learning techniques, which can easily obtain an optimal strategy to allocate power efficiently to maximize the sum data-rate of the NOMA system. In addition, they also proposed a channel gain-based user clustering technique that contributes to the maximization of sum data-rate. At the output it is found that the proposed power allocation algorithm with user clustering has achieved the highest throughput compared to other scenarios. **Saggese et al., 2020 [46]** investigated the joint clustering, beamforming, and power allocation problem for the downlink of multi-user MIMO-NOMA cellular system. They have proposed a scheme where strong and weak users are paired together to form NOMA clusters. Simulations results show that the proposed MIMO-NOMA scheme outperforms both classical MIMO-OMA and state-of-the-art MIMO-NOMA algorithms. **Ali et al., 2016 [47]** investigated the application of non-orthogonal multiple access (NOMA) with successive interference cancellation (SIC) in downlink multiuser multiple-input multiple-output (MIMO) cellular systems, where the total number of receive antennas at user equipment (UE) ends in a cell is more than the number of transmit antennas at the base station (BS). They first dynamically grouped the UE receive antennas into a number of clusters equal to or more than the number of BS transmit antennas. They have proposed a linear beamforming technique in which all the receive antennas can significantly cancel the inter-cluster interference. They have also provided dynamic power allocation solution for inter-cluster and intra-cluster power allocation in downlink MIMO-NOMA system to mitigate inter-cluster interference in order to maximize the overall throughput in a cell. Simulation results have demonstrated the spectral efficiency enhancement due to the proposed MIMO-NOMA model over the MIMO-OMA and other existing MIMO-NOMA solutions. **Liu et al., 2015 [48]** proposed a user selection algorithm to reduce the interference and improve the system information rate. They also proposed user power allocation scheme to make the proposed NOMA based multi-user beamforming system achieve higher information rate than traditional downlink multi-user beamforming system. **Guo et al., 2016 [49]** proposed two sort-based user pairing schemes in a multiuser Downlink NOMA system to decrease Symbol Error Rate (SER) and improve system capacity. A power allocation method was also proposed to maximize the system spectral efficiency. **Zeng et al., 2017 [50]** have compared the sum rates of MIMO-NOMA and MIMO-OMA. At output it has been proved analytically that MIMO-NOMA

outperforms MIMO-OMA in terms of both sum rate and ergodic sum rate for a simple two-user scenario. Then they have considered multiple user scenario in which users are paired into clusters. At the output it was observed that in order for MIMO-NOMA to achieve better performance than MIMO-OMA, user pairing should be conducted such that the two users have a large distance disparity. **Liang et al., 2017 [51]** proposed a user pairing in a downlink non-orthogonal multiple access (NOMA) network, where a user with poor channel condition is paired with a user with good channel condition, when both their rate requirements are satisfied, and the base station allocates the power to the pairwise users within the cluster. They also proposed a distributed matching algorithm in the downlink NOMA network, aiming to optimize the user pairing and power allocation between weak users and strong users, subject to the users' target rate requirements. Output results showed that the proposed algorithm outperforms the conventional orthogonal multiple access scheme. **Mahmoudi et al., 2022 [52]** tackled the problem of optimizing user clustering, power, and resource (time slot or bandwidth) allocation in the downlink of a hybrid non-orthogonal multiple access (NOMA)-orthogonal multiple access (OMA) system. In such system, users are organized into several clusters under: (1) fixed cluster size, (2) fixed number of clusters, and (3) variable number of clusters and variable cluster size. A power domain NOMA (PD-NOMA) scheme is used in each cluster, while OMA is employed for allocating resources to different clusters. The goal is to maximize the minimum success probability (which is equivalent to minimizing the maximum outage probability) among all users to guarantee fairness.

Summary of the chapter:

This chapter offers a review of the literature on the various NOMA and NOMA Clustering systems that have been performed in the past by various researchers and the overview of the results that they have got in their experiments.

Chapter-3

Fundamental Concept of NOMA

3.1 Basics of NOMA:

NOMA stands for Non-Orthogonal Multiple access. NOMA is a multiple access technique used in wireless communication systems where multiple users share the same time-frequency resources non-orthogonally. Unlike Orthogonal multiple access (OMA) techniques, such as TDMA and FDMA, where users are allocated separate and mutually exclusive resource blocks, NOMA allows simultaneous transmission of multiple users on the same resources. The main advantage of NOMA is that there is no need to share neither frequency nor time among users, since they are superimposed in the power domain, they can use the same frequency and time. It supports more number of users compared to OMA technique. Non-orthogonal multiple access (NOMA) has emerged as a potential technology for the fifth generation (5G) of wireless networks due to the increased demands on data rates and ever-increasing traffic.

NOMA can be classified into 2 major categories [53].

i. Power Domain NOMA (PD-NOMA),
ii. Code Domain NOMA (CD-NOMA).

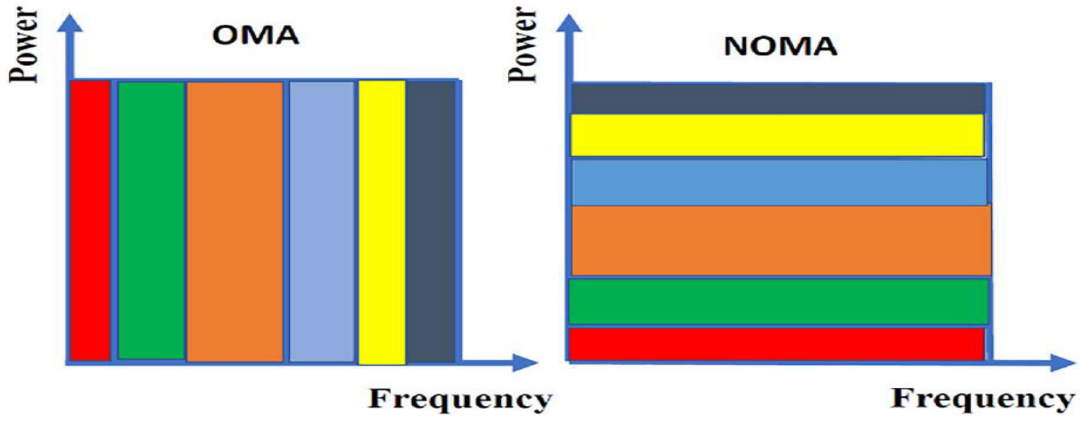


Fig 3.1: Graphical representation between OMA and NOMA [54]

i. **Power Domain NOMA (PD-NOMA):** Power Domain NOMA assigns a unique power level to every user, sharing the same time-frequency-code resources. The level of power for a user is decided based on its channel gain: a user with higher channel gain is assigned a lower power level. Consider at receiver there are 2 users: Near user (strong channel gain) and Far user (weak channel gain). Both served on same time and frequency. Transmitted power is splitted between them. High power is allocated to the far user (FU) and weak power is allocated to near user (NU). Typically interference

should happen. FU signal has small interference from NU signal. FU decodes it signal first and suffers from slight extra interference. NU signal has large interference from FU. NU decodes (detects) FU signal first and subtracts the interference from the composite received signal. Hence FU interference is cancelled. NU detects its data from cleaned signal [55].

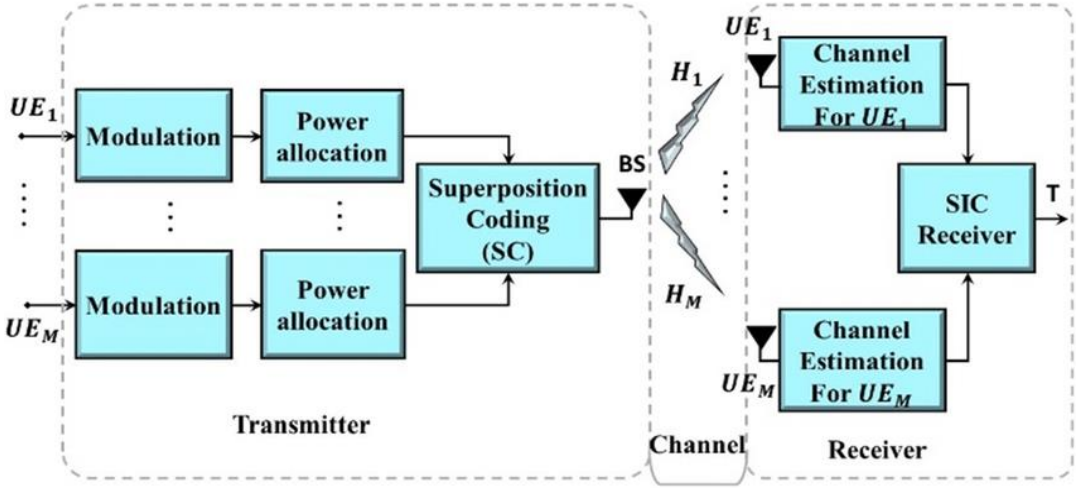


Fig 3.2: Block diagram of the conventional PD-NOMA system [56]

ii. Code Domain NOMA (CD-NOMA): It is another type of NOMA technique where multiple users share the same time and frequency resources simultaneously to transmit the data, but they use different spreading codes [53]. At the receiver side receiver has the knowledge about spreading codes. Receiver uses those spreading codes to decode the data. Figure below shows the image of Code domain NOMA.

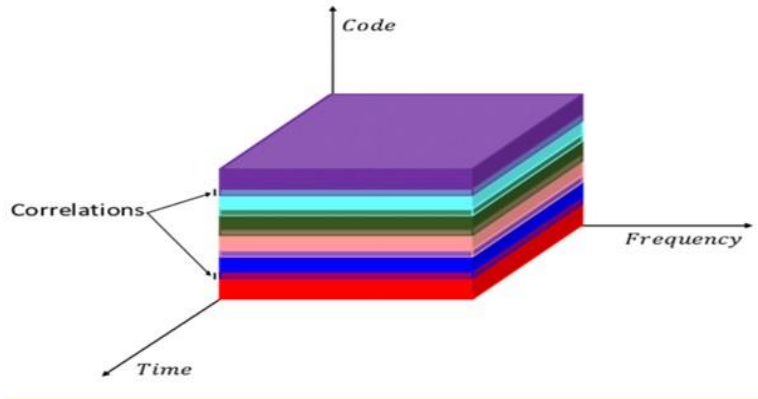


Fig 3.3: Pictorial representation of Code domain NOMA [57]

PD-NOMA accommodates Superposition Coding (SC) in the base station transmitter and Successive Interference Cancellation (SIC) in the receiver side to enhance spectrum efficiency. At the transmitter side various signals coming from different users are superposed by Superposition Coding (SC) technique and then transmitted over the same channel. At the receiver side, Successive Interference Cancellation (SIC) is applied to detect desired signals.

3.1.1 Superposition Coding (SC):

In Superposition Coding (SC) technique transmitter allows different user's signal to be superposed and transmitted through the same channel. Each signal at transmitter side is multiplied with some power levels and then added together to transmit through the channel. The power level allocation is decided based on the position of the users from the base station (BS). In Downlink NOMA system, more power is allocated to UE located farther from the BS and least power is allocated to the UE located closest to the BS [58].

For example, consider a two users NOMA scenario where UE1 is the NU and UE2 is the FU. $x_1(t)$ and $x_2(t)$ are the signals of UE1 and UE2 respectively. P_t is the total available power at BS. α_1 and α_2 are the power allocation coefficient for UE1 and UE2 respectively such that $\alpha_1 < \alpha_2$. Then the superimposed signal that is transmitted by the BS can be mathematically written as -

$$X(t) = \sqrt{P_t \alpha_1}\, x_1(t) + \sqrt{P_t \alpha_2}\, x_2(t)$$

Where $\alpha_1 + \alpha_2 = 1$.

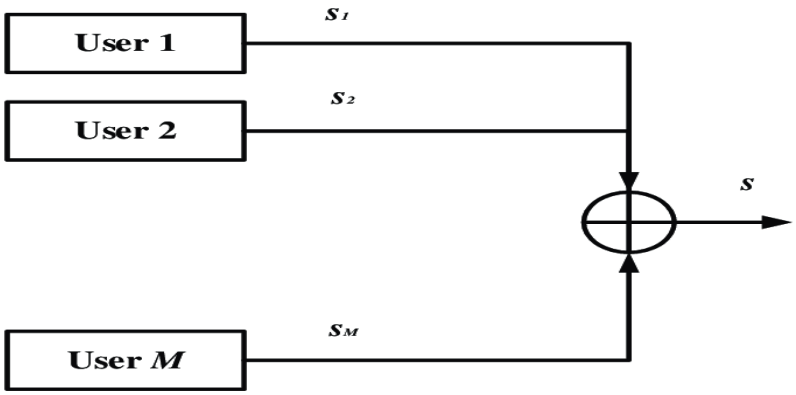


Fig 3.4: Transmitter implementing Superposition coding (SC) [59]

3.1.2 Successive Interference Cancellation (SIC):

The SIC is the most powerful interference cancellation-based scheme in terms of Bit-Error-Rate (BER) performance [60]. The concept behind this scheme is that the users can decode the received signal efficiently. In this technique, FU signal is decoded first, treating the other user signal as an interference, then subtracts the decoded signal from the composite signal and decodes the signal to get other user's signal. Each user decodes it signal treating other user's signal as interference. SIC aims to improve system capacity and performance gain.

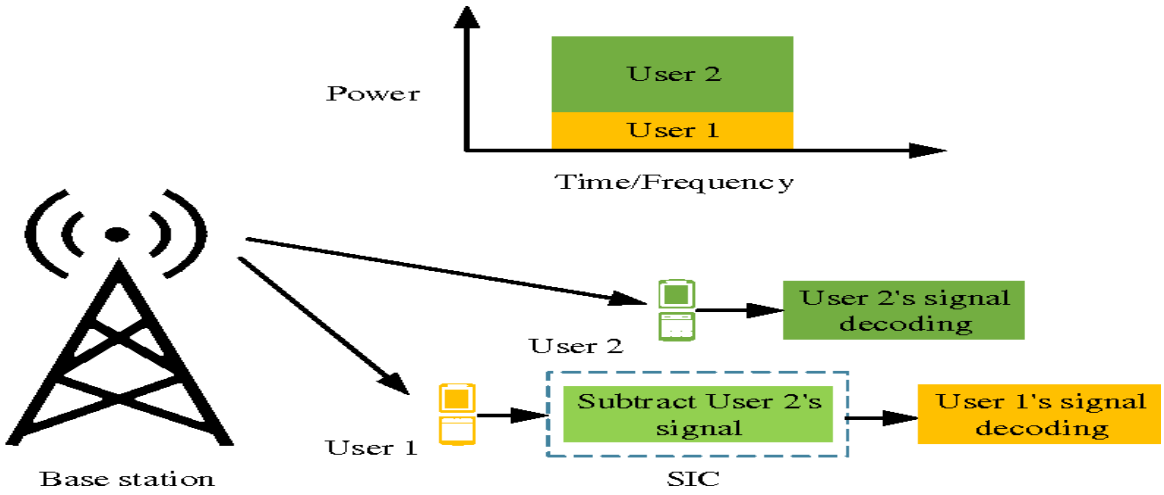


Fig 3.5: Pictorial representation of Successive Interference Cancellation process [61]

3.2 System Model Description:

In this thesis, two cases of PD-NOMA in a downlink scenario are explored. In the first case Single Input Multiple Output PD-NOMA (SIMO PD-NOMA) is explained and in the second case Multiple Input Multiple Output PD-NOMA (MIMO PD-NOMA) is explained. The system models for two cases are presented and discussed as follows:

CASE-I:

a) **Downlink 1x2 SIMO PD-NOMA system.**

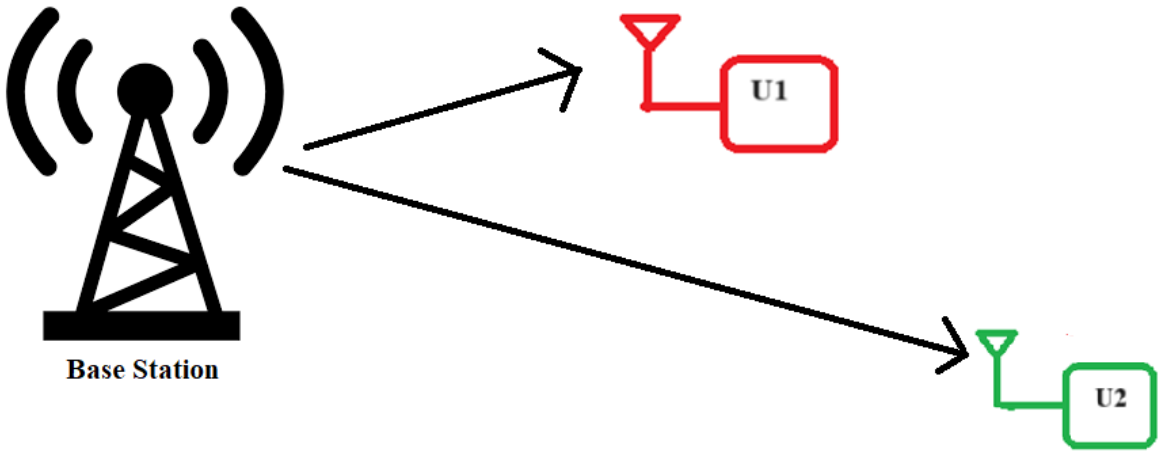


Fig 3.6: Illustration of Downlink 1x2 SIMO PD-NOMA system

Fig 3.6 represents a Downlink 1x2 SIMO PD-NOMA system where a single base station (BS) communicates with 2 users at the receiver end. U1 is situated at the closest distance from the BS, whereas U2 is located at the farthest distance from the BS. So, U1 is called as NU and U2 is called as FU. The system has (2x1) communication channel between the BS and users at the receiver end. Assumed that total transmitter power is P_t. The effective channel gains of the users are sorted as:

$|z_1 H_1 p_1|^2 \geq |z_2 H_2 p_2|^2$, where H_i indicates the channel matrix from BS to i^{th} user, p_i and z_i are the precoding and post-coding matrices of the i^{th} user respectively if and only if the precoding technique is applied to the system. Here, $i \in 1,2$. Therefore U1 has the highest channel gain and is hence referred to as the strong user while other user is termed as weak user. As per the NOMA principle, at the BS, the signals of different users are allocated different fractions of the total power, and the superposed signal is transmitted through the channel. The strong user is allocated a small fraction of the total power compared to the weak user. So, the power allocation order of the users are as follows: $P_1 < P_2$, where, $P_1 + P_2 = P_t$. If Precoding technique is applied, then the superposed signal is precoded and the resultant signal is transmitted through the antenna of the BS. At the receiver end each user receives the transmitted signal and apply the post-coding technique if precoding technique is applied at the transmitter end. At the receiver end, FU applies direct decoding to the received signal while NU performs SIC subtract the signal of FU from the received signal and decode it. NU treats the FU signal as interference.

b) Downlink 1x3 SIMO PD-NOMA system.

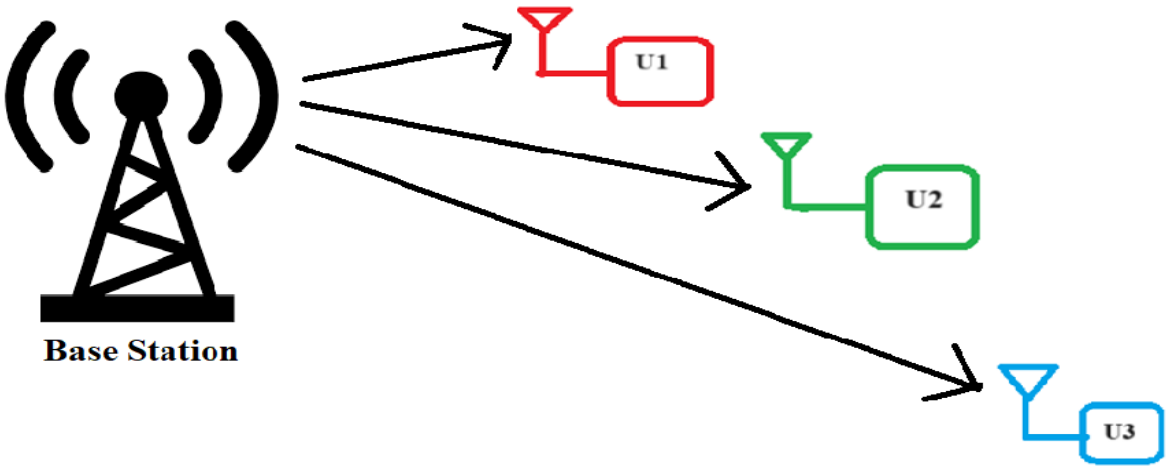


Fig 3.7: Illustration of Downlink 1x3 SIMO PD-NOMA system

Fig 3.7 represents a Downlink 1X3 SIMO PD-NOMA system where a single base station (BS) communicates with 3 users at the receiver end. U1 is situated at the closest distance from the BS, U3 is located at the farthest distance from the BS and U3 is located between U1 and U2. So, U1 is called NU, U2 is called Intermediary user (IU) and U3 is called FU. The system has (3x1) communication channel between the BS and users at the receiver end. Assumed that total transmitter power is P_t. The effective channel gains of the users are sorted as: $|z_1 H_1 p_1|^2 \geq |z_2 H_2 p_2|^2 \geq |z_3 H_3 p_3|^2$, where H_i indicates the channel matrix from BS to i^{th} user, p_i and z_i are the precoding and post-coding matrices of the i^{th} user respectively if and only if the precoding technique is applied to the system. Here, $i \in 1,2,3$. Therefore U1 has the highest channel gain and is hence referred to as the strong user while other users are termed as weak users. as per the NOMA principle, at the BS, the signals of different

users are allocated different fraction of the total power, and the superposed signal is transmitted through the channel. The strong user is given small fraction of power compared to weak users. So, the power allocation order of the users are as follows: $P_1 < P_2 < P_3$, where, $P_1 + P_2 + P_3 = P_t$. If Precoding technique is applied, then the superposed signal is precoded and the resultant signal is transmitted through the antenna of the BS. At the receiver end each user receives the transmitted signal and apply the post-coding technique if precoding technique is applied at the transmitter end. At the receiver end, FU applies direct decoding to the received signal. Then IU performs SIC to subtract the signal of FU and decode it to get its signal. After that NU performs SIC to subtract the signal of FU and IU from the received signal and decode it to get its signal. NU treats other signals as interference.

CASE-II:

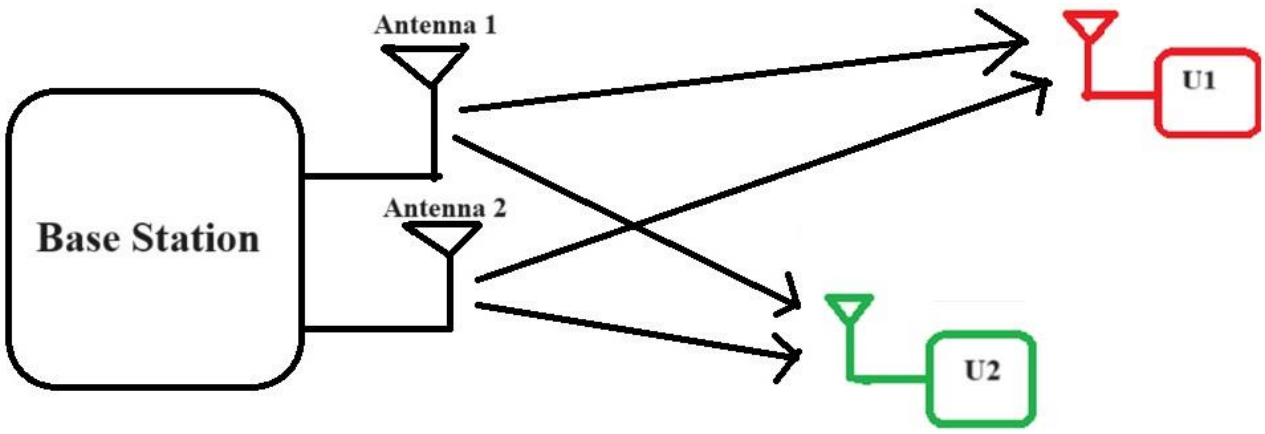


Fig 3.8: Illustration of Downlink 2x2 MIMO PD-NOMA system

Fig 3.8 represents a Downlink 2X2 MIMO PD-NOMA system [62] where 2 antennas at the transmitter side communicate with 2 users at the receiver end. U2 is situated at the smallest distance from the BS, whereas U1 is located at the farthest distance from the BS. So, U1 is called FU and U2 is called NU. The system has (2x2) communication channel between the transmitter and users at the receiver end. It is assumed that the total transmitter power is P_t. The effective channel gains of the users are sorted as: $|z_2 H_2 p_2|^2 \geq |z_1 H_1 p_1|^2$, where H_i indicates the channel matrix from transmitter to i^{th} user, p_i and z_i are the precoding and post-coding matrices respectively for the i^{th} user if and only if the concept of precoding is applied to the system. Here, $i \in 1,2$. Therefore U2 has the highest channel gain and is hence referred to as the strong user while other user is termed as weak user. At the transmitter, as per the NOMA principle, the signals of different users are allocated different fractions of the total power, and the superposed signal is transmitted over the same channel. The strong user is given small fraction of power compared to weak user. So, the power allocation order of the users are as follows: $P_2 < P_1$, where, $P_1 + P_2 = P_t$. The superposed signal may thereafter be

precoded and the resultant signal is transmitted through all the antennas of the BS. At the receiver end each user receives the transmitted signal and apply the post-coding technique if precoding technique is applied at the transmitter end. At the receiver end, FU applies direct decoding to the received signal while NU Perform SIC. NU employs SIC to decode and subtract the signal of FU from the received signal. NU treats the FU signal as interference.

3.3 Precoding Technique:

Precoding is a method of signal processing used in wireless communication at the transmitter side to optimize the transmission of signals before they are transmitted through the wireless channel. In order to achieve specific goals, such as improving received signal quality, enhancing overall system performance, and mitigating the effects of interference and other channel impairments, it entails processing the transmitted signals based on the channel conditions, characteristics, and system requirements in a way that optimizes system performance. So, the Precoding technique relies on knowledge of the channel's characteristics, referred to as Channel State Information (CSI). This information describes how signals propagate from the transmitter to the receiver, considering factors like fading, interference, and other environmental influences. The primary goal of precoding is to maximize the signal-to-noise ratio (SNR) and throughput, reducing interference among users, and increase the overall system capacity.

3.3.1 Processing Flow of Precoding:

The processing flow of precoding typically involves the following steps:

i. **Channel State Information (CSI) Calculation:** The transmitter needs accurate Channel State Information before applying the precoding technique. CSI is obtained by transmitting training sequence from transmitter to receiver. Based on the received signal, the transmitter then calculates the channel's information.

ii. **Calculation of Precoding Matrix:** The transmitter computes the precoding matrix after obtaining the CSI. The purpose of the precoding matrix is to convert the data symbols into a precise spatial pattern that may be transmitted via a wireless channel.

iii. **Precoding the Data:** After calculating precoding matrix, the data symbols are multiplied with the precoding matrix to produce a precoded signal. This signal is then transmitted over the wireless channel.

iv. **Reception and Decoding:** The transmitted data is extracted at the receiving end by processing the received signal. In order for the receiver to precisely estimate the channel's response, CSI is necessary. The receiver can recover the original data symbols by reversing the precoding process

and knowing the precoding matrix used at the transmitter.

We have used here Singular Value Decomposition (SVD) precoding technique.

3.3.2 Singular Value Decomposition (SVD) precoding:

Singular Value Decomposition (SVD) precoding is a technique used in wireless communication to optimize the transmission and reception of signals. It optimizes the transmit signal based on the channel condition, as a result maximizes the system's capacity, and improves the signal quality at the receiver end. SVD precoding involves computing the SVD of the channel matrix and then using the resulting matrices to shape the transmitted and received signals. This requires the knowledge of the channel, which can be obtained through channel estimation techniques. Then the transmit signal is multiplied by the Precoding matrix at the transmitter side. As a result enhance the signal quality at the receiver side, improve the system capacity.

In SVD technique, channel matrix (H) is decomposed into 3 matrices: U, D, V^H [63].

where, U and V^H are Unitary matrices, D is a diagonal matrix.

Channel matrix (H) can be written as:

$$H = UDV^H \qquad (1)$$

Here, V is the Precoding matrix that is applied at the transmitter side and U^H is the post-coding matrix that is applied at the receiver side.

The mathematical analysis of SVD Precoding technique is as follows:

Let us consider, N and M are the number of receiver and transmitter antennas respectively and H is a (NxM) channel matrix. Then, received Signal is written as

$$r = HPs + w \qquad (2)$$

where, r is a (Nx1) received signal vector,

s is a (Mx1) transmitted signal vector,

P is a (MxM) precoding matrix,

W is a (Nx1) Additive White Gaussian Noise (AWGN) vector.

The SVD of the channel matrix can be written from equation (1) as:

$$H = UDV^H$$

where, U and V are (NxN) and (MxM) unitary matrices respectively.

Therefore, replacing P with the precoding vector V and H with its SVD form in equation (2) we get,

$$r = UDV^H Vs + w \quad (3)$$

At the receiver side, the received signal is multiplied by post-coding vector U^H. So, at receiver end the received signal becomes:

$$U^H r = U^H(UDV^H Vs + w) \quad (4)$$

$$\Rightarrow \quad r' = U^H UDV^H Vs + U^H w \quad (5)$$

$$\Rightarrow \quad r' = (U^H U)D(V^H V)s + U^H w \quad (6)$$

Since U and V are unitary matrices, therefore by the property of Unitary matrices,

$$U^H U = I = UU^H \quad (7)$$

$$V^H V = I = VV^H \quad (8)$$

Thus, the received signal after post-coding process is as follows:

$$r' = Ds + w' \quad (9)$$

Where, $w' = U^H w$

Therefore it can be seen from equation (9) that the transmitted signal will be received with a gain matrix D.

3.4 Mathematical Model of PD-NOMA system:

Let us consider, K and M are the number of receiver and transmitter antennas respectively.

The expression for the superposed signal transmitted by the BS, in a downlink PD-NOMA system, is given as follows:

x = s, when no precoding is employed

= Ps, when precoding is employed

Where, s is (Mx1) superposed signal.

P is the (MxM) precoding matrix, which varies according to the precoding scheme used at transmitter side.

The superposed signal is given as follows:

$$s = \sum_{i=1}^{K} \sqrt{P_t \alpha_i} m_i$$

where, m_i is the transmitted signal of i^{th} user,

P_t is the total transmission power at BS,

α_i is the power coefficient of i^{th} user, subjected to the following condition:

$$\sum_{i=1}^{K} \alpha_i = 1$$

and $\alpha_1 \leq \alpha_2 \leq \ldots\ldots \leq \alpha_K$.

Effective channel gains of the system to be in the following order:

$$|z_1 H_1 p_1|^2 \geq |z_2 H_2 p_2|^2 \geq \ldots\ldots\ldots \geq |z_K H_K p_K|^2$$

Where, p_i and z_i are precoding and post-coding matrices respectively, that depends on the applied precoding scheme.

$|z_1 p_1| = 1$, when no precoding is applied.

H_i is a (KxM) channel matrix from BS to i^{th} user of the system.

The expression for the received signal at the i^{th} user is as follows:

$$r_i = H_i x + g_i$$

Where, g_i is a (Kx1) zero mean AWGN noise vector with a variance of σ_n^2.

After applying post-coding matrix, if required as per applied Precoding scheme, the modified received signal can be written as follows:

$$y_i = z_i H_i x + z_i g_i$$

The Signal to Interference plus Noise ratio (SINR) of the i^{th} user, except the 1^{st} user, can be expressed as follows [65]:

$$SINR_i = \frac{P_t \alpha_i |z_i H_i p_i|^2}{P_t |z_i H_i p_i|^2 \sum_{q=1}^{i-1} \alpha_q + \sigma_n^2}, \; i \neq 1$$

The Signal to Interference plus Noise ratio (SINR) of the 1^{st} user can be expressed as:

$$SINR_1 = \frac{P_t \alpha_1 |z_1 H_1 p_1|^2}{\sigma_n^2}$$

The Throughput of the i^{th} user can be expressed as:

$$R_i = Blog_2(1 + SINR_i)$$

Where, B is the available transmission Bandwidth.

Sum Capacity of the system can be written as [64]:

$$R = \sum_{i=1}^{K} R_i$$

3.5 Power Allocation strategy:

Power allocation strategy in Power domain Non-Orthogonal Multiple Access (PD-NOMA) system refers to method that is used to distribute total transmission power among multiple users sharing the same time, frequency resources in enhancing the system performance [66]. In NOMA, multiple users transmit their signals simultaneously over the same frequency band. To separate these signals at the receiver side, Successive Interference Cancellation (SIC) technique is used, where FU's signals are decoded first. This approach requires careful planning of power allocation to avoid interference and ensure correct decoding. Effective power allocation strategy is essential for managing interference, maximizing overall system capacity, and ensuring fairness among the users. So, efficient power allocation is crucial for improving the system's performance. Furthermore, in order to enhance system performance, power allocation in NOMA can be done in conjunction with other strategies like precoding and clustering. There are different power allocation strategies that can be employed in the NOMA system.

In this thesis we have discussed 2 types of power allocation strategies.

i. **Fixed Power Allocation:** Fixed Power Allocation strategy involves allocating fixed power levels to each user. In this strategy, each user is assigned a specific power level that remains constant during transmission, providing a simple and efficient way to implement NOMA [67]. In Fixed Power Allocation, power levels for each user are pre-determined based on channel conditions, or system requirements. The usual approach is to allocate more power to users with weaker channel conditions (those farther from the base station) and less power to users with stronger conditions (those closer from the base station).

ii. **Dynamic Power Allocation:** Dynamic Power Allocation in Non-Orthogonal Multiple Access (NOMA) is a strategy where the transmission power allocated to each user is adjusted based on various factors like channel conditions and system constraints. It involves continuously adjusting the power levels assigned to users based on changing network conditions. This approach is designed to

maximize system performance and reduce interference in NOMA systems, where multiple users share the same resources by transmitting at different power levels. It allows greater flexibility and adaptability compared to fixed power allocation, enabling more effective management of interference and system capacity. In Dynamic power allocation, power levels are adjusted to optimize system performance, reduce interference, and maximize system performance.

We have used a Dynamic Power Allocation scheme, whose main goal is to maximize the sum Capacity, Spectral efficiency, Energy Efficiency, minimize the Interference among the users.

Here, first we have considered a minimum Target Capacity for every users. Here we have applied the Dynamic Power Allocation scheme for 2 users and 3 users Downlink PD-NOMA system.

3.5.1 Derivation of Dynamic Power Allocation coefficients:

Case - I: 2 users Downlink NOMA System:

Capacity equations for NOMA near and far users can be written as follows:

$$R_f = B * \log_2(1 + \frac{P\alpha_f |h_f|^2}{|h_f|^2 P\alpha_n + \sigma_n^2}) \quad (10)$$

$$R_n = B * \log_2(1 + \frac{P\alpha_n |h_n|^2}{\sigma_n^2}) \quad (11)$$

Where, R_f is the Capacity of FU,

R_n is the Capacity of NU,

B is the available Bandwidth,

P is the total transmit Power,

α_n is the Power coefficient of NU,

α_f is the Power coefficient of FU,

h_f is the channel gain of FU,

h_n is the channel gain of NU,

σ_n^2 is the Noise Power.

α_n and α_f should be calculated such that -

$$\alpha_n + \alpha_f = 1 \text{ and } \alpha_f > \alpha_n.$$

We consider a minimum Capacity of the FU is R′.

Our goal is to calculate α_n and α_f such that $R_f \geq R'$.

Calculation of $\boldsymbol{\alpha_n}$ and $\boldsymbol{\alpha_f}$:

$$R_n \geq R' \tag{12}$$

Replacing the value of R_n from equation (11) we get,

$$B * \log_2(1 + \frac{P\alpha_n|h_n|^2}{\sigma_n^2}) \geq R' \tag{13}$$

$$\Rightarrow \log_2(1 + \frac{P\alpha_n|h_n|^2}{\sigma_n^2}) \geq R'/B$$

$$\Rightarrow (1 + \frac{P\alpha_n|h_n|^2}{\sigma_n^2}) \geq 2^{(R'/B)} \tag{14}$$

$$\Rightarrow \frac{P\alpha_n|h_n|^2}{\sigma_n^2} \geq 2^{(R'/B)} - 1 \tag{15}$$

Consider, $2^{(R'/B)} - 1 = \xi$

So, equation (15) becomes,

$$\frac{P\alpha_n|h_n|^2}{\sigma_n^2} \geq \xi$$

$$\Rightarrow P\alpha_n|h_n|^2 \geq \xi[\sigma_n^2]$$

$$\Rightarrow \boldsymbol{\alpha_n \geq \frac{\xi[\sigma_n^2]}{P|h_n|^2}} \tag{16}$$

Again, $\boldsymbol{\alpha_n + \alpha_f = 1}$

Once α_n is calculated using equation (16), we can easily calculate α_f as:

$$\boldsymbol{\alpha_f = 1 - \alpha_n} \tag{17}$$

Case - II: 3 users Downlink NOMA System:

Capacity equations for NOMA near, intermediary and far users can be written as follows:

$$R_f = B * \log_2(1 + \frac{P\alpha_f|h_f|^2}{|h_f|^2 P\alpha_n + |h_f|^2 P\alpha_i + \sigma_n^2}) \tag{18}$$

$$R_i = B * \log_2(1 + \frac{P\alpha_i|h_i|^2}{|h_i|^2 P\alpha_n + |h_i|^2 P\alpha_f + \sigma_n^2}) \tag{19}$$

$$R_n = B * \log_2(1 + \frac{P\alpha_n|h_n|^2}{\sigma_n^2}) \quad (20)$$

Where, R_f is the Capacity of FU,

R_i is the Capacity of IU,

R_n is the Capacity of NU,

B is the available Bandwidth,

P is the total transmit Power,

α_n is the Power coefficient of NU,

α_i is the Power coefficient of IU,

α_f is the Power coefficient of FU,

h_f is the channel gain of FU,

h_i is the channel gain of IU,

h_n is the channel gain of NU,

σ_n^2 is the Noise Power.

α_n , α_i and α_i should be calculated such that -

$$\alpha_n + \alpha_i + \alpha_f = 1 \text{ and } \alpha_f > \alpha_i > \alpha_n.$$

We consider a minimum Capacity of every user R_{min}.

Our goal is to calculate α_n , α_i and α_f such that $R_n \geq R_{min}$, $R_i \geq R_{min}$.

Calculation of α_n , α_i and α_f :

$$R_n \geq R_{min} \quad (21)$$

Replacing the value of R_n from equation (20) we get,

$$B * \log_2(1 + \frac{P\alpha_n|h_n|^2}{\sigma_n^2}) \geq \text{Rmin} \quad (22)$$

$$\log_2(1 + \frac{P\alpha_n|h_n|^2}{\sigma_n^2}) \geq \text{Rmin/B} \quad (23)$$

$$(1 + \frac{P\alpha_n|h_n|^2}{\sigma_n^2}) \geq 2^{(\text{Rmin/B})} \quad (24)$$

$$\frac{P\alpha_n|h_n|^2}{\sigma_n^2} \geq 2^{(\mathrm{Rmin/B})} - 1 \quad (25)$$

Consider, $2^{(\mathrm{Rmin/B})} - 1 = \xi$

So, equation (25) becomes,

$$\frac{P\alpha_n|h_n|^2}{\sigma_n^2} \geq \xi$$

$$\boldsymbol{\alpha_n \geq \frac{\xi[\sigma_n^2]}{P|h_n|^2}} \quad (26)$$

Again,

$$R_i \geq R_{min} \quad (27)$$

Replacing the value of R_i from equation (19) we get,

$$B * \log_2(1 + \frac{P\alpha_i|h_i|^2}{|h_i|^2 P\alpha_n + |h_i|^2 P\alpha_f + \sigma_n^2}) \geq \mathrm{Rmin} \quad (28)$$

$$\log_2(1 + \frac{P\alpha_i|h_i|^2}{|h_i|^2 P\alpha_n + |h_i|^2 P\alpha_f + \sigma_n^2}) \geq \mathrm{Rmin/B}$$

$$(1 + \frac{P\alpha_i|h_i|^2}{|h_i|^2 P\alpha_n + |h_i|^2 P\alpha_f + \sigma_n^2}) \geq 2^{(\mathrm{Rmin/B})} \quad (29)$$

$$\frac{P\alpha_i|h_i|^2}{|h_i|^2 P\alpha_n + |h_i|^2 P\alpha_f + \sigma_n^2} \geq 2^{(\mathrm{Rmin/B})} - 1 \quad (30)$$

Again,

$$\alpha_n + \alpha_i + \alpha_f = 1$$

So, $\alpha_n + \alpha_f = 1 - \alpha_i$

So, equation (30) becomes,

$$\frac{P\alpha_i|h_i|^2}{|h_i|^2 P(1-\alpha_i) + \sigma_n^2} \geq 2^{(\mathrm{Rmin/B})} - 1 \quad (31)$$

Consider, $2^{(\mathrm{Rmin/B})} - 1 = \xi$

So, equation (31) becomes,

$$\frac{P\alpha_i|h_i|^2}{|h_i|^2 P(1-\alpha_i) + \sigma_n^2} \geq \xi$$

$$P\alpha_i|h_i|^2 \geq \xi[|h_i|^2 P(1-\alpha_i) + \sigma_n^2]$$

$$P\alpha_i|h_i|^2[1+\xi] \geq \xi[|h_i|^2 P + \sigma_n^2]$$

$$\boldsymbol{\alpha_i \geq \frac{\xi[|h_i|^2 P + \sigma_n^2]}{P|h_i|^2[1+\xi]}} \quad (32)$$

Once α_n and α_i are calculated using equation (26) and (32), we can easily calculate α_f as:

$$\boldsymbol{\alpha_f = 1 - (\alpha_n + \alpha_i)} \quad (33)$$

In the same way, we can calculate the Dynamic Power Allocation coefficients if the number of users are increased.

3.6 Digital Modulation Techniques:

Modulation is defined as the process by which some characteristics of a carrier signal are varied in accordance with the message signal. The modulation technique in which transmitted signal is in the form of digital pulses is called Digital modulation [68]. Normally, the signals produced from different sources is analog in nature like audio signal captured in microphone, video signal etc. These can be converted into digital form using ADC (Analog to Digital converter) because there are certain advantages of digital modulation over analog modulation. Due to digital nature of transmitted signals, the interference of additive noise is less. Hence digital modulation provides better noise immunity. In Digital modulation channel coding techniques make it possible to detect and correct the errors introduced during transmission.

The following techniques give a brief description of the linear modulation schemes that we have used in our work.

3.6.1 Binary Phase Shift Keying (BPSK):

Phase Shift Keying (PSK) refers to a digital modulation technique in which the sine and cosine inputs of a radio wave vary at a specific time, altering the phase of the carrier signal. Binary PSK is the simplest type of phase-shift keying. It is also known as Phase Reversal Keying (PRK) or 2-phase PSK [69]. In BPSK, the carrier signal has two possible phase states. A binary '0' is represented by a carrier with one phase, while a binary '1' is represented by the same carrier with a phase shift of 180 degrees. In BPSK system, the pair of signals $S_1(t)$ and $S_2(t)$ used to represent binary symbols 1 and 0 respectively, is defined by-

$$S_1(t) = \sqrt{\frac{2E_b}{T_b}}\, cos(2\Pi f_c t) \;\&\; S_2(t) = \sqrt{\frac{2E_b}{T_b}}\, cos(2\Pi f_c t + \pi) \;;\; 0 \leq t \leq T_b \quad (34)$$

Where T_b is the bit duration and E_b is transmitted signal energy per bit.

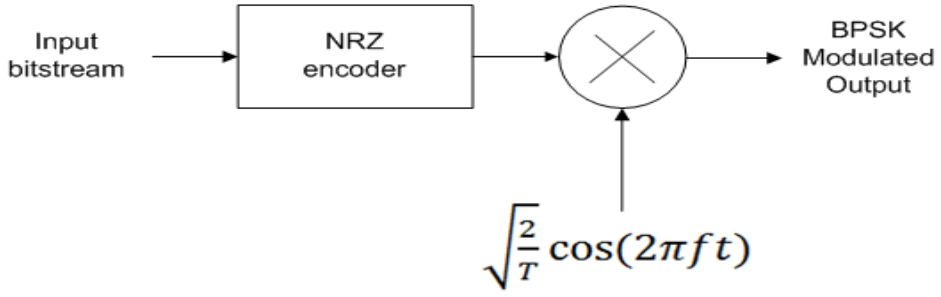


Fig 3.9: Block diagram of BPSK Transmitter side [70]

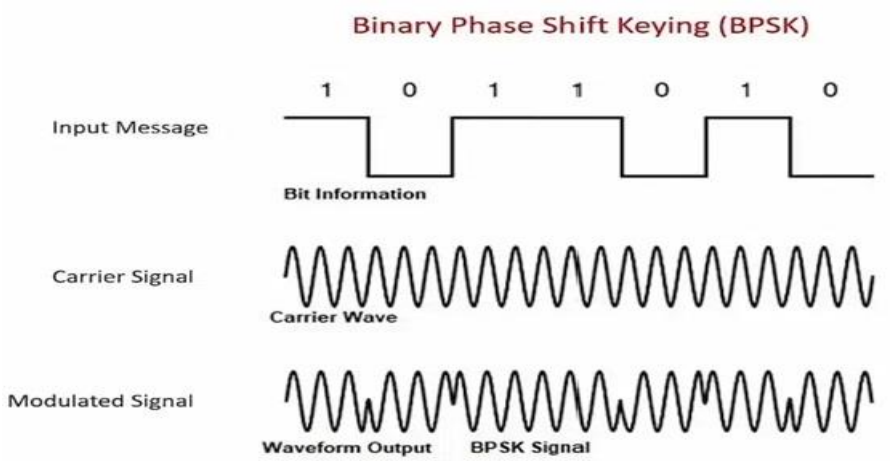


Fig 3.10: BPSK modulated waveform [71]

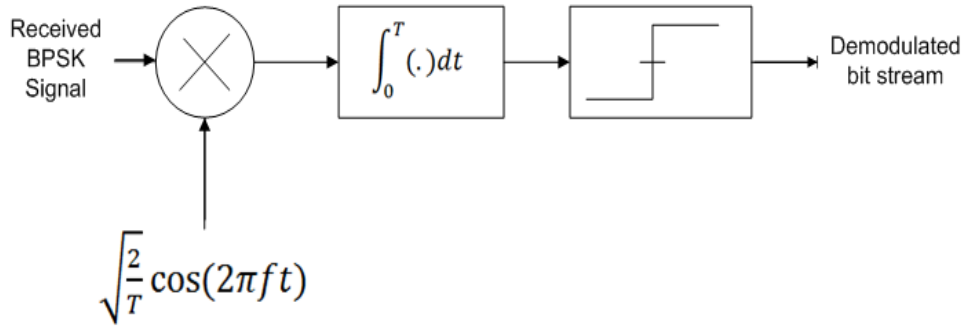


Fig 3.11: Block diagram of BPSK Receiver side [72]

3.6.2 Quadrature Phase Shift Keying (QPSK):

Quadrature Phase Shift Keying (QPSK) is a digital modulation method where, the phase of the carrier waveform is changed according to the digital baseband signal. The phase of the carrier remains the same when the input logic is the 1 but goes a phase shift when the logic is 0. In Quadrature Phase Shift Keying, two information bits are transmitted per symbol whereas in Binary Phase Shift Keying only one bit is passed per symbol. Here, there are four carrier phase offsets with a phase

difference of ±90° for four possible combinations of two bits (00, 01, 10, 11). Symbol duration in this modulation is twice the bit duration. The phase of the carrier takes one of the four equally spaced values, such as 0, $\Pi/2$, Π ,$3\Pi/2$, where each value of phase corresponds to a unique pair of message bits. QPSK allows the signal to carry twice as much information as ordinary PSK using the same bandwidth [73].

At the transmitter side, the message signal bits are separated as even bits and odd bits using a bit splitter. These bits are then multiplied with the same carrier waveform to generate Even QPSK and Odd QPSK signals. The Even QPSK signal is phase shifted by 90°, using a phase shifter, before modulation. Here, the Local Oscillator is used for generating the carrier waveform. After separation of bits, a 2-bit serial to parallel converter is used. After multiplying with the carrier waveform, both Even QPSK and Odd QPSK are given to the summer when modulation output is obtained.

QPSK transmitted signal may be defined as:

$$S(t) = \sqrt{\frac{2E_s}{T_s}}\, cos(2\Pi f_c t + (i-1)\frac{\Pi}{2}) \quad , \; 0 \le t \le T_s, \quad i = 1,2,3,4. \tag{35}$$

Where, T_s is the symbol duration,

E_s is the transmitted signal energy per symbol.

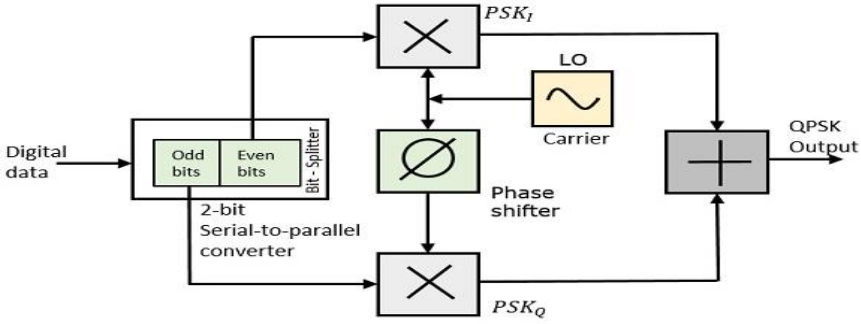


Fig 3.12: Block diagram of QPSK Transmitter side [74]

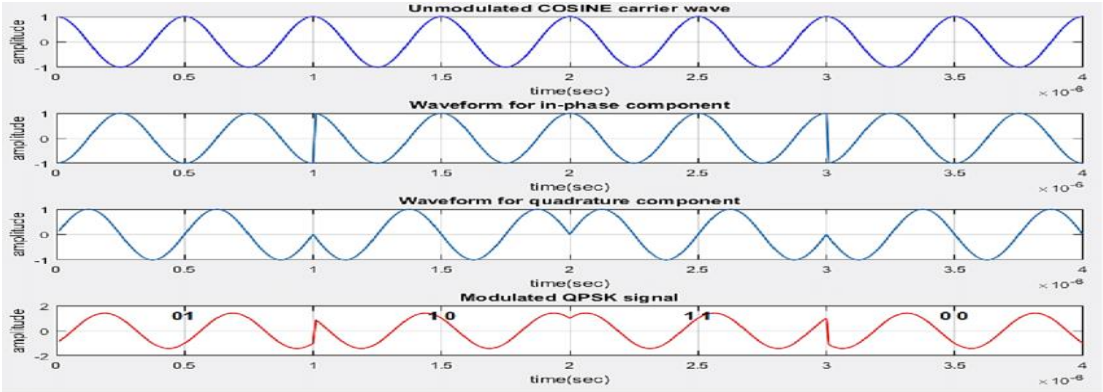


Fig 3.13: QPSK modulated waveform [75]

At the receiver end for demodulation, two product detectors are used. This product detectors convert the modulated QPSK signal into Even QPSK and Odd QPSK signals. Then the signals are passed through two bandpass filters and two integrators. After processing the signals are applied to the 2-bit parallel- to-serial converter, whose output is the reconstructed signal.

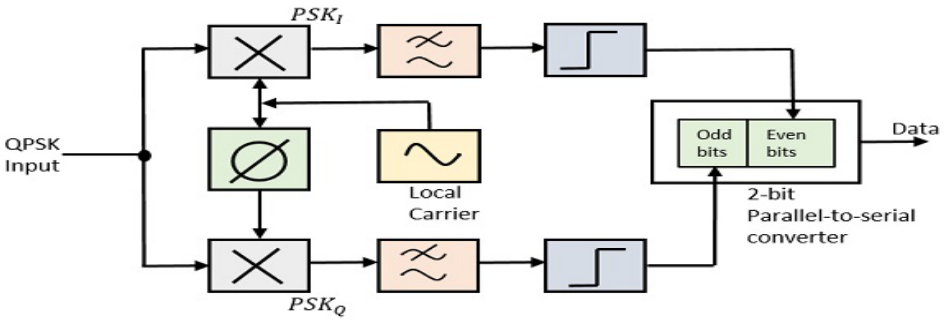


Fig 3.14: Block diagram of QPSK Receiver side [76]

3.6.3 Quadrature Amplitude Modulation (QAM):

In PSK technique, one symbol is distinguished from other symbols in phase, but all the symbols are same in amplitude. As we know that, the ability of receiver to distinguish between one signal vector from other depends on distance between vector end points. Hence noise immunity will improve if signals differ not only in phase but also in amplitude. Such a system is called Amplitude and Phase Shift Keying system. It is also known as Quadrature Amplitude modulation. So, QAM is a modulation scheme where its amplitude is allowed to vary with phase [69]. If N represents the number of bits and M is the number of possible combinations corresponding to any given number of N bits i.e the number of constellation points, the number of bits supported by M-ary QAM is given by the following Equation:

$$M = 2^N \qquad (36)$$

16-QAM is a type of Quadrature Amplitude Modulation (QAM) in which a carrier wave of a fixed frequency can exist in one of sixteen different states, where each state is a symbol that contains one of 16 different amplitude and phase levels. Each symbol contains up to 4 bits (0s and 1s) in a 16-QAM scheme. Therefore, the number of combinations that are possible using 4 binary bits is $2^4 = 16$, with each state or symbol containing a value from 0000 to 1111.

Similarly, in a **64-QAM** scheme each symbol contains up to 6 bits (0s and 1s). Therefore, the number of combinations that are possible using 6 binary bits is $2^6 = 64$, with each state or symbol containing a value from 000000 to 111111.

3.7 Performance Analysis Parameters:

Performance Analysis parameters in wireless communication systems are used to evaluate and measure the performance of the system.

The following parameters are some performance analysis parameters those have been explored in our work.

3.7.1 Sum Capacity:

The total throughput that every user contributes to the system is known as sum capacity. The amount of data that is successfully transferred via a wireless communication system in a specific amount of time is referred to as throughput. Typically, throughput is expressed in bits per second (bps). Thus, bits per second (bps) is the unit of measurement for sum capacity. The expression of Sum Capacity is as follows [77]:

$$\textbf{Sum Capacity} = \mathbf{R} = \sum_{i=1}^{n} R_i \qquad (37)$$

Where, n is the total number of users in the system,

R_i is the throughput of i^{th} user in the system.

3.7.2 Spectral Efficiency:

Spectral Efficiency (SE) or Bandwidth Efficiency measures how efficiently a communication system uses the available bandwidth to transmit data. It is a measure of the amount of data rate (throughput) that can be transmitted over a given bandwidth in a specific time. A higher spectral efficiency indicates that more data can be transmitted in less bandwidth, leading to more efficient use of the frequency spectrum. Therefore, it indicates how efficiently the allocated bandwidth is utilized. It is expressed in bits per second per hertz (bps/Hz). Mathematically SE is defined as follows [78]:

$$\textbf{SE} = \frac{R}{B} \qquad (38)$$

Where, R is the Sum Capacity of the system in bps,

B is the available bandwidth in Hz.

3.7.3 Energy Efficiency:

In NOMA system Energy Efficiency (EE) is defined as the ratio of Sum Capacity of the system to the total power consumption in the system. Sum Capacity refers to the sum of amount of data successfully transmitted and received by the users. Total power consumed by the system is the sum

of power required for transmitting the signal and power lost during Successive Interference Cancellation (SIC) process. The unit of EE is bps/Watt. Mathematically EE is defined as follows [79]:

$$\mathbf{EE} = \frac{\boldsymbol{R}}{\boldsymbol{P}} \quad (39)$$

Where, R is the Sum Capacity of the system in bps,

P is the total power consumption in Watt.

3.7.4 Total Interference:

In a Non-Orthogonal Multiple Access (NOMA) system, total interference can be computed as the sum of interference experienced by all users sharing the same resource. Consider a 3 users downlink NOMA system where User 1 is the NU, User 2 is the IU and User 3 is the FU. Signal to Interference plus Noise ratio (SINR) of the system can be written as:

$$\text{SINR of User 1} = \frac{(\boldsymbol{a_1} * |\mathbf{h_1}|^2)}{\boldsymbol{N_0}} \quad (40)$$

$$\text{SINR of User 2} = \frac{(\mathbf{a_2} * |\mathbf{h_2}|^2)}{((\mathbf{a_1} * |\mathbf{h_2}|^2) + \mathbf{N_0})} \quad (41)$$

$$\text{SINR of User 3} = \frac{(\mathbf{a_3} * |\mathbf{h_3}|^2)}{((\mathbf{a_1} * |\mathbf{h_3}|^2) + (\mathbf{a_2} * |\mathbf{h_3}|^2) + \mathbf{N_0})} \quad (42)$$

Where, a_1 is the power allocation coefficient for User 1,

a_2 is the power allocation coefficient for User 2,

a_3 is the power allocation coefficient for User 3,

h_1 is the channel gain of User 1,

h_2 is the channel gain of User 2,

h_3 is the channel gain of User 3,

N_0 is the Noise Power.

Then interference of User 1 = 0,

Interference of User 2 = $(\boldsymbol{a_1} * |\boldsymbol{h_2}|^2)$,

Interference of User 3 = $(\boldsymbol{a_1} * |\boldsymbol{h_3}|^2) + (\boldsymbol{a_2} * |\boldsymbol{h_3}|^2)$.

So, total interference of the system = interference of User 1+ interference of User 2+ interference of User 3 = $(\boldsymbol{a_1} * |\boldsymbol{h_2}|^2) + (\boldsymbol{a_1} * |\boldsymbol{h_3}|^2) + (\boldsymbol{a_2} * |\boldsymbol{h_3}|^2)$.

3.7.5 Constellation Diagram:

A constellation diagram in a communication system is a graphical representation that illustrates how data is transmitted using different modulation techniques. It provides a visual depiction of the various symbols used in digital modulation schemes, typically on a two-dimensional plane. It plots symbols in a complex plane, illustrating the amplitude and phase variations used to encode data. The horizontal axis (usually labeled "In-Phase" or "I") represents the real part of the complex signal, while the vertical axis (often labeled "Quadrature" or "Q") represents the imaginary part [80]. Points on the diagram represent different symbols used in the modulation scheme. Each symbol corresponds to a unique combination of phase and amplitude. Different modulation schemes have different Constellation patterns. Thus, Constellation diagrams are an invaluable tool for evaluating a digital communication system's performance.

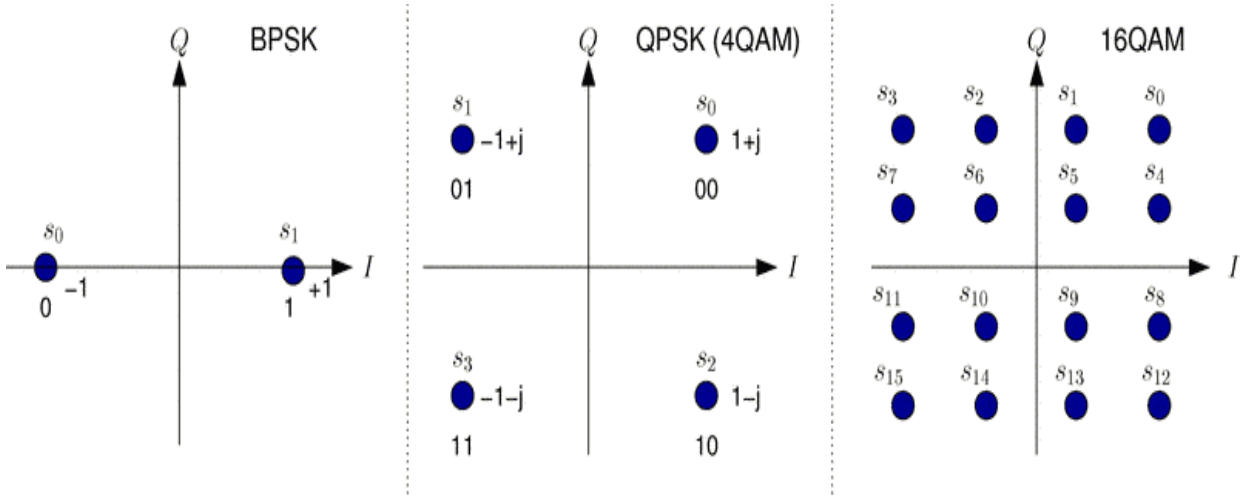


Fig 3.15: Constellation Diagram of BPSK, QPSK and 16 QAM modulation technique [81]

3.8 Summary of the chapter:

The fundamentals of NOMA technique as well as the two distinct methods (SC and SIC) those are used at the transmitter and receiver sides, respectively, of various NOMA system types, are covered in this chapter. This chapter also covered system model descriptions and related mathematical models. We also learned about the precoding technique, various power allocation schemes, modulation strategies, and performance analysis parameters from this chapter, that we have employed in our work.

Chapter-4

Concept of NOMA Clustering Technique:

4.1 Basics of NOMA Clustering:

NOMA is a powerful multiple access technique. But it faces several challenges in terms of Interference management that NOMA Clustering aims to address. Since NOMA allows multiple users to share the same frequency and time resources, interference is a significant challenge with the increase in the number of users in the system. Clustering technique in NOMA aims to address these challenges. Clustering helps in managing the complexity of SIC by reducing the number of users in each cluster. This can lead to more efficient SIC processing and reduced computational overhead. By simplifying SIC and reducing interference through clustering, NOMA systems can become more scalable, supporting a larger number of users without significant degradation in performance. NOMA clustering technique involves grouping users into different clusters for effective implementation of NOMA, enabling optimized power allocation, reduced interference, and enhanced system capacity. Clusters are formed based on various criteria, such as signal strength, spatial location, or channel conditions. Within each cluster NOMA technique is applied individually. In NOMA clustering system 2 types of interference needs to be handled. First is Intra-Cluster Interference (Interference between users within a Cluster) that is handled by SIC technique and the second one is Inter-Cluster Interference (Interference between different Clusters) that is handled by appropriate precoding technique. In our work we have applied clustering in Downlink SIMO-PD-NOMA systems, and we have clustered the users based on their power allocation coefficient. The goal of NOMA clustering technique is to enhance the system performance in terms of Sum Capacity, Spectral Efficiency, and Energy Efficiency by optimizing the allocation of resources and managing interference among users. We have worked on 3 types of Clustering. These clustering techniques are:

1. Near-Near Clustering (NN Clustering),
2. Near-Far Clustering (NF Clustering),
3. Far-Far Clustering (FF Clustering).

The power allocation strategies that we have used in our work are: Fixed Power Allocation (FPA) and Dynamic Power Allocation. We have analyzed their performances with the performances of downlink PD-NOMA system under different modulation techniques, different power allocation schemes and in presence and absence of precoding technique in terms of Sum Capacity, Spectral

Efficiency, Energy Efficiency and total amount of Interference. We have used Singular Value Decomposition (SVD) precoding technique.

4.2 System Model Description:

In this thesis, Single Input Multiple Output PD-NOMA Clustering (SIMO PD-NOMA Clustering) in a downlink scenario are explored. The system models are presented and discussed as follows:

a) Downlink 1x3 PD-NOMA NN Clustering system.

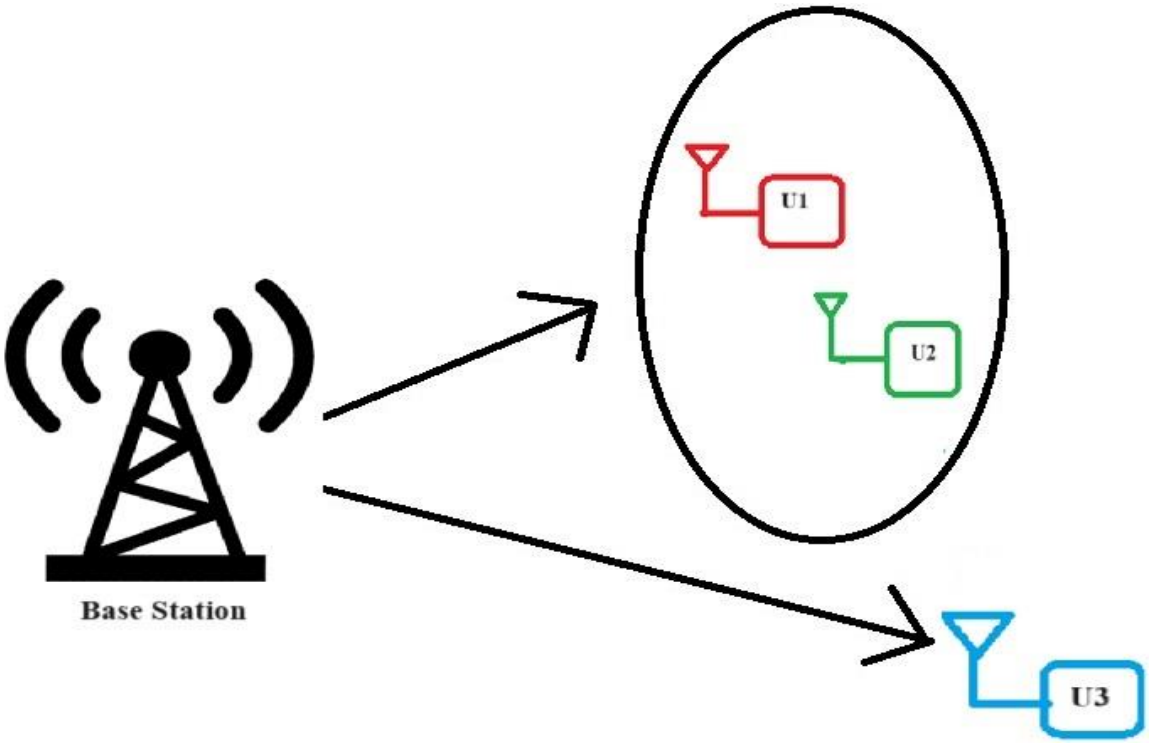


Fig 4.1: Illustration of Downlink 1x3 PD-NOMA system model with NN Clustering

Fig 4.1 represents a 1x3 PD-NOMA system in a Downlink scenario, where there is a single base station that communicates with 3 users at the receiver end. At the receiver end 2 users are grouped in a cluster based on the power allocation coefficients of the users. U1 is situated at the smallest distance from the BS, U3 is located at the farthest distance from the BS and U2 is located between U1 and U3. So, U1 is called NU, U2 is called IU and U3 is called FU. At the BS, as per the NOMA principle, the signals of different users are allocated different fraction of the total power. The NU is given the least fraction of power, and the FU is given highest fraction of power. So, the power allocation order of the users are as follows: $P_1<P_2<P_3$. In NN Clustering technique the NU and IU are grouped in a cluster. Within the cluster NOMA principle is employed, i.e. among the users in the cluster.

b) Downlink 1x3 PD-NOMA NF Clustering system.

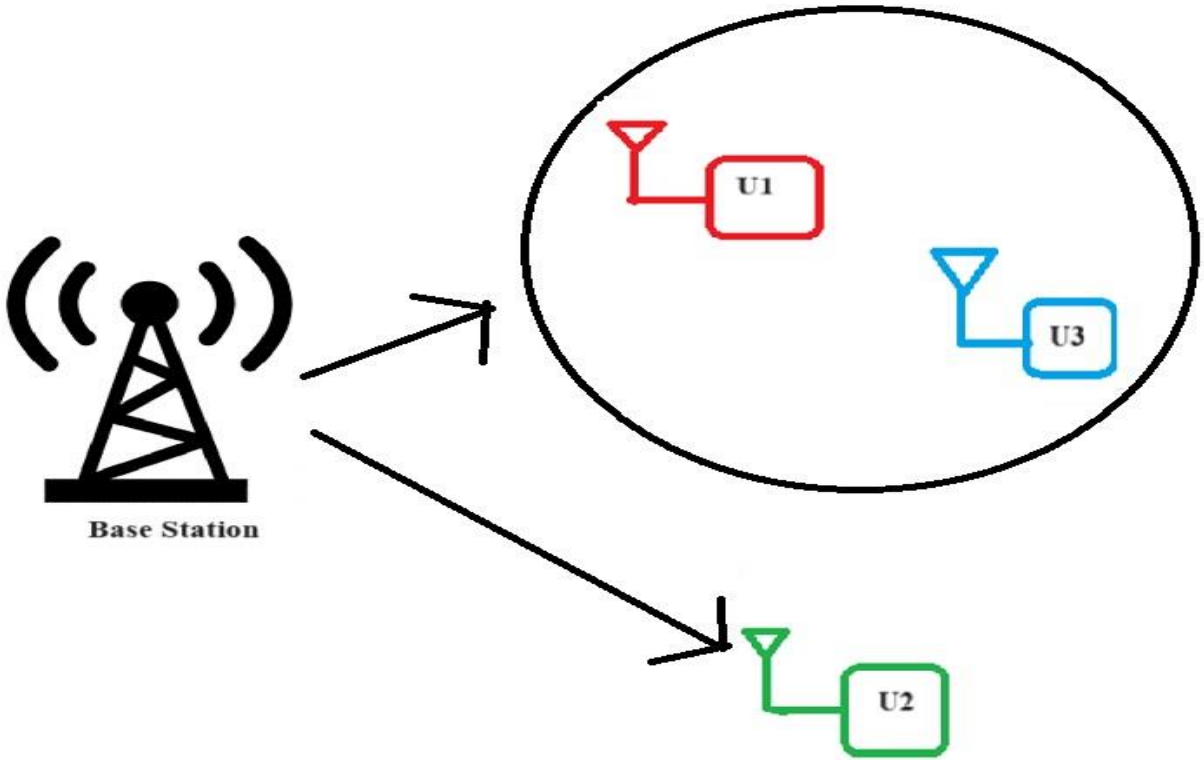


Fig 4.2: Illustration of Downlink 1x3 PD-NOMA system model with NF Clustering

Fig 4.2 represents a 1x3 PD-NOMA system in a Downlink scenario, where there is a single base station that communicates with 3 users at the receiver end. At the receiver end 2 users are grouped in a cluster based on the power allocation coefficients of the users. U1 is situated at the smallest distance from the BS, U3 is located at the farthest distance from the BS and U2 is located between U1 and U3. So, U1 is called NU, U2 is called IU and U3 is called FU. At the BS, as per the NOMA principle, the signals of different users are allocated different fraction of the total power. The NU is given the least fraction of power, and the FU is given highest fraction of power. So, the power allocation order of the users are as follows: $P_1<P_2<P_3$. In NF Clustering technique the NU and FU are grouped in a cluster. Within the cluster NOMA principle is employed, i.e. only among the users in the respective cluster.

c) Downlink 1x3 PD-NOMA FF Clustering system.

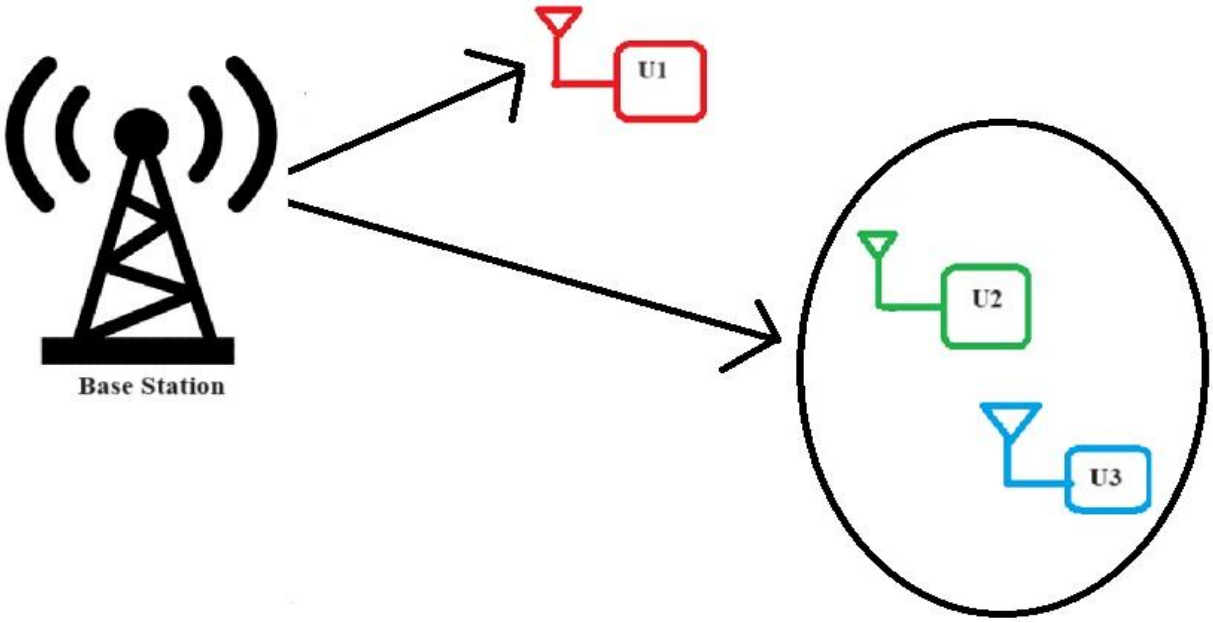


Fig 4.3: Illustration of Downlink 1x3 PD-NOMA system model with FF Clustering

Fig 4.3 represents a 1x3 PD-NOMA system in a Downlink scenario, where there is a single base station that communicates with 3 users at the receiver end. At the receiver end 2 users are grouped in a cluster based on the power allocation coefficients of the users. U1 is situated at the smallest distance from the BS, U3 is located at the farthest distance from the BS and U2 is located between U1 and U3. So, U1 is called NU, U2 is called IU and U3 is called FU. At the BS, as per the NOMA principle, the signals of different users are allocated different fraction of the total power. The NU is given the least fraction of power, and the FU is given highest fraction of power. So, the power allocation order of the users are as follows: $P_1<P_2<P_3$. In FF Clustering technique the Intermediary and FUs are grouped in a cluster. Within the cluster NOMA principle is employed, i.e. only among the users in the respective cluster.

We have increased the number of users up to 16 users at the receiver side and analyzed their performance with the NOMA systems and (1x3) NOMA system with Cluster. We have analyzed the performances of (1x4), (1x8) and (1x16) Downlink PD NOMA clustering systems.

d) Downlink 1x4 PD-NOMA NN Clustering system.

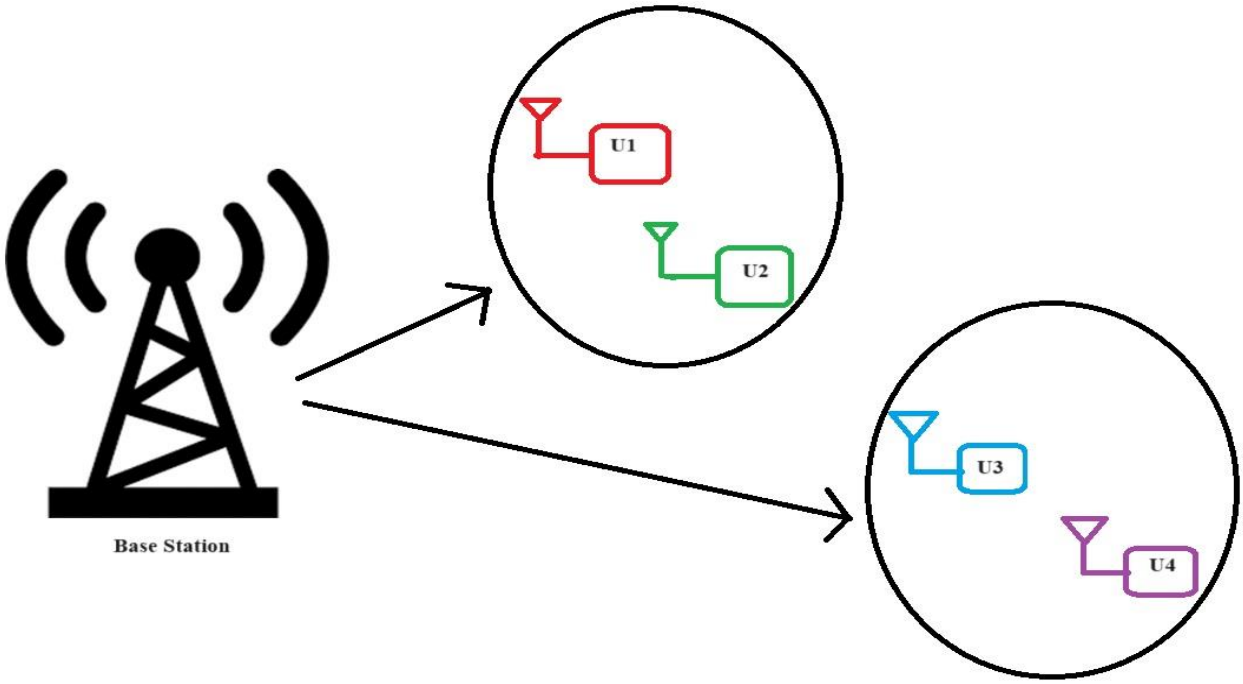


Fig 4.4: Illustration of Downlink 1x4 PD-NOMA system model with NN Clustering

Fig 4.4 represents a 1x4 PD-NOMA system in a Downlink scenario, where there is a single base station that communicates with 4 users at the receiver end. At the receiver end 2 users are grouped in a cluster based on the power allocation coefficients of the users. U1 is situated at the smallest distance from the BS, U4 is located at the farthest distance from the BS and U2 and U3 are located between U1 and U4. So, U1 is called NU, U2, U3 are called IUs and U4 is called FU. At the BS, as per the NOMA principle, the signals of different users are allocated different fraction of the total power. The NU is given the least fraction of power, and the FU is given highest fraction of power. So, the power allocation order of the users are as follows: $P_1<P_2<P_3<P_4$. In NN Clustering technique 2 nearest users from the BS are grouped together in a Cluster and the rest two users are grouped in another cluster. Within the cluster NOMA principle is employed, i.e. only among the users in the respective cluster.

e) Downlink 1x4 PD-NOMA NF Clustering system.

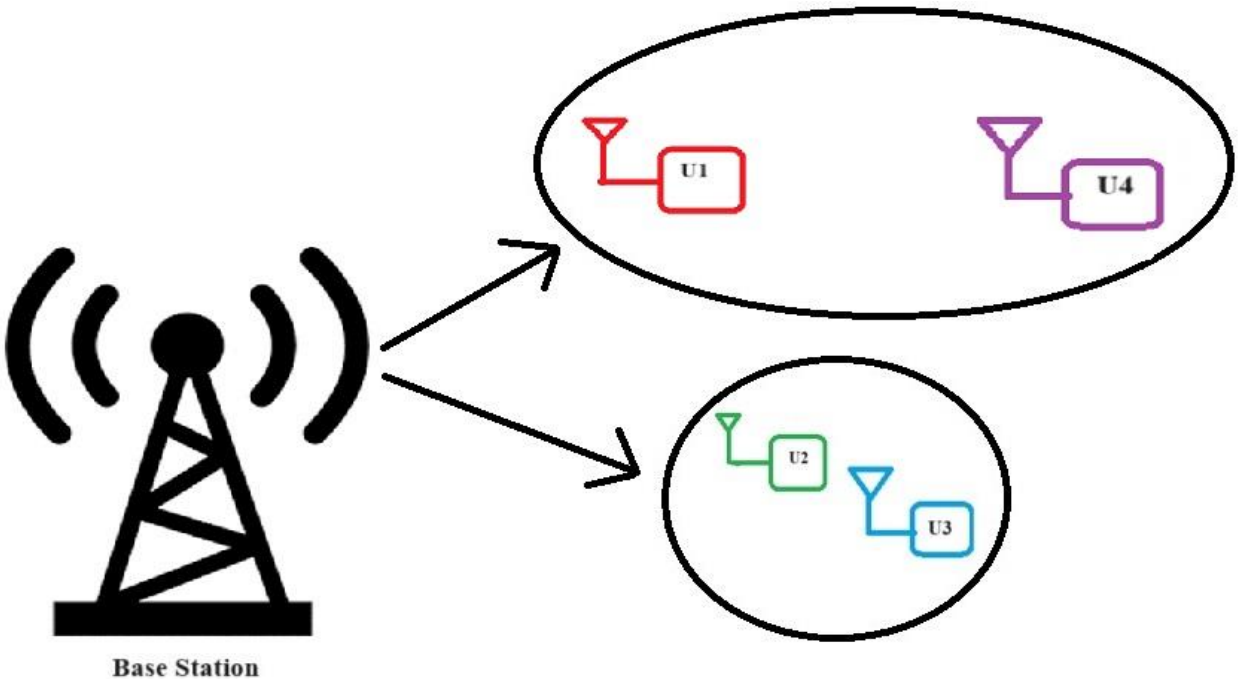


Fig 4.5: Illustration of Downlink 1x4 PD-NOMA system model with NF Clustering

Fig 4.5 represents a 1x4 PD-NOMA system in a Downlink scenario, where there is a single base station that communicates with 4 users at the receiver end. At the receiver end 2 users are grouped in a cluster based on the power allocation coefficients of the users. U1 is situated at the smallest distance from the BS, U4 is located at the farthest distance from the BS and U2 and U3 are located between U1 and U4. So, U1 is called NU, U2, U3 are called IUs and U4 is called FU. At the BS, as per the NOMA principle, the signals of different users are allocated different fraction of the total power. The NU is given the least fraction of power, and the FU is given highest fraction of power. So, the power allocation order of the users are as follows: $P_1<P_2<P_3<P_4$. In NF Clustering technique the NU and FU from the BS are grouped together in a Cluster and the rest two users are grouped in another cluster. Within the cluster NOMA principle is employed, i.e. only among the users in the respective cluster.

f) Downlink 1x8 PD-NOMA NN Clustering system.

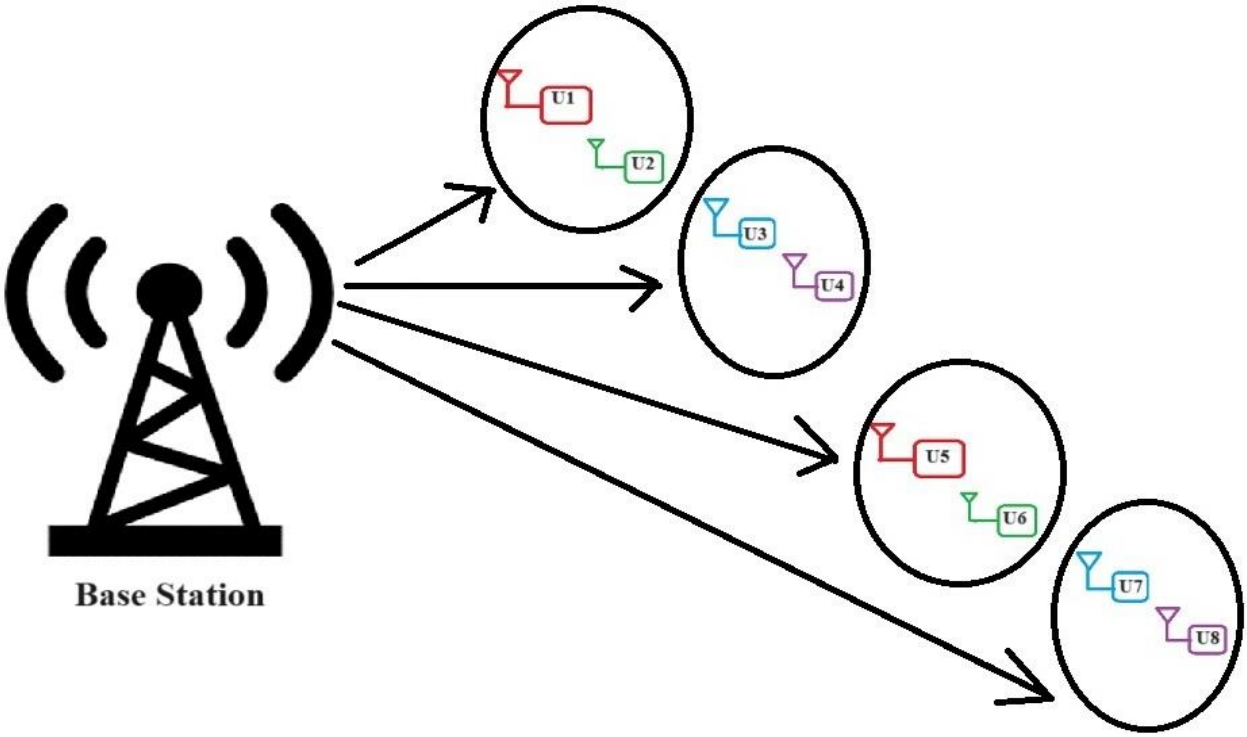


Fig 4.6: Illustration of Downlink 1x8 PD-NOMA system model with NN Clustering

Fig 4.6 represents a 1x8 PD-NOMA system in a Downlink scenario, where there is a single base station that communicates with 8 users at the receiver end. At the receiver end 2 users are grouped into clusters based on the power allocation coefficients of the users. U1 is situated at the smallest distance from the BS, U8 is located at the farthest distance from the BS and other users are located between U1 and U8. So, U1 is called NU, and U8 is called FU. At the BS, as per the NOMA principle, the signals of different users are allocated different fraction of the total power. The NU is given the least fraction of power, and the FU is given highest fraction of power. So, the power allocation order of the users are as follows: $P_1<P_2<P_3<P_4$ $P_5<P_6<P_7<P_8$. In NN Clustering technique a total of 4 clusters have been formed, each cluster contains 2 users as shown in Fig 4.6. Within each cluster NOMA principle is employed, i.e. only among the users in the respective cluster.

g) Downlink 1x8 PD-NOMA NF Clustering system.

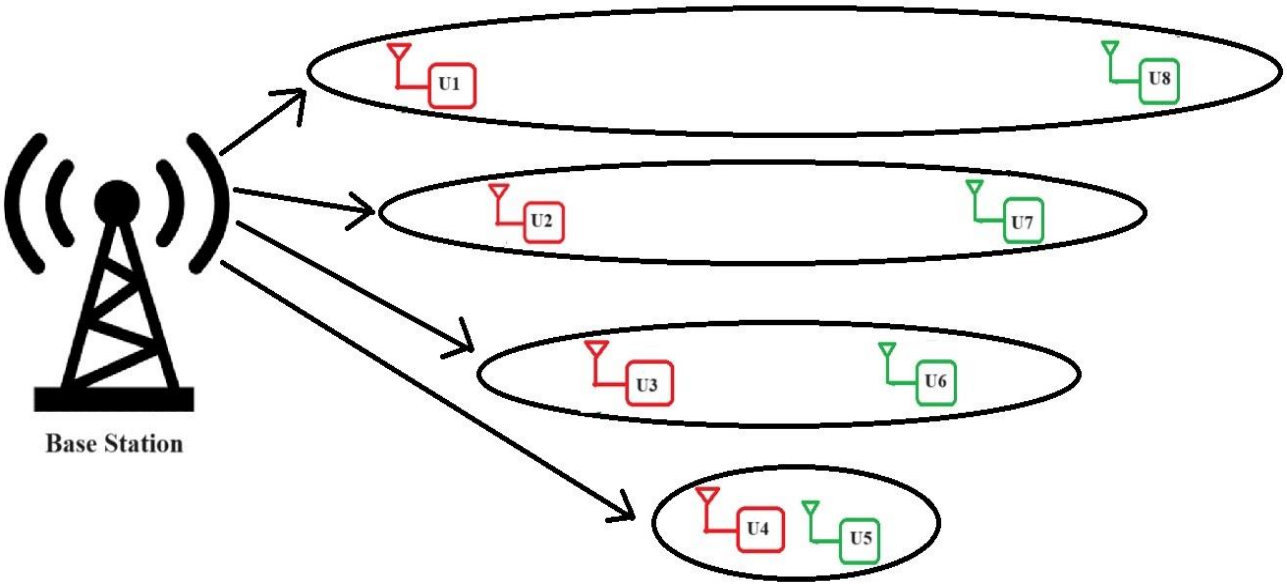


Fig 4.7: Illustration of Downlink 1x8 PD-NOMA system model with NF Clustering

Fig 4.7 represents a 1x8 PD-NOMA system in a Downlink scenario, where there is a single base station that communicates with 8 users at the receiver end. At the receiver end 2 users are grouped into clusters based on the power allocation coefficients of the users. U1 is situated at the smallest distance from the BS, U8 is located at the farthest distance from the BS and other users are located between U1 and U8. So, U1 is called NU, and U8 is called FU. At the BS, as per the NOMA principle, the signals of different users are allocated different fraction of the total power. The NU is given the least fraction of power, and the FU is given highest fraction of power. So, the power allocation order of the users are as follows: $P_1<P_2<P_3<P_4$ $P_5<P_6<P_7<P_8$. In NF Clustering technique a total of 4 clusters have been formed, each cluster contains 2 users as shown in Fig 4.7. Within each cluster NOMA principle is employed, i.e. only among the users in the respective cluster.

h) Downlink 1x16 PD-NOMA NN Clustering system.

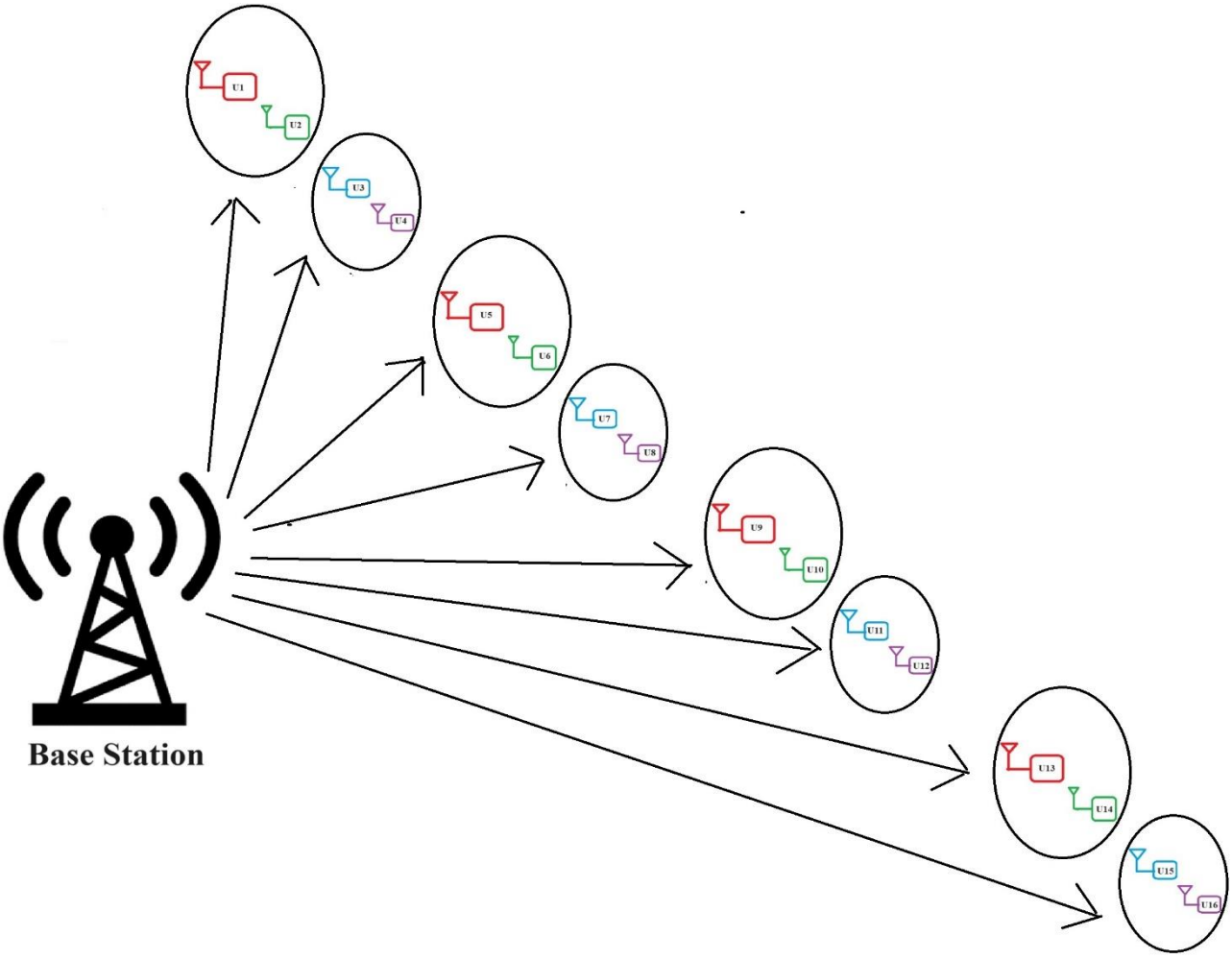


Fig 4.8: Illustration of Downlink 1x16 PD-NOMA system model with NN Clustering

Fig 4.8 represents a 1x16 PD-NOMA system in a Downlink scenario, where there is a single base station that communicates with 16 users at the receiver end. At the receiver end 2 users are grouped into clusters based on the power allocation coefficients of the users. U1 is situated at the smallest distance from the BS, U16 is located at the farthest distance from the BS and other users are located between U1 and U16. So, U1 is called NU, and U16 is called FU. At the BS, as per the NOMA principle, the signals of different users are allocated different fraction of the total power. The NU is given the least fraction of power, and the FU is given highest fraction of power. So, the power allocation order of the users are as follows: $P_1<P_2<P_3<P_4$ $P_5<P_6<P_7<P_8<$ $P_9<P_{10}<P_{11}<P_{12}$ $P_{13}<P_{14}<P_{15}<P_{16}$. In NN Clustering technique a total of 8 clusters have been formed, each cluster contains 2 users as shown in Fig 4.8. Within each cluster NOMA principle is employed, i.e. only among the users in the respective cluster.

i) Downlink 1x16 PD-NOMA NF Clustering system.

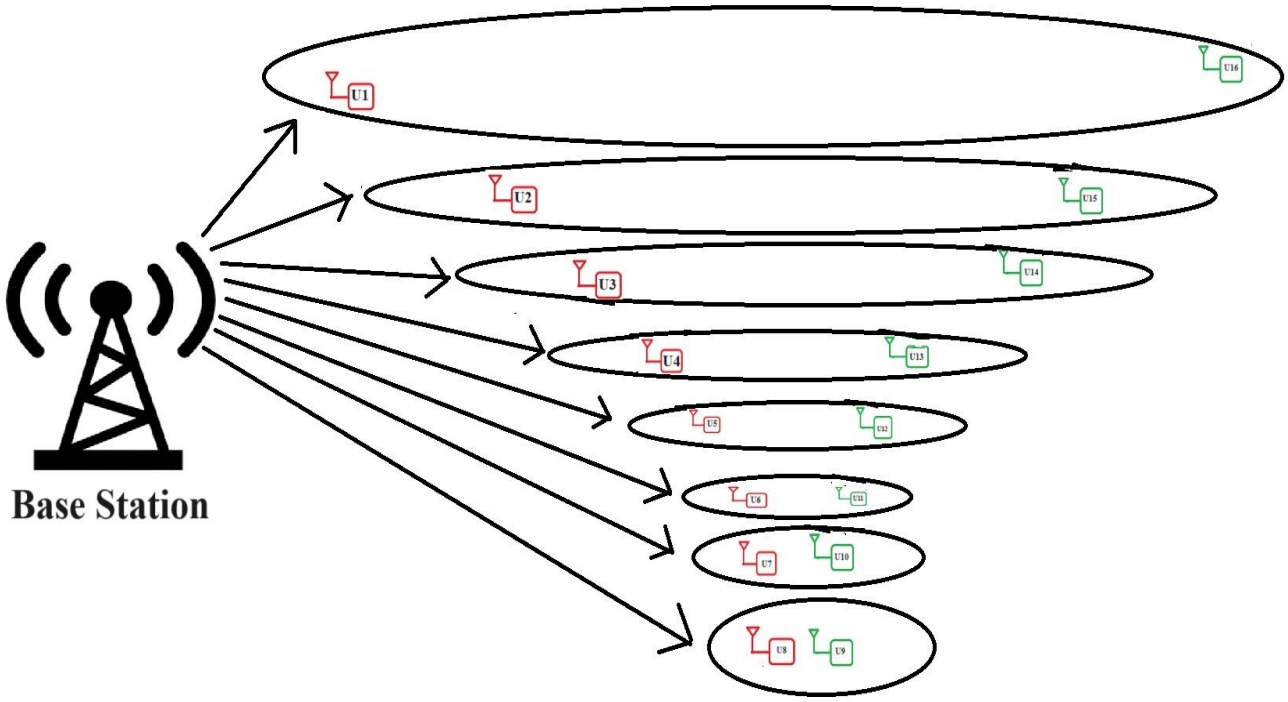


Fig 4.9: Illustration of Downlink 1x16 PD-NOMA system model with NF Clustering

Fig 4.9 represents a 1x16 PD-NOMA system in a Downlink scenario, where there is a single base station that communicates with 16 users at the receiver end. At the receiver end 2 users are grouped into clusters based on the power allocation coefficients of the users. U1 is situated at the smallest distance from the BS, U16 is located at the farthest distance from the BS and other users are located between U1 and U16. So, U1 is called NU, and U16 is called FU. At the BS, as per the NOMA principle, the signals of different users are allocated different fraction of the total power. The NU is given the least fraction of power, and the FU is given highest fraction of power. So, the power allocation order of the users are as follows: $P_1<P_2<P_3<P_4$ $P_5<P_6<P_7<P_8<$ $P_9<P_{10}<P_{11}<P_{12}$ $P_{13}<P_{14}<P_{15}<P_{16}$. In NF Clustering technique a total of 8 clusters have been formed, each cluster contains 2 users as shown in Fig 4.9. Within each cluster NOMA principle is employed, i.e. only among the users in the respective cluster.

4.3 Summary of the chapter:

This chapter gave us an overview of the NOMA Clustering technique and its necessity. We have covered three NOMA clustering techniques (Near-Near NOMA Clustering, Near-Far NOMA Clustering, and Far-Far NOMA Clustering) and their corresponding system models for varying number of users in downlink scenarios.

Chapter-5

WARP Hardware Setup:

5.1 Description of WARP V3 board:

Wireless Open Access Research Platform (WARP) is a scalable, extensible, and programmable wireless platform designed for wireless communication research and development. It is a transceiver board. WARP is developed by the RICE University research team and distributed by Mango Communication. The heart of a WARP node is the Xilinx FPGA which is located in the heart of the board provides all the node's processing resources. The WARP comprises of the FPGA boards along with clock and radio boards, WARPLAB repositories, OFDM Reference Designs, Medium Access Layer components, etc. It is able to operate in two frequency bands: 2.4 GHz and 5GHz.

Mango Communications WARP version 3 (WARP V3) is the latest generation of WARP hardware, integrating a high-performance FPGA, two flexible RF interfaces and multiple peripherals to facilitate rapid prototyping of custom wireless design. WARP V3 hardware runs the latest WARPLAB 7 reference design [82].

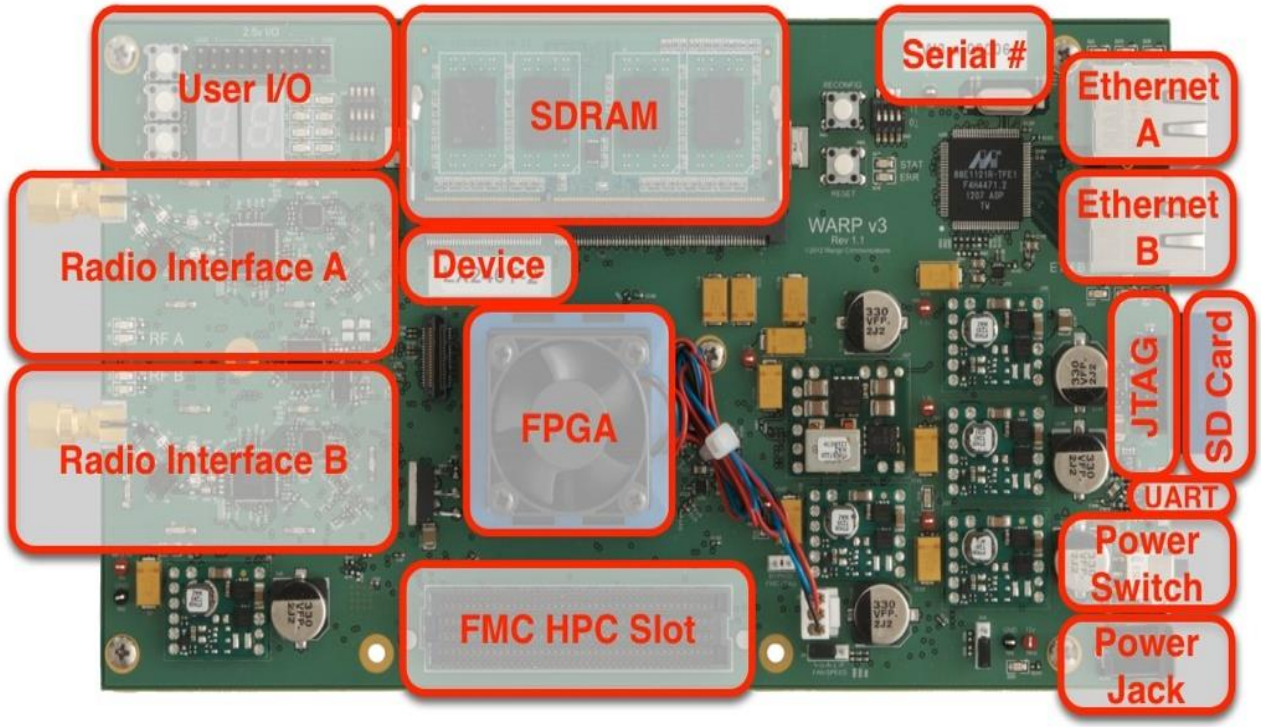


Fig 5.1: Hardware diagram of WARP [83]

5.1.1 Hardware components of WARP V3 Board:

The hardware features of WARP V3 are listed below [83].

i) **User I/O:** This collection of push buttons, LEDs, hexadecimal displays, dip switches, and debug header pins is used for interacting with the board. Designs can read values from the switches and push buttons and can write values to the displays and LEDs. The debug header can be used for any number of purposes, such as providing a convenient way for one WARP board to trigger the action of another board over a wire.

ii) **Radio Interfaces A & B:** These interfaces provide the radios that allow designs to communicate at the 2.4GHz and 5GHz bands. For each radio interface, digital I and Q values from the FPGA are taken through digital-to-analog converters and are delivered to the transceiver for upconversion (i.e. wireless transmission). Wireless reception follows the reciprocal process where I and Q analog streams are taken from the transceiver through analog-to-digital conversion and are then delivered to the FPGA. The interfaces are labeled as "RF A" and "RF B" on the board and in our reference designs.

iii) **SDRAM:** This DDR3 SO-DIMM provides extra memory beyond the block RAM inside the FPGA. The WARP v3 kit ships with a pre-tested 2GB SO-DIMM.

iv) **Device label:** This label shows the FPGA device on the WARP v3 board. This device is used in a number of places during the development process (such as exporting a peripheral core from Xilinx System Generator), so this label is present for convenient lookup.

v) **Virtex-6 FPGA:** Under the fan, the FPGA serves as the central processing system for the WARP board.

vi) **FMC HPC Slot:** The FPGA Mezzanine Card High Pin Count slot provides connectivity to an existing ecosystem of hardware as well as future WARP-specific modules.

vii) **Serial Number:** This is the unique serial number for the WARP board. This number is also programmed into an EEPROM on the board prior to shipping, allowing software running on the hardware to read this information.

viii) **Ethernet A/B:** The two 10/100/1000 Ethernet ports provide high-speed connectivity between the board and a wired network. The ports are labelled "ETH A" and "ETH B" on the WARP v3 board and in our reference designs.

ix) **JTAG:** The JTAG connector allows direct programming of the Virtex-6 FPGA using a Digilent or Xilinx JTAG cable.

x) **SD Card:** An alternative to programming the board over JTAG is to use the SD card. This allows non-volatile storage of programs that will automatically download and execute upon insertion of the SD card.

xi) **UART:** The micro-USB connector on the board allows programs on the board to print messages to a terminal running on a computer.

xii) **Power Switch:** The power switch controls power to the board. The "off" position is where the switch is furthest away from the power jack. The "on" position is where the switch is closest to the power jack.

xiii) **Power Jack:** The power jack is where the 12V power supply that comes with the WARP hardware should be plugged in. It is important to note that the power switch should be in the "off" position whenever the power plug is inserted or removed. This allows the circuitry controlled by the switch to properly sequence the power regulators on the board.

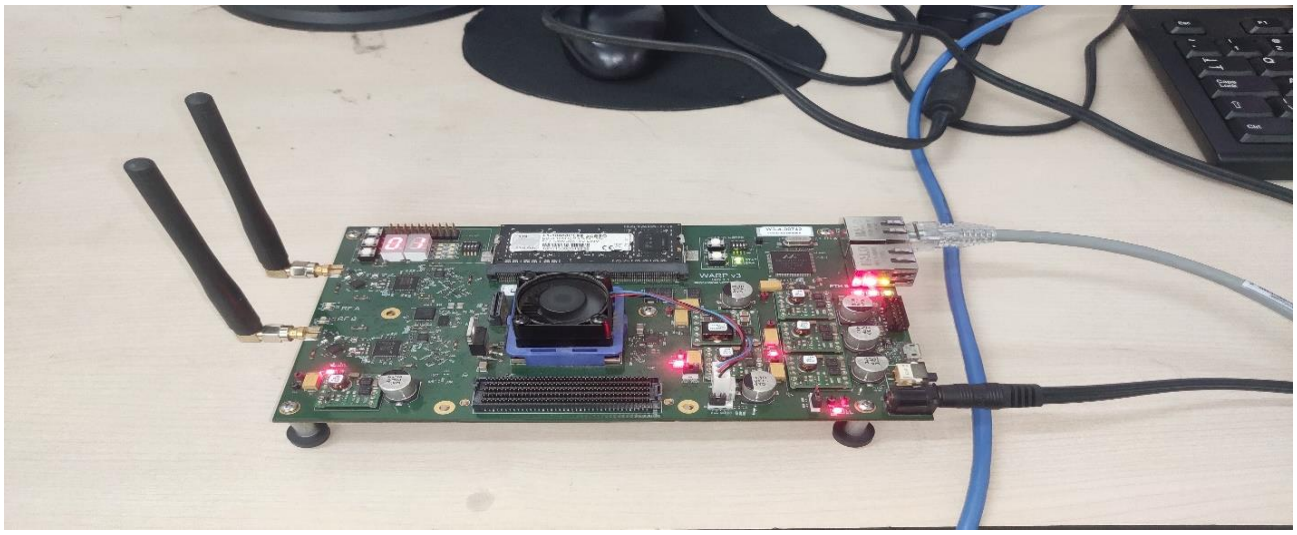


Fig 5.2: Figure of WARP V3 board

5.1.2 Integration of WARP Hardware with WARPLab Framework:

In order to integrate the MATLAB software with WARP board, WARP makes use of the WARPLab framework. The implementation of the WARPLab framework is represented by the WARPLab reference design [84]. This reference design offers a high-level flexibility and adaptability by integrating MATLAB and FPGA implementations of WARPLab framework modules. The WARPLab framework includes the necessary software components to facilitate convenient interaction with WARP nodes directly from the MATLAB workspace.

Hardware Requirements:

- For WARP V3 hardware, the version of WARPLab used is WARPLab 7.

- For 2-radio WARPLab reference design, WARP V3 board uses the RF interfaces those are present in the board.
- For 4-radio WARPLab reference design, a FMC-RF-2X245 radio FMC module must be connected with the WARP Board, to provide two more RF interfaces, with the RF interfaces present in the board.

Software Requirements:

- MATLAB 2014a.

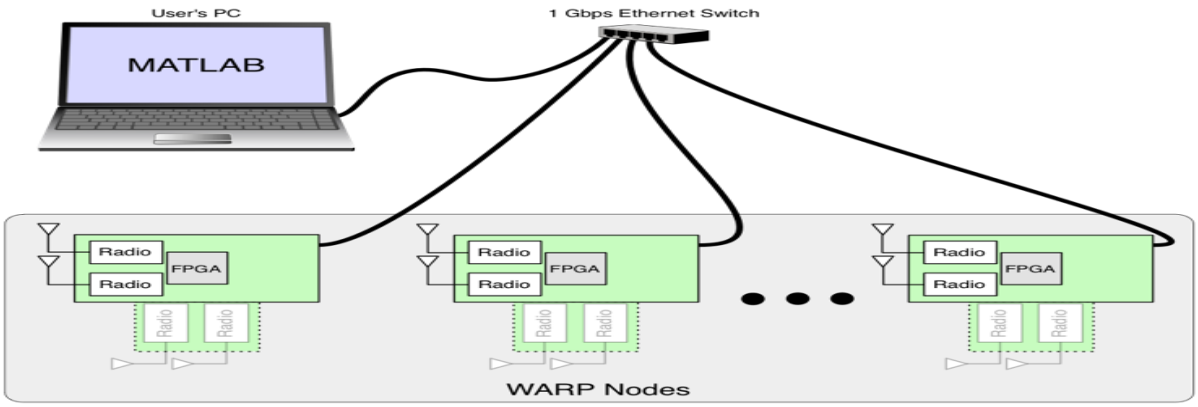


Fig 5.3: Experimental setup using WARP [84]

5.2 Transmitter Receiver Block Diagram:

The operations that have been implemented at transmitter and receiver side are shown in the block diagram below.

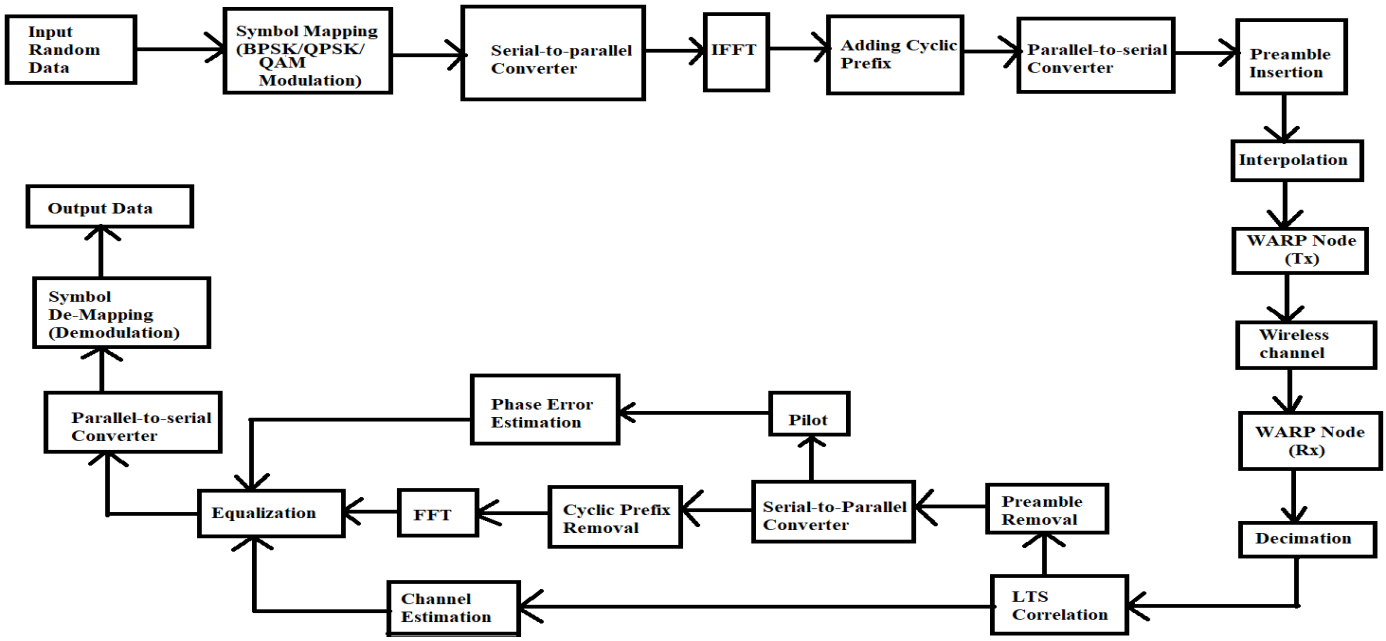


Fig 5.4: Transmitter Receiver Block diagram

Operations performed at the Transmitter Side:

- Input random data is generated. The transmit data bit is modulated as per the modulation scheme used (BPSK/QPSK/QAM). Then Superposition Coding (SC) technique is performed.
- Then, the serial-to-parallel converter block converts the entire data sequence into a matrix of size (N_{data} x N_{sym}), where N_{data} is the number of data subcarrier, while N_{sym} refers to the total number of OFDM symbols per subcarrier that will be transmitted in a single transmission. In our work we have used 64 sub-carriers, out of which 48 sub-carriers are used as data subcarriers, 4 sub-carriers for pilots.
- Then, insert the data symbols and pilots to the corresponding data and pilot subcarrier respectively and apply the whole sequence to the IFFT block, where 64-point IFFT is performed. Cyclic Prefix is added to each OFDM symbol.
- After addition of Cyclic Prefix, the output of IFFT block is transformed into serial form by parallel-to-serial converter.
- To estimate the channel, a preamble is added at the beginning of overall OFDM frame. The preamble contains two training sequences: Long Training Sequence (LTS) and Short Training Sequence (STS). Then to increase the sample rate, the signal is subjected to Interpolation process. The Interpolation process involves Up-sampling and Low-Pass Filter (LPF). The whole signal is multiplied with precoding matrix if Precoding technique is applied at the transmitter side. Then the signal is transmitted through all the transmitting antennas to the channel.

Operations performed at the Receiver Side:

- After receiving the received signal, the signal is multiplied with Post Coding matrix, as per applied precoding scheme. Then the signal is decimated. The Decimation process includes Low-Pass filter and down-sampling.
- Then, the received signal is cross correlated with the LTS reference sequence. The cross-correlation process is performed to estimate the start of each frame.
- The next step is the removal of cyclic prefix for each OFDM symbol, after which 64-point FFT is performed.
- The FFT process is followed by Doppler frequency estimation and correction.
- The effects of the channel impairments the signal experienced during channel transmission are then countered by applying equalization.
- Finally, the data symbols are converted to the respective bit sequence, through the process of de-mapping (Demodulation) as per applied modulation scheme.

5.2.1 CFO, Phase Error and SFO:

Generally, a transmitter and receiver are each clocked independently, therefore resulting to three distinct degradation issues that must be corrected at the receiving end. These are as follows [85]:

i. **Carrier Frequency Offset (CFO):** The center frequency of the transmitter will not perfectly match the center frequency of the receiver. The difference in frequency between the transmitter and the receiver in a communication system is referred to as Carrier Frequency Offset (CFO). This can result in a frequency offset. This offset can cause the received signal to deviate from its intended frequency, leading to distortion and degradation in the signal quality. It will de-orthogonalize the OFDM subcarriers and cause inter-carrier interference (ICI). CFO is typically corrected in the time domain via multiplication with a digital carrier whose frequency negates the CFO estimate.

ii. **Phase Error:** Even after CFO is corrected in the time domain, there is typically a residual phase error component that must be corrected in the frequency domain and tracked over time. OFDM systems employ multiple pilot subcarriers to enable this correction system. These pilot subcarriers contain known reference signals. All data subcarriers in each OFDM symbol are phase-rotated to match any residual rotation observed in the known pilot subcarriers. By applying this phase correction, the receiver ensures that the data subcarriers maintain the correct phase relationship, compensating for any residual rotation that may have occurred during transmission.

iii. **Sampling Frequency Offset (SFO):** The presence of different sampling clocks at transmitter and receiver side causes the temporal duration of a sample to vary slightly between them. As a result, over time, the relative sample periods of samples will drift apart from each other during reception. This drift introduces large phase errors. To address this issue, each data subcarrier within each OFDM symbol undergoes a unique phase rotation based on its subcarrier index.

5.3 Components required to perform the experiments:

1) One WARP V3 board,
2) 12V DC power supply,
3) One FPGA Mezzanine Card (FMC) Slot that is used to provide more number of antennas,
4) 4 Antennas,
5) Ethernet cable for connecting WARP board with computer,
6) JTAG Cable,
7) Network Switch,
8) iMPACT Software,
9) MATLAB 2014a Software.

5.3.1 Experimental setup and steps for performing the experiments:

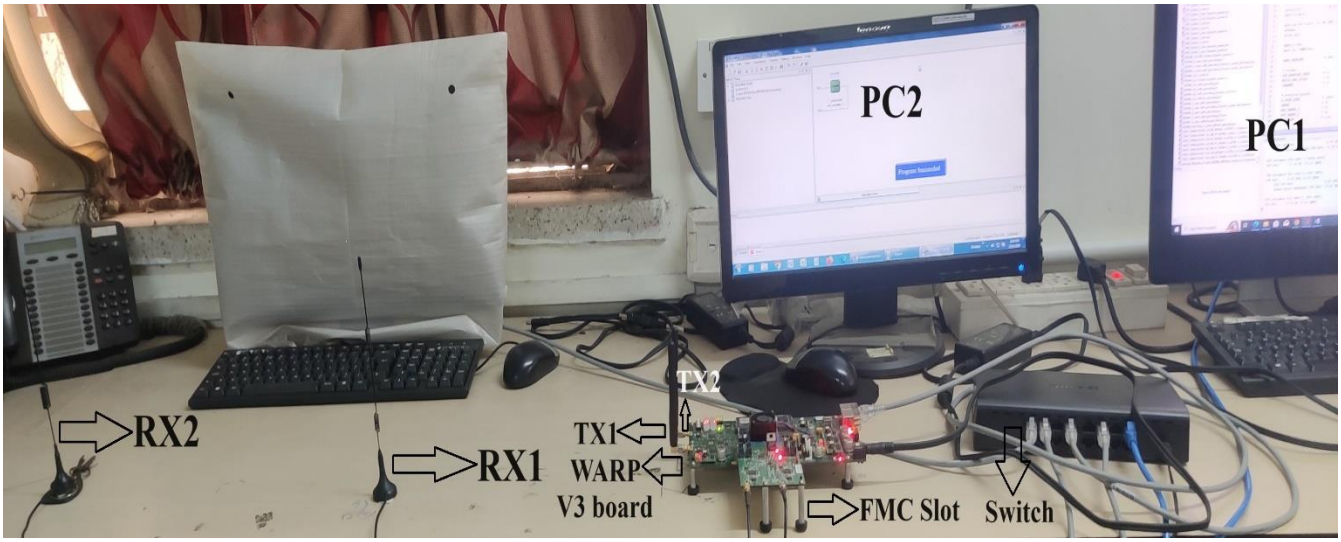


Fig 5.5: Experimental setup for (2x2) PD-NOMA system

Fig 5.5 shows the setup required for implementing Downlink (2x2) PD-NOMA system using WARP V3 board. Here, TX1 and TX2 are 2 transmitter antennas located at base station. Antennas RX1 and RX2 are two receiver antennas located at the receiver side. Antenna RX1 is located at the smallest distance from the base station, whereas RX2 is located at farthest distance from the base station. So, RX1 is termed as **Near User** and RX2 is termed as **Far User**. PC2 is used to program the WARP board, for which iMPACT software is required and PC1 is used for writing MATLAB code.

5.3.2 Steps required for performing the Experiments:

1. First connect the FMC slot and 4 antennas to the WARP board.
2. Connect the Ethernet cable from the Switch to the Ethernet port of the board.
3. Connect the power jack to the power port of the board and toggle the switch to ON position.
4. Connect the JTAG cable to the JTAG connector of the board from the CPU of PC2, where the iMPACT software is present.
5. Open the iMPACT software in the PC2 and select the "**Boundary Scan**" option, right click on the screen, and select "**Initialize Chain**" option.
6. Click on the "**Bitstream Reference**" option. Under "**Bitstream Reference**" option select 4RF option if 4 RF nodes have been used. If 2RF nodes have been used, then select 2RF option. In our work we as 4RF nodes have been used, we have selected 4RF option.
7. Again right click on the screen and select "**Program**" option to program the board.
8. Finally, JTAG is disconnected, and iMPACT software is closed after "**Program Succeeded**" is shown on the screen of the computer.

9. All these devices i.e. PC1, PC2 and WARP board are connected with one another via the network switch.
10. Then, open the MATLAB software is opened in PC1 to run the program using the WARP V3 board, based on the respective experiment, through the switch.

Table 5.1 illustrates the parameters used for implementing (2x2) PD-NOMA Experiment:

Table 5.1: Parameters for (2x2) PD-NOMA

PARAMETERS	VALUES
Transmitter Power	1 Watt
Number of Transmitter antenna at Base Station	2
Number of Users at Receiver end	2
Number of OFDM symbols	1000
Number of OFDM Subcarriers	64
Cyclic Prefix Length	16
Power Allocation Coefficient for NU when employing FPA	0.27
Power Allocation Coefficient for FU when employing FPA	0.73
Target Capacity when employing Dynamic Power Allocation (DPA)	10^8 bps
Modulation Techniques used	i)BPSK, QPSK,16 QAM, 64 QAM modulation schemes for both NU and FU, ii)Adaptive modulation scheme, i.e., QPSK modulation scheme for NU and BPSK for FU.
Bandwidth	80 MHz

Table 5.2 illustrates the parameters used for implementing (1x2) PD-NOMA Experiment:

Table 5.2: Parameters for (1x2) PD-NOMA

PARAMETERS	VALUES
Transmitter Power	1 Watt
Number of Transmitter antenna at Base Station	1
Number of Users at Receiver end	2
Number of OFDM symbols	1000
Number of OFDM Subcarriers	64
Cyclic Prefix Length	16
Power Allocation Coefficient for NU when employing FPA	0.27
Power Allocation Coefficient for FU when employing FPA	0.73
Target Capacity when employing Dynamic Power Allocation (DPA)	10^8 bps
Modulation Techniques used	i)BPSK, QPSK,16 QAM, 64 QAM modulation schemes for both NU and FU, ii) Adaptive modulation scheme, i.e., QPSK modulation scheme for NU and BPSK for FU.
Bandwidth	80 MHz

Table 5.3 illustrates the parameters used for implementing (1x3) PD-NOMA with and without Clustering Experiment:

Table 5.3: Parameters for (1x3) PD-NOMA

PARAMETERS	VALUES
Transmitter Power	1 Watt
Number of Transmitter antenna at Base Station	1
Number of Users at Receiver end	3
Number of OFDM symbols	1000
Number of OFDM Subcarriers	64
Cyclic Prefix Length	16
Power Allocation Coefficient for NU when employing FPA	0.05
Power Allocation Coefficient for IU when employing FPA	0.20
Power Allocation Coefficient for FU when employing FPA	0.75
Target Capacity when employing Dynamic Power Allocation (DPA)	10^8 bps
Modulation Techniques used	i)BPSK, QPSK,16 QAM, 64 QAM modulation schemes for all users, ii) Adaptive modulation scheme, i.e., QPSK modulation scheme for NU and BPSK for IU and 16 QAM for FU.
Bandwidth	80 MHz

5.4 Experimental Results:

I. Constellation diagram of Downlink (2x2) PD-NOMA system with and without Precoding, for different Power Allocation Scheme and for different modulation techniques:

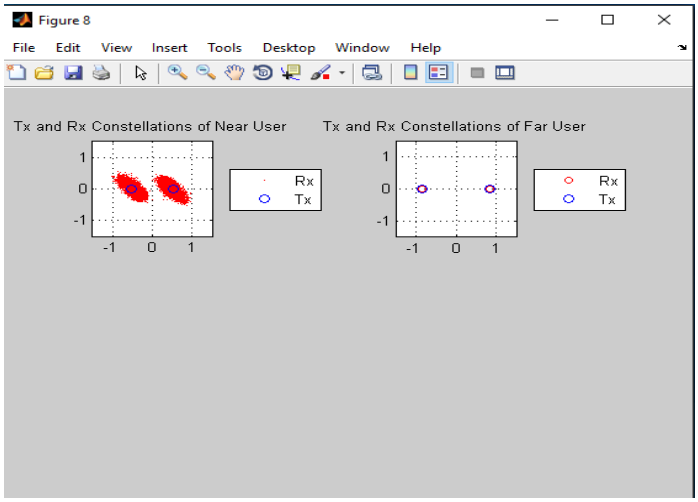


Fig 5.6: Constellation Diagram of (2x2) NOMA for BPSK modulation without Precoding employing FPA

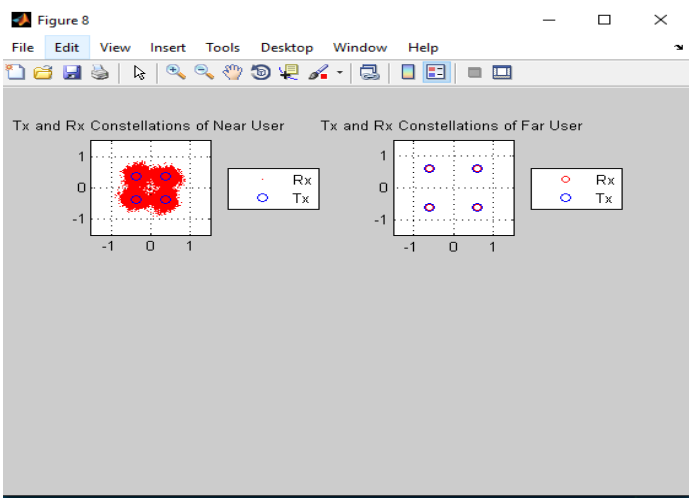


Fig 5.7: Constellation Diagram of (2x2) NOMA for QPSK modulation without Precoding employing FPA

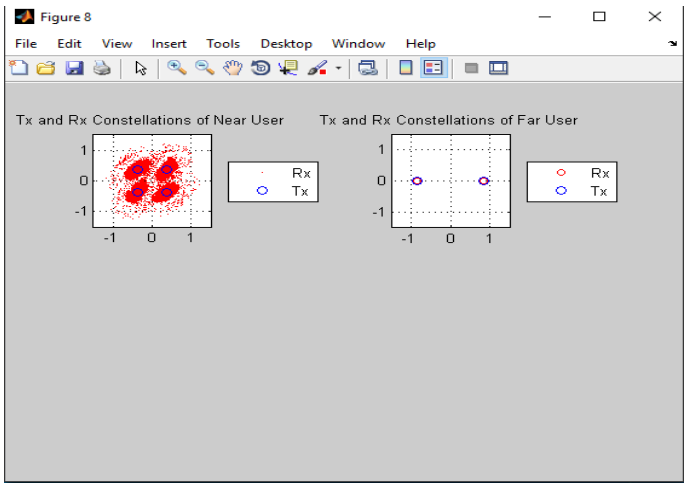


Fig 5.8: Constellation Diagram of (2x2) NOMA for Adaptive modulation without Precoding employing FPA

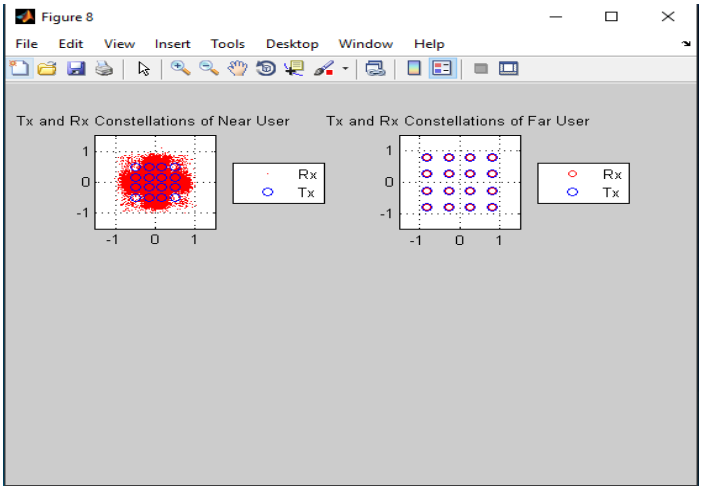


Fig 5.9: Constellation Diagram of (2x2) NOMA for 16 QAM modulation without Precoding employing FPA

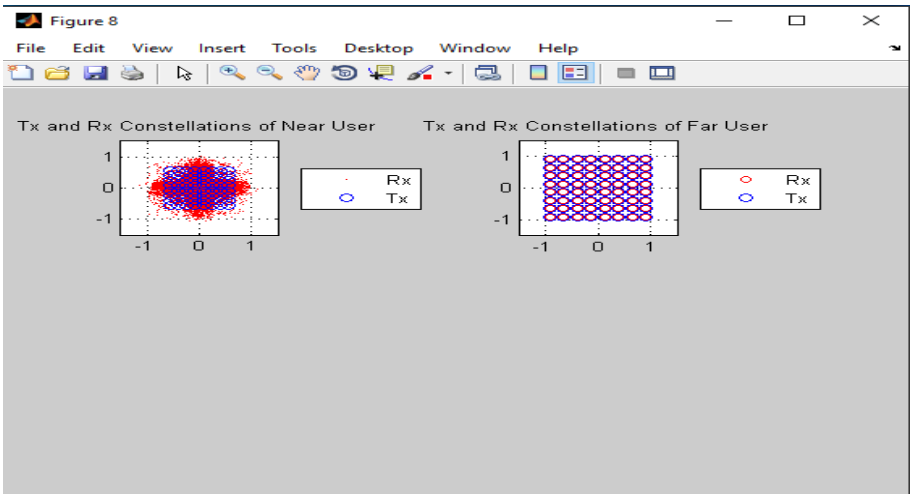


Fig 5.10: Constellation Diagram of (2x2) NOMA for 64 QAM modulation without Precoding employing FPA

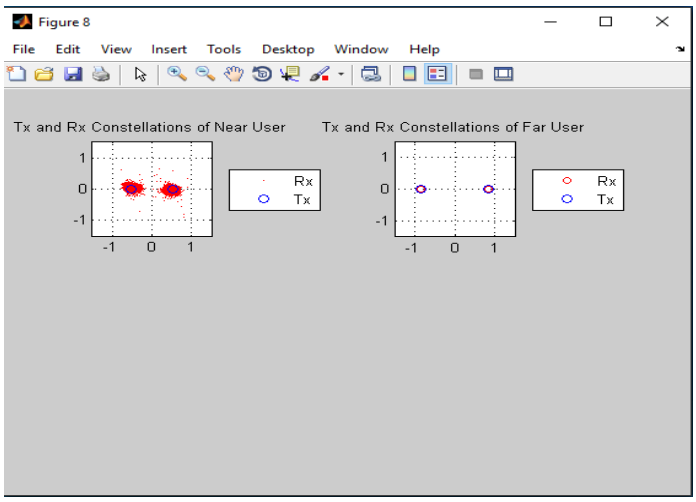


Fig 5.11: Constellation Diagram of (2x2) NOMA for BPSK modulation with SVD Precoding employing FPA

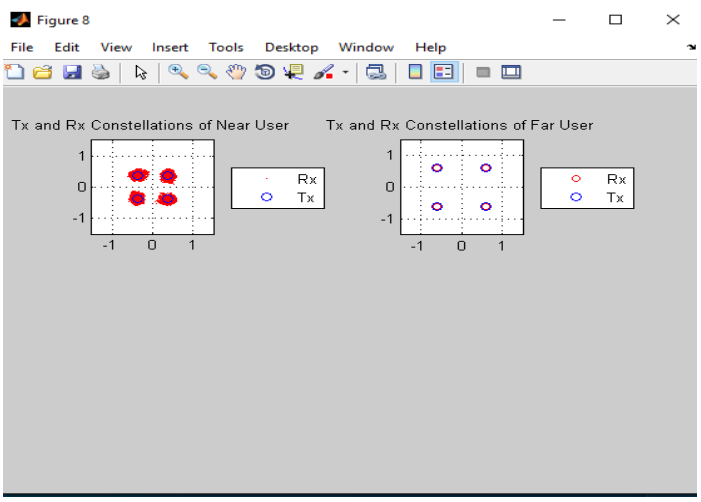


Fig 5.12: Constellation Diagram of (2x2) NOMA for QPSK modulation with SVD Precoding employing FPA

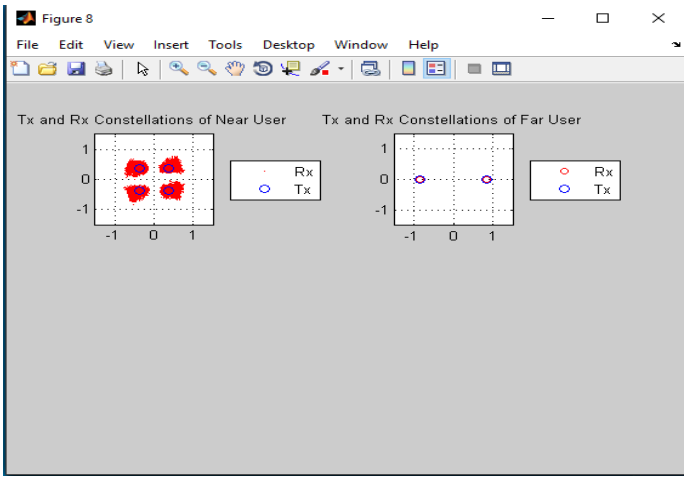


Fig 5.13: Constellation Diagram of (2x2) NOMA for Adaptive modulation with SVD Precoding employing FPA

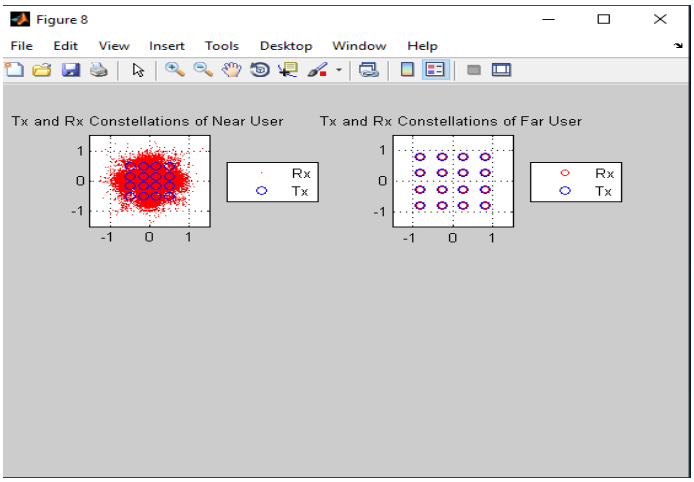


Fig 5.14: Constellation Diagram of (2x2) NOMA for 16 QAM modulation with SVD Precoding employing FPA

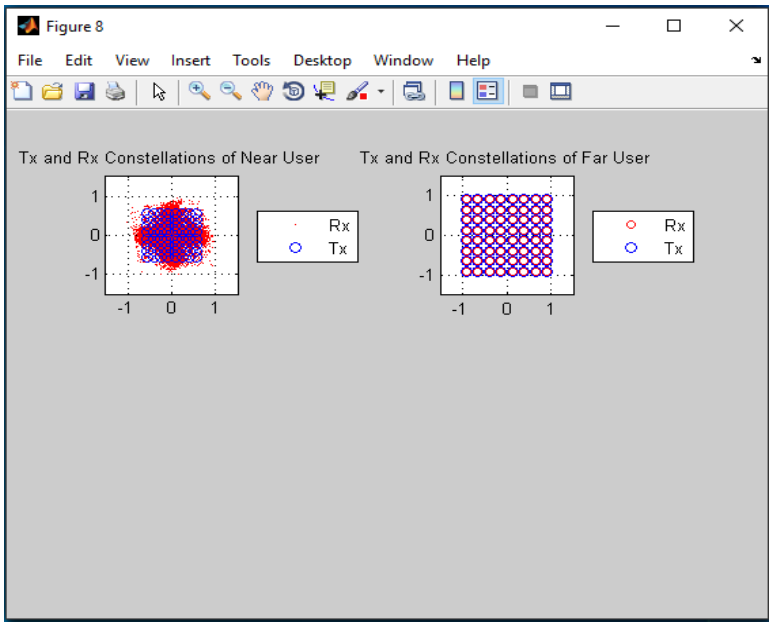


Fig 5.15: Constellation Diagram of (2x2) NOMA for 64 QAM modulation with SVD Precoding employing FPA

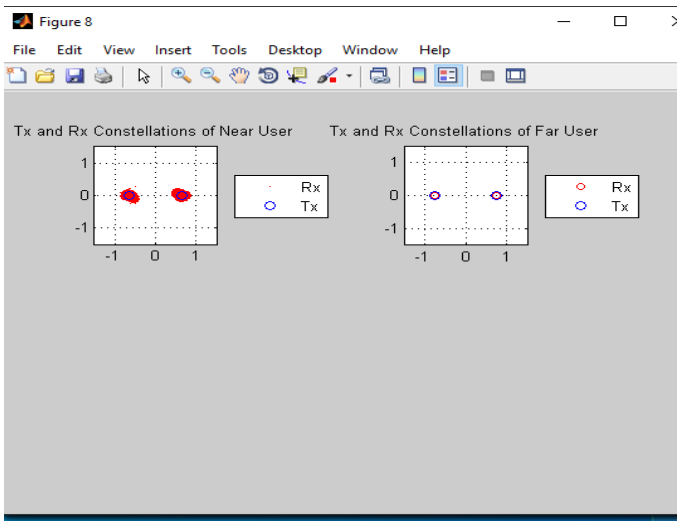


Fig 5.16: Constellation Diagram of (2x2) NOMA for BPSK modulation with SVD Precoding employing DPA

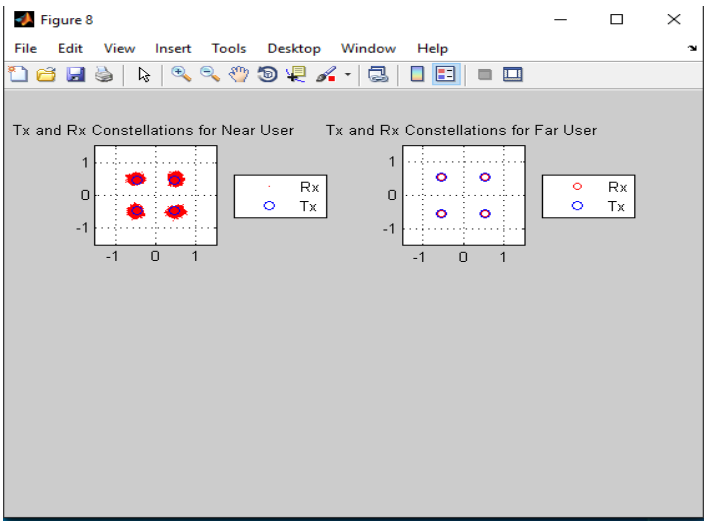


Fig 5.17: Constellation Diagram of (2x2) NOMA for QPSK modulation with SVD Precoding employing DPA

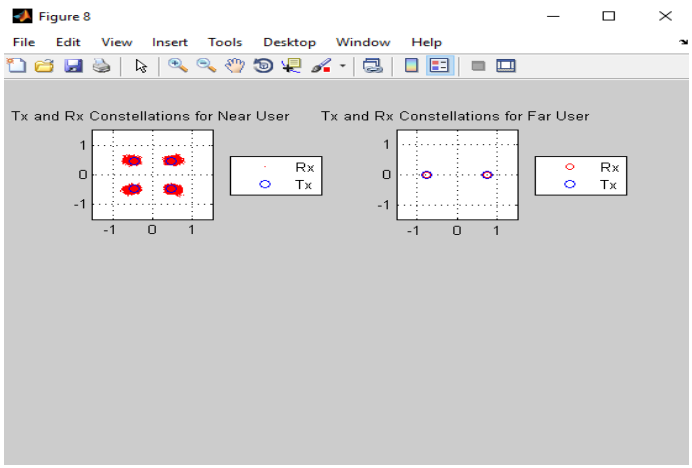


Fig 5.18: Constellation Diagram of (2x2) NOMA for Adaptive modulation with SVD Precoding employing DPA

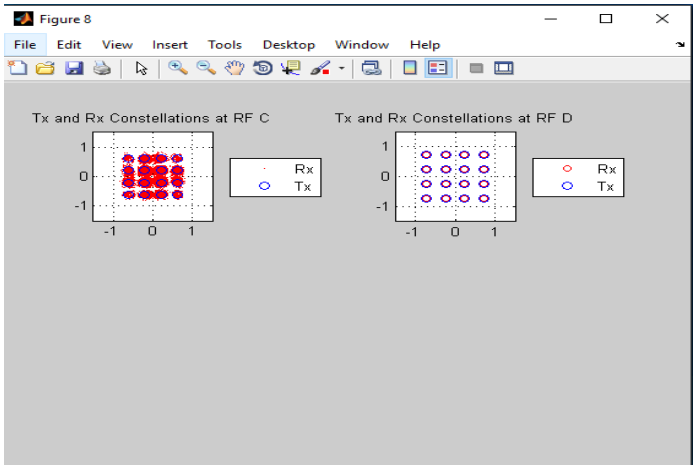


Fig 5.19: Constellation Diagram of (2x2) NOMA for 16 QAM modulation with SVD Precoding employing DPA

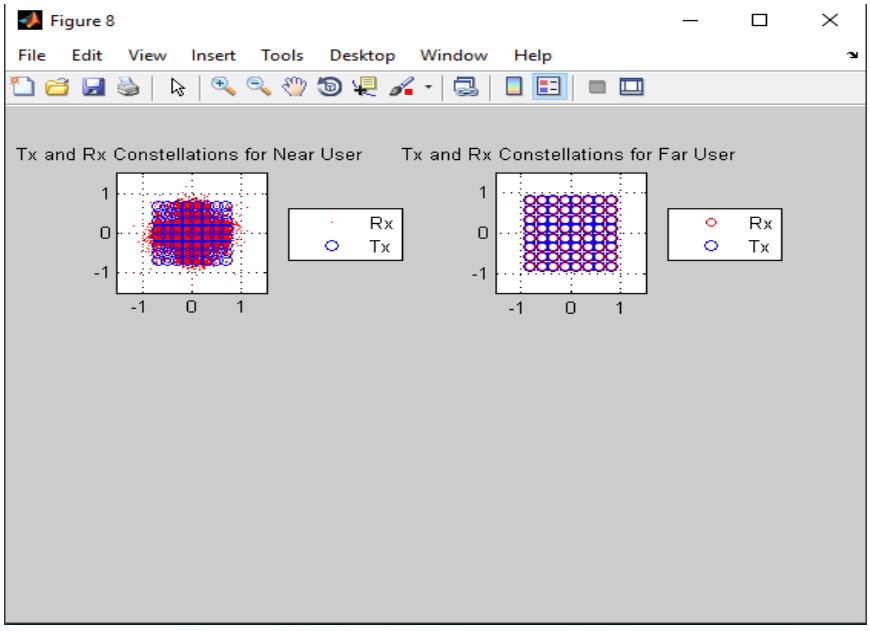


Fig 5.20: Constellation Diagram of (2x2) NOMA for 64 QAM modulation with SVD Precoding employing DPA

Fig 5.6, Fig 5.7, Fig 5.8, Fig 5.9, and Fig 5.10 represent the Constellation diagram of Downlink (2x2) PD-NOMA system for different modulation techniques, without using Precoding technique and employing Fixed Power Allocation (FPA) scheme. Left side of each figure represents the Constellation diagram of NU and right side represents Constellation diagram of FU. From the figures we can see that in case of BPSK modulation each received symbols can be distinguished in the Constellation diagram corresponding to each transmitted symbols. But in case of QPSK, Adaptive modulation, 16 QAM and 64 QAM, received symbols of NU cannot be distinguished properly in the Constellation diagram corresponding to each transmitted symbols.

Fig 5.11, Fig 5.12, Fig 5.13, Fig 5.14, and Fig 5.15 represent the Constellation diagram of Downlink (2x2) PD-NOMA system for different modulation techniques, with SVD Precoding technique and employing Fixed Power Allocation (FPA) scheme. From the figures we can observe that in case of BPSK, QPSK and Adaptive modulation each received symbols can be distinguished in the Constellation diagram corresponding to each transmitted symbols. But in case of 16 QAM and 64 QAM, received symbols of NU cannot be distinguished properly in the Constellation diagram corresponding to each transmitted symbols. So, applying SVD Precoding technique provides better Constellation Diagram than without applying Precoding technique.

Fig 5.16, Fig 5.17, Fig 5.18, Fig 5.19, and Fig 5.20 represent the Constellation diagram of Downlink (2x2) PD-NOMA system for different modulation techniques, with SVD Precoding technique and employing Dynamic Power Allocation (DPA) scheme. From the figures we can observe that in almost every modulation schemes each received symbols can be distinguished in the Constellation diagram corresponding to each transmitted symbols.

For every cases, received symbols can be distinguished more accurately for FU than NU because FU performs direct decoding on the received signal while NU performs SIC to eliminate FU's signal before applying decoding and SIC can never be perfect and depends on the quality of the received signal.

So, SVD Precoding with Dynamic Power Allocation scheme provides the best Constellation Diagram among these three techniques.

II. Constellation diagram of Downlink (1x2) PD-NOMA system with and without Precoding for different Power Allocation Scheme, for different modulation techniques:

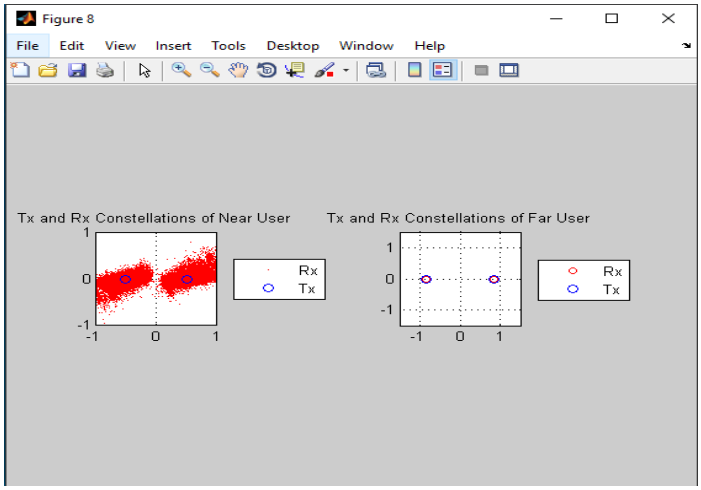


Fig 5.21: Constellation Diagram of (1x2) NOMA for BPSK modulation without Precoding employing FPA

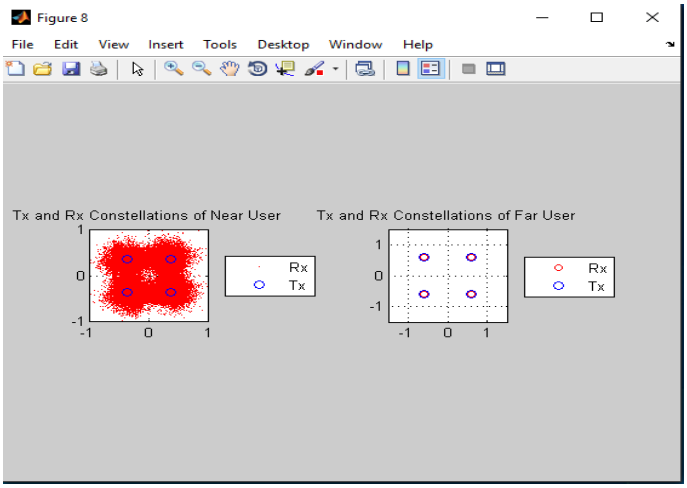


Fig 5.22: Constellation Diagram of (1x2) NOMA for QPSK modulation without Precoding employing FPA

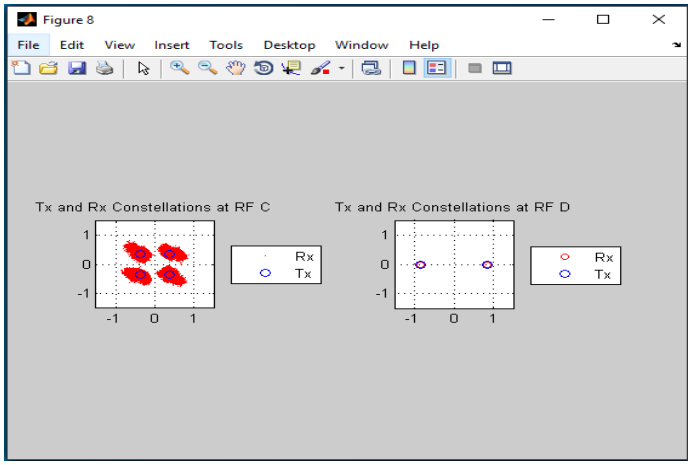


Fig 5.23: Constellation Diagram of (1x2) NOMA for Adaptive modulation without Precoding employing FPA

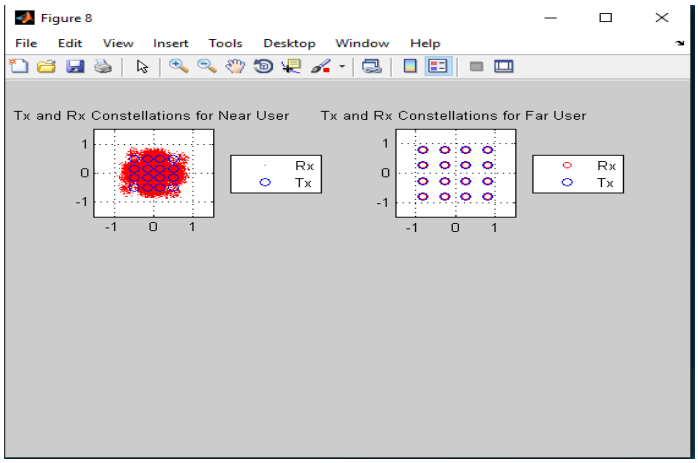


Fig 5.24: Constellation Diagram of (1x2) NOMA for 16 QAM modulation without Precoding employing FPA

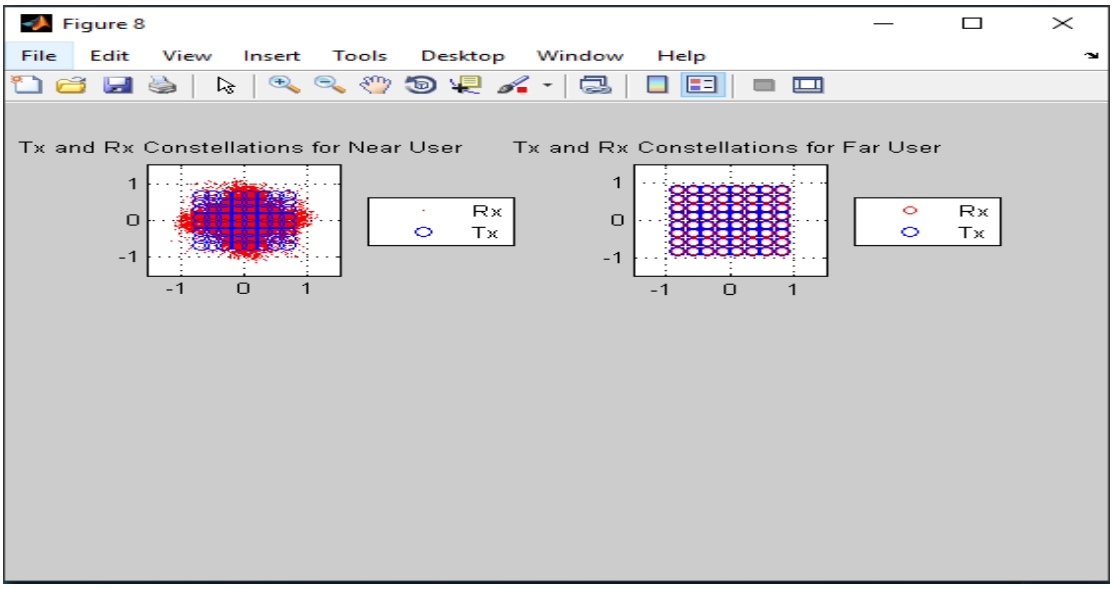


Fig 5.25: Constellation Diagram of (1x2) NOMA for 64 QAM modulation without Precoding employing FPA

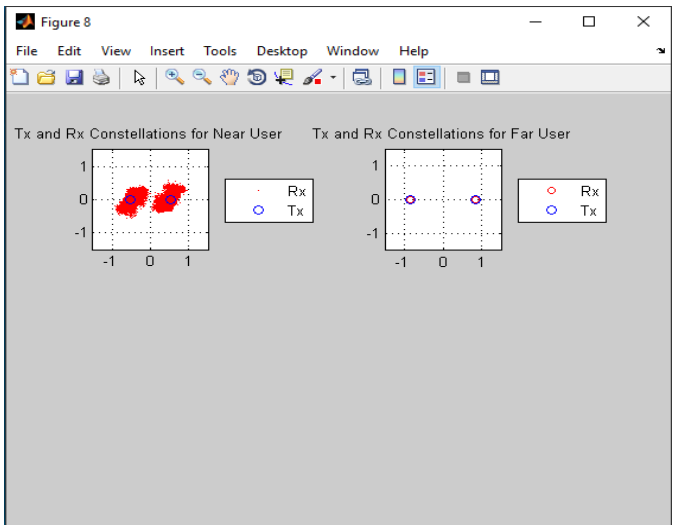


Fig 5.26: Constellation Diagram of (1x2) NOMA for BPSK modulation with SVD Precoding employing FPA

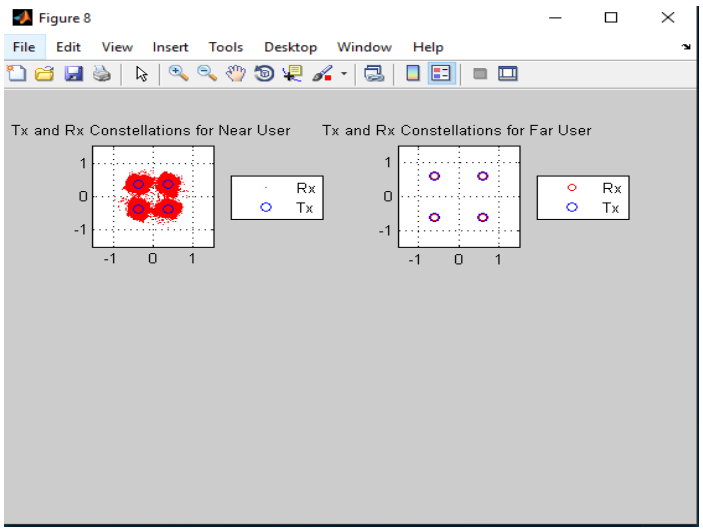


Fig 5.27: Constellation Diagram of (1x2) NOMA for QPSK modulation with SVD Precoding employing FPA

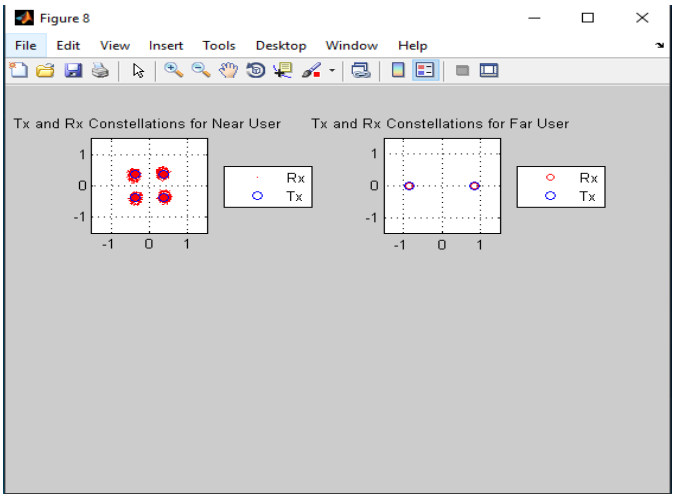


Fig 5.28: Constellation Diagram of (1x2) NOMA for Adaptive modulation with SVD Precoding employing FPA

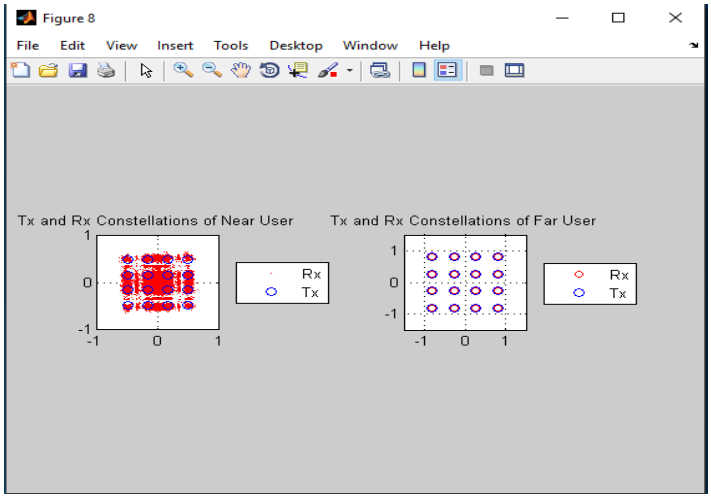


Fig 5.29: Constellation Diagram of (1x2) NOMA for 16 QAM modulation with SVD Precoding employing FPA

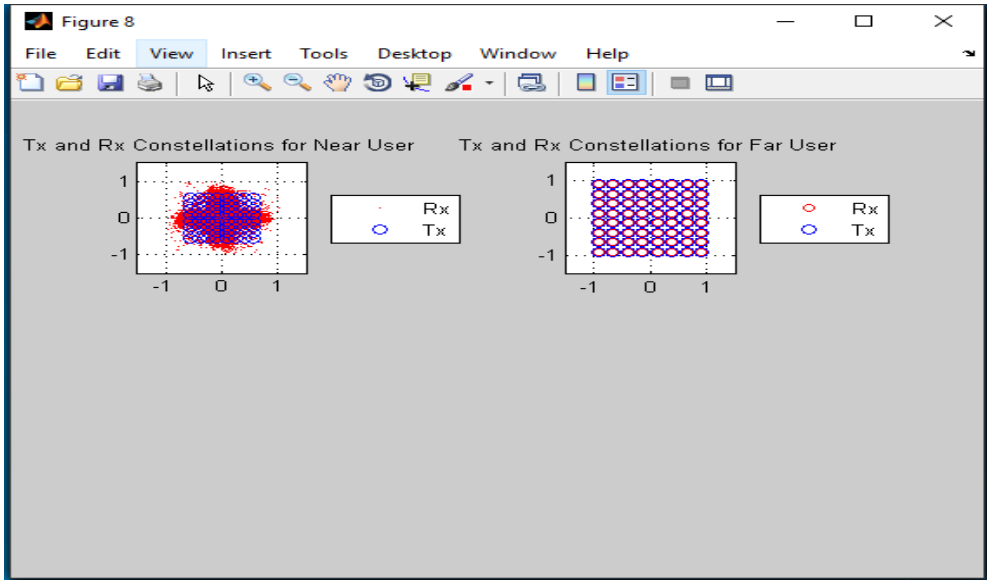


Fig 5.30: Constellation Diagram of (1x2) NOMA for 64 QAM modulation with SVD Precoding employing FPA

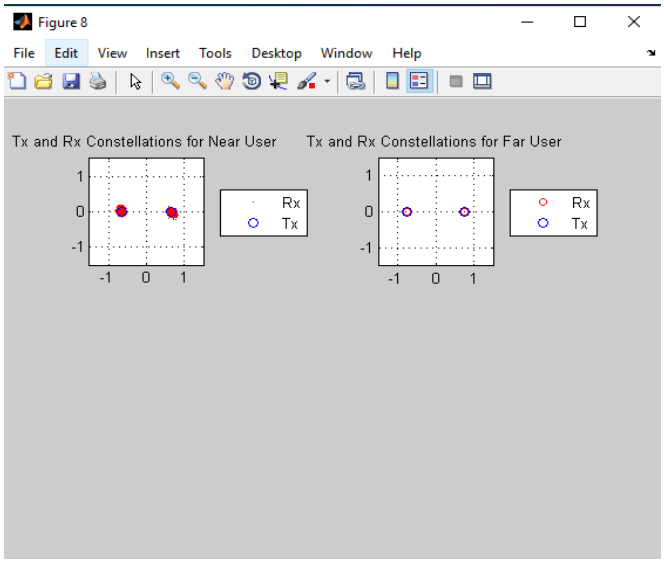


Fig 5.31: Constellation Diagram of (1x2) NOMA for BPSK modulation with SVD Precoding employing DPA

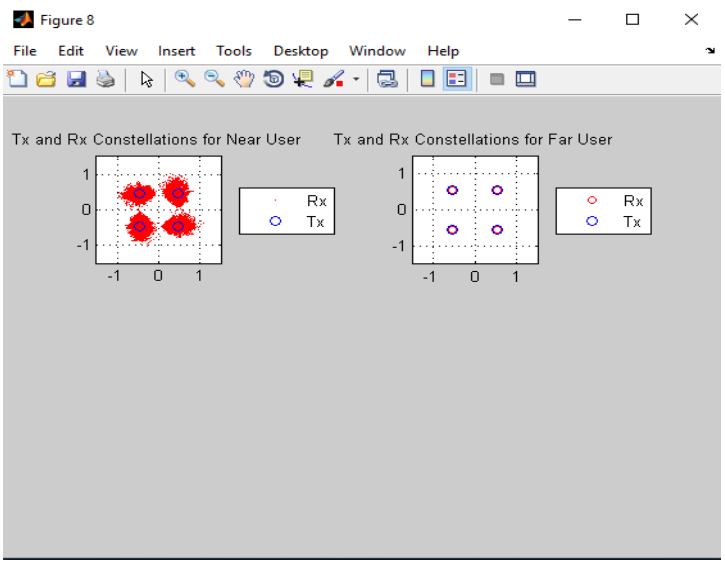


Fig 5.32: Constellation Diagram of (1x2) NOMA for QPSK modulation with SVD Precoding employing DPA

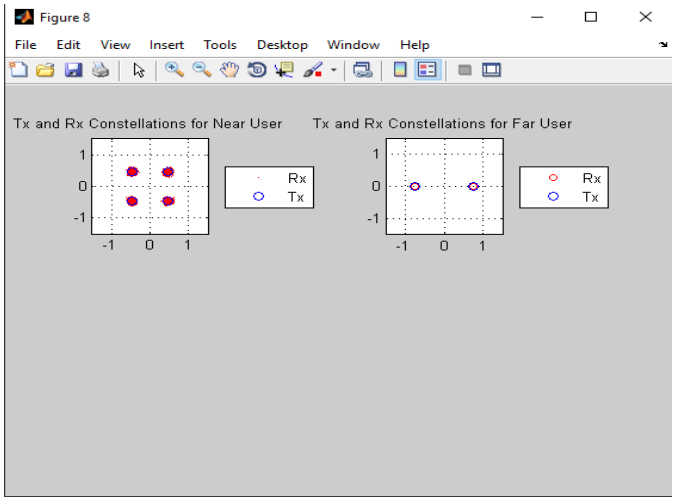


Fig 5.33: Constellation Diagram of (1x2) NOMA for Adaptive modulation with SVD Precoding employing DPA

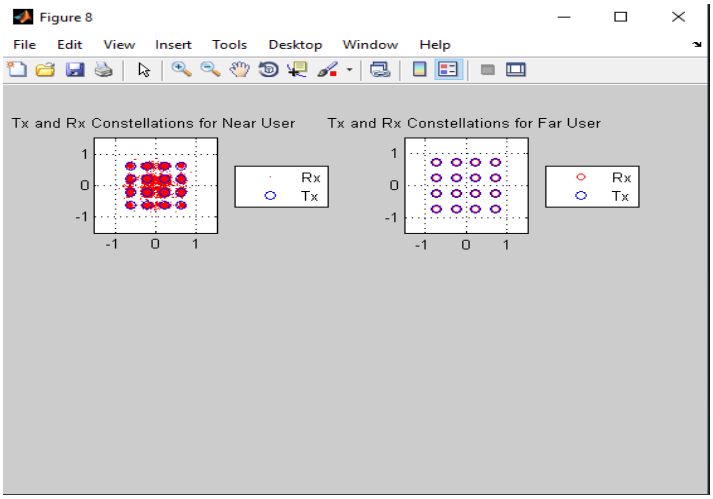


Fig 5.34: Constellation Diagram of (1x2) NOMA for 16 QAM modulation with SVD Precoding employing DPA

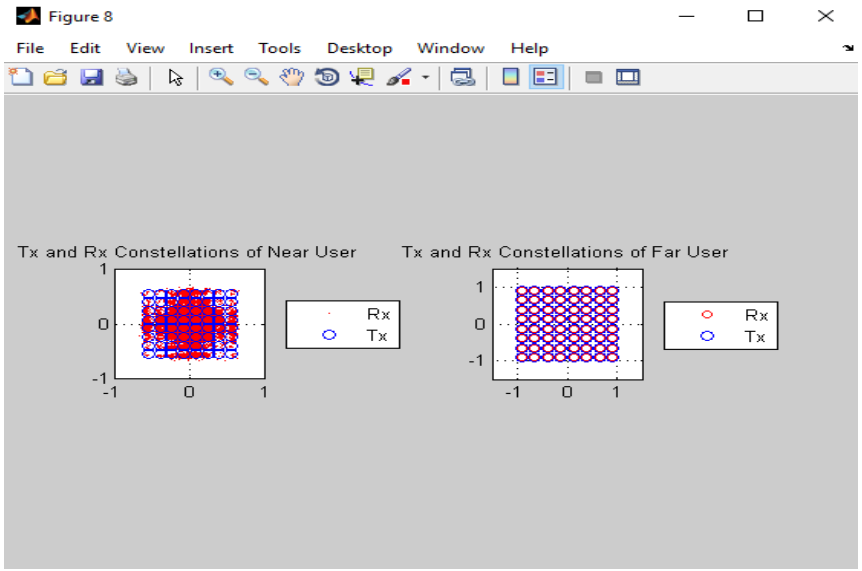


Fig 5.35: Constellation Diagram of (1x2) NOMA for 64 QAM modulation with SVD Precoding employing DPA

Fig 5.21, Fig 5.22, Fig 5.23, Fig 5.24, and Fig 5.25 represent the Constellation diagram of Downlink (1x2) PD-NOMA system for different modulation techniques, without using Precoding technique and employing Fixed Power Allocation (FPA) scheme. Left side of each figure represents the Constellation diagram of NU and right side represents Constellation diagram of FU. From the figures we can see that in case of BPSK and Adaptive modulation each received symbols can be distinguished in the Constellation diagram corresponding to each transmitted symbols. But in case of QPSK, 16 QAM and 64 QAM, received symbols of NU cannot be distinguished properly in the Constellation diagram corresponding to each transmitted symbols.

Fig 5.26, Fig 5.27, Fig 5.28, Fig 5.29, and Fig 5.30 represent the Constellation diagram of Downlink (1x2) PD-NOMA system for different modulation techniques, with SVD Precoding technique and employing Fixed Power Allocation (FPA) scheme. From the figures we can observe that in case of BPSK, QPSK and Adaptive modulation each received symbols can be distinguished in the Constellation diagram corresponding to each transmitted symbols. But in case of 16 QAM and 64 QAM, received symbols of NU cannot be distinguished properly in the Constellation diagram corresponding to each transmitted symbols. So, applying SVD Precoding technique provides better Constellation Diagram than without applying Precoding technique.

Fig 5.31, Fig 5.32, Fig 5.33, Fig 5.34, and Fig 5.35 represent the Constellation diagram of Downlink (1x2) PD-NOMA system for different modulation techniques, with SVD Precoding technique and employing Dynamic Power Allocation (DPA) scheme. From the figures we can observe that in almost every modulation schemes each received symbols can be distinguished in the Constellation diagram corresponding to each transmitted symbols.

So, SVD Precoding with Dynamic Power Allocation scheme provides the best Constellation Diagram among these three techniques.

III. Constellation diagram of Downlink (1x3) PD-NOMA system with and without Precoding for different Power Allocation Scheme, for different modulation techniques:

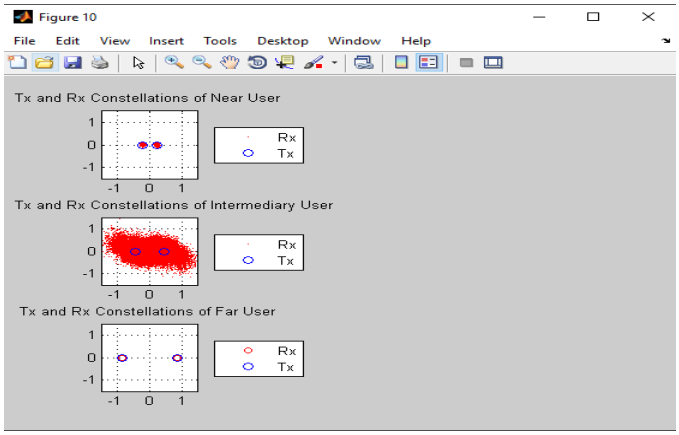


Fig 5.36: Constellation Diagram of (1x3) NOMA for BPSK modulation without Precoding employing FPA

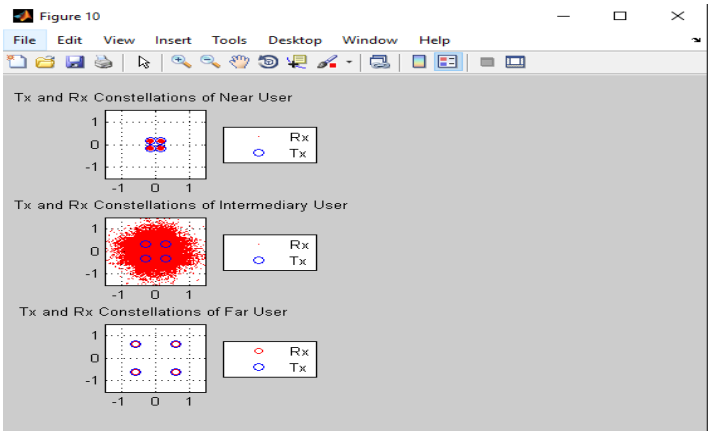


Fig 5.37: Constellation Diagram of (1x3) NOMA for QPSK modulation without Precoding employing FPA

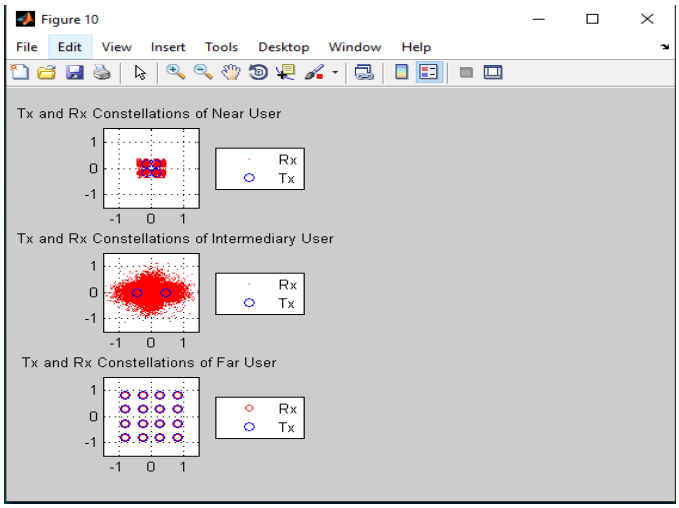


Fig 5.38: Constellation Diagram of (1x3) NOMA for Adaptive modulation without Precoding employing FPA

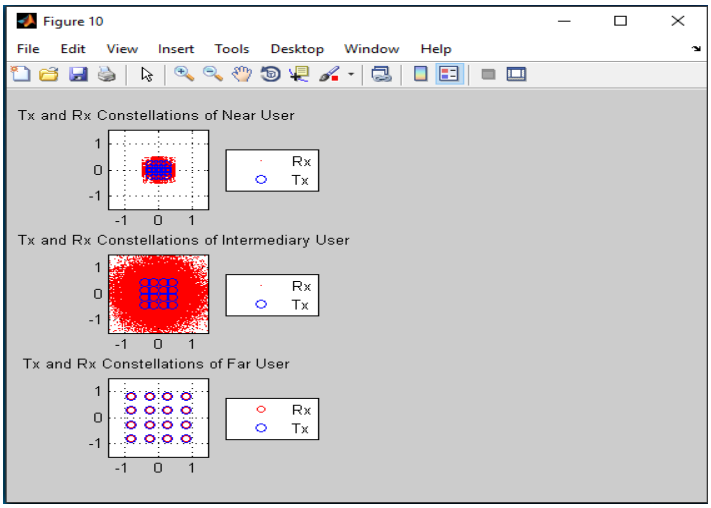


Fig 5.39: Constellation Diagram of (1x3) NOMA for 16 QAM modulation without Precoding employing FPA

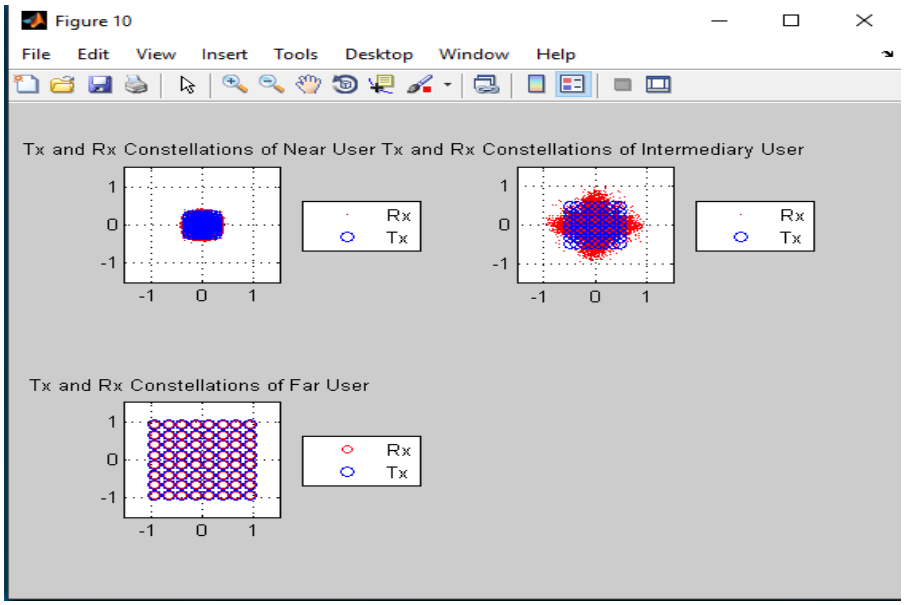


Fig 5.40: Constellation Diagram of (1x3) NOMA for 64 QAM modulation without Precoding employing FPA

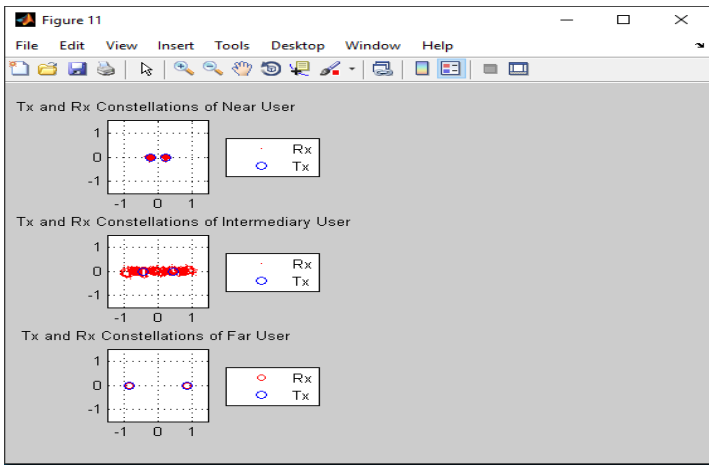


Fig 5.41: Constellation Diagram of (1x3) NOMA for BPSK modulation with SVD Precoding employing FPA

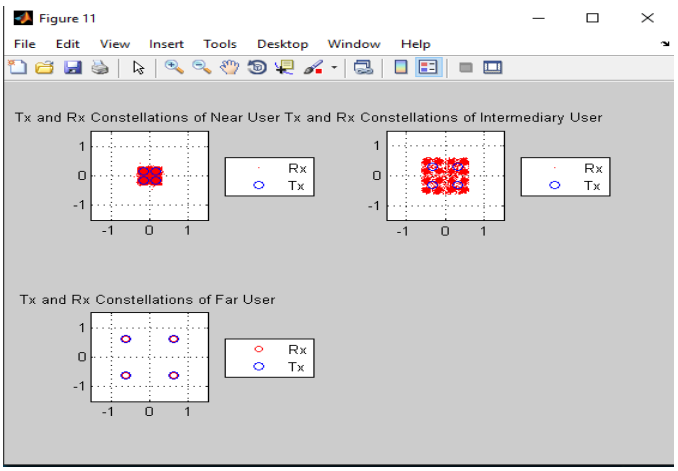


Fig 5.42: Constellation Diagram of (1x3) NOMA for QPSK modulation with SVD Precoding employing FPA

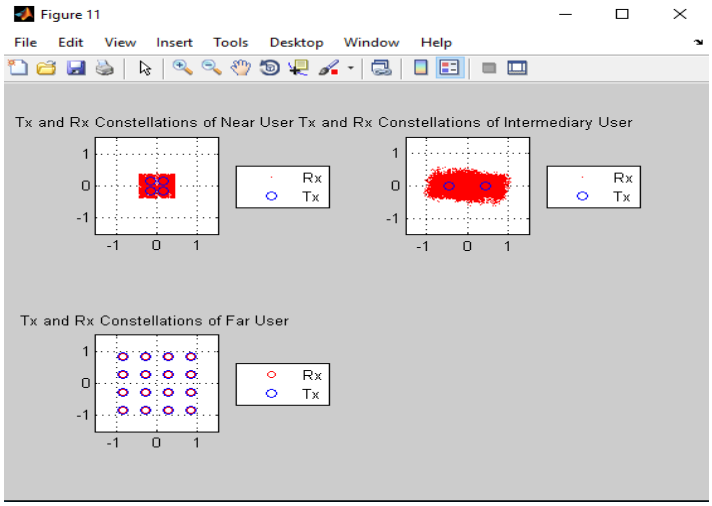


Fig 5.43: Constellation Diagram of (1x3) NOMA for Adaptive modulation with SVD Precoding employing FPA

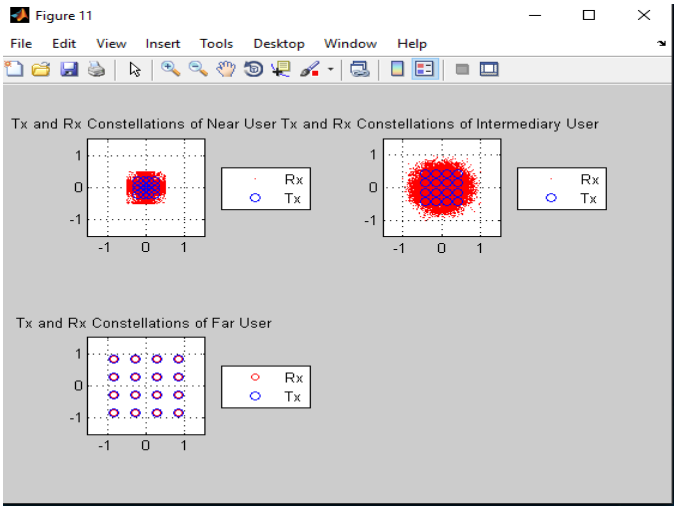


Fig 5.44: Constellation Diagram of (1x3) NOMA for 16 QAM modulation with SVD Precoding employing FPA

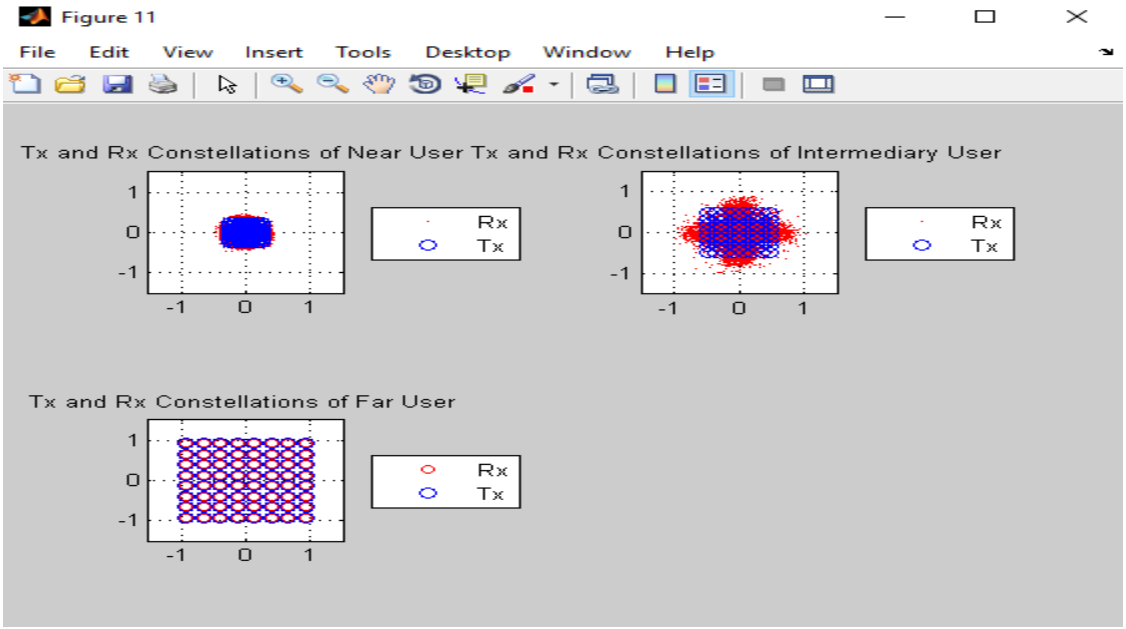


Fig 5.45: Constellation Diagram of (1x3) NOMA for 64 QAM modulation with SVD Precoding employing FPA

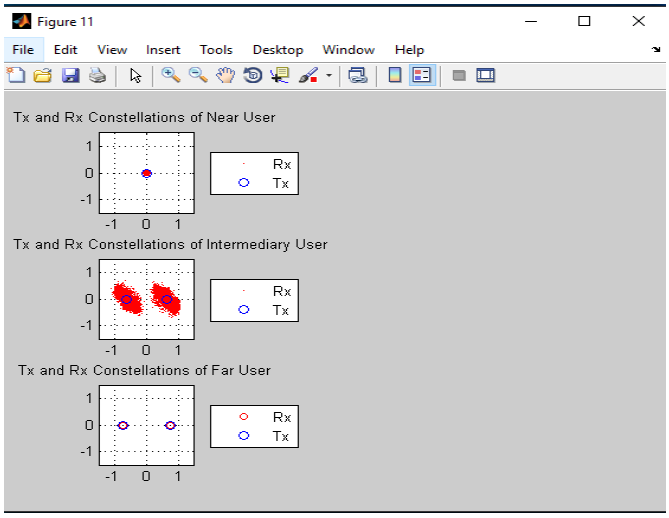


Fig 5.46: Constellation Diagram of (1x3) NOMA for BPSK modulation with SVD Precoding employing DPA

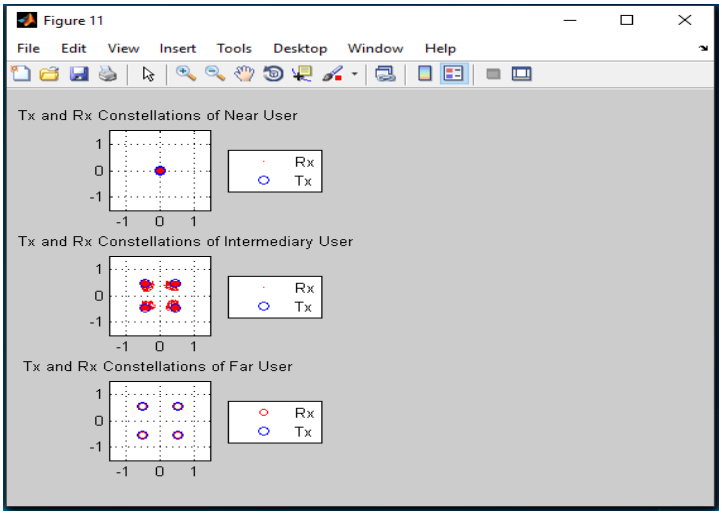


Fig 5.47: Constellation Diagram of (1x3) NOMA for QPSK modulation with SVD Precoding employing DPA

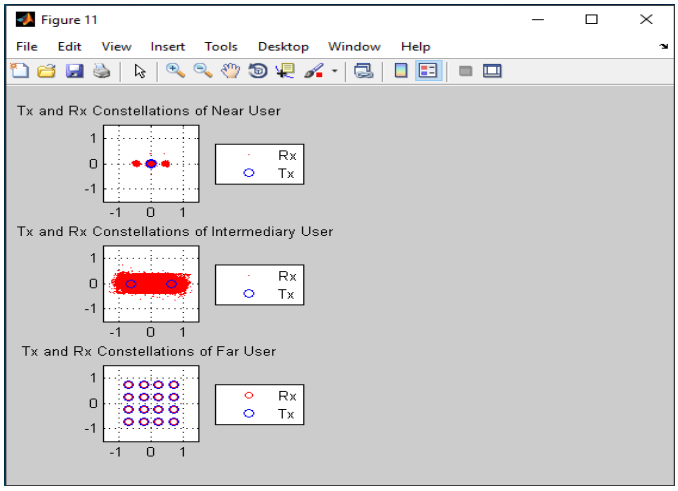


Fig 5.48: Constellation Diagram of (1x3) NOMA for Adaptive modulation with SVD Precoding employing DPA

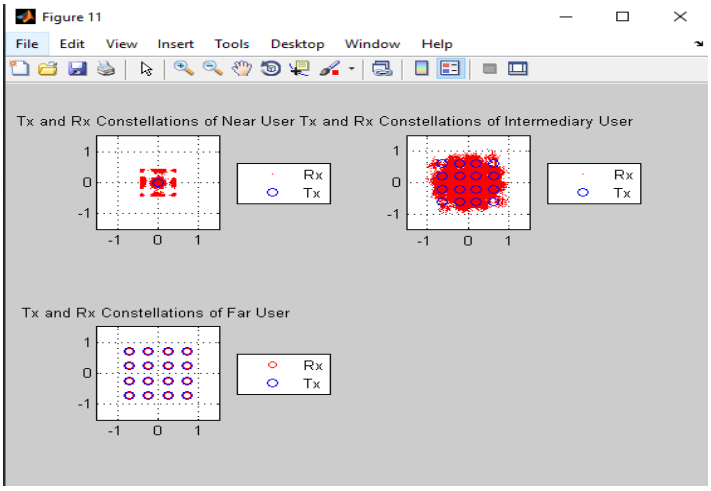


Fig 5.49: Constellation Diagram of (1x3) NOMA for 16 QAM modulation with SVD Precoding employing DPA

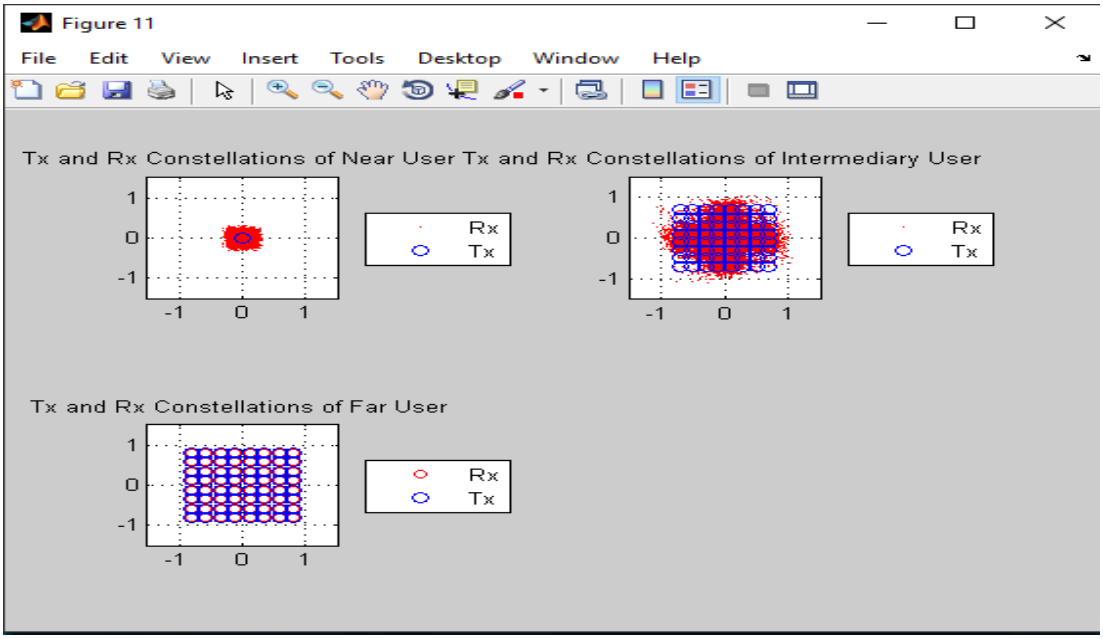


Fig 5.50: Constellation Diagram of (1x3) NOMA for 64 QAM modulation with SVD Precoding employing DPA

Fig 5.36, Fig 5.37, Fig 5.38, Fig 5.39, and Fig 5.40 represent the Constellation diagram of Downlink (1x3) PD-NOMA system for different modulation techniques, without using Precoding technique and employing Fixed Power Allocation (FPA) scheme. From the figures we can see that in every cases, received symbols of IU cannot be distinguished and in case of BPSK and QPSK modulation, received symbols of NU and FU can be distinguished in the Constellation diagram corresponding to each transmitted symbols. But in case of Adaptive, 16 QAM and 64 QAM, received symbols of NU cannot be distinguished properly in the Constellation diagram corresponding to each transmitted symbols.

Fig 5.41, Fig 5.42, Fig 5.43, Fig 5.44, and Fig 5.45 represent the Constellation diagram of Downlink (1x3) PD-NOMA system for different modulation techniques, with SVD Precoding technique and employing Fixed Power Allocation (FPA) scheme. From the figures we can observe that applying SVD Precoding technique provides better Constellation Diagram than without applying Precoding technique.

Fig 5.46, Fig 5.47, Fig 5.48, Fig 5.49, and Fig 5.50 represent the Constellation diagram of Downlink (1x3) PD-NOMA system for different modulation techniques, with SVD Precoding technique and employing Dynamic Power Allocation (DPA) scheme. From the figures we can observe that in almost every modulation schemes each received symbols can be distinguished in the Constellation diagram corresponding to each transmitted symbols.

So, SVD Precoding with Dynamic Power Allocation scheme provides the best Constellation Diagram among these three techniques.

IV. Constellation diagram of Downlink (1x3) PD-NOMA system with Clustering and SVD Precoding for different Power Allocation Schemes, and for different modulation techniques:

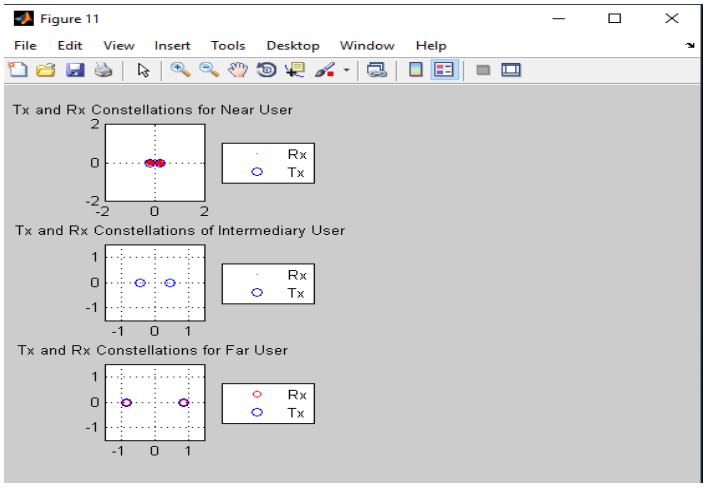


Fig 5.51: Constellation Diagram of (1x3) NN NOMA Cluster for BPSK modulation employing FPA

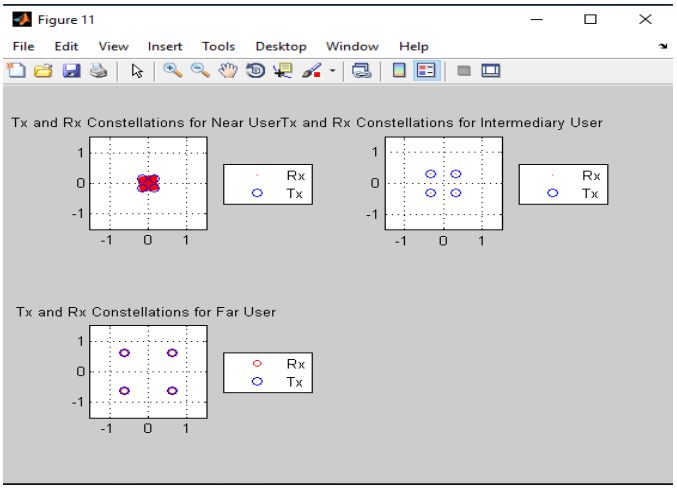


Fig 5.52: Constellation Diagram of (1x3) NN NOMA Cluster for QPSK modulation employing FPA

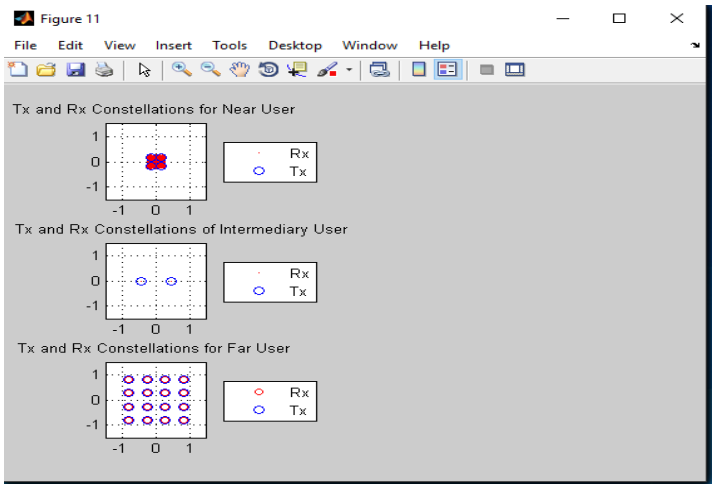


Fig 5.53: Constellation Diagram of (1x3) NN NOMA Cluster for Adaptive modulation employing FPA

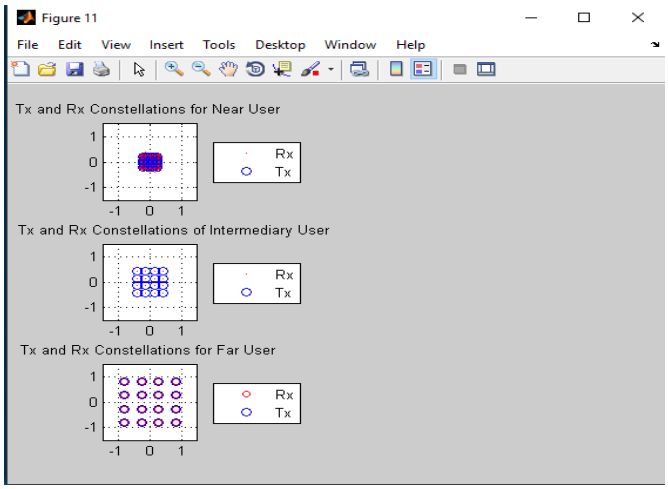


Fig 5.54: Constellation Diagram of (1x3) NN NOMA Cluster for 16 QAM modulation employing FPA

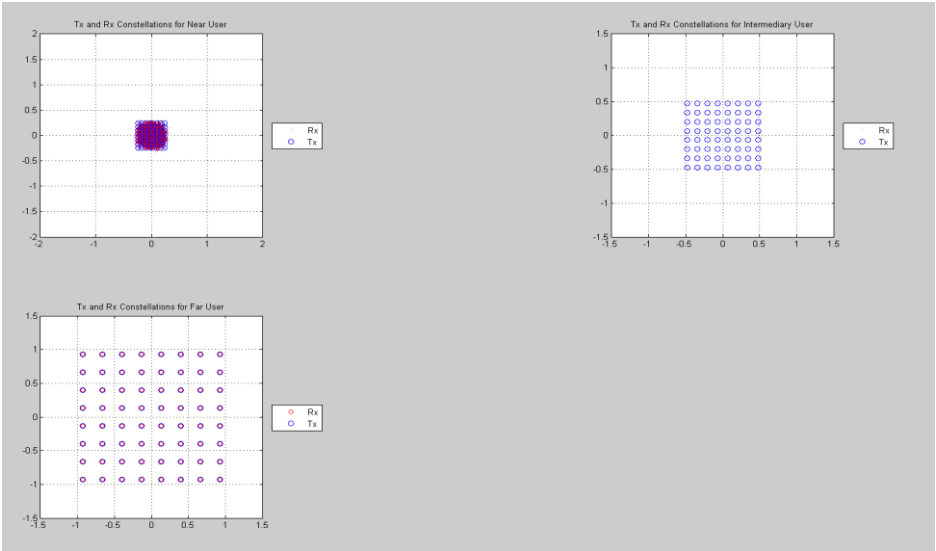


Fig 5.55: Constellation Diagram of (1x3) NN NOMA Cluster for 64 QAM modulation employing FPA

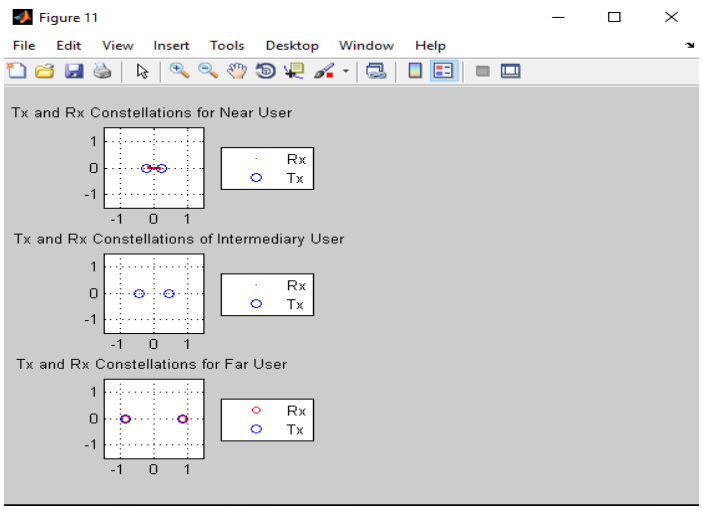


Fig 5.56: Constellation Diagram of (1x3) NF NOMA Cluster for BPSK modulation employing FPA

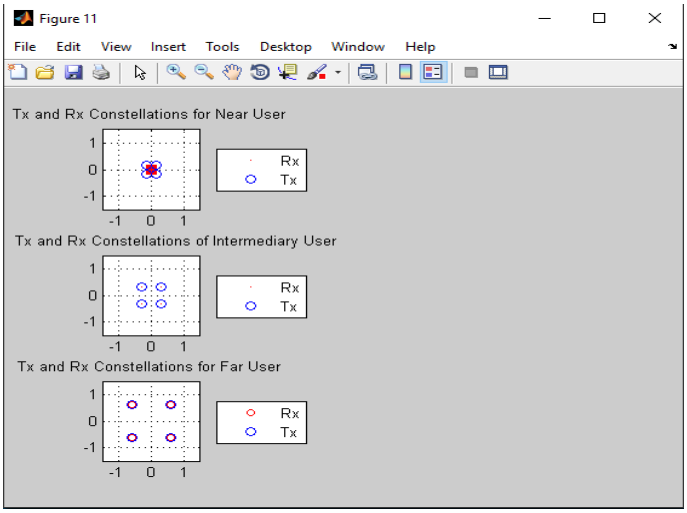


Fig 5.57: Constellation Diagram of (1x3) NF NOMA Cluster for QPSK modulation employing FPA

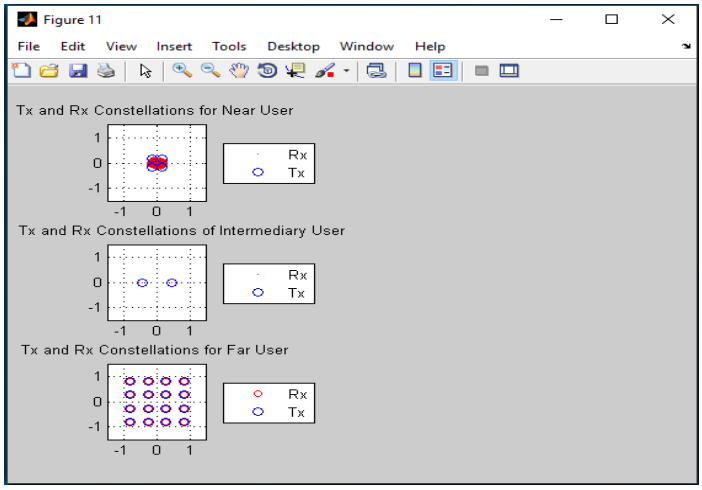


Fig 5.58: Constellation Diagram of (1x3) NF NOMA Cluster for Adaptive modulation employing FPA

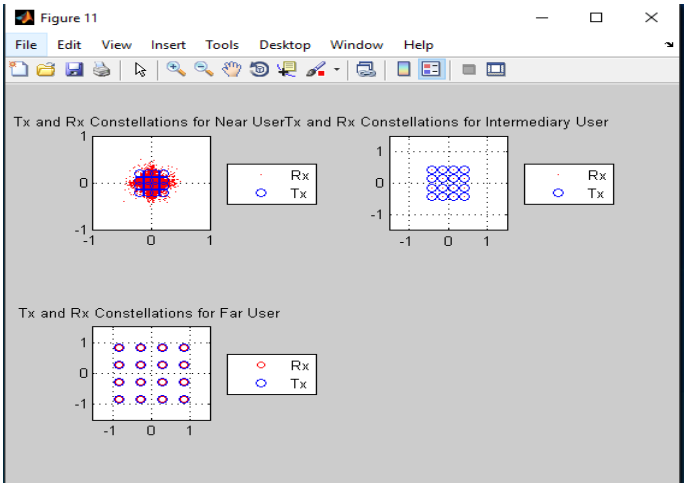


Fig 5.59: Constellation Diagram of (1x3) NF NOMA Cluster for 16 QAM modulation employing FPA

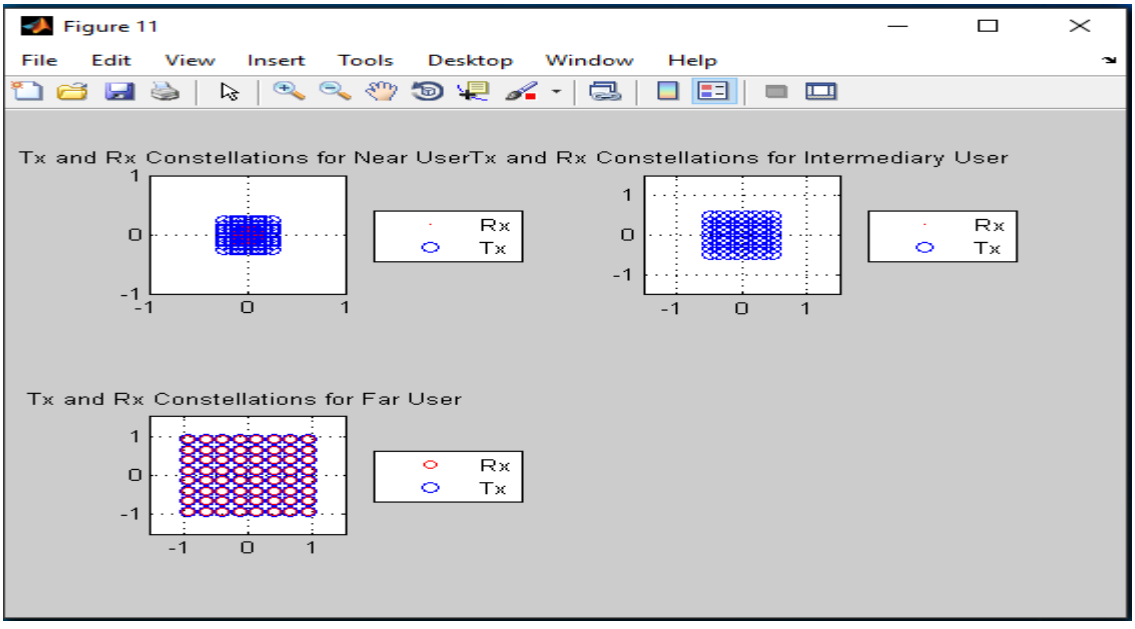


Fig 5.60: Constellation Diagram of (1x3) NF NOMA Cluster for 64 QAM modulation employing FPA

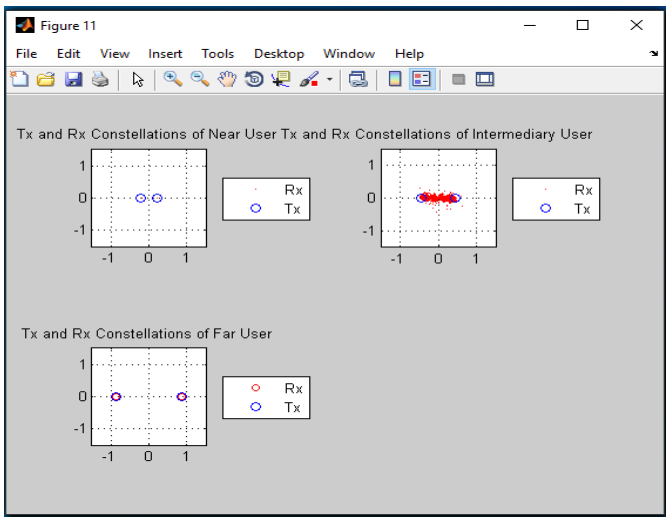


Fig 5.61: Constellation Diagram of (1x3) FF NOMA Cluster for BPSK modulation employing FPA

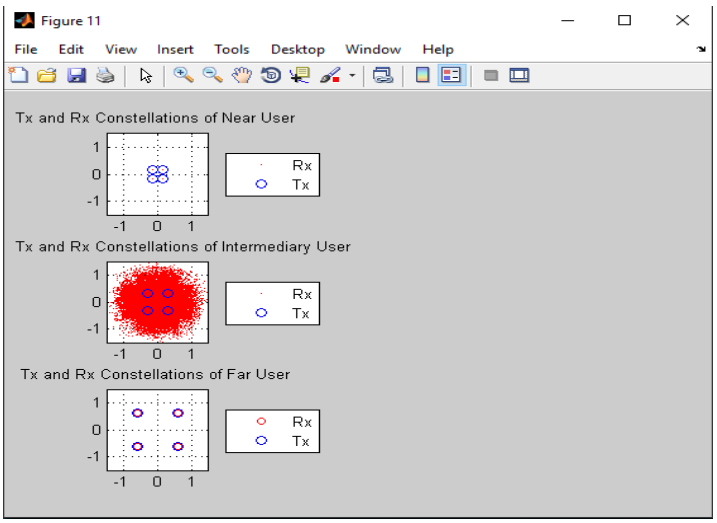


Fig 5.62: Constellation Diagram of (1x3) FF NOMA Cluster for QPSK modulation employing FPA

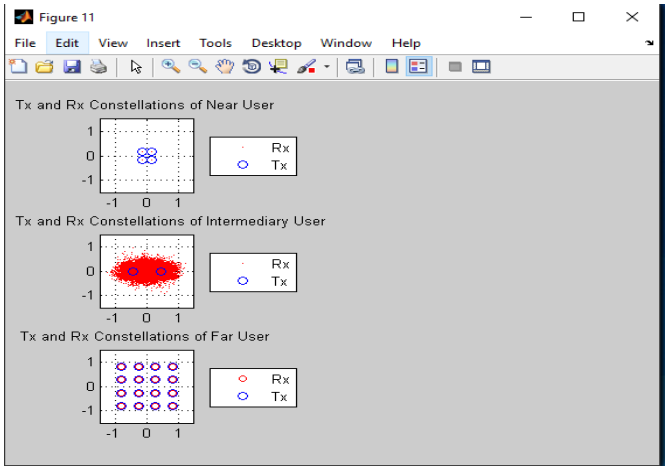


Fig 5.63: Constellation Diagram of (1x3) FF NOMA Cluster for Adaptive modulation employing FPA

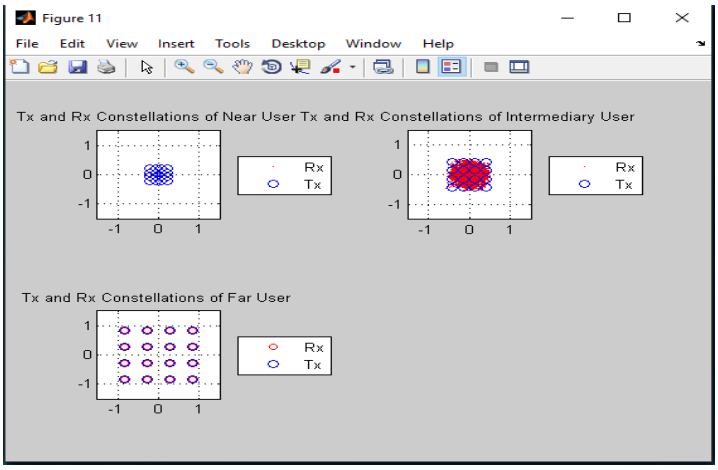


Fig 5.64: Constellation Diagram of (1x3) FF NOMA Cluster for 16 QAM modulation employing FPA

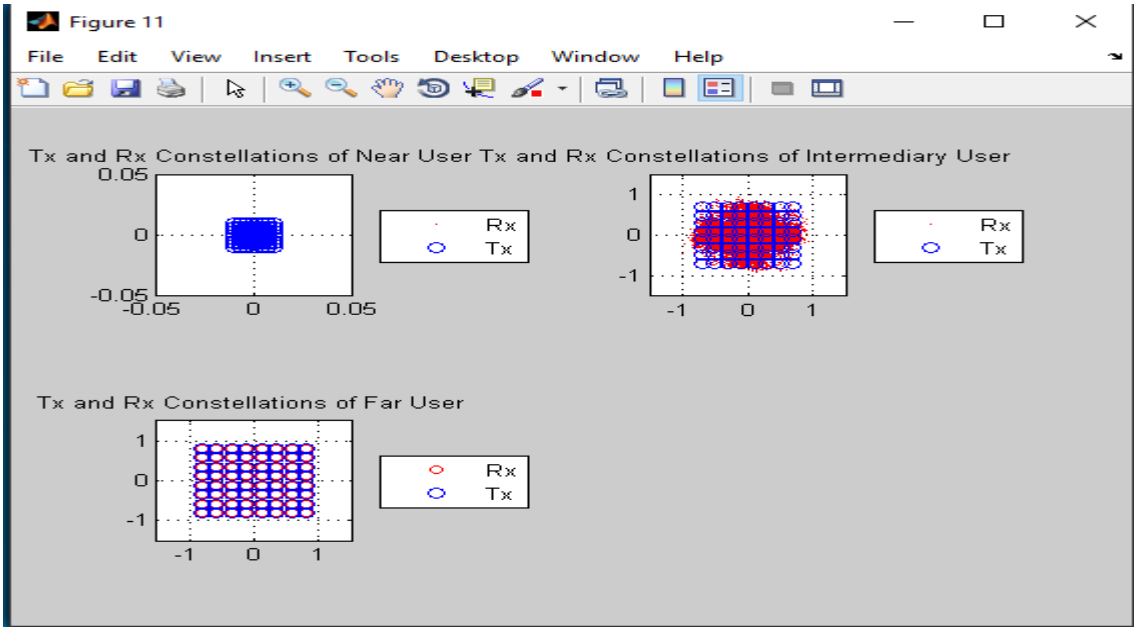


Fig 5.65: Constellation Diagram of (1x3) FF NOMA Cluster for 64 QAM modulation employing FPA

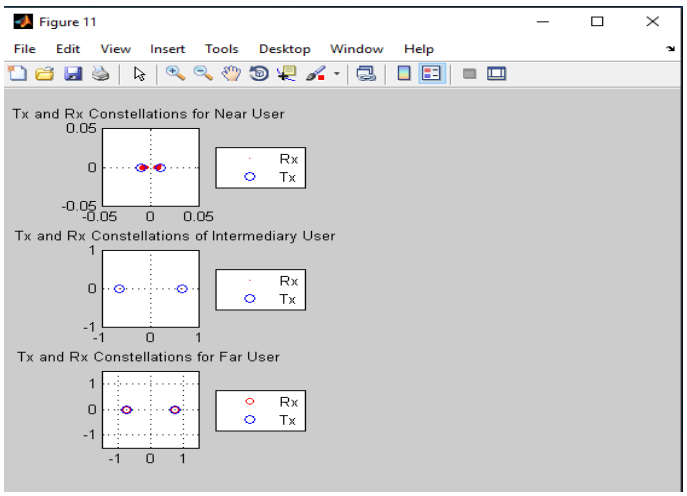


Fig 5.66: Constellation Diagram of (1x3) NN NOMA Cluster for BPSK modulation employing DPA

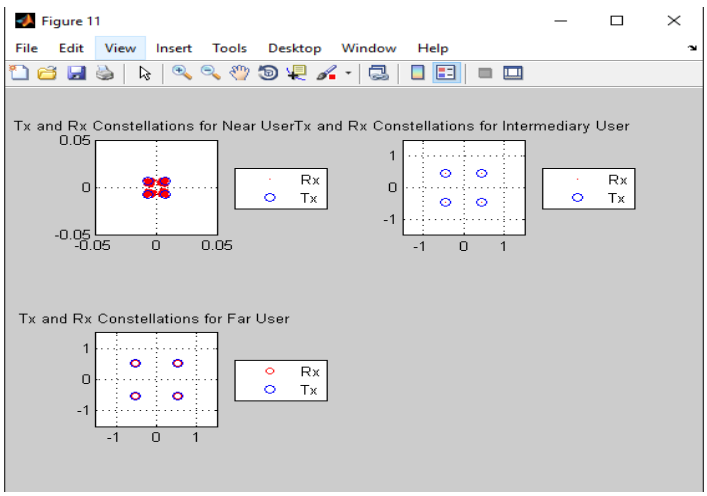


Fig 5.67: Constellation Diagram of (1x3) NN NOMA Cluster for QPSK modulation employing DPA

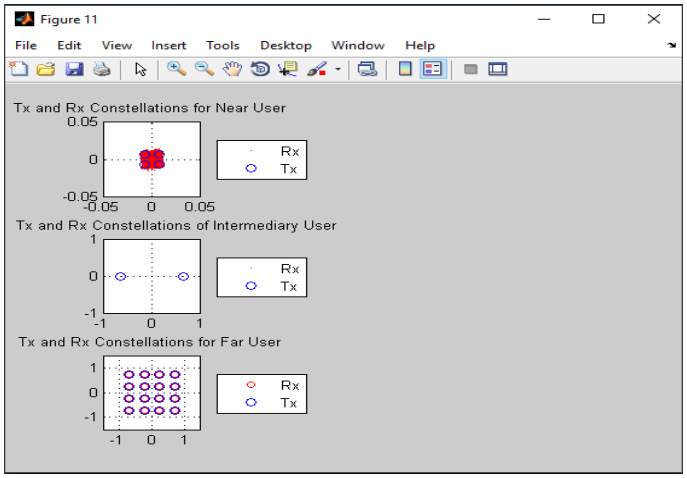


Fig 5.68: Constellation Diagram of (1x3) NN NOMA Cluster for Adaptive modulation employing DPA

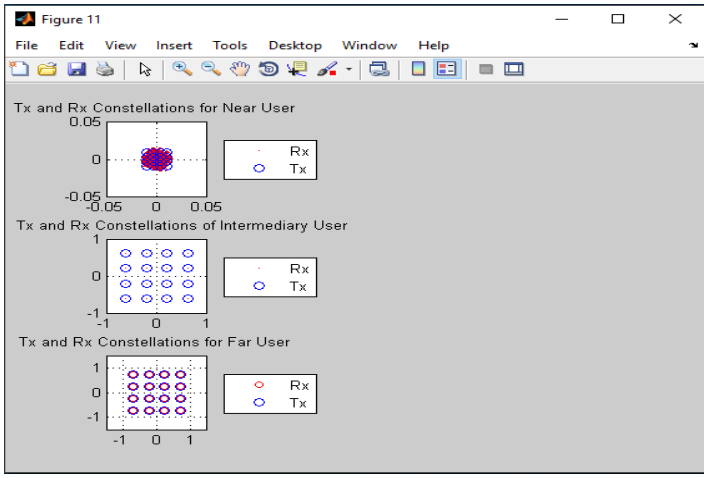


Fig 5.69: Constellation Diagram of (1x3) NN NOMA Cluster for 16 QAM modulation employing DPA

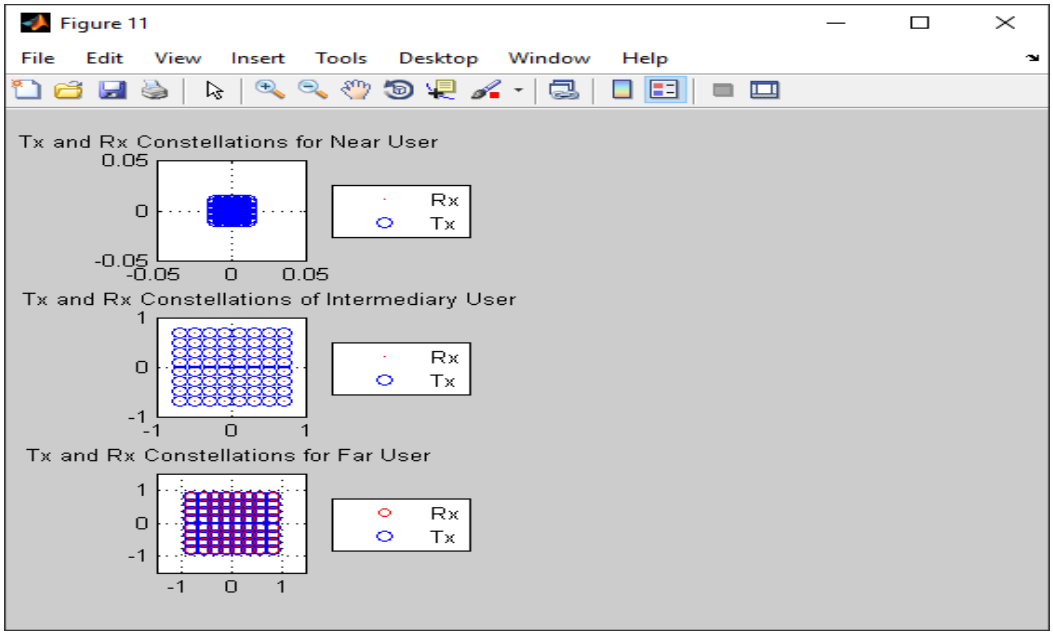


Fig 5.70: Constellation Diagram of (1x3) NN NOMA Cluster for 64 QAM modulation employing DPA

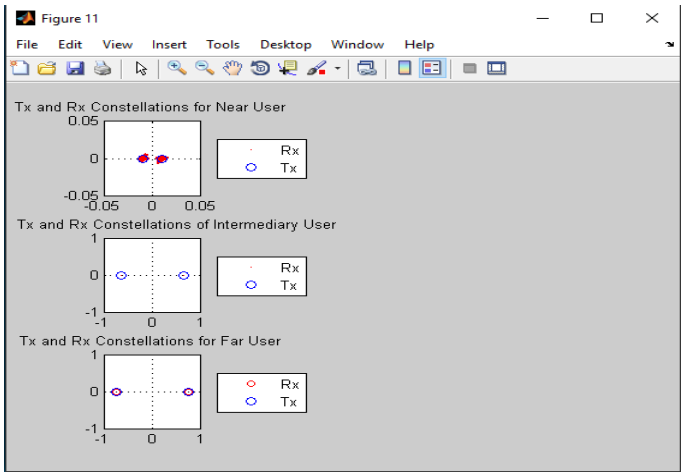


Fig 5.71: Constellation Diagram of (1x3) NF NOMA Cluster for BPSK modulation employing DPA

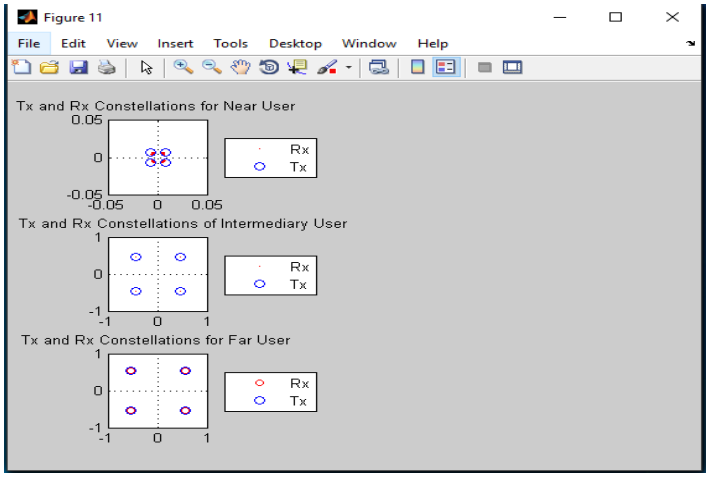


Fig 5.72: Constellation Diagram of (1x3) NF NOMA Cluster for QPSK modulation employing DPA

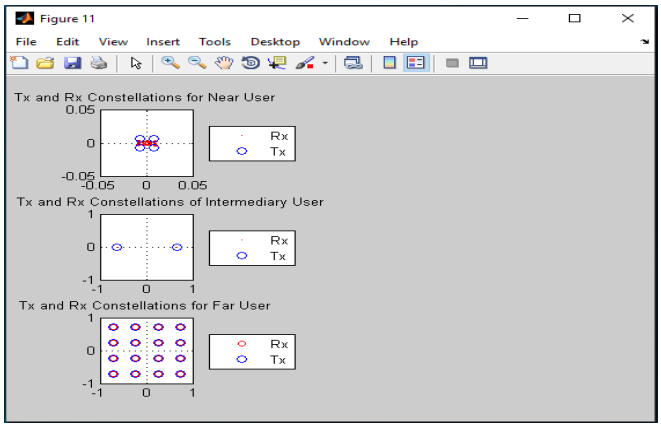


Fig 5.73: Constellation Diagram of (1x3) NF NOMA Cluster for Adaptive modulation employing DPA

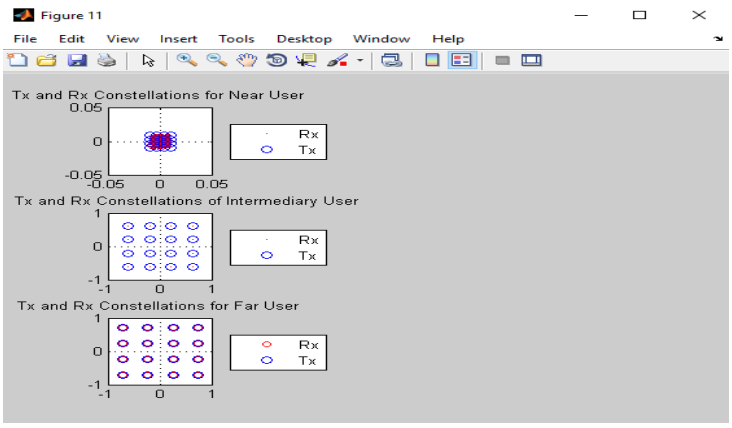


Fig 5.74: Constellation Diagram of (1x3) NF NOMA Cluster for 16 QAM modulation employing DPA

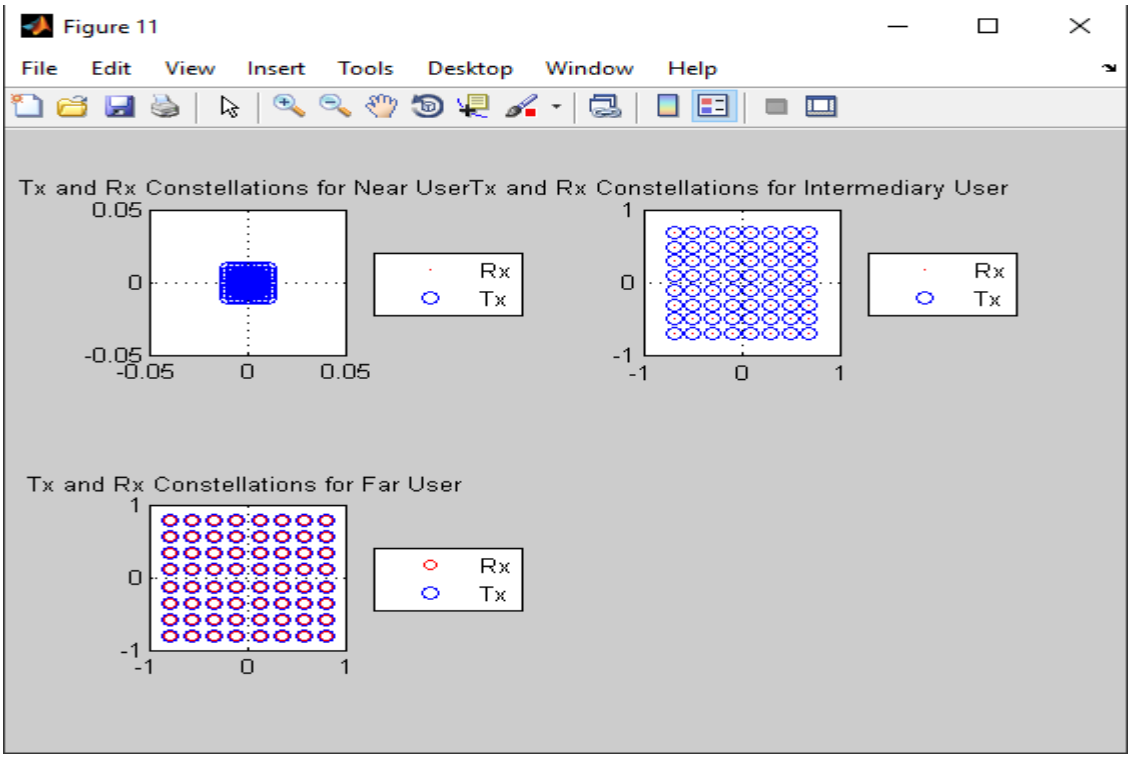


Fig 5.75: Constellation Diagram of (1x3) NF NOMA Cluster for 64 QAM modulation employing DPA

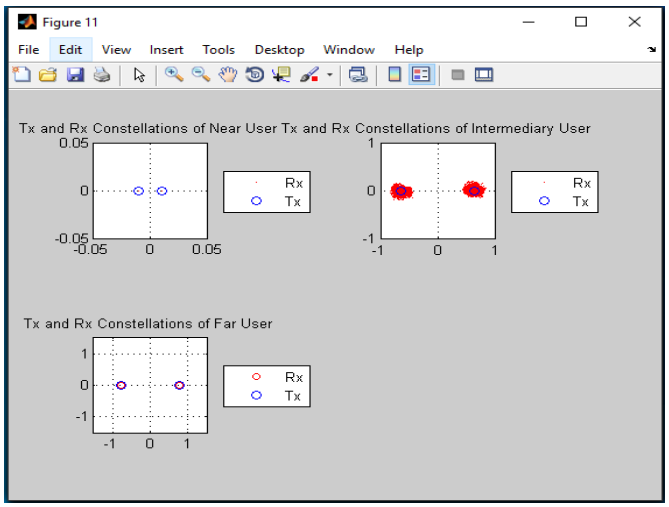


Fig 5.76: Constellation Diagram of (1x3) FF NOMA Cluster for BPSK modulation employing DPA

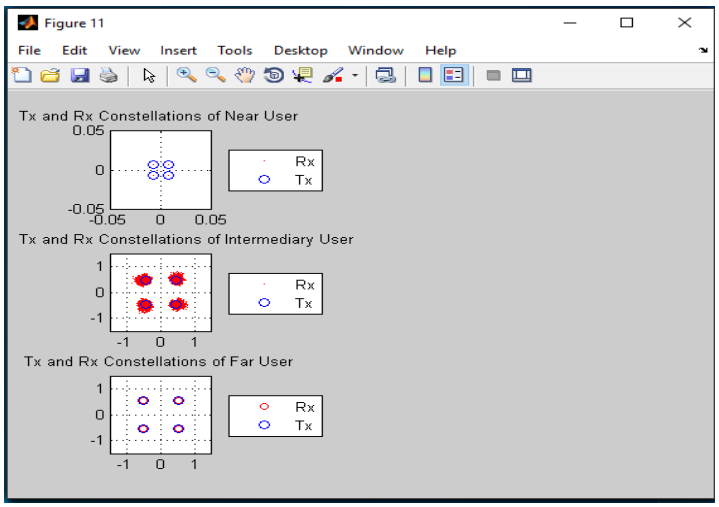


Fig 5.77: Constellation Diagram of (1x3) FF NOMA Cluster for QPSK modulation employing DPA

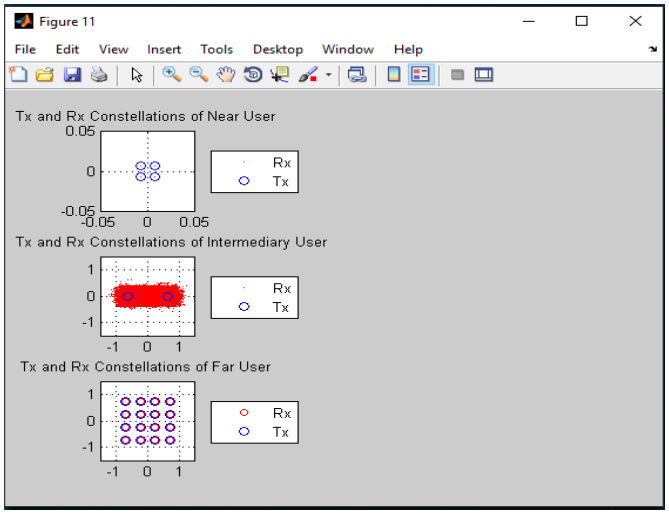


Fig 5.78: Constellation Diagram of (1x3) FF NOMA Cluster for Adaptive modulation employing DPA

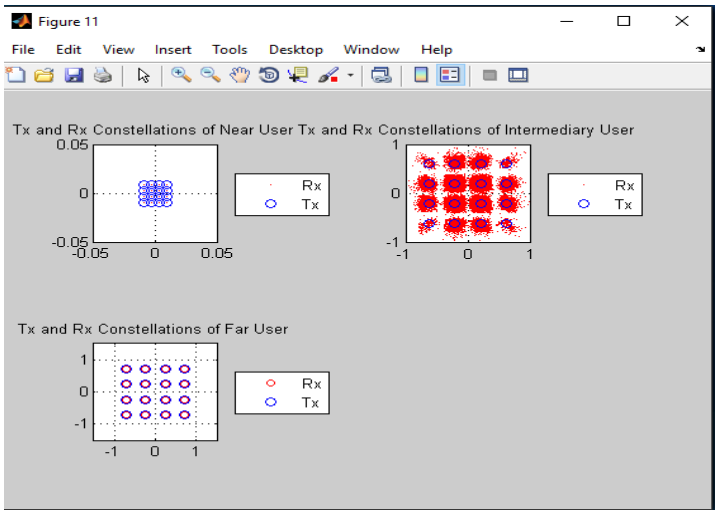


Fig 5.79: Constellation Diagram of (1x3) FF NOMA Cluster for 16 QAM modulation employing DPA

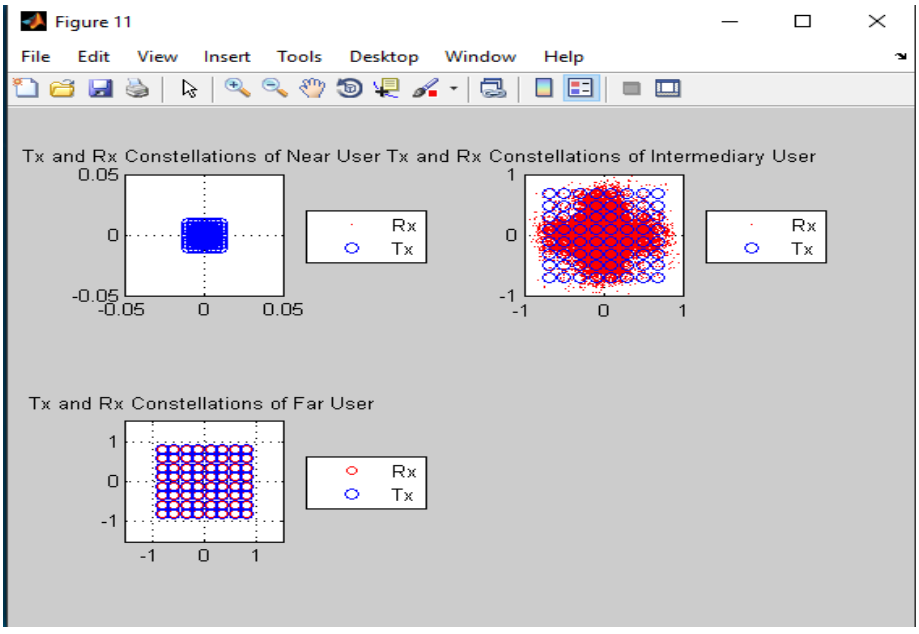


Fig 5.80: Constellation Diagram of (1x3) FF NOMA Cluster for 64 QAM modulation employing DPA

With the increase in number of Users in a NOMA system, SIC becomes more imperfect. To solve this problem, Clustering technique is required. In case of (1x3) PD-NOMA system we can observe that received symbols of IU cannot be distinguished in every modulation technique.

Fig 5.51, Fig 5.52, Fig 5.53, Fig 5.54, and Fig 5.55 represent the Constellation diagram of Downlink (1x3) NN NOMA Clustering system for different modulation techniques, with SVD Precoding technique and employing Fixed Power Allocation (FPA) scheme. Fig 5.56, Fig 5.57, Fig 5.58, Fig 5.59, and Fig 5.60 represent the Constellation diagram of Downlink (1x3) NF NOMA Clustering system for different modulation techniques, with SVD Precoding technique and employing Fixed Power Allocation (FPA) scheme. Fig 5.61, Fig 5.62, Fig 5.63, Fig 5.64, and Fig 5.65 represent the Constellation diagram of Downlink (1x3) FF NOMA Clustering system for different modulation techniques, with SVD Precoding technique and employing Fixed Power Allocation (FPA) scheme. In every NOMA Clustering system, we can see that it provides better Constellation Diagram than Downlink PD-NOMA system.

Fig 5.66, Fig 5.67, Fig 5.68, Fig 5.69, and Fig 5.70 represent the Constellation diagram of Downlink (1x3) NN NOMA Clustering system for different modulation techniques, with SVD Precoding technique and employing Dynamic Power Allocation (DPA) scheme. Fig 5.71, Fig 5.72, Fig 5.73, Fig 5.74, and Fig 5.75 represent the Constellation diagram of Downlink (1x3) NF NOMA Clustering system for different modulation techniques, with SVD Precoding technique and employing Dynamic Power Allocation (DPA) scheme. Fig 5.76, Fig 5.77, Fig 5.78, Fig 5.79, and Fig 5.80 represent the Constellation diagram of Downlink (1x3) FF NOMA Clustering system for different modulation techniques, with SVD Precoding technique and employing Dynamic Power Allocation (DPA) scheme. In every NOMA Clustering system employing SVD Precoding and Dynamic Power Allocation scheme each received symbols can be distinguished in the Constellation diagram corresponding to each transmitted symbols in every modulation schemes.

5.5 Summary of the chapter:

The transceiver board, WARP V3, that we have used for all of our experiments is described in this chapter. This chapter presents constellation diagrams of several user PD-NOMA and PD-NOMA clustering systems using various modulation and power allocation algorithms, both with and without precoding.

Chapter-6

Simulation and hardware-based Results:

In this chapter, an extensive analysis of performances, with respect to Sum Capacity, Spectral Efficiency, Energy Efficiency and Total amount of Interference, of different users downlink PD-NOMA system with downlink PD-NOMA Clustering system has been presented for different Power Allocation strategies and different modulation techniques. Fixed Power Allocation (FPA) and Dynamic Power Allocation schemes are the power allocation techniques used. The results are conducted using MATLAB software. To account for various aspects of fading environment, each simulation is performed multiple times, and the ensemble average of the results is considered. This approach ensures that different realizations of the fading phenomenon are considered and provides a comprehensive understanding of its effects.

I. Performance analysis of (2x2) PD-NOMA system in presence and absence of precoding for different power allocation schemes and different modulation techniques:

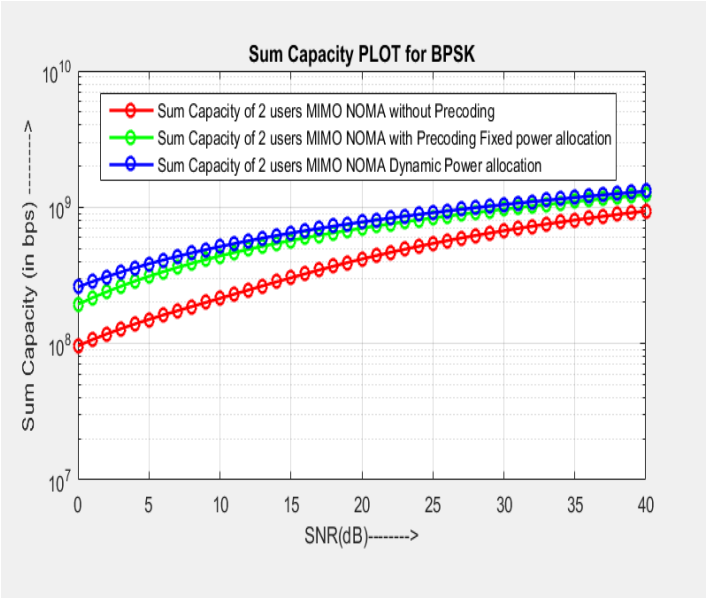


Fig 6.1: Comparison of Sum Capacity of (2x2) PD-NOMA system for BPSK modulation

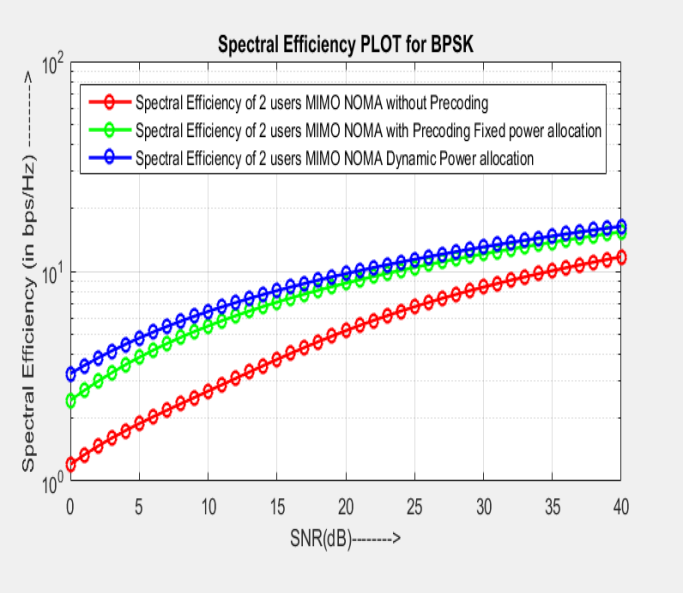


Fig 6.2: Comparison of Spectral Efficiency of (2x2) PD-NOMA system for BPSK modulation

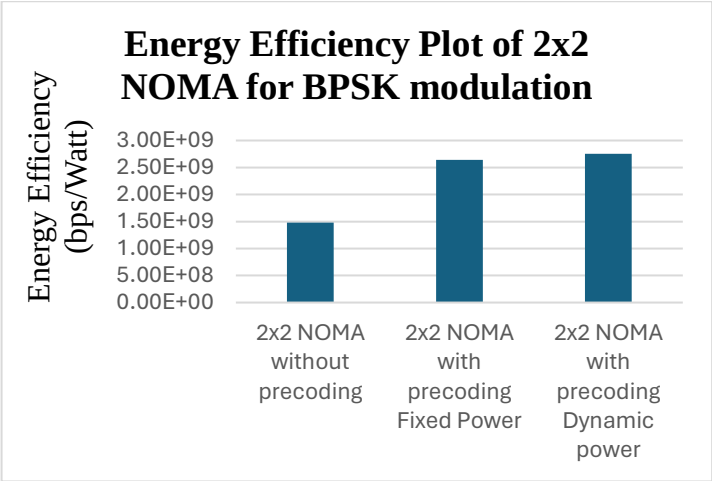


Fig 6.3: Comparison of Energy Efficiency of (2x2) PD-NOMA system for BPSK modulation

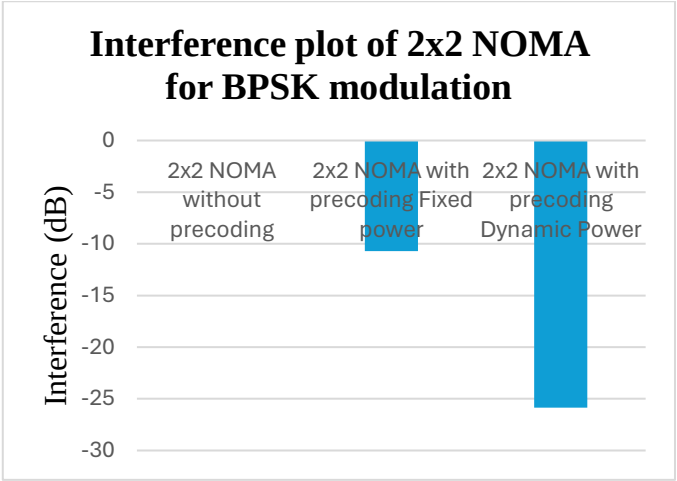


Fig 6.4: Comparison of total Interference of (2x2) PD-NOMA system for BPSK modulation

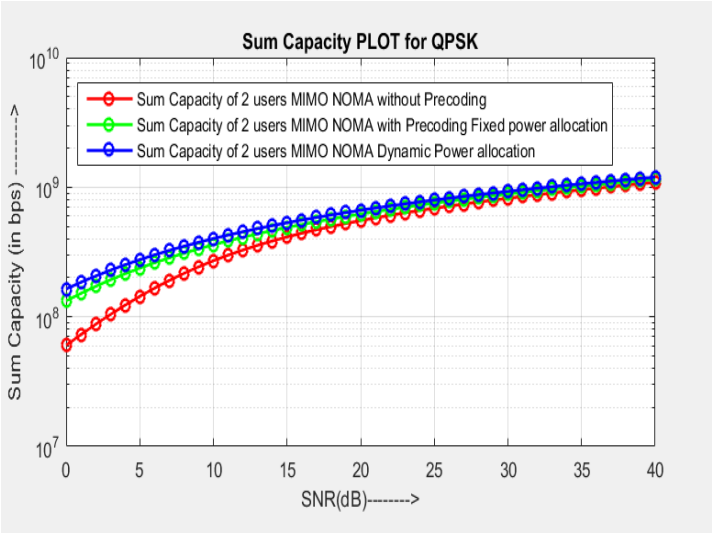


Fig 6.5: Comparison of Sum Capacity of (2x2) PD-NOMA system for QPSK modulation

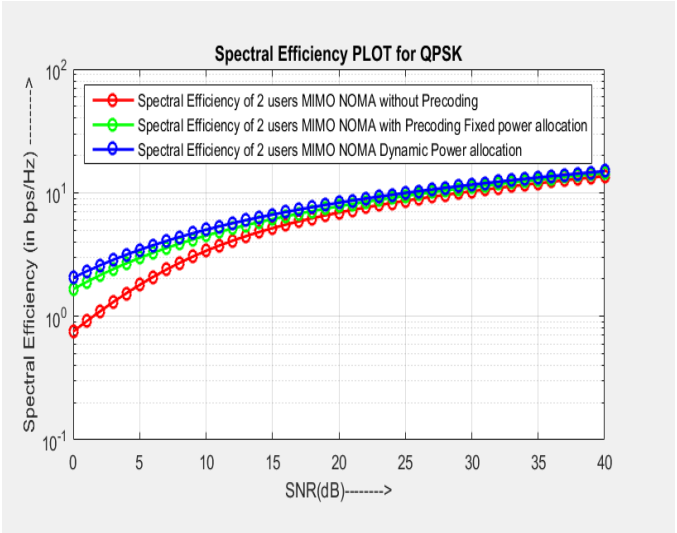


Fig 6.6: Comparison of Spectral Efficiency of (2x2) PD-NOMA system for QPSK modulation

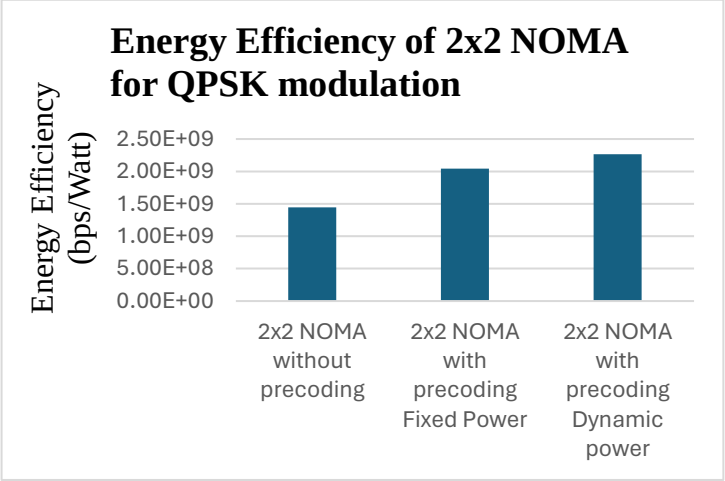


Fig 6.7: Comparison of Energy Efficiency of (2x2) PD-NOMA system for QPSK modulation

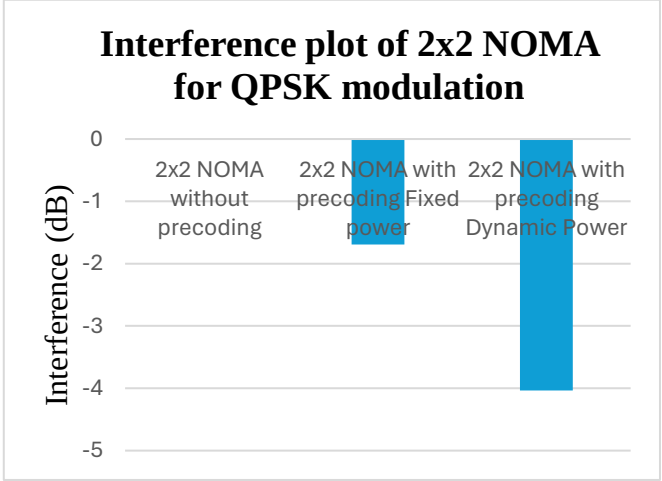


Fig 6.8: Comparison of total Interference of (2x2) PD-NOMA system for QPSK modulation

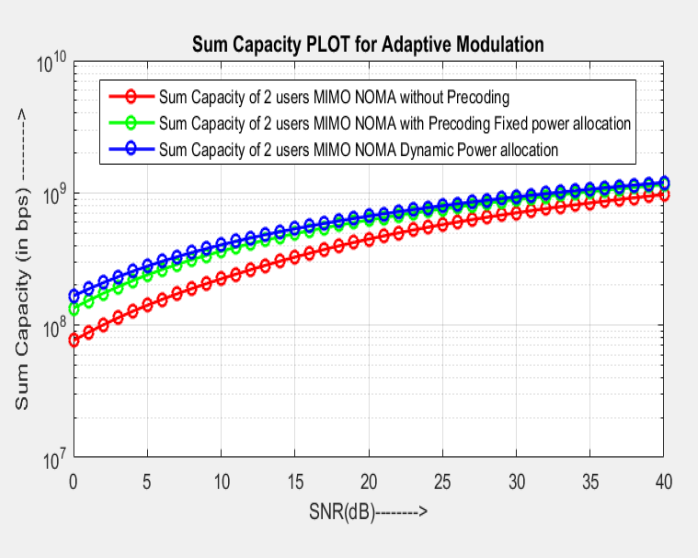


Fig 6.9: Comparison of Sum Capacity of (2x2) PD-NOMA system for Adaptive modulation

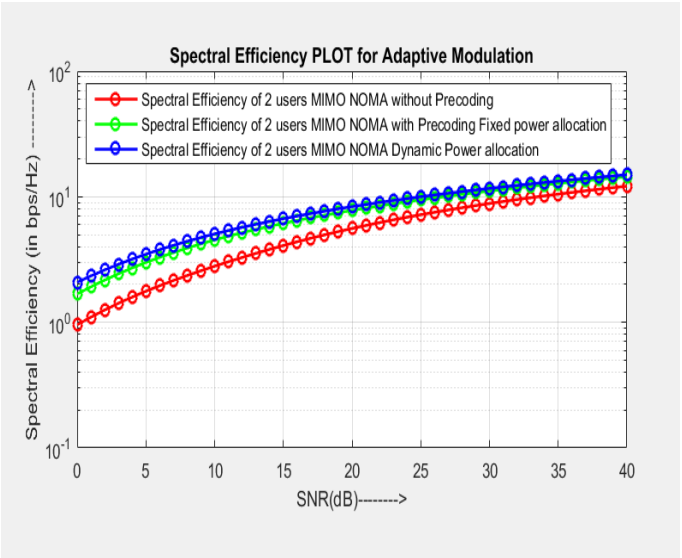


Fig 6.10: Comparison of Spectral Efficiency of (2x2) PD-NOMA system for Adaptive modulation

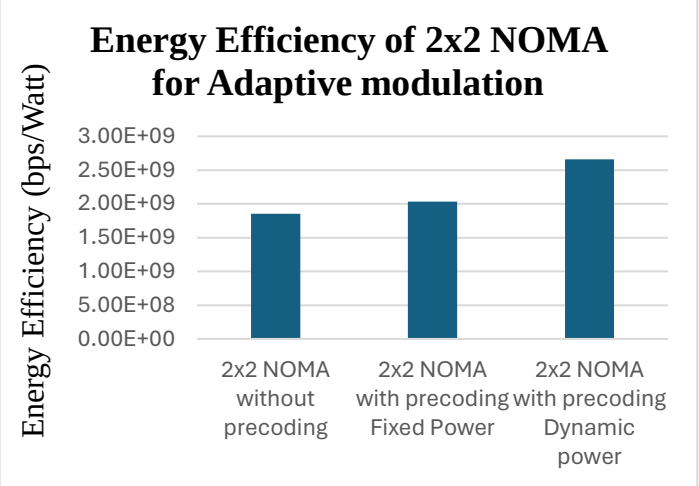


Fig 6.11: Comparison of Energy Efficiency of (2x2) PD-NOMA system for Adaptive

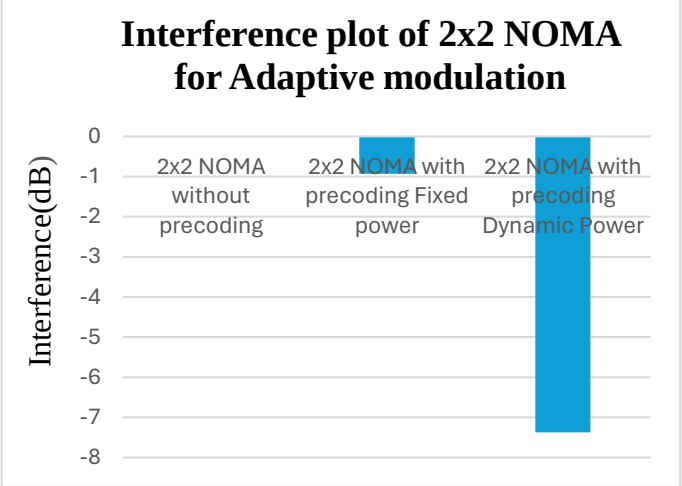


Fig 6.12: Comparison of total Interference of (2x2) PD-NOMA system for Adaptive

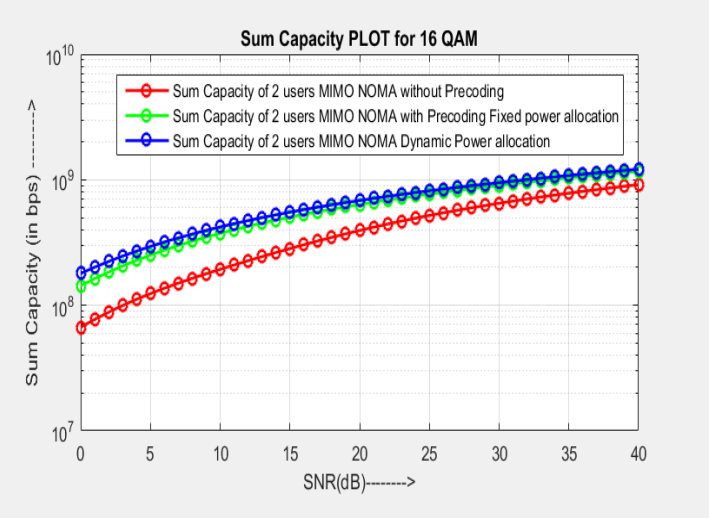


Fig 6.13: Comparison of Sum Capacity of (2x2) PD-NOMA system for 16 QAM

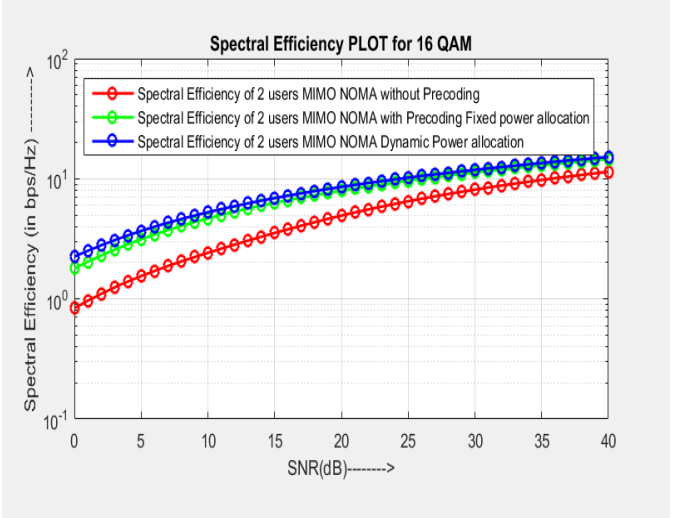


Fig 6.14: Comparison of Spectral Efficiency of (2x2) PD-NOMA system for 16 QAM

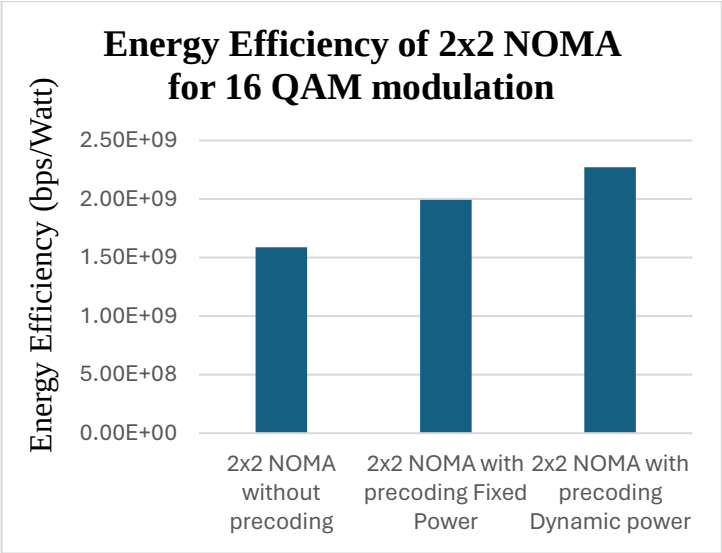


Fig 6.15: Comparison of Energy Efficiency of (2x2) PD-NOMA system for 16 QAM

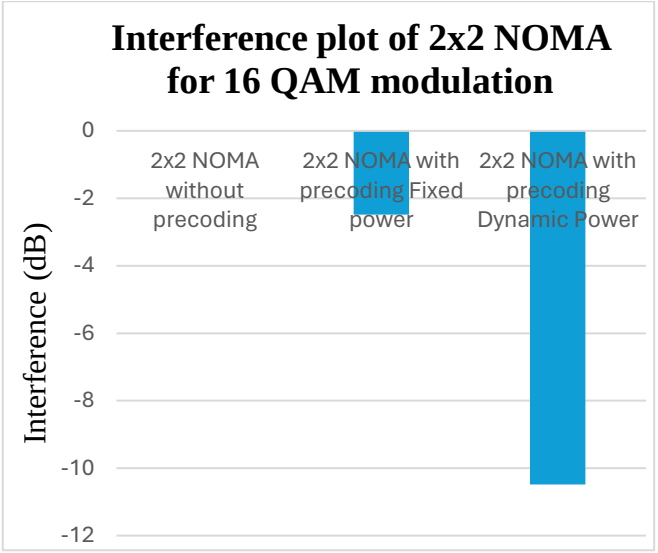


Fig 6.16: Comparison of total Interference of (2x2) PD-NOMA system for 16 QAM

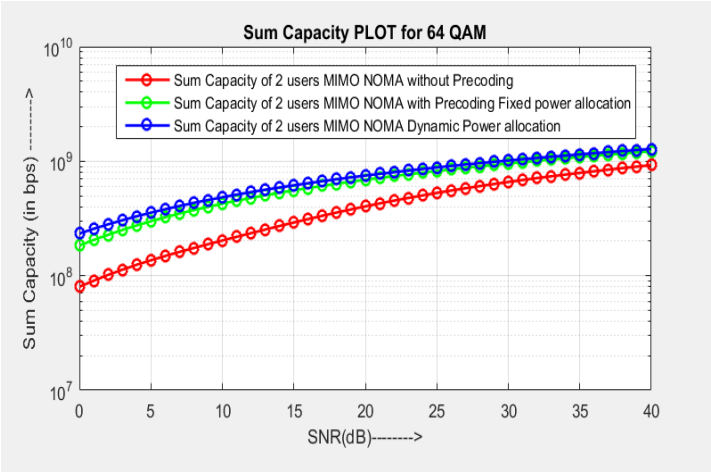


Fig 6.17: Comparison of Sum Capacity of (2x2) PD-NOMA system for 64 QAM

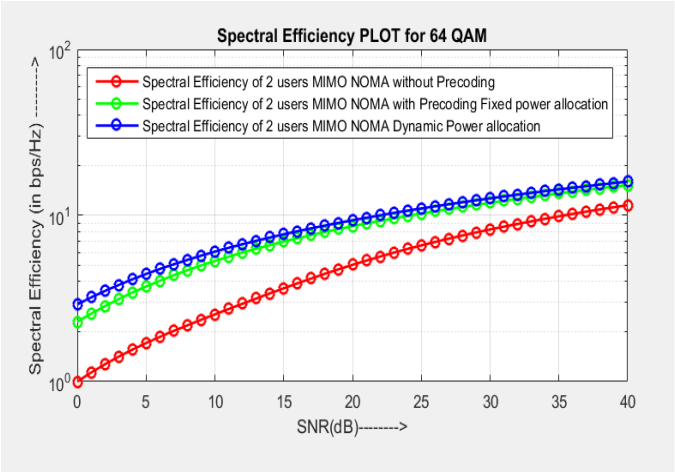


Fig 6.18: Comparison of Spectral Efficiency of (2x2) PD-NOMA system for 64 QAM

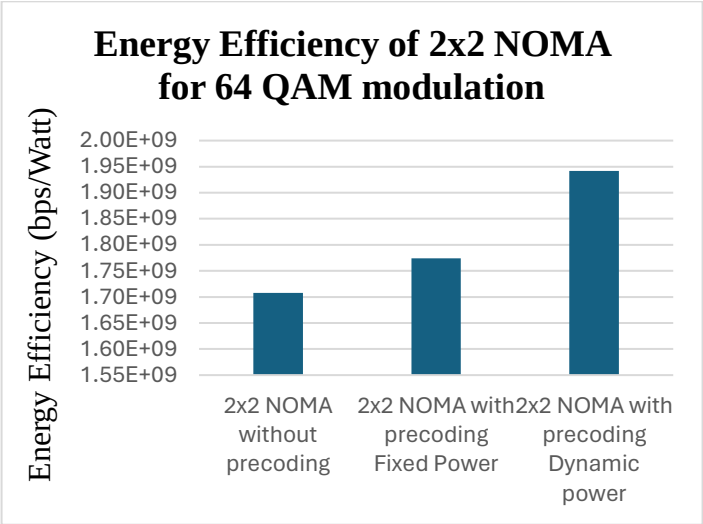


Fig 6.19: Comparison of Energy Efficiency of (2x2) PD-NOMA system for 64 QAM

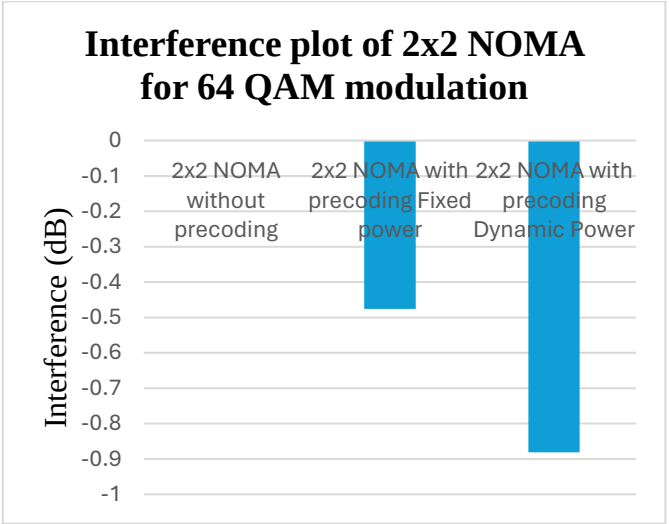


Fig 6.20: Comparison of total Interference of (2x2) PD-NOMA system for 64 QAM

Fig 6.1, Fig 6.5, Fig 6.9, Fig 6.13, and Fig 6.17 represent the comparison of Sum Capacity of a (2x2) Downlink-MIMO-PD-NOMA system in the presence and absence of SVD Precoding for 2 different power allocation schemes (FPA and Dynamic Power Allocation) using different modulation schemes. It is observed that Sum Capacity of the system increased when SVD Precoding technique is applied. Dynamic Power allocation scheme with SVD precoding technique provides the highest Sum Capacity of the system in all modulation schemes. This is because in Dynamic Power allocation scheme, power is allocated to the users based on the varying channel conditions and the user's throughput is influenced by the power allocation coefficient assigned to it. So, the Sum Capacity of the entire system increases.

Fig 6.2, Fig 6.6, Fig 6.10, Fig 6.14, and Fig 6.18 represent the comparison of Spectral Efficiency of a (2x2) Downlink-MIMO-PD-NOMA system in the presence and absence of SVD Precoding for 2 different power allocation schemes (FPA and Dynamic Power Allocation) using different modulation schemes. It is observed that Dynamic Power allocation scheme with SVD precoding technique provides the highest Spectral Efficiency of the system in all modulation schemes. This is because from Equation (38) we can see that Spectral Efficiency is directly proportional to Sum Capacity. So, Dynamic Power allocation scheme with SVD precoding technique provides the highest Spectral Efficiency.

Fig 6.4, Fig 6.8, Fig 6.12, Fig 6.16, and Fig 6.20 represent the comparison of Total Interference of a (2x2) Downlink-MIMO-PD-NOMA system in the presence and absence of SVD Precoding for 2 different power allocation schemes (FPA and Dynamic Power Allocation) using different modulation techniques. It is observed that Dynamic Power allocation scheme with SVD precoding technique provides the least Interference of the system in all modulation schemes. This is because in Dynamic Power allocation scheme, power is allocated to the users based on the varying channel conditions and the amount of Interference of any user is influenced by the power allocation coefficient assigned to it.

Fig 6.3, Fig 6.7, Fig 6.11, Fig 6.15, and Fig 6.19 represent the comparison of Energy Efficiency of a (2x2) Downlink-MIMO-PD-NOMA system in the presence and absence of SVD Precoding for 2 different power allocation schemes (FPA and Dynamic Power Allocation) using different modulation techniques. It is observed that Dynamic Power allocation scheme with SVD precoding technique provides the highest Energy Efficiency of the system in all modulation schemes. This is because from Equation (39) we can see that Energy Efficiency is related to total interference of the system and Dynamic Power allocation scheme with SVD precoding technique provides the least Interference of the system.

II. Performance analysis of different users SIMO-PD-NOMA system in presence and absence of precoding for different power allocation schemes and different modulation techniques:

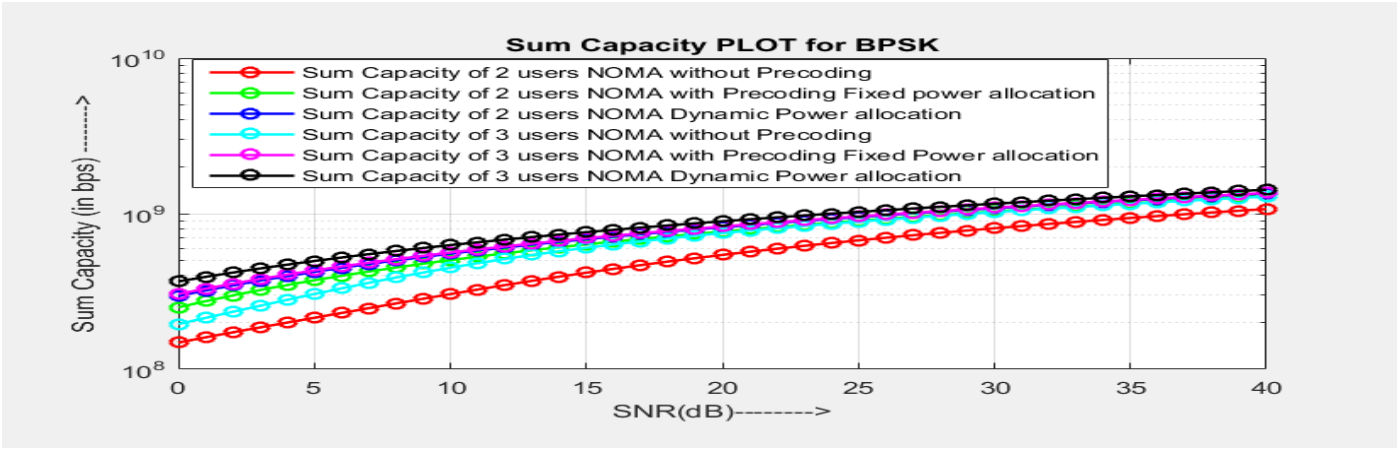


Fig 6.21: Comparison of Sum Capacity of different users SIMO-NOMA system for BPSK modulation

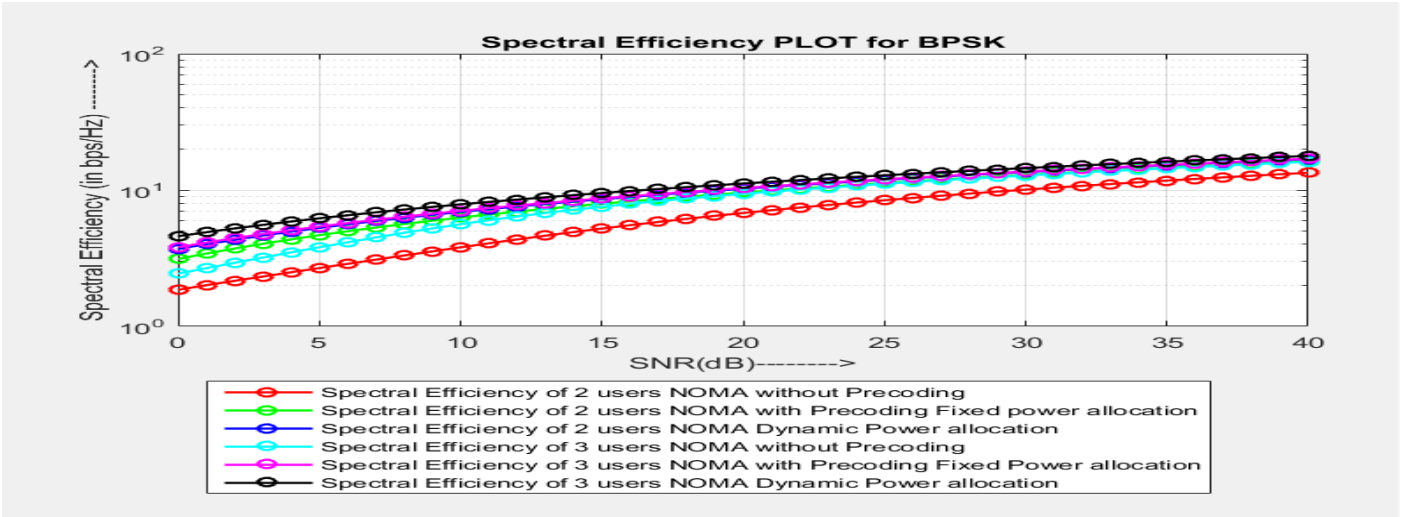


Fig 6.22: Comparison of Spectral Efficiency of different users SIMO-NOMA system for BPSK modulation

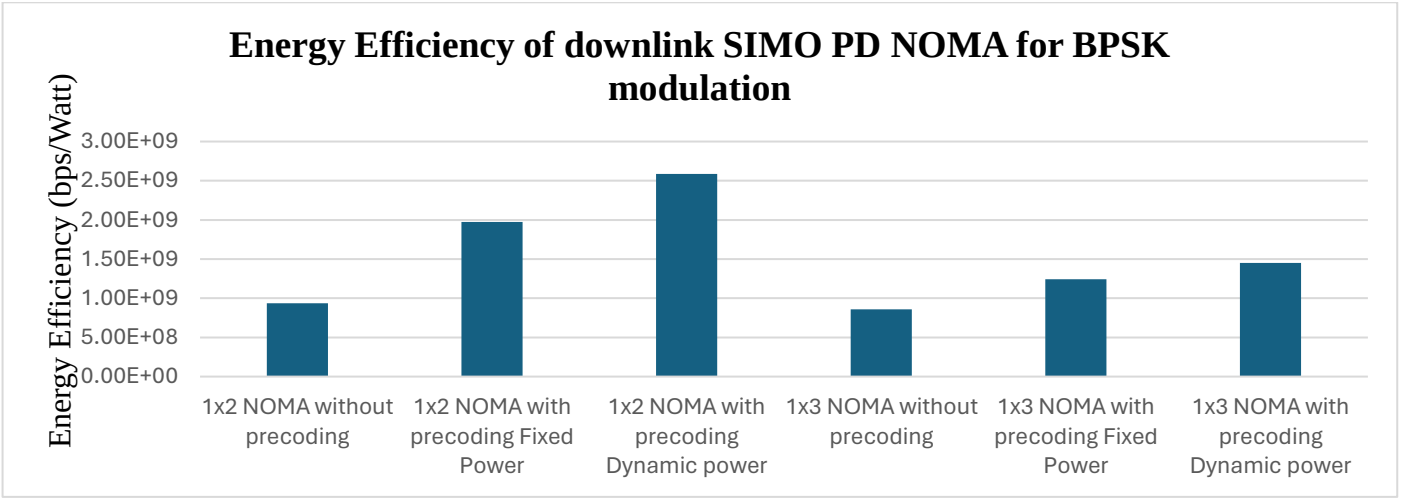


Fig 6.23: Comparison of Energy Efficiency of different users SIMO-NOMA system for BPSK modulation

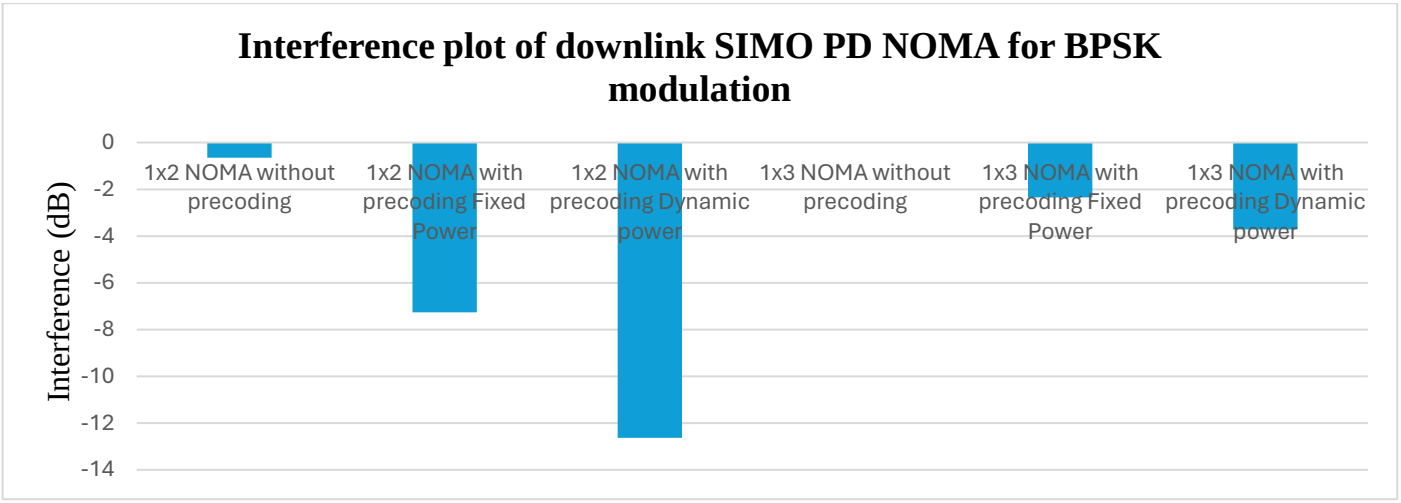


Fig 6.24: Comparison of total Interference of different users SIMO-NOMA system for BPSK modulation

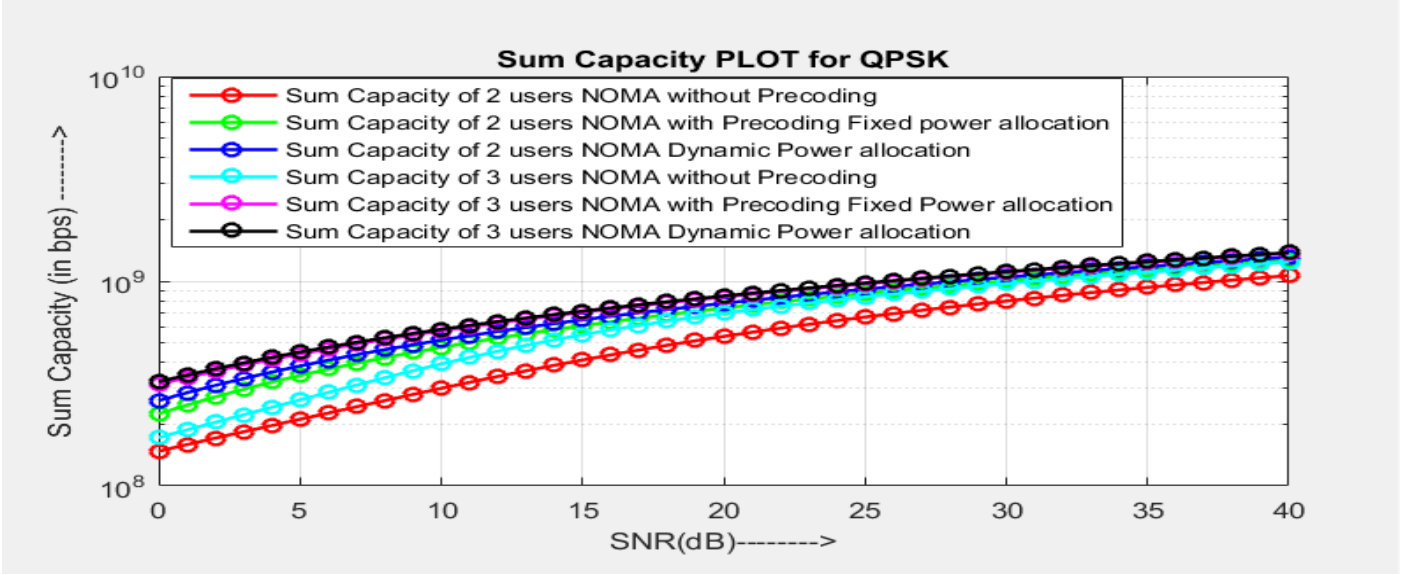


Fig 6.25: Comparison of Sum Capacity of different users SIMO-NOMA system for QPSK modulation

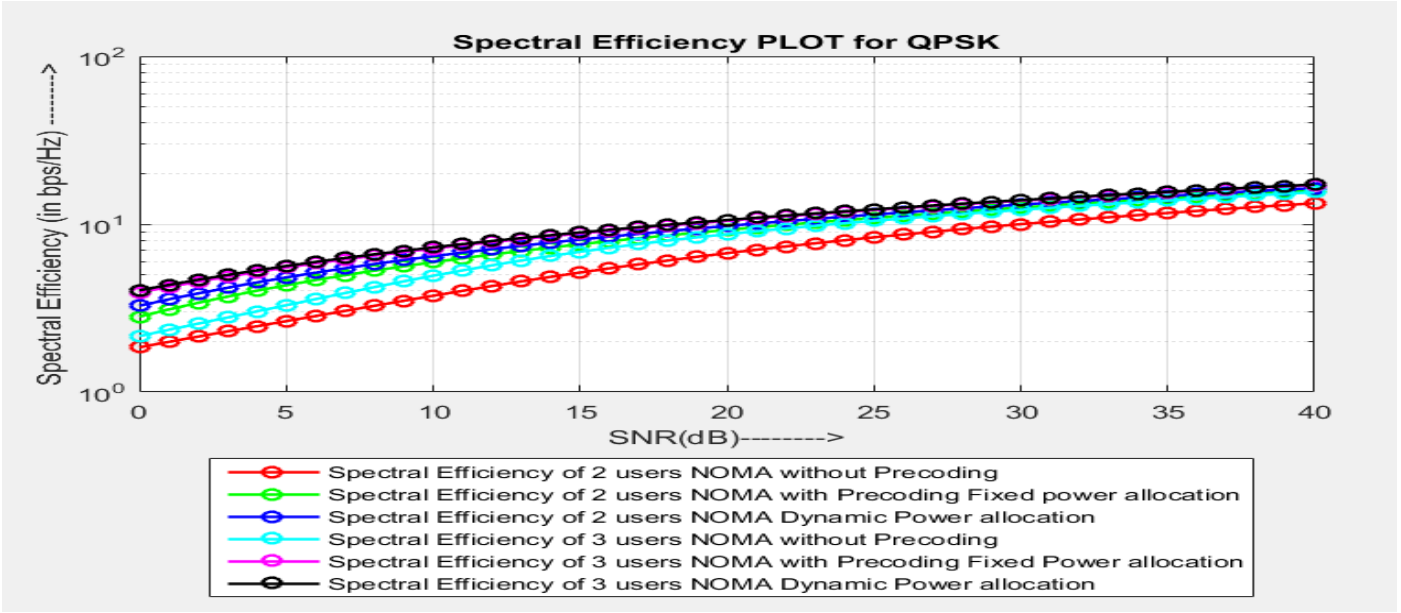


Fig 6.26: Comparison of Spectral Efficiency of different users SIMO-NOMA system for QPSK modulation

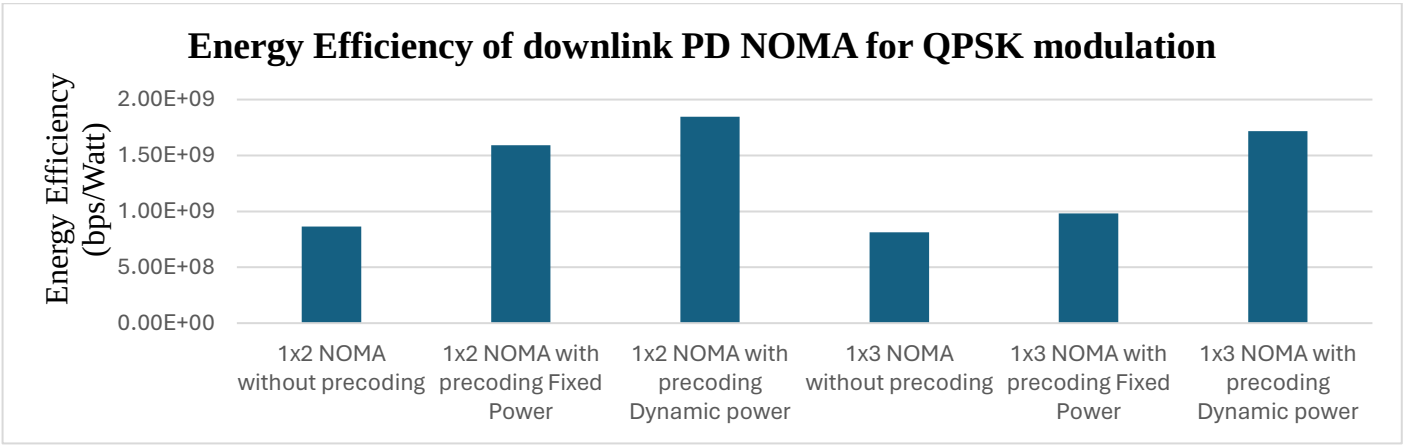


Fig 6.27: Comparison of Energy Efficiency of different users SIMO-NOMA system for QPSK modulation

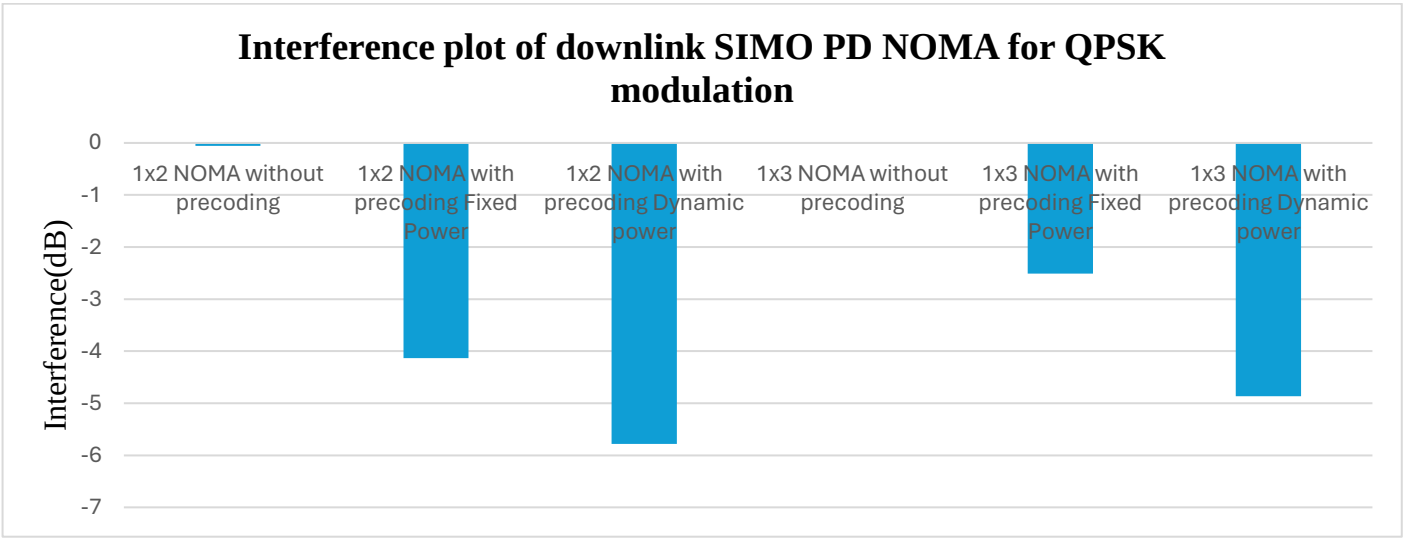


Fig 6.28: Comparison of total Interference of different users SIMO-NOMA system for QPSK modulation

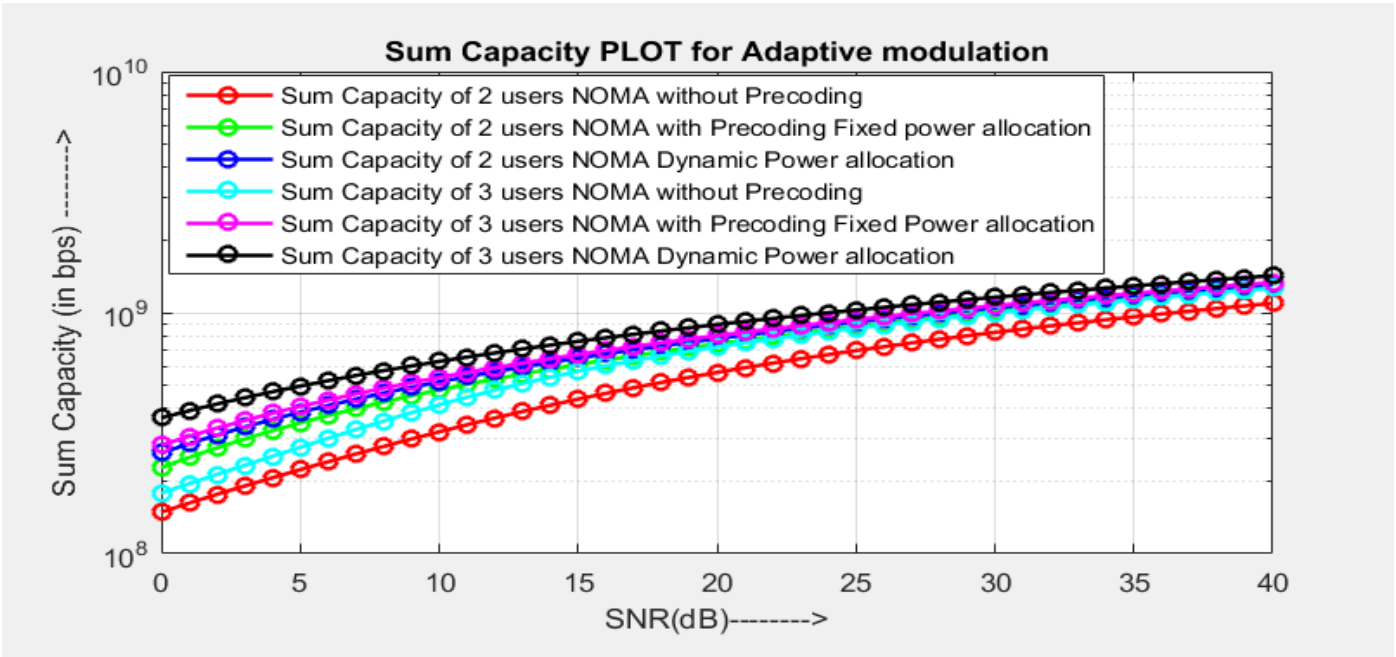


Fig 6.29: Comparison of Sum Capacity of different users SIMO-NOMA system for Adaptive modulation

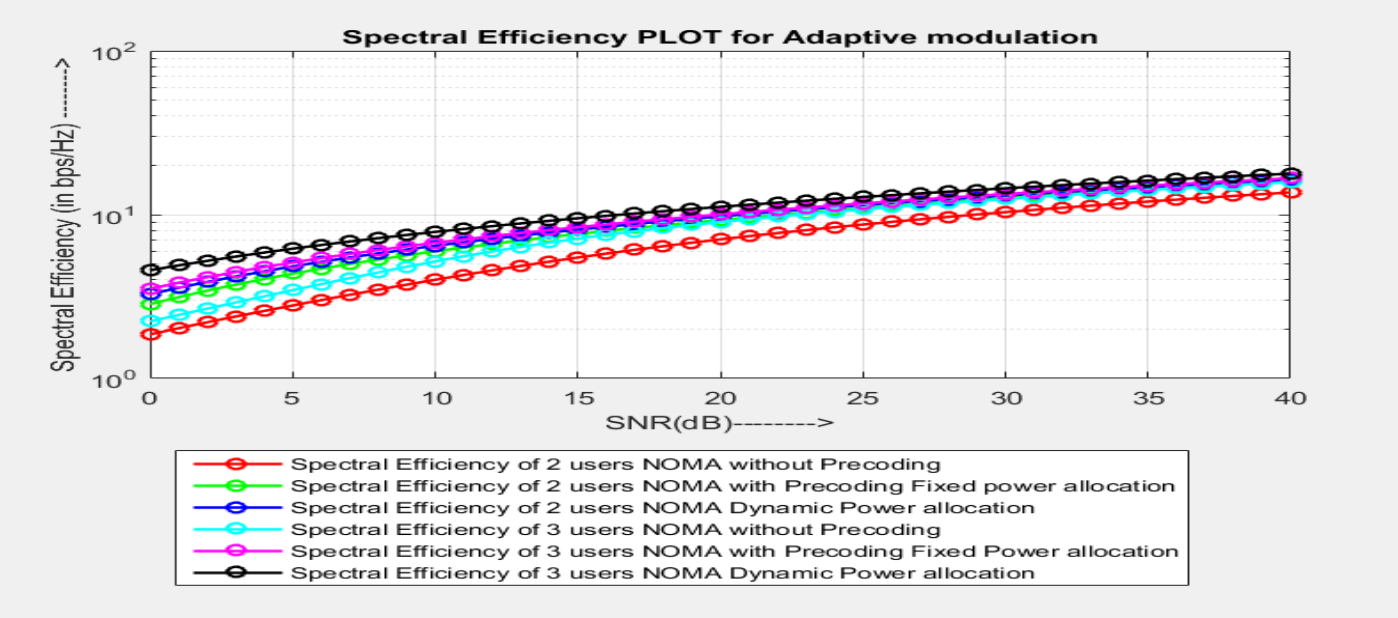


Fig 6.30: Comparison of Spectral Efficiency of different users SIMO-NOMA system for Adaptive modulation

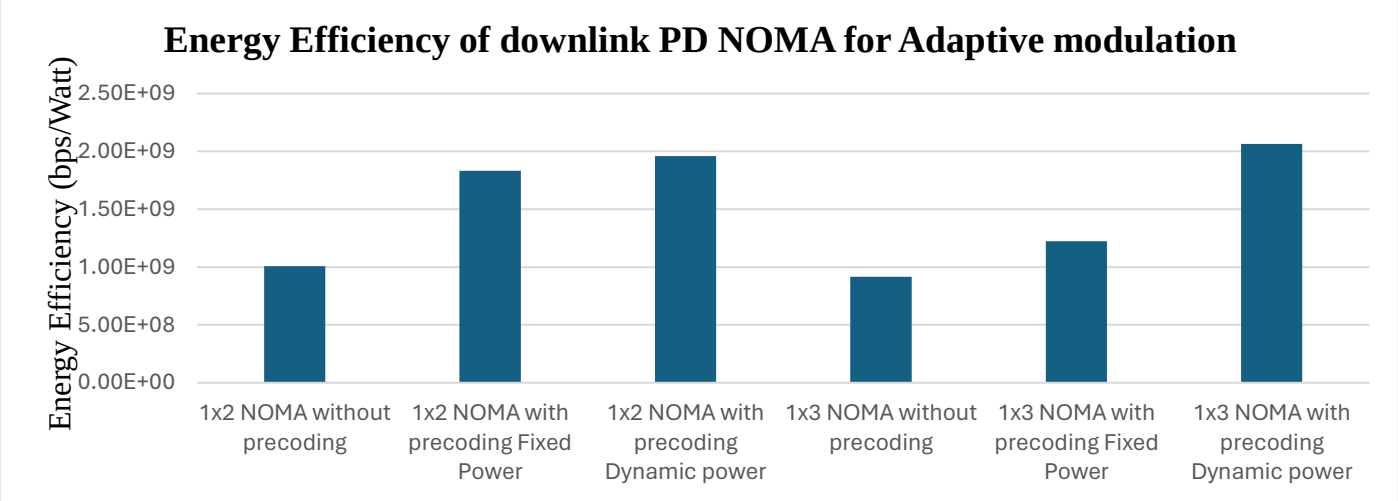


Fig 6.31: Comparison of Energy Efficiency of different users SIMO-NOMA system for Adaptive modulation

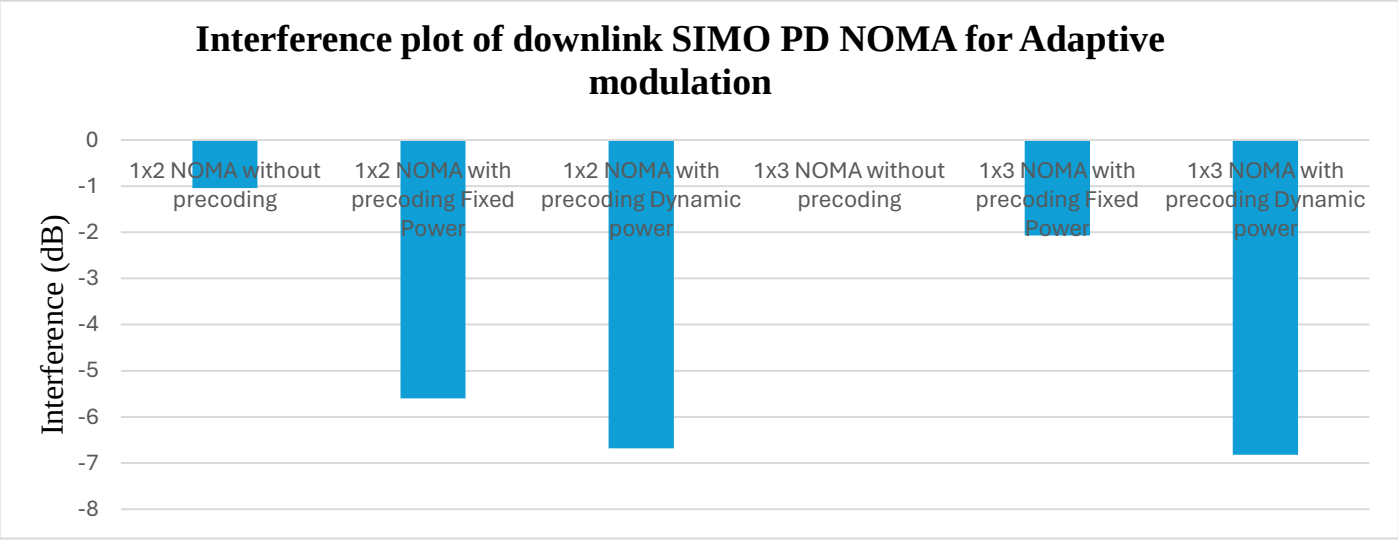


Fig 6.32: Comparison of total Interference of different users SIMO-NOMA system for Adaptive modulation

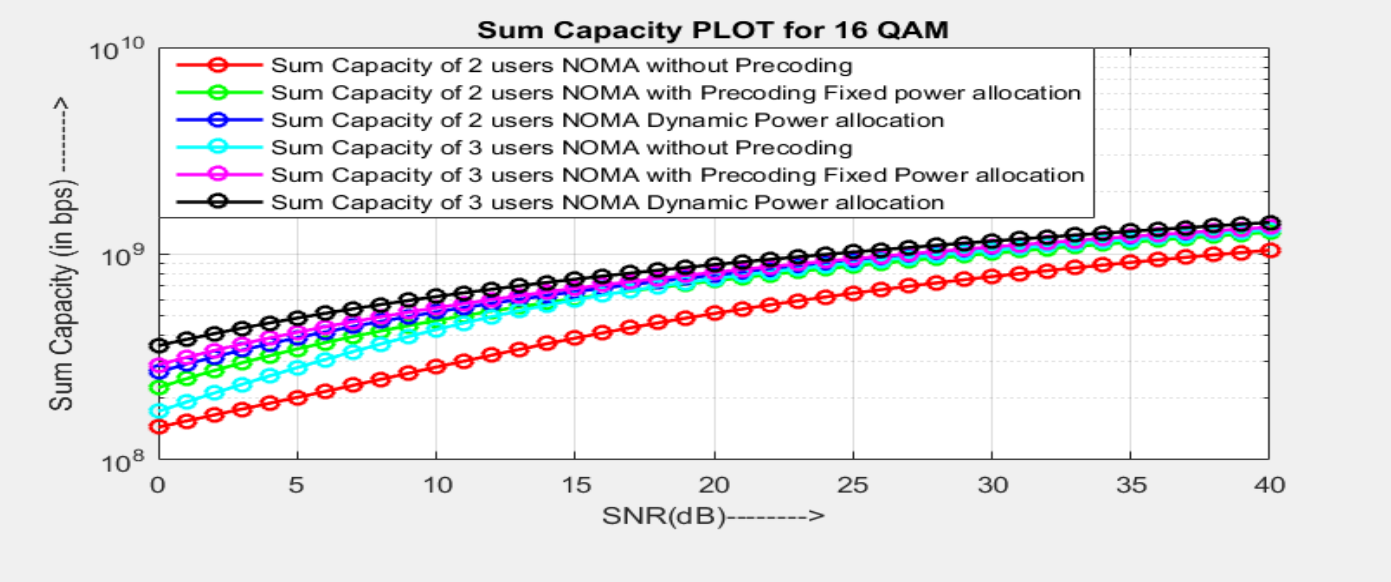


Fig 6.33: Comparison of Sum Capacity of different users SIMO-NOMA system for 16 QAM modulation

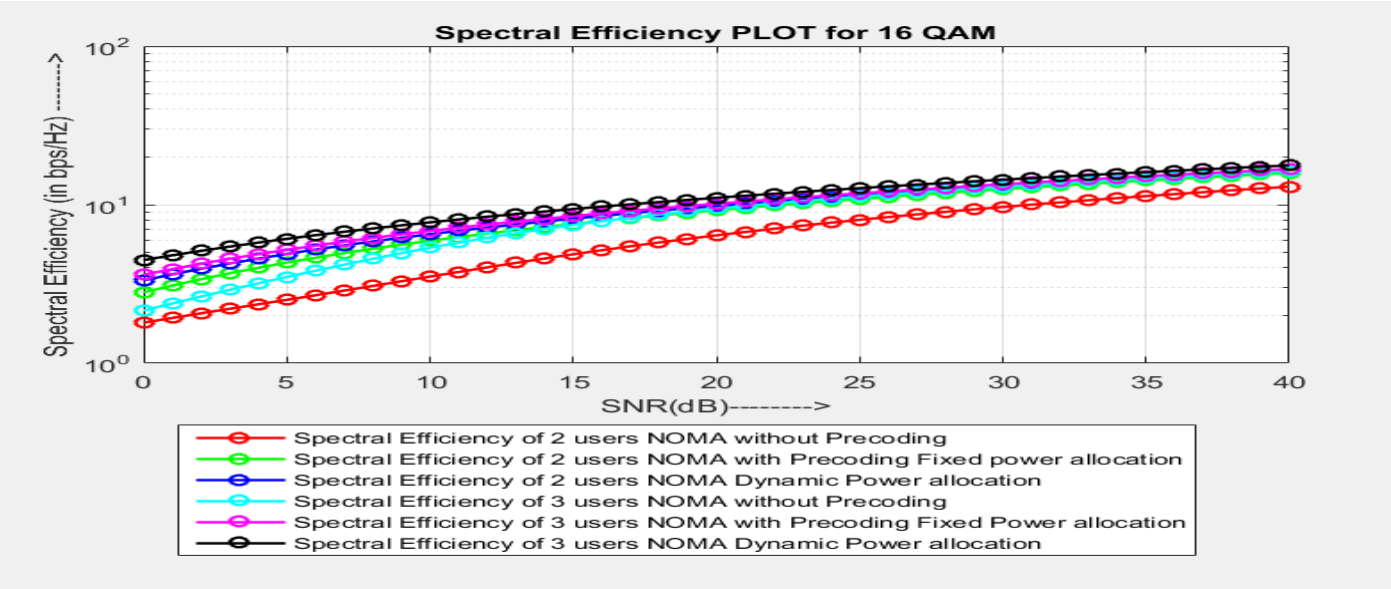


Fig 6.34: Comparison of Spectral Efficiency of different users SIMO-NOMA system for 16 QAM modulation

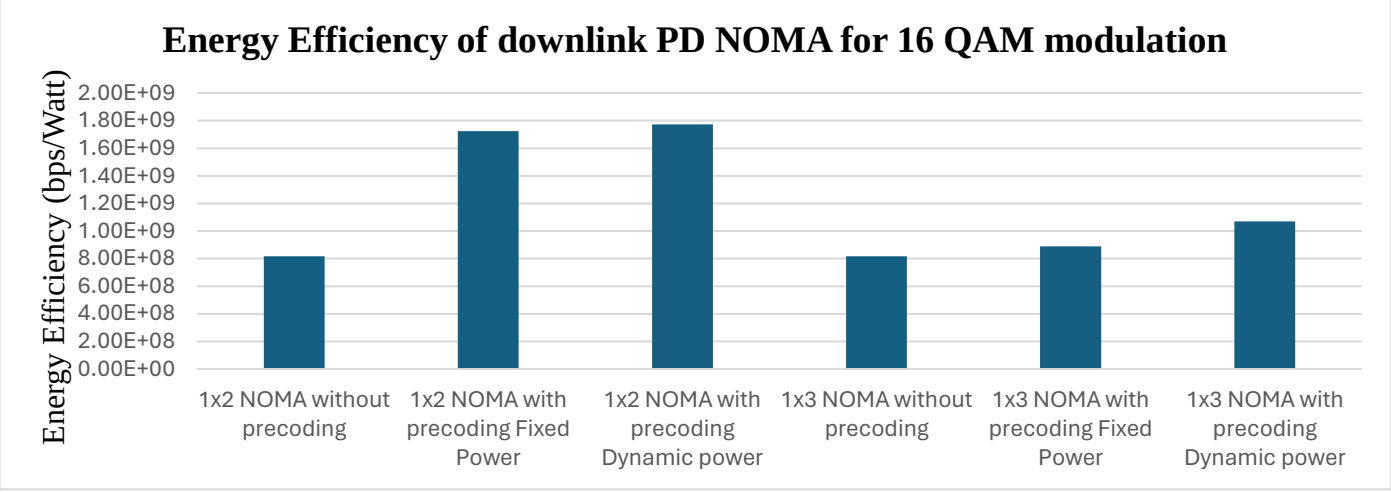


Fig 6.35: Comparison of Energy Efficiency of different users SIMO-NOMA system for 16 QAM modulation

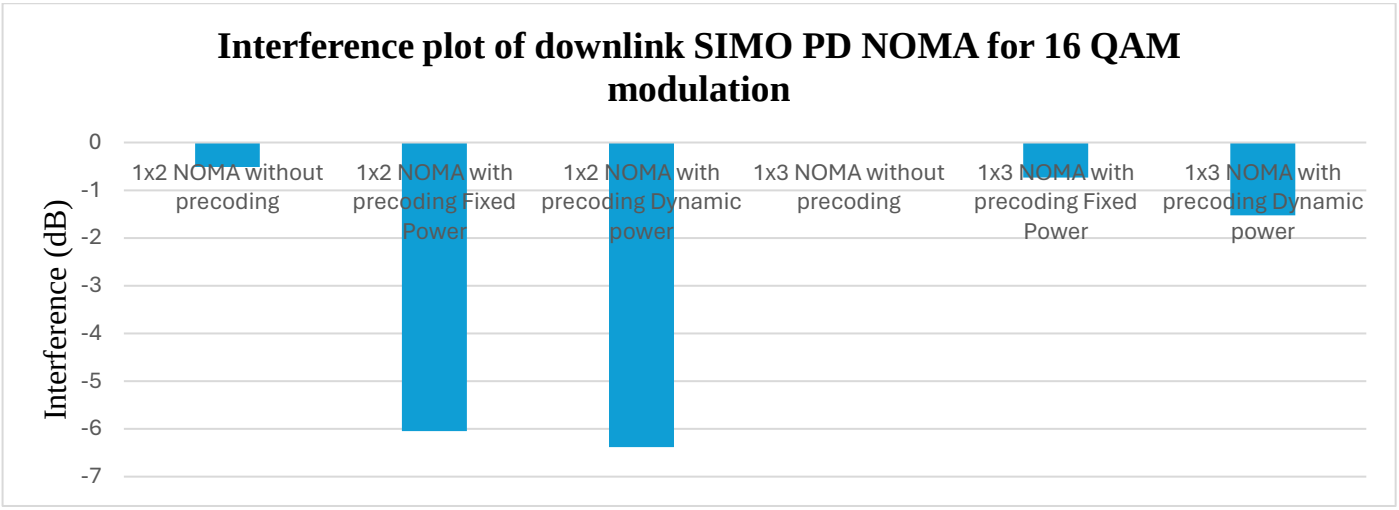


Fig 6.36: Comparison of total Interference of different users SIMO-NOMA system for 16 QAM modulation

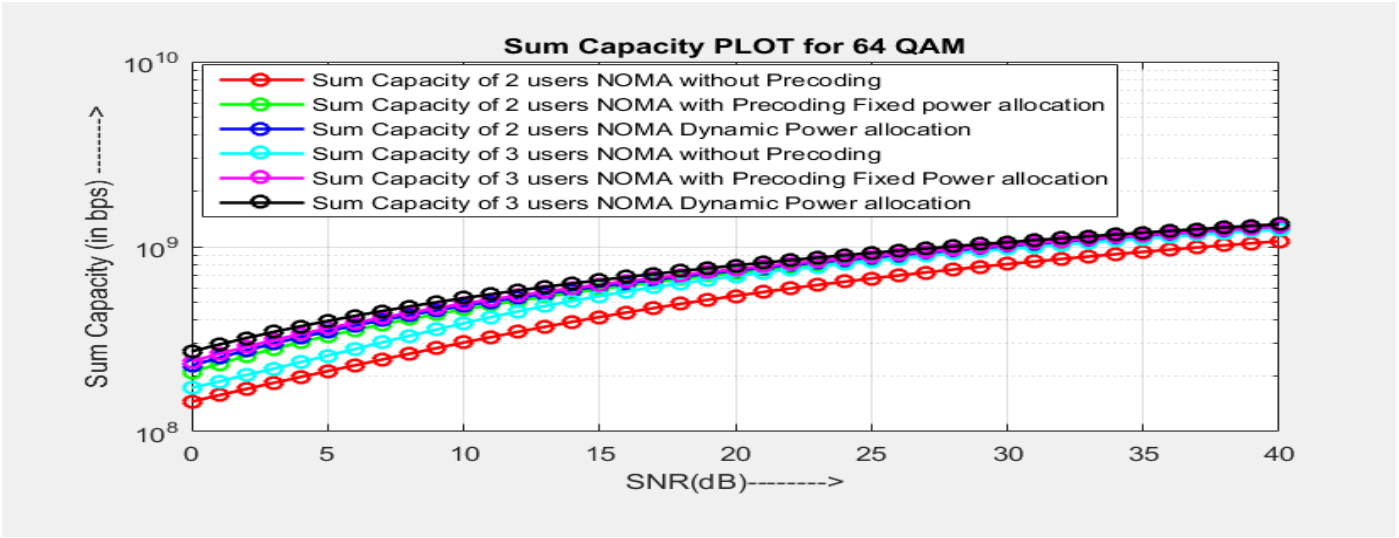


Fig 6.37: Comparison of Sum Capacity of different users SIMO-NOMA system for 64 QAM modulation

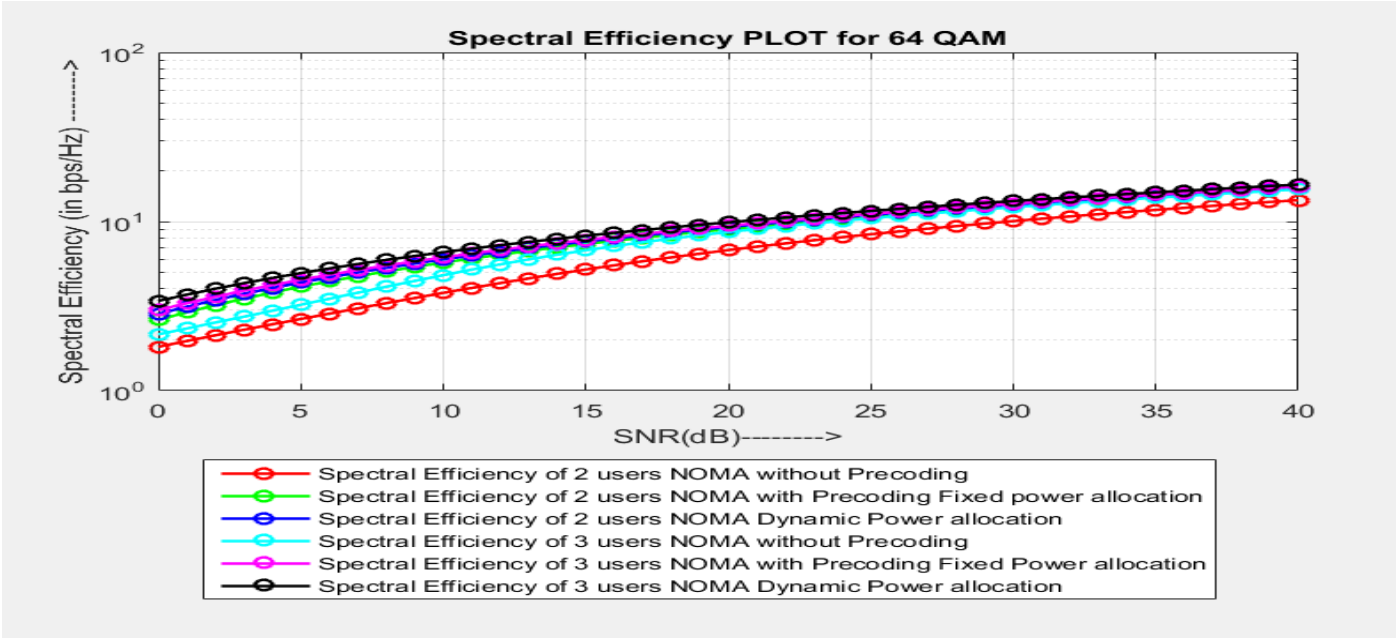


Fig 6.38: Comparison of Spectral Efficiency of different users SIMO-NOMA system for 64 QAM modulation

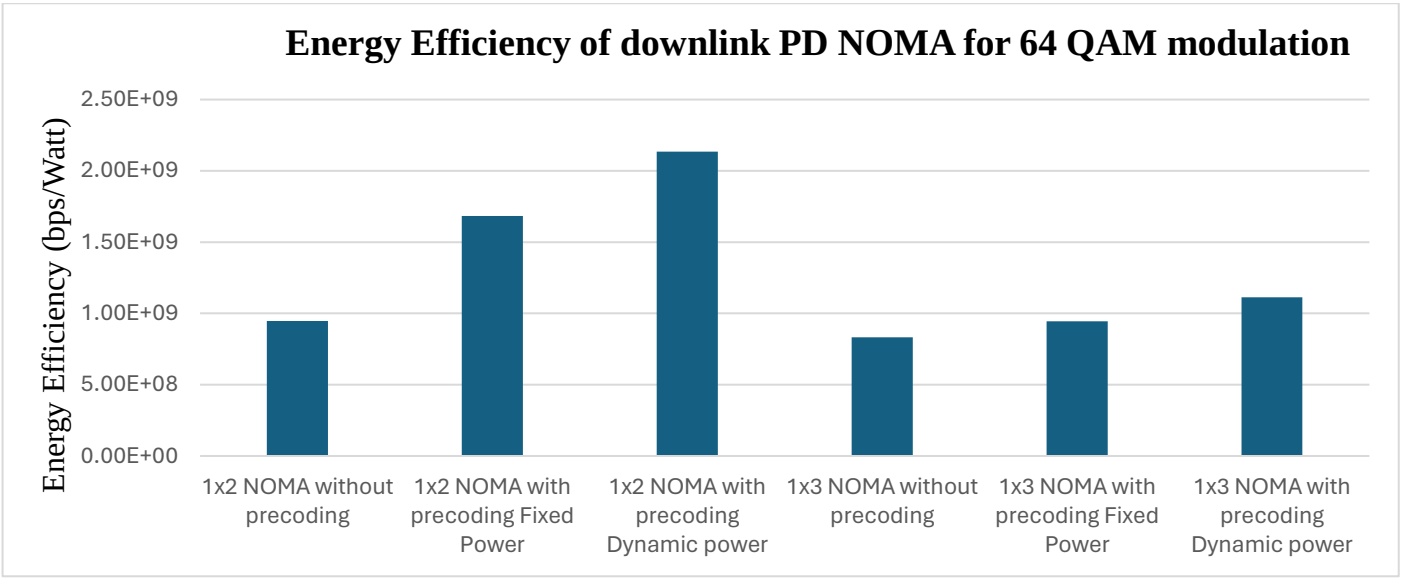


Fig 6.39: Comparison of Energy Efficiency of different users SIMO-NOMA system for 64 QAM modulation

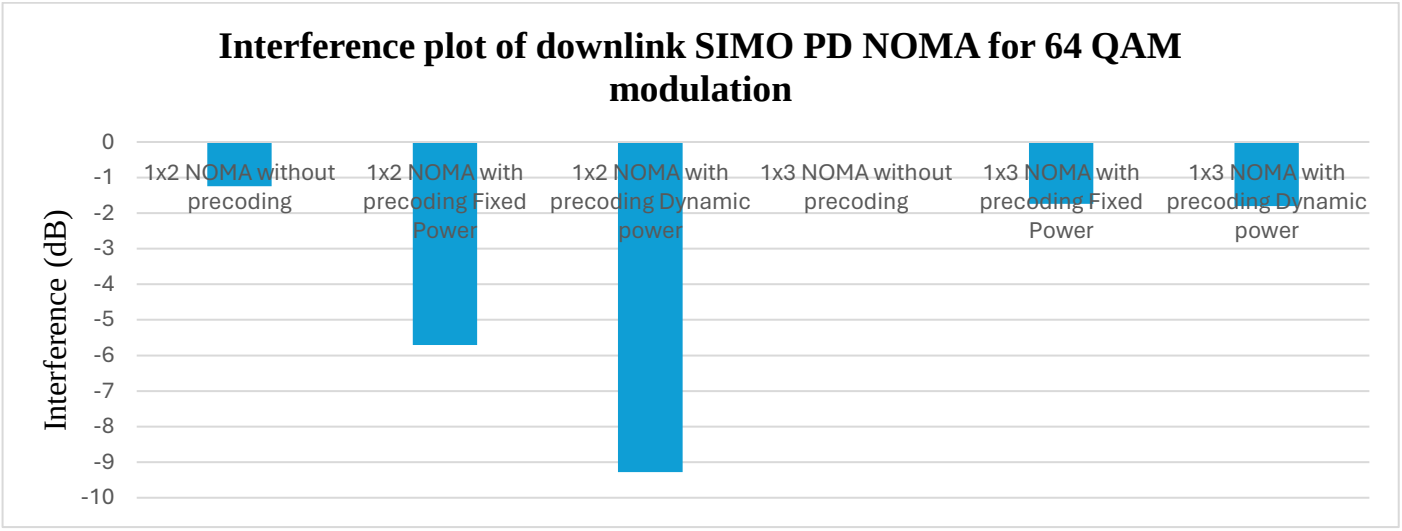


Fig 6.40: Comparison of total Interference of different users SIMO-NOMA system for 64 QAM modulation

Fig 6.21, Fig 6.25, Fig 6.29, Fig 6.33, and Fig 6.37 represent the comparison of Sum Capacity of different users SIMO Downlink-PD-NOMA system in the presence and absence of SVD Precoding for 2 different power allocation schemes (FPA and Dynamic Power Allocation) using different modulation schemes. It is observed that as the number of users is increased, Sum Capacity of the system is increased in the presence of SVD Precoding technique under Dynamic power allocation. This is because with the increase in the number of users, throughput of the system increases. Precoding technique is used to reduce the interference and channel impairments. In Dynamic power allocation scheme, power is distributed to all the users in accordance with changing channel circumstances, and the power allocation coefficient assigned to each user affects its throughput.

Fig 6.22, Fig 6.26, Fig 6.30, Fig 6.34, and Fig 6.38 represent the comparison of Spectral Efficiency of different users SIMO Downlink-PD-NOMA system in the presence and absence of SVD

Precoding for 2 different power allocation schemes (FPA and Dynamic Power Allocation) using different modulation schemes. It is observed that as the number of users is increased, Spectral Efficiency of the system is increased in the presence of SVD Precoding technique under Dynamic power allocation. This is because Spectral Efficiency is directly proportional to the Sum Capacity of the system and the maximum Sum Capacity is achieved under SVD Precoding technique in conjunction with dynamic power allocation scheme.

Fig 6.24, Fig 6.28, Fig 6.32, Fig 6.36, and Fig 6.40 represent the comparison of total Interference of different users SIMO Downlink-PD-NOMA system in the presence and absence of SVD Precoding for 2 different power allocation schemes (FPA and Dynamic Power Allocation) using different modulation techniques. It is observed that as the number of users is increased, total Interference of the system is increased. For any particular number of users, in the presence of SVD Precoding technique under Dynamic power allocation provides less amount of Interference compared to NOMA without precoding system. This is because Precoding technique is used to reduce the channel impairments. In dynamic power allocation scheme, power is allocated to all the users based on the channel condition and the amount of Interference of any user is affected by the power allocation coefficient assigned to it.

Fig 6.23, Fig 6.27, Fig 6.31, Fig 6.35, and Fig 6.39 represent the comparison of Energy Efficiency of different users SIMO Downlink-PD-NOMA system in the presence and absence of SVD Precoding for 2 different power allocation schemes (FPA and Dynamic Power Allocation) using different modulation schemes. It is observed that as the number of users is increased, Energy Efficiency of the system is decreased. For any particular number of users, in the presence of SVD Precoding technique under Dynamic power allocation provides more Energy Efficiency compared to NOMA without precoding system. This is because Energy Efficiency is related to the amount of interference of the system. SVD precoding technique along with Dynamic power allocation scheme provides least amount of Interference.

Performance analysis of 1x3 SIMO-PD-NOMA Clustering system with 1x3 SIMO-PD-NOMA system in presence and absence of precoding for different power allocation schemes and different modulation techniques:

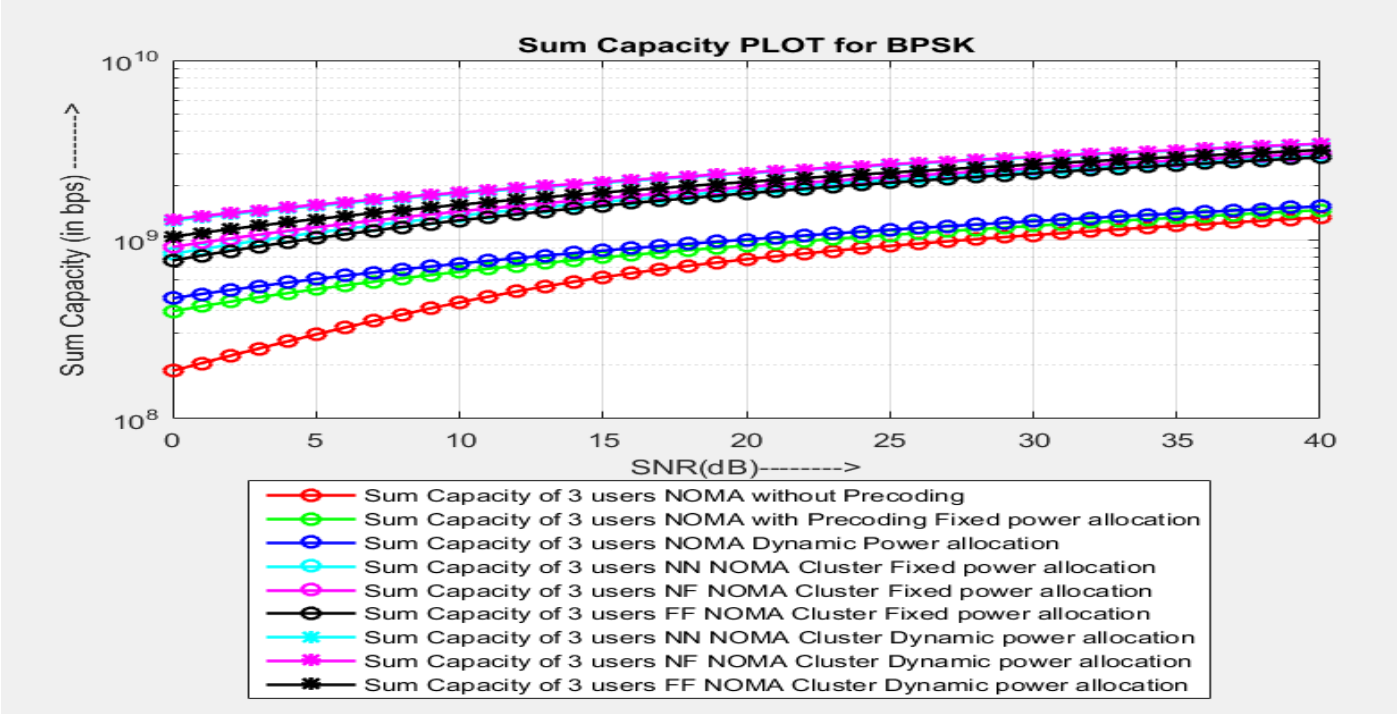


Fig 6.41: Comparison of Sum Capacity of 1x3 NOMA with NOMA Clustering system for BPSK modulation

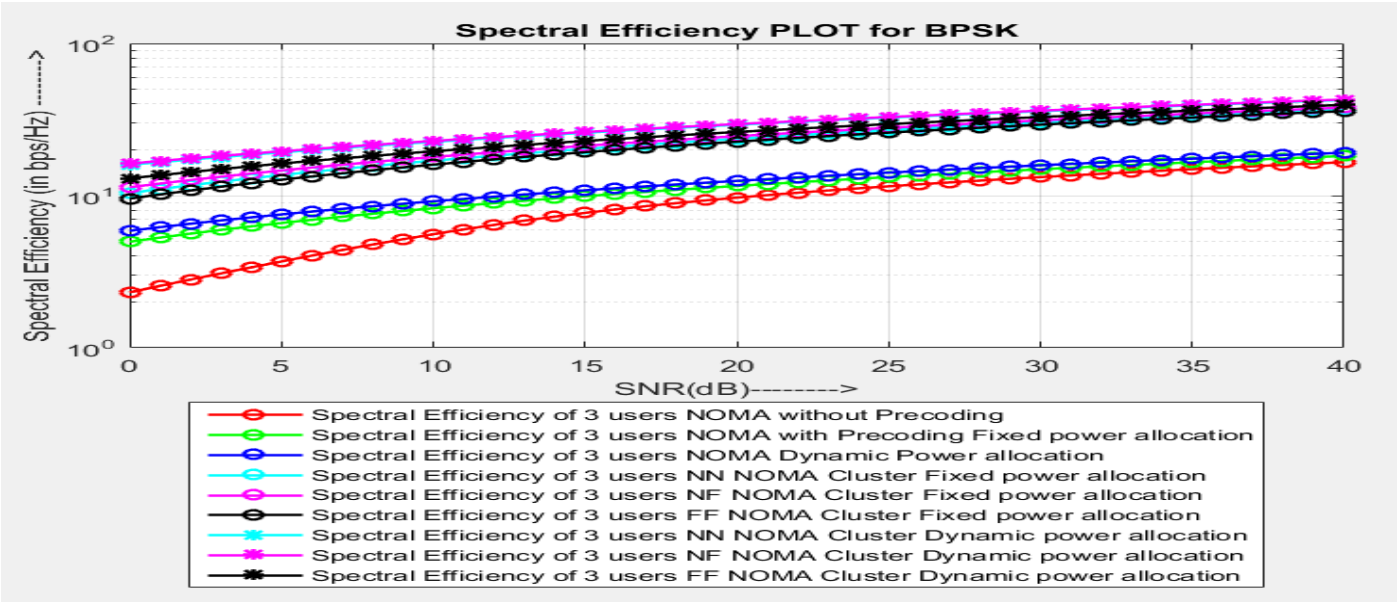


Fig 6.42: Comparison of Spectral Efficiency of 1x3 NOMA with NOMA Clustering system for BPSK modulation

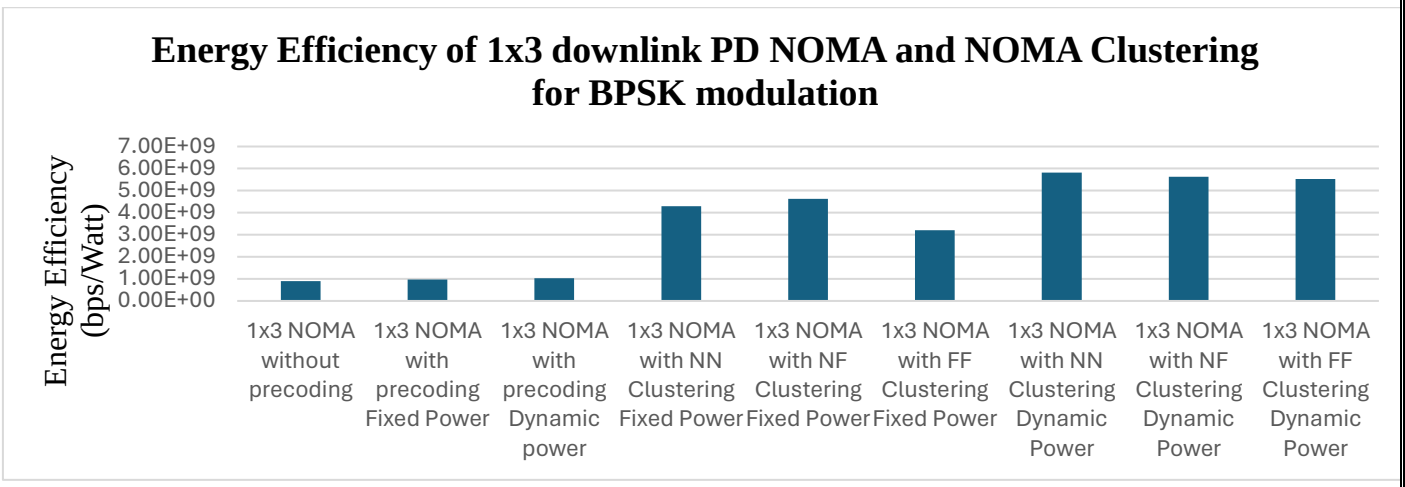


Fig 6.43: Comparison of Energy Efficiency of 1x3 NOMA with NOMA Clustering system for BPSK modulation

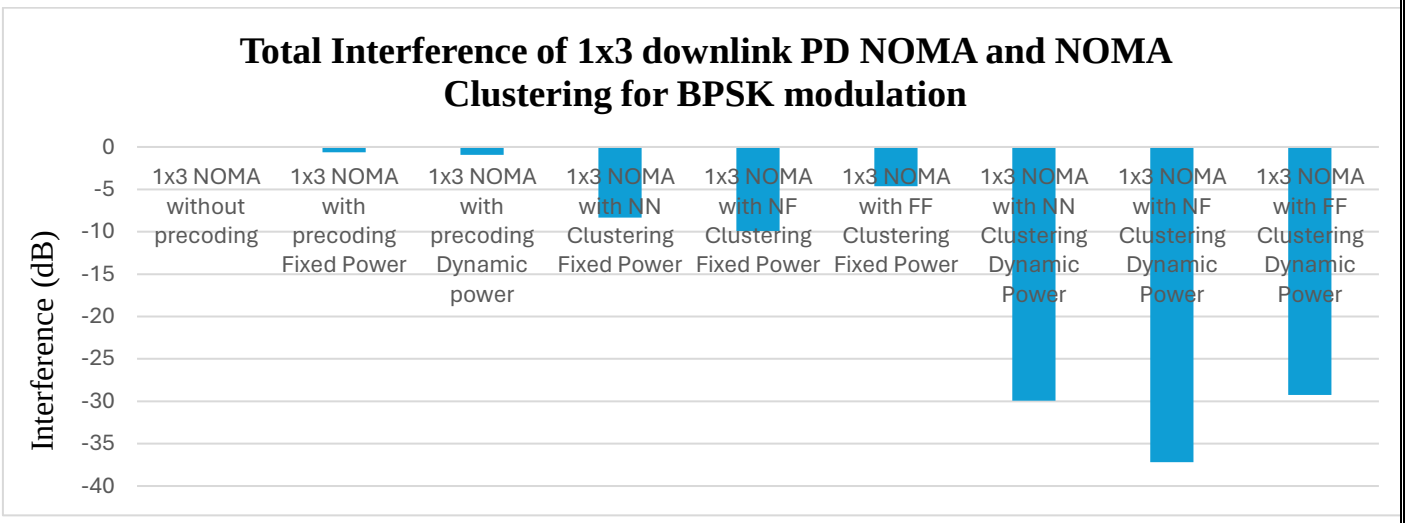


Fig 6.44: Comparison of total Interference of 1x3 NOMA with NOMA Clustering system for BPSK modulation

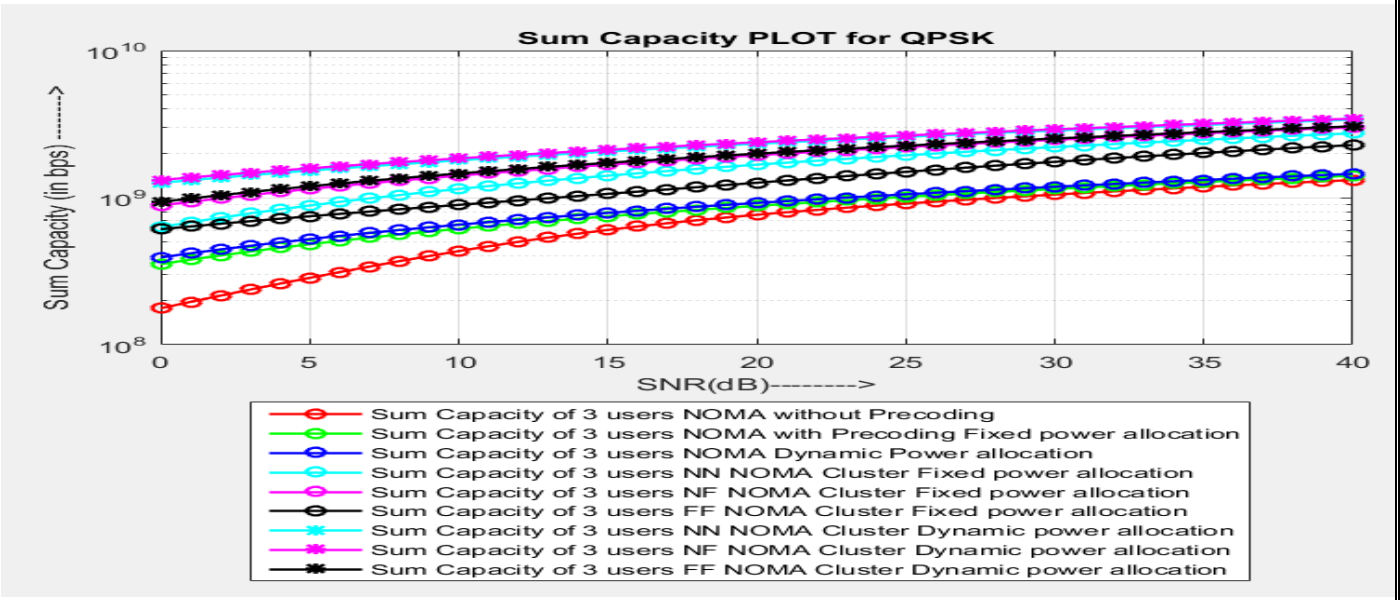


Fig 6.45: Comparison of Sum Capacity of 1x3 NOMA with NOMA Clustering system for QPSK modulation

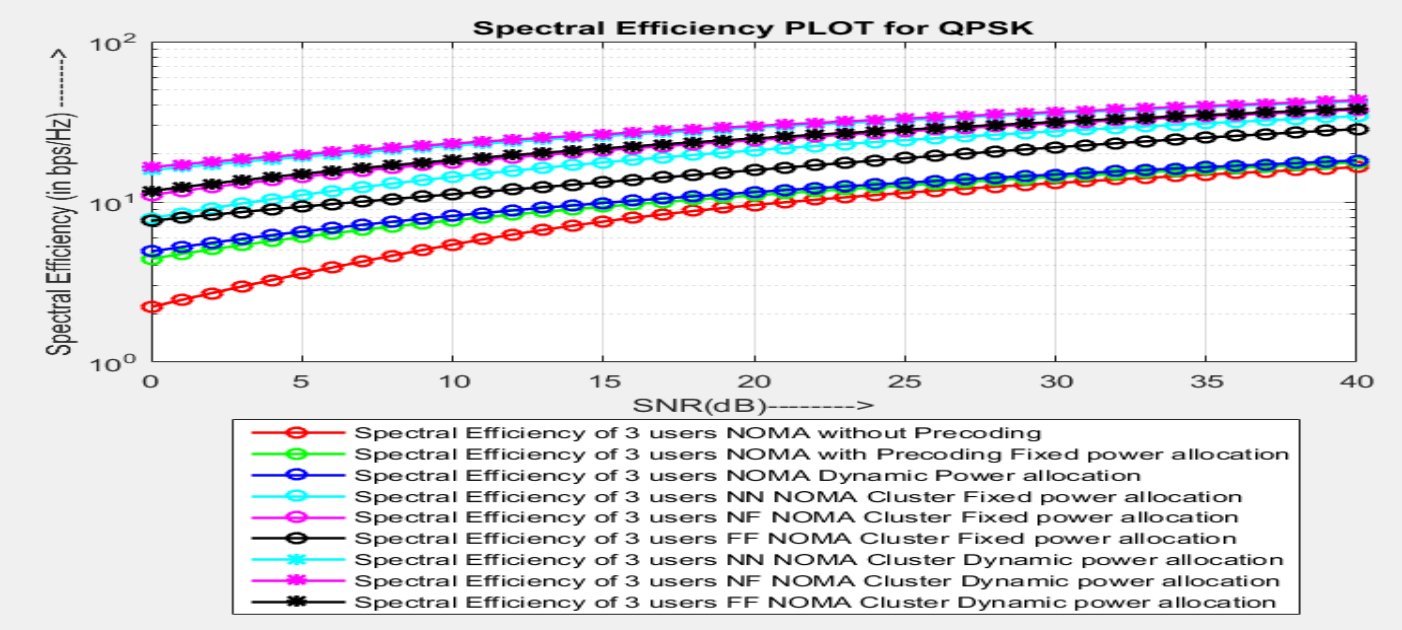


Fig 6.46: Comparison of Spectral Efficiency of 1x3 NOMA with NOMA Clustering system for QPSK modulation

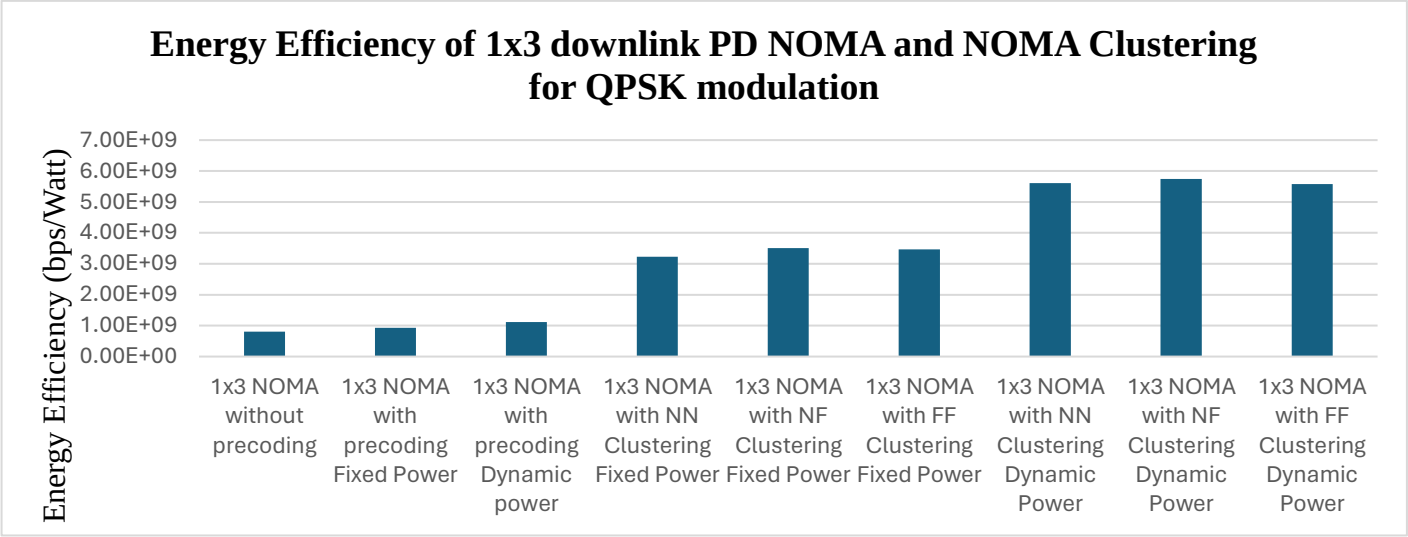


Fig 6.47: Comparison of Energy Efficiency of 1x3 NOMA with NOMA Clustering system for QPSK modulation

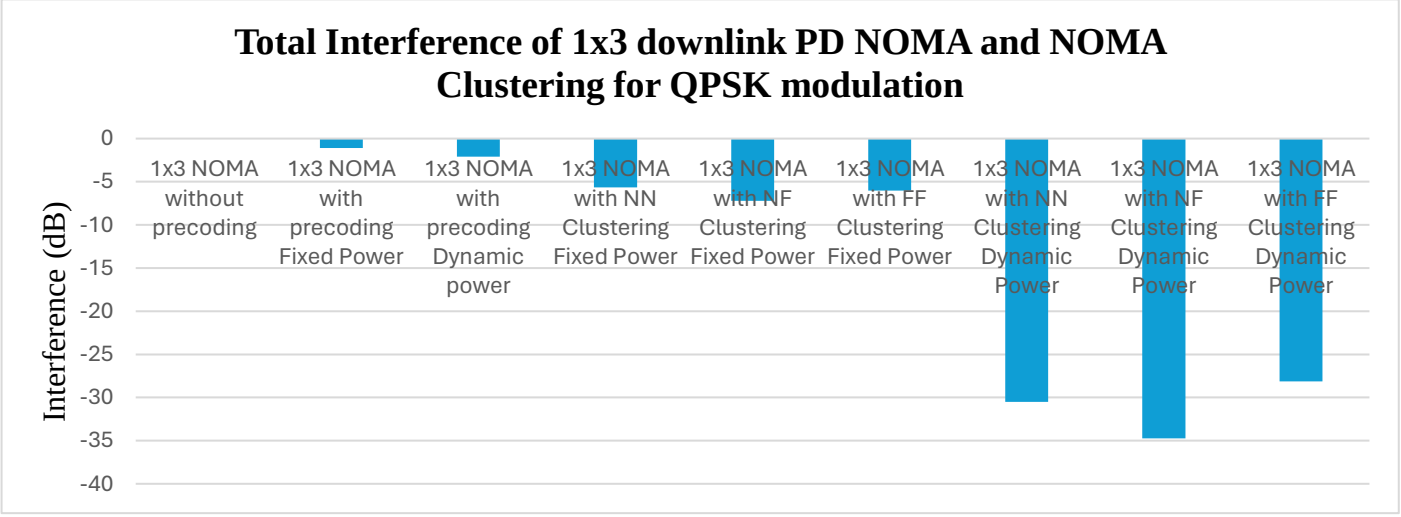


Fig 6.48: Comparison of total Interference of 1x3 NOMA with NOMA Clustering system for QPSK modulation

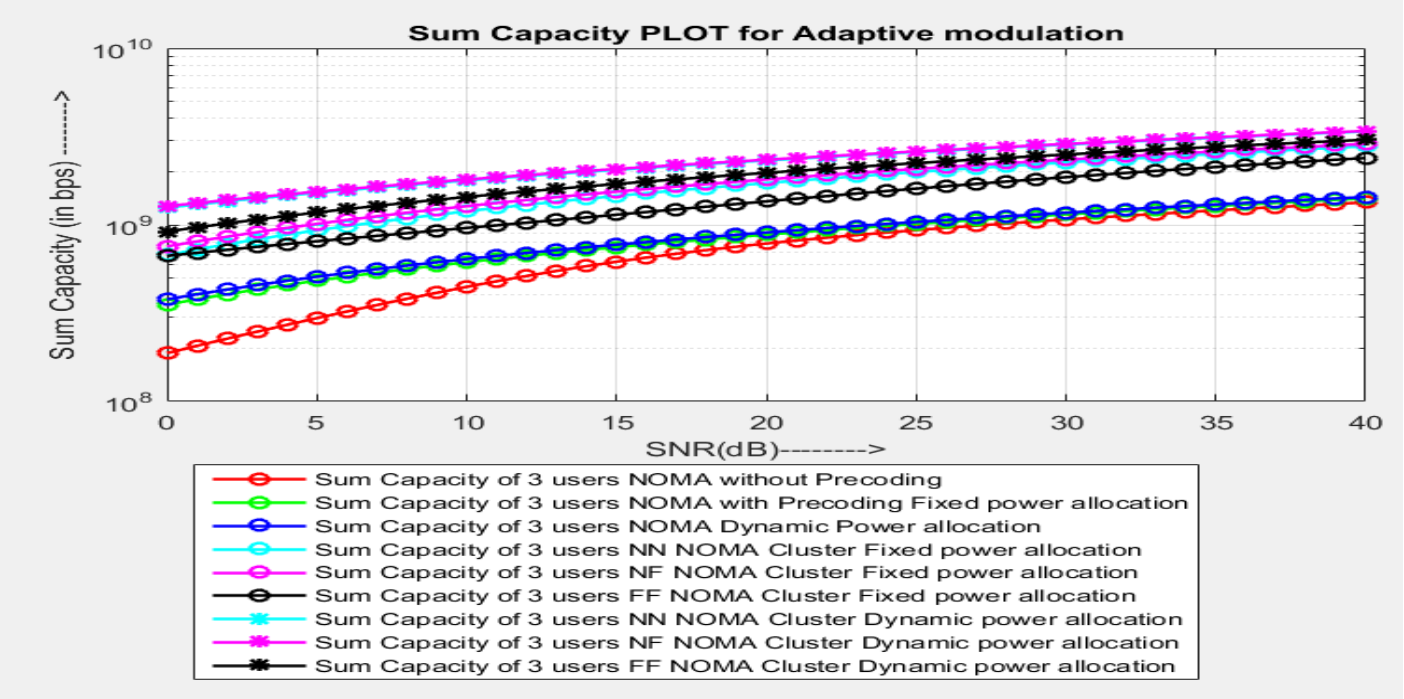


Fig 6.49: Comparison of Sum Capacity of 1x3 NOMA with NOMA Clustering system for Adaptive modulation

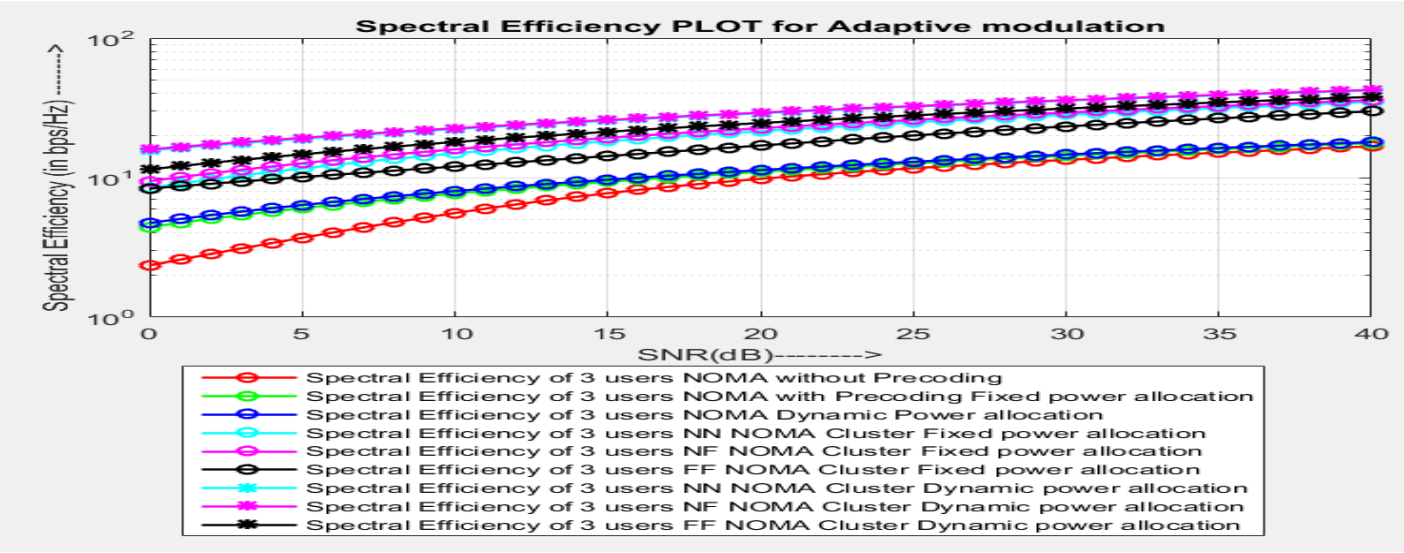


Fig 6.50: Comparison of Spectral Efficiency of 1x3 NOMA with NOMA Clustering system for Adaptive modulation

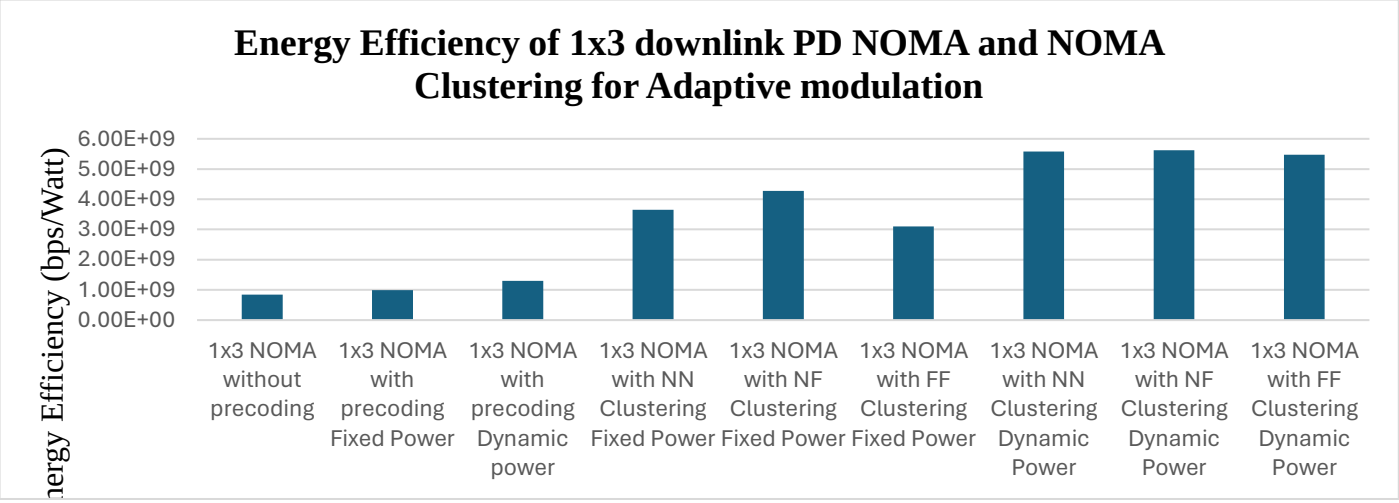


Fig 6.51: Comparison of Energy Efficiency of 1x3 NOMA with NOMA Clustering system for Adaptive modulation

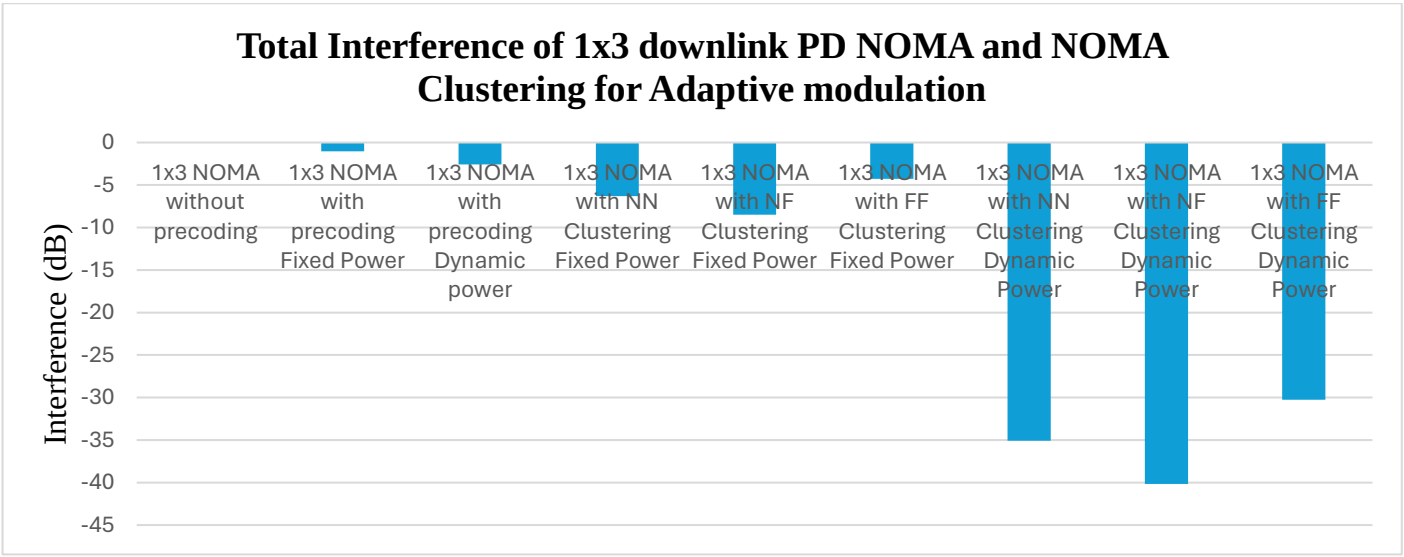


Fig 6.52: Comparison of total Interference of 1x3 NOMA with NOMA Clustering system for Adaptive modulation

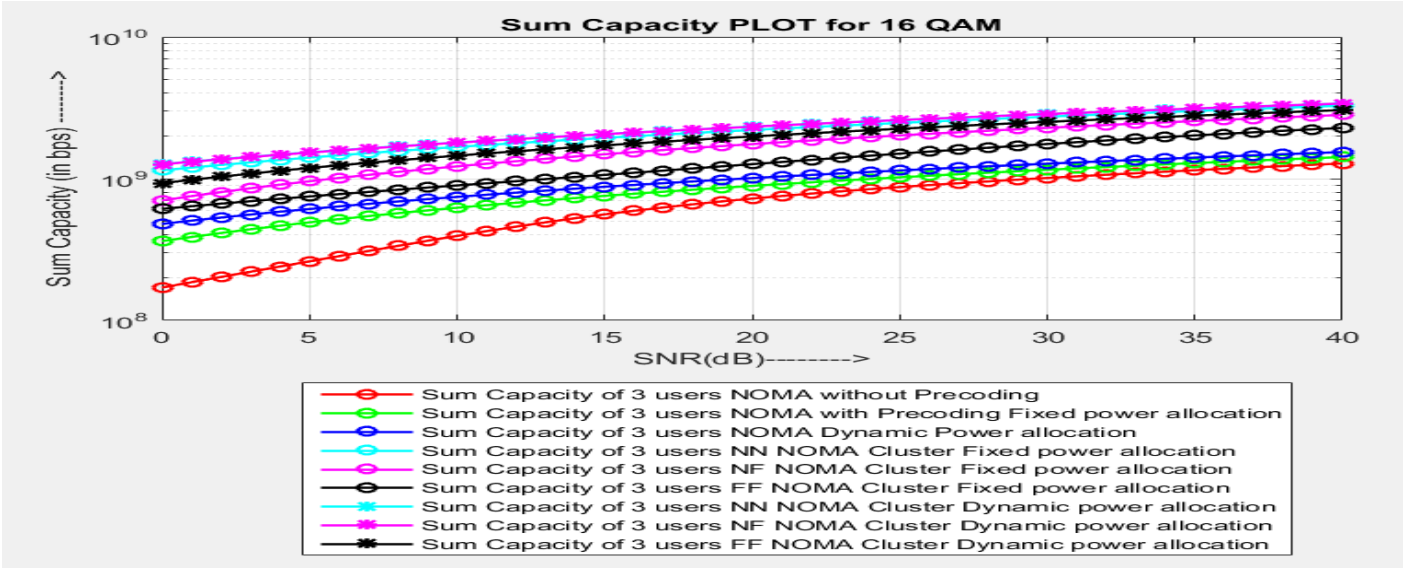


Fig 6.53: Comparison of Sum Capacity of 1x3 NOMA with NOMA Clustering system for 16 QAM modulation

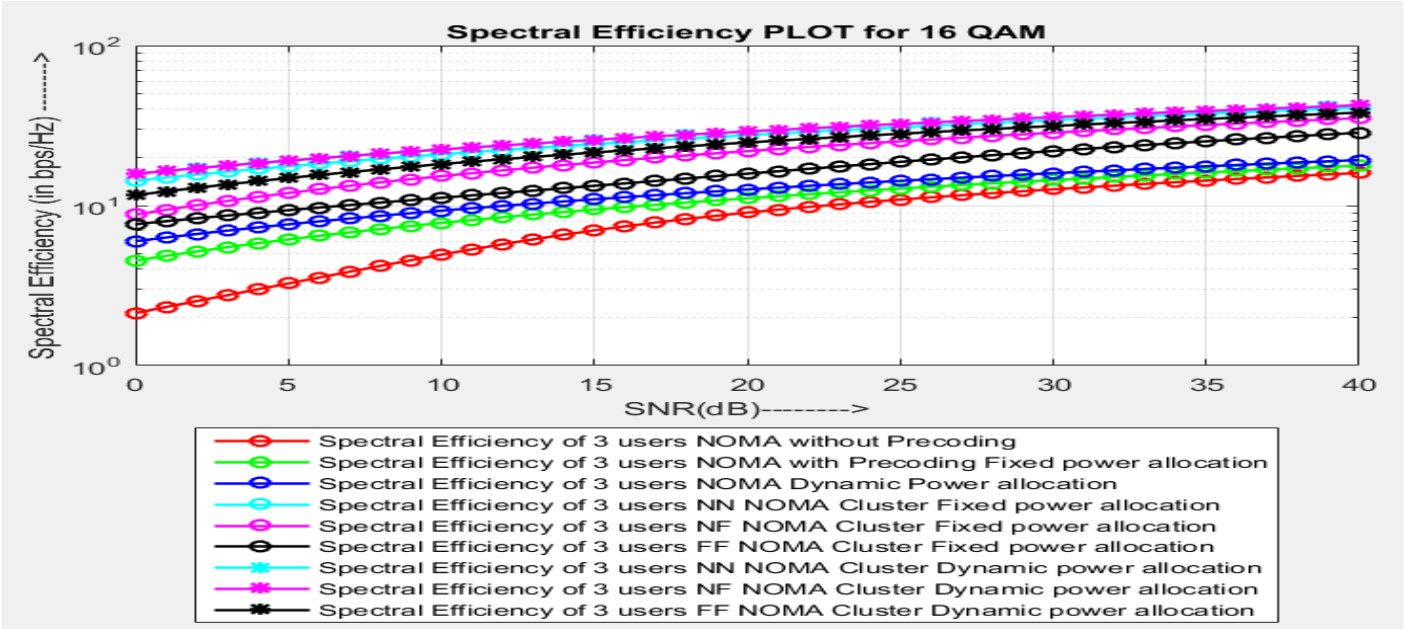


Fig 6.54: Comparison of Spectral Efficiency of 1x3 NOMA with NOMA Clustering system for 16 QAM modulation

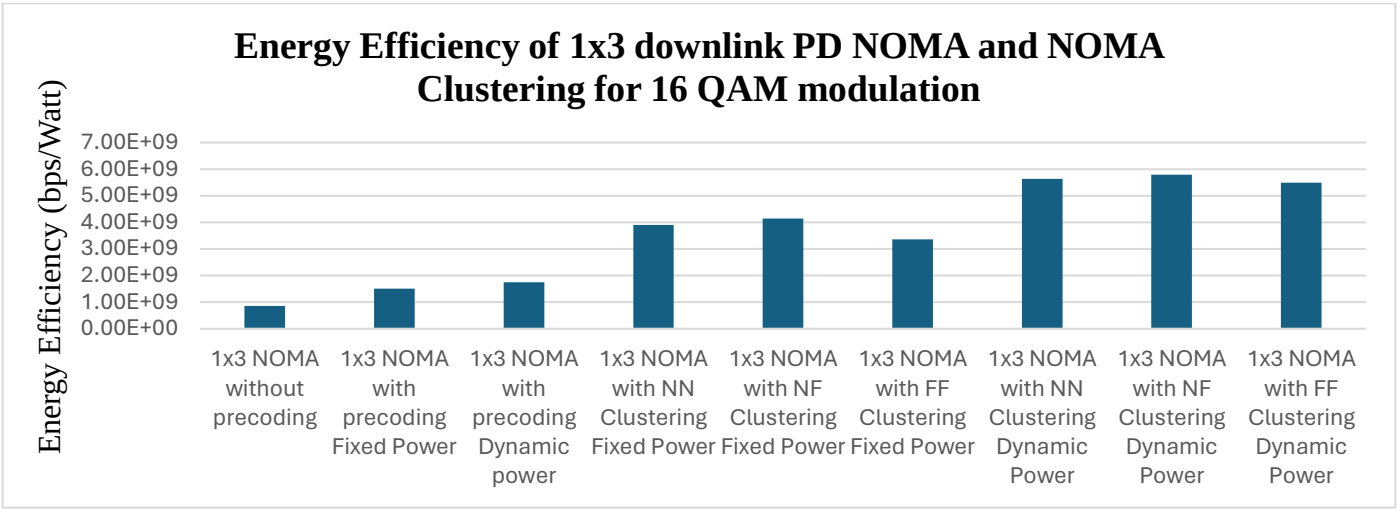


Fig 6.55: Comparison of Energy Efficiency of 1x3 NOMA with NOMA Clustering system for 16 QAM modulation

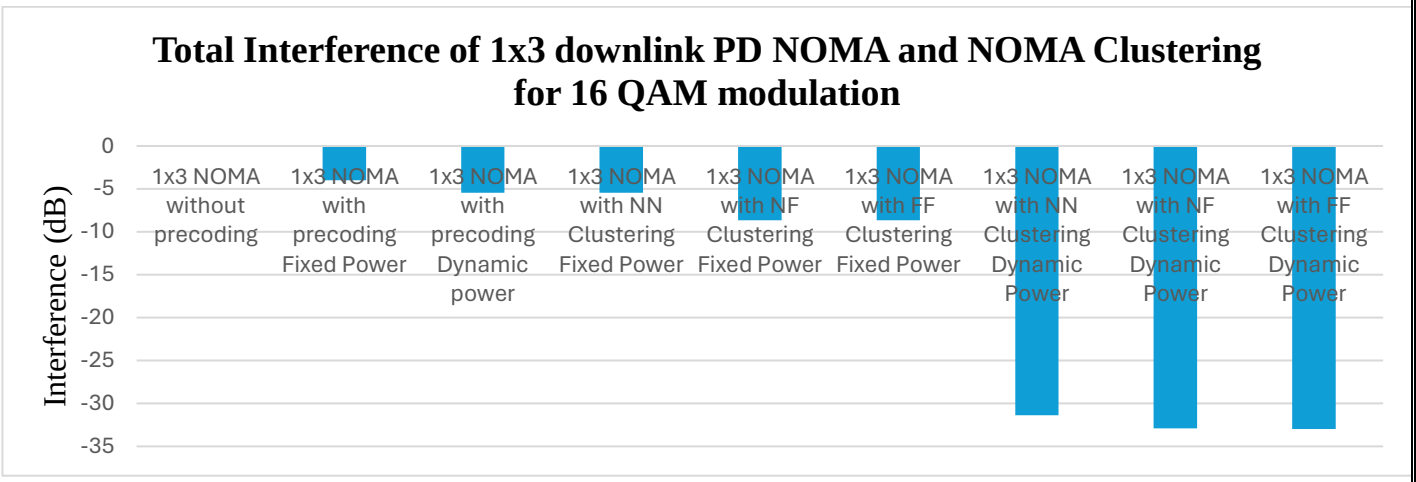


Fig 6.56: Comparison of total Interference of 1x3 NOMA with NOMA Clustering system for 16 QAM modulation

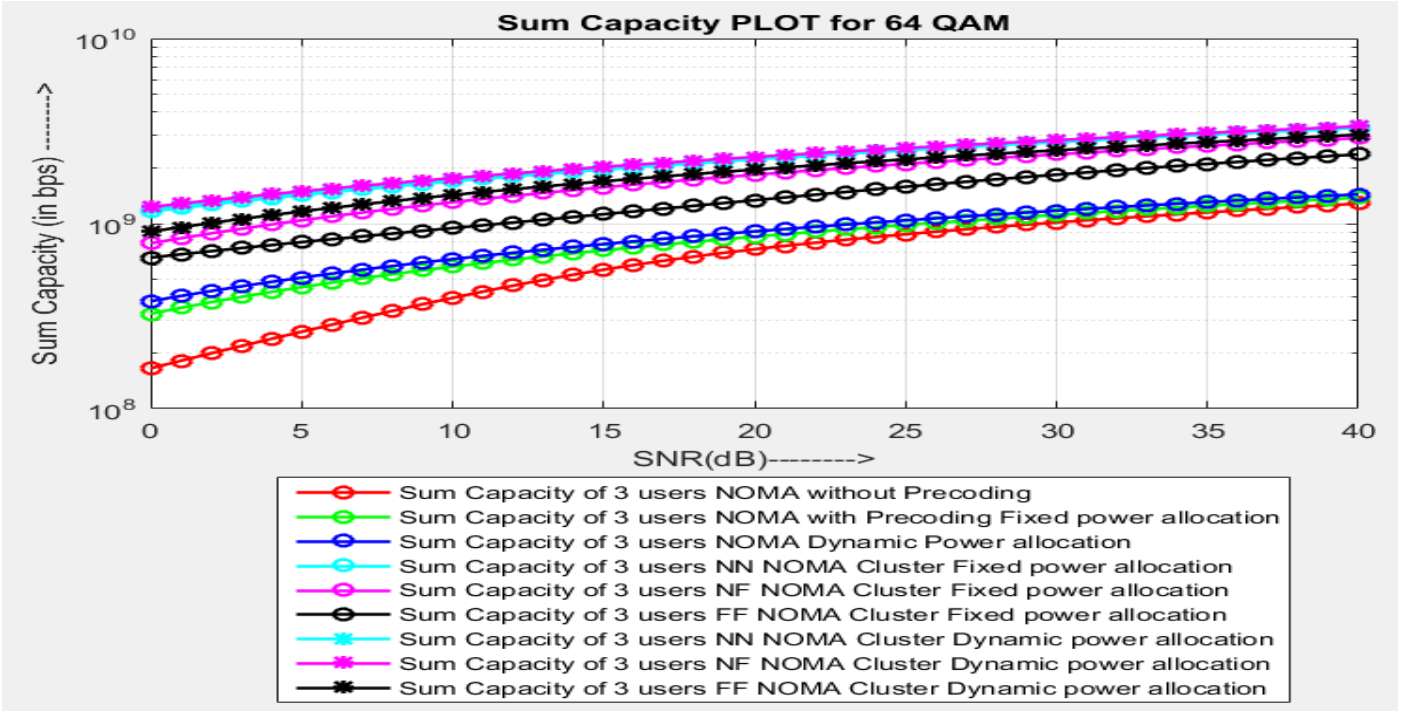


Fig 6.57: Comparison of Sum Capacity of 1x3 NOMA with NOMA Clustering system for 64 QAM modulation

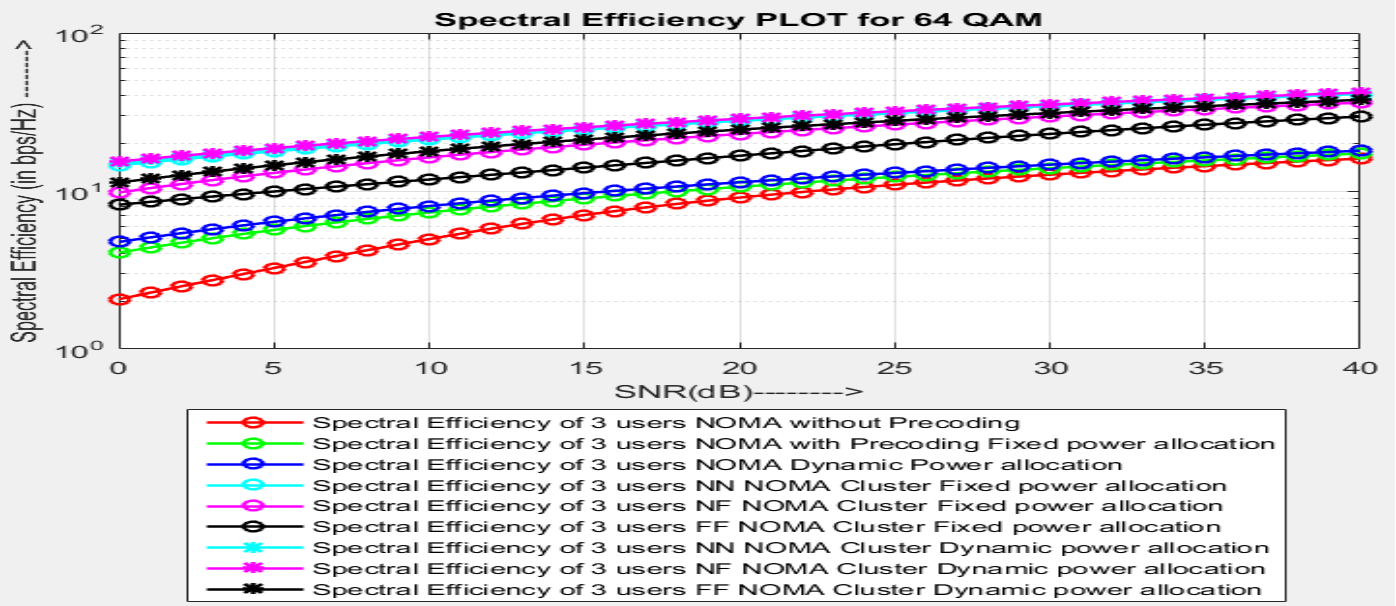


Fig 6.58: Comparison of Spectral Efficiency of 1x3 NOMA with NOMA Clustering system for 64 QAM modulation

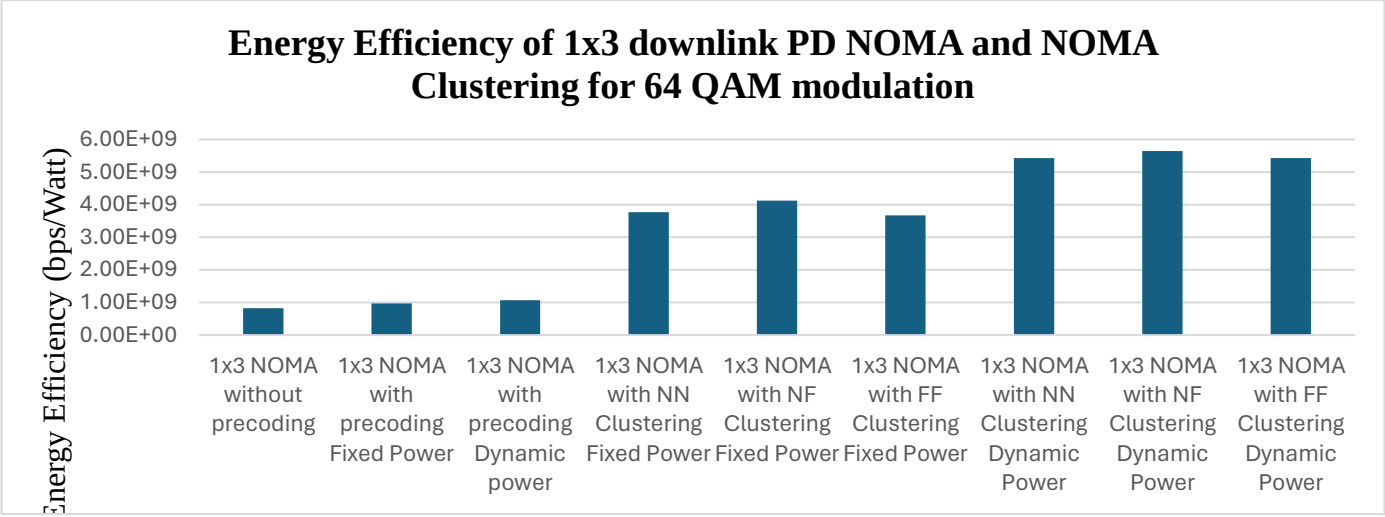


Fig 6.59: Comparison of Energy Efficiency of 1x3 NOMA with NOMA Clustering system for 64 QAM modulation

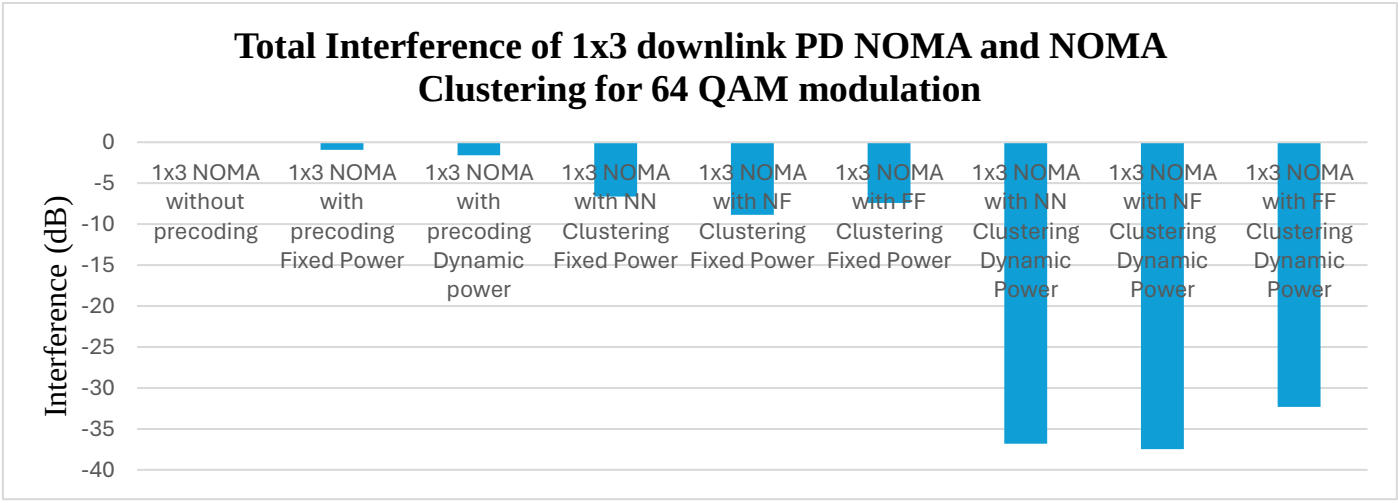


Fig 6.60: Comparison of total Interference of 1x3 NOMA with NOMA Clustering system for 64 QAM modulation

Fig 6.41, Fig 6.45, Fig 6.49, Fig 6.53, and Fig 6.57 represent the comparison of Sum Capacity of 3 users SIMO Downlink-PD-NOMA system with and without clustering in the presence and absence of SVD Precoding for 2 different power allocation schemes (FPA and Dynamic Power Allocation) using different modulation techniques. In clustering technique, users are clustered in such a way so that Interference among the users is minimized. So, Clustering technique leads to higher probability of efficient SIC as well as direct decoding processes, of the corresponding users. It is observed that NF Clustering technique with SVD precoding technique and Dynamic Power allocation scheme provides the highest Sum Capacity of the system in all modulation schemes. This is because near user and far user constitute a cluster and there is a significant variance in channel gain between them. Thus it results in the least amount of interference between them.

Fig 6.42, Fig 6.46, Fig 6.50, Fig 6.54, and Fig 6.58 represent the comparison of Spectral Efficiency of 3 users SIMO Downlink-PD-NOMA system with and without clustering in the presence and absence of SVD Precoding for 2 different power allocation schemes (FPA and Dynamic Power Allocation) using different modulation schemes. It is observed that NF Clustering technique with SVD precoding technique and Dynamic Power allocation scheme provides the highest Spectral Efficiency of the system in all modulation schemes. This is because NF Clustering with SVD precoding technique and Dynamic Power allocation scheme provides highest Sum Capacity and Spectral Efficiency is directly related to the Sum Capacity.

Fig 6.44, Fig 6.48, Fig 6.52, Fig 6.56, and Fig 6.60 represent the comparison of Total Interference of 3 users SIMO Downlink-PD-NOMA system with and without clustering in the presence and absence of SVD Precoding for 2 different power allocation schemes (FPA and Dynamic Power Allocation) using the above-stated modulation schemes. It is observed that NF Clustering technique with SVD precoding technique and Dynamic Power allocation scheme provides the least Interference of the system in all modulation schemes. This is caused by the variation in channel gain that separates the far user from the near user, which form a cluster.

Fig 6.43, Fig 6.47, Fig 6.51, Fig 6.55, and Fig 6.59 represent the comparison of Energy Efficiency of 3 users SIMO Downlink-PD-NOMA system with and without clustering in the presence and absence of SVD Precoding for 2 different power allocation schemes (FPA and Dynamic Power Allocation) using the above-stated modulation schemes. It is observed that NF Clustering technique with SVD precoding technique and Dynamic Power allocation scheme provides the highest Energy Efficiency of the system in all modulation schemes. This is due to the fact that NF Clustering offers the least amount of interference when combined with the SVD precoding technique and the dynamic power allocation scheme.

Due to hardware constraint in WARP V3 board we have performed up to (1x3) NOMA and NOMA clustering system using WARP hardware. We have increased the number of users and calculated their performance using MATLAB software and compared their performance with the (1x3) NOMA clustering system.

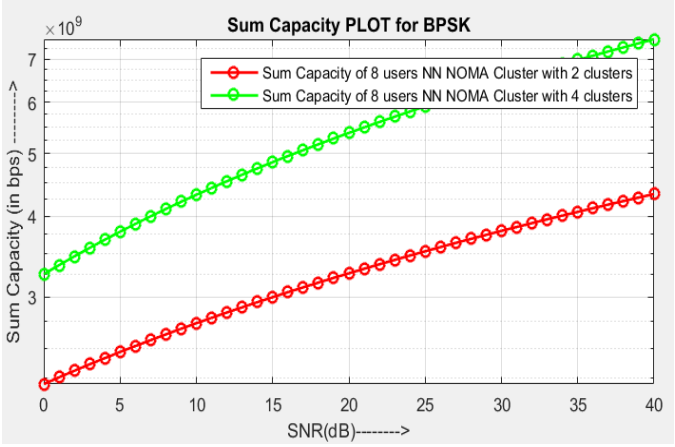


Fig 6.61: Comparison of Sum Capacity of 1x8 NOMA Cluster with different number of users in each cluster for BPSK modulation

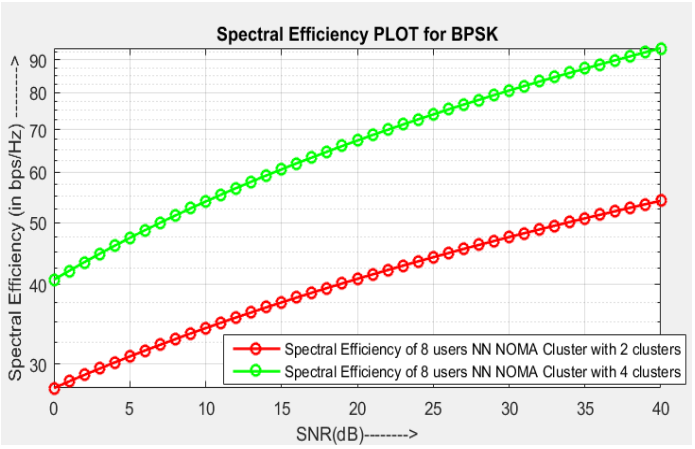


Fig 6.62: Comparison of Spectral Efficiency of 1x8 NOMA Cluster with different number of users in each cluster for BPSK modulation

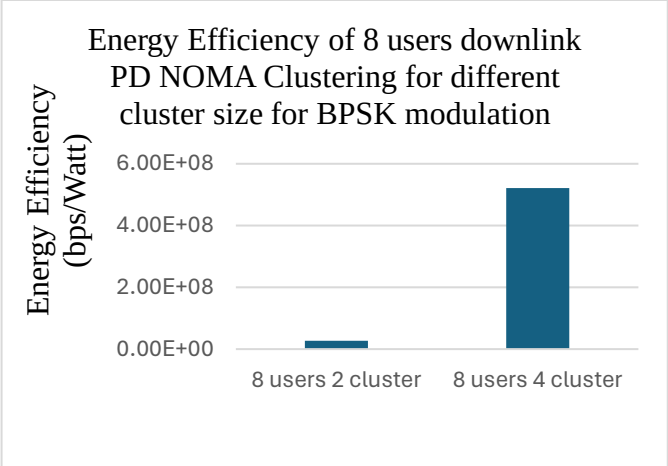


Fig 6.63: Comparison of Energy Efficiency of 1x8 NOMA Cluster with different number of users in each cluster for BPSK modulation

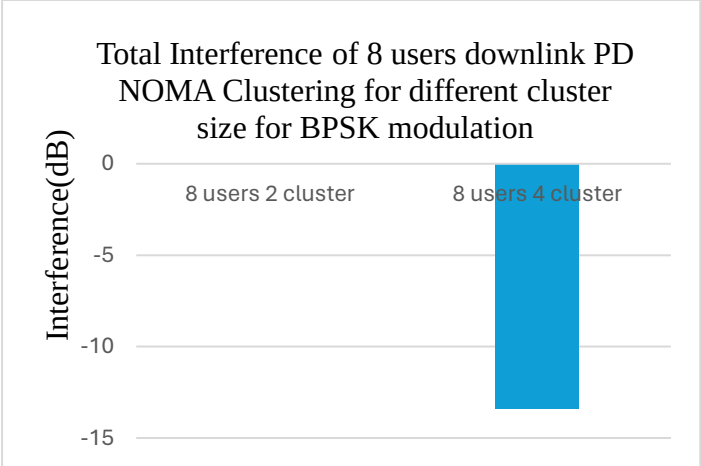


Fig 6.64: Comparison of total Interference of 1x8 NOMA Cluster with different number of users in each cluster for BPSK modulation

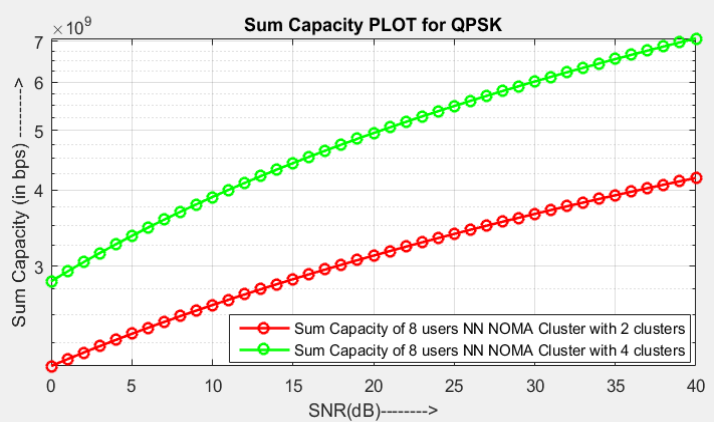


Fig 6.65: Comparison of Sum Capacity of 1x8 NOMA Cluster with different number of users in each cluster for QPSK modulation

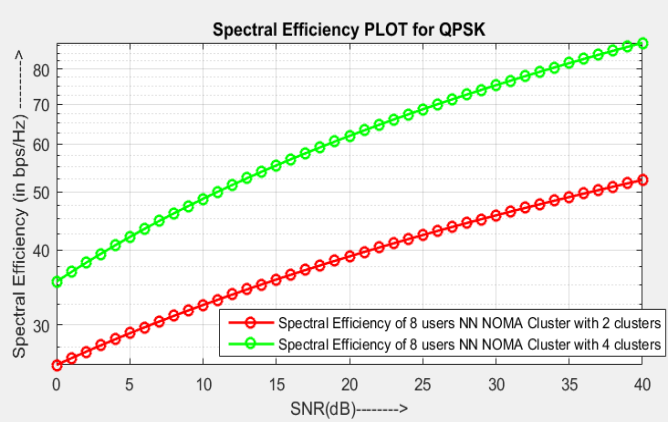


Fig 6.66: Comparison of Spectral Efficiency of 1x8 NOMA Cluster with different number of users in each cluster for QPSK modulation

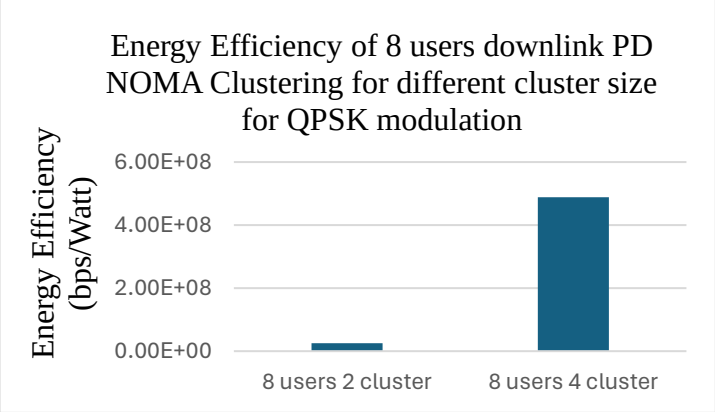


Fig 6.67: Comparison of Energy Efficiency of 1x8 NOMA Cluster with different number of users in each cluster for QPSK modulation

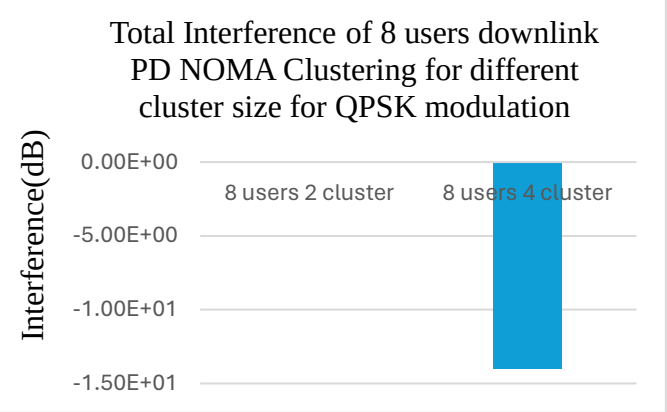


Fig 6.68: Comparison of total Interference of 1x8 NOMA Cluster with different number of users in each cluster for QPSK modulation

Fig 6.61 and Fig 6.65 represent the comparison of Sum Capacity of 8 users SIMO Downlink-PD-NOMA Clustering system with different number of users in each cluster in the presence of SVD Precoding for 2 different modulation schemes. From the figures we can observe that as the number of users increases within each cluster, amount of Sum Capacity of the system decreases. This is because with the increase in number of users in each cluster, amount of Interference of the system increases as we can see from Fig 6.64 and Fig 6.68. As a result we can from Fig 6.62 and Fig 6.66 that Spectral Efficiency of the system decreases as Sum Capacity of the system decreases. Energy Efficiency of the system also decreases as shown in Fig 6.63 and Fig 6.67. This is because Energy Efficiency is influenced by the amount of Interference.

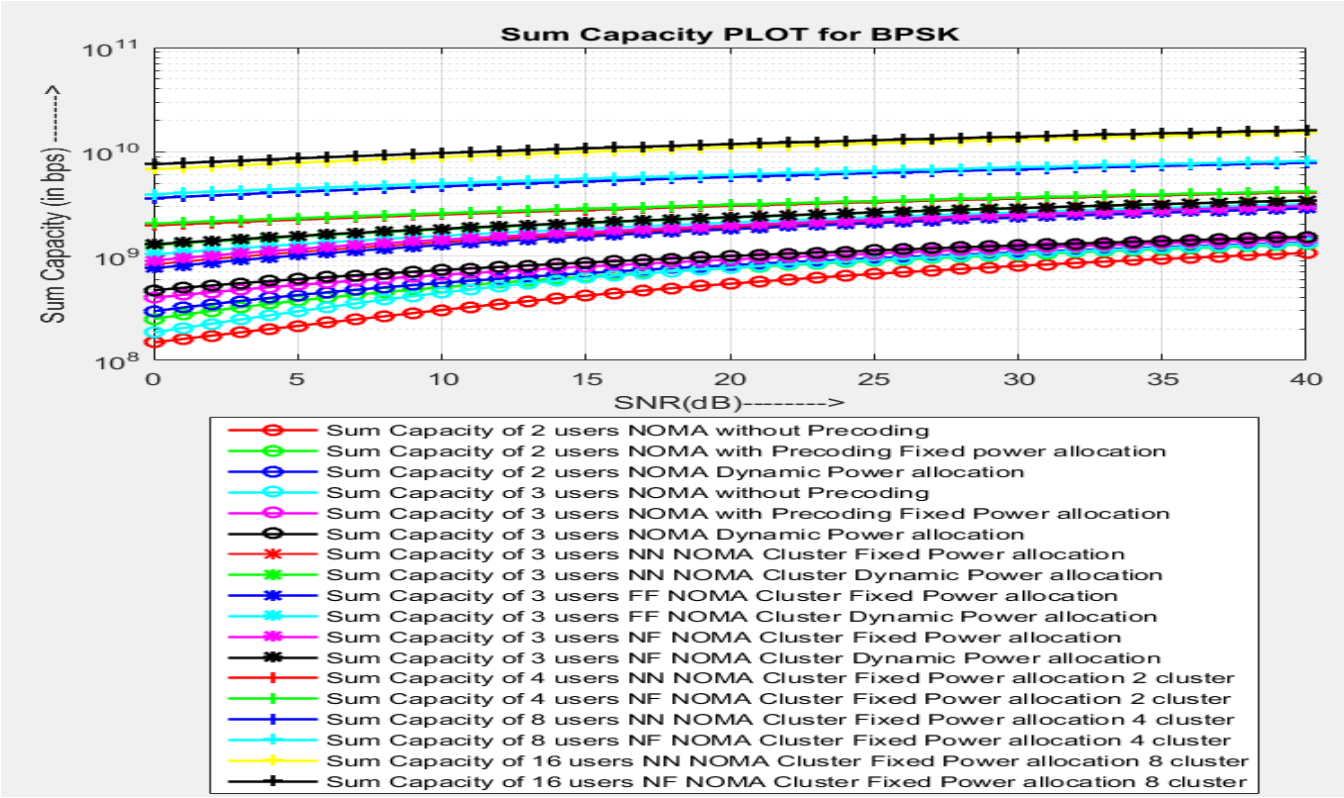


Fig 6.69: Comparison between Sum Capacity performed by Simulation and WARP V3 board of different users PD-NOMA with and without Clustering for BPSK modulation

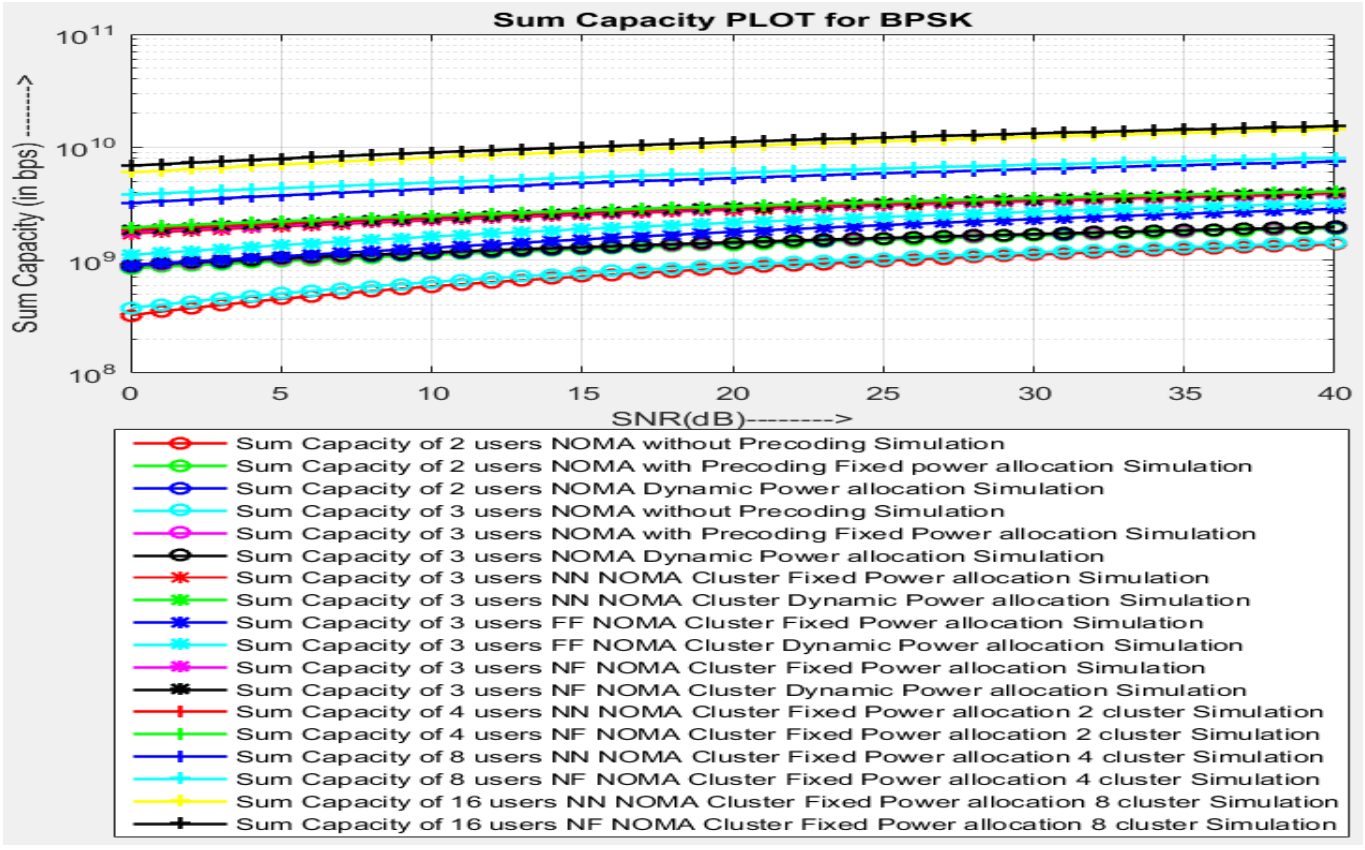


Fig 6.70: Comparison between Sum Capacity performed by Simulation of different users PD-NOMA with and without Clustering for BPSK modulation

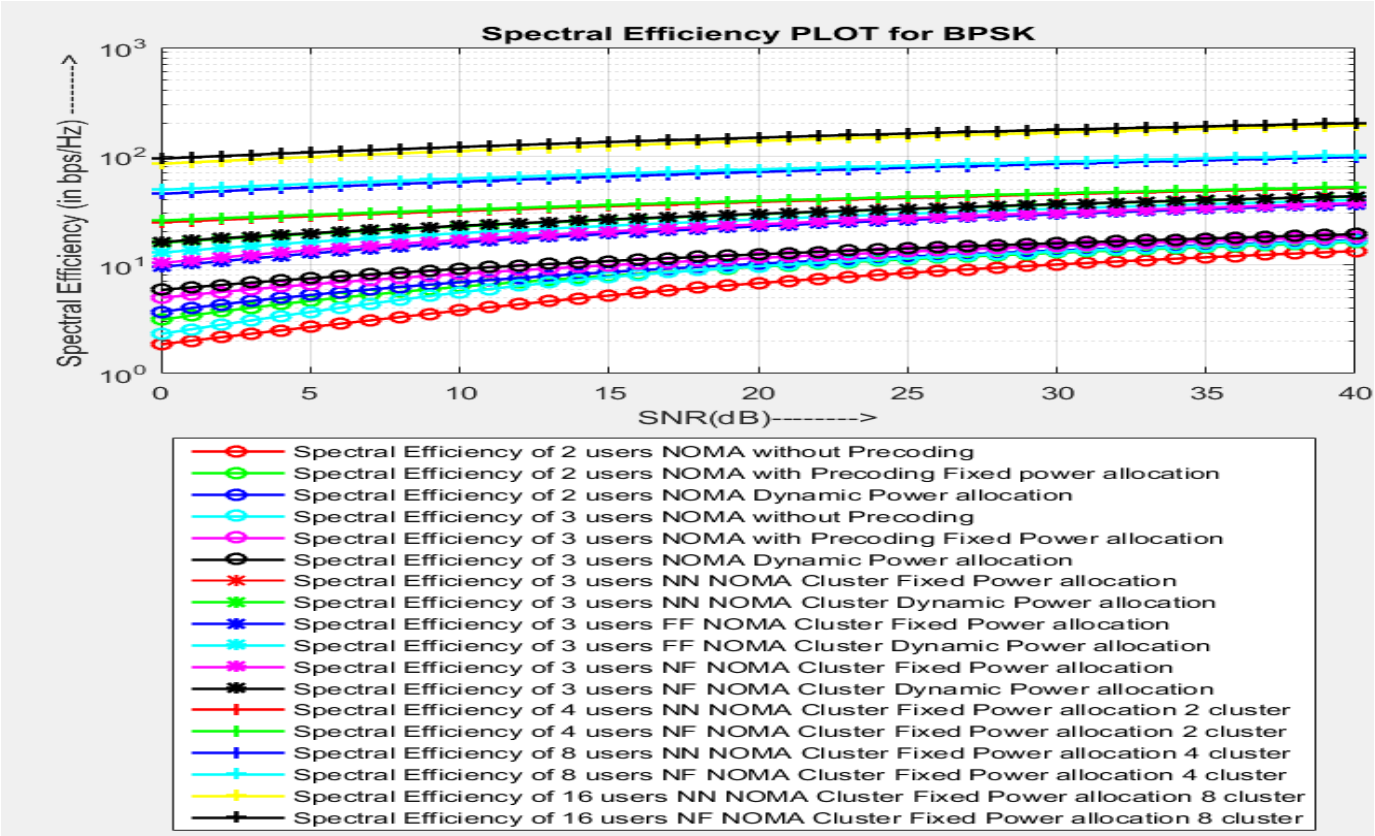


Fig 6.71: Comparison between Spectral Efficiency performed by Simulation and WARP V3 board of different users PD-NOMA with and without Clustering for BPSK modulation

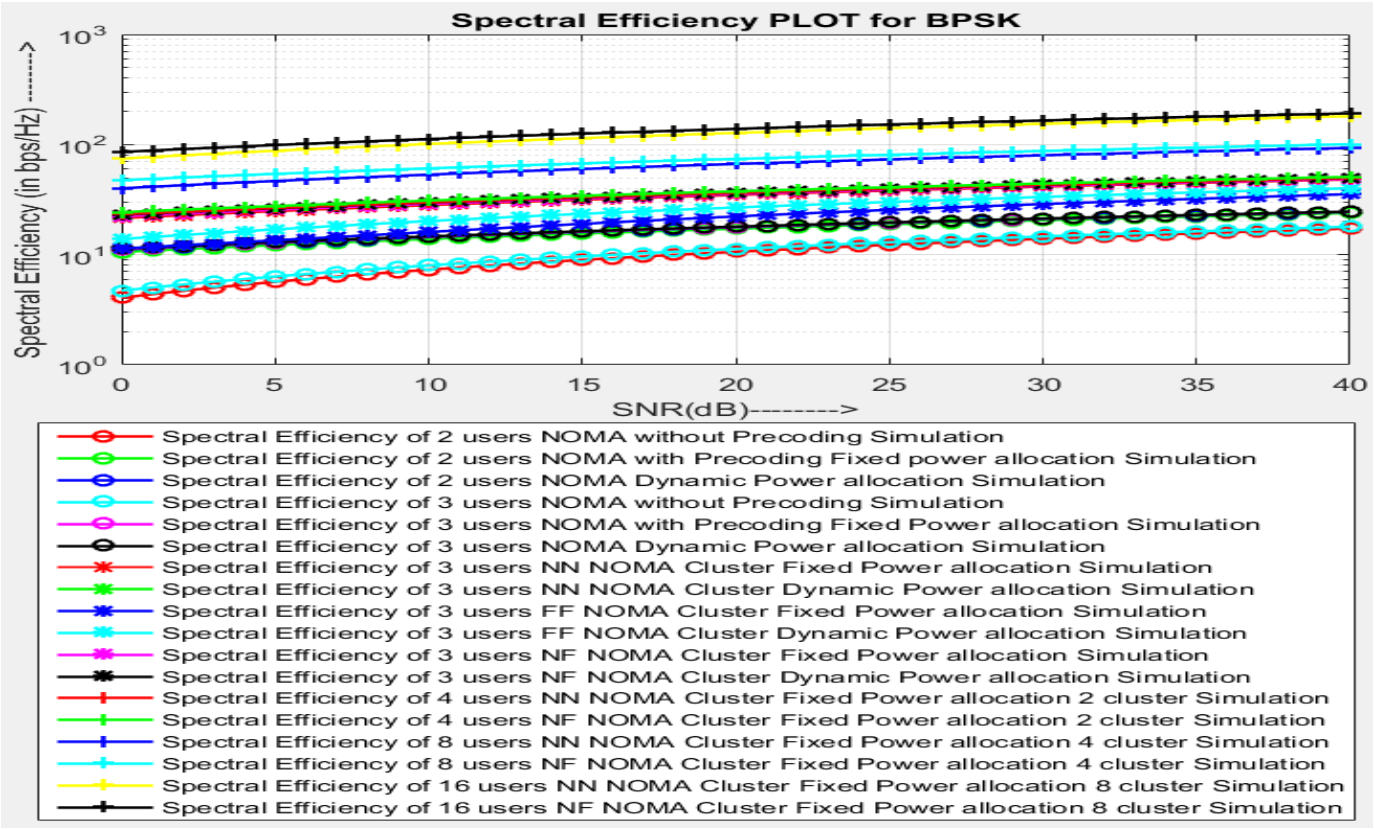


Fig 6.72: Comparison between Spectral Efficiency performed by Simulation of different users PD-NOMA with and without Clustering for BPSK modulation

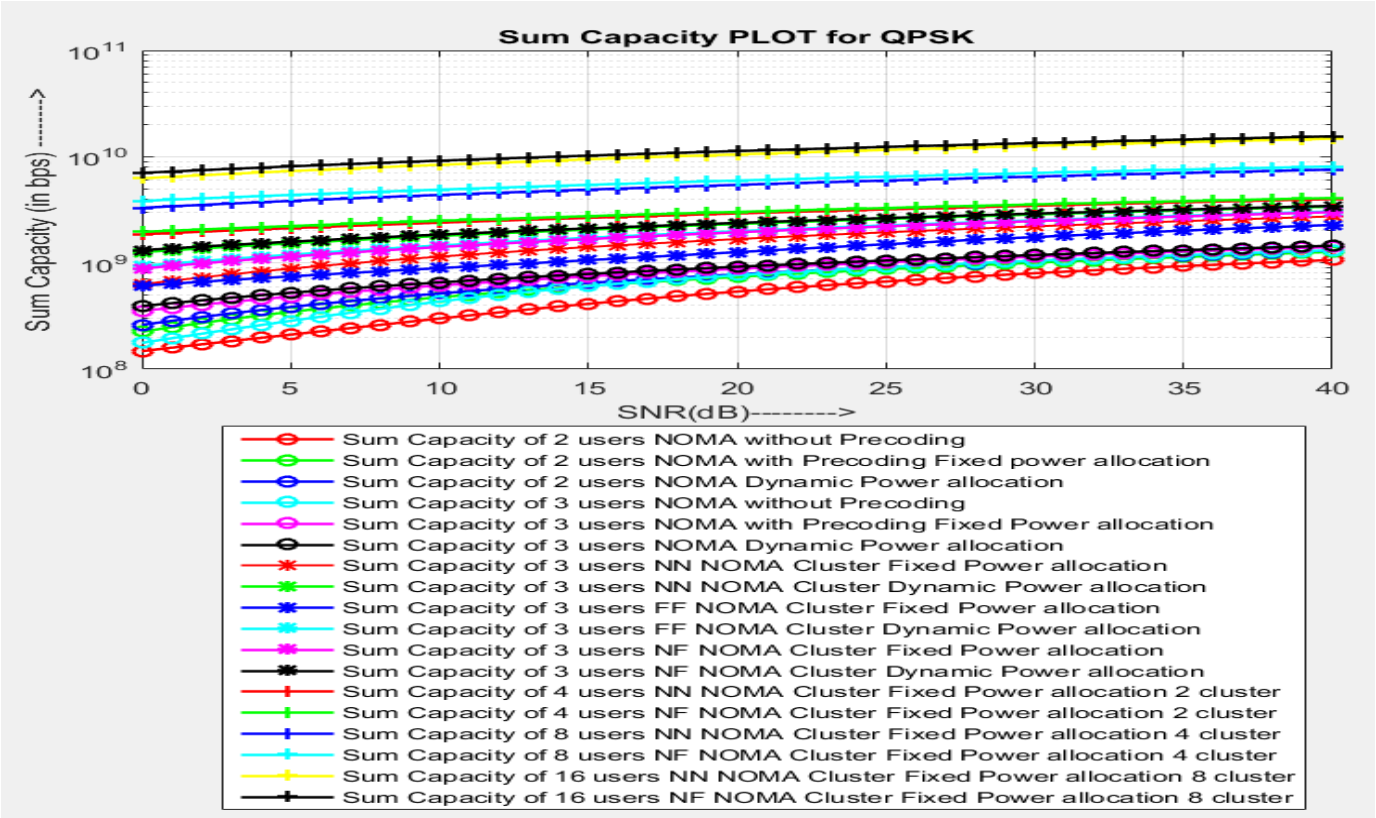


Fig 6.73: Comparison between Sum Capacity performed by Simulation and WARP V3 board of different users PD-NOMA with and without Clustering for QPSK modulation

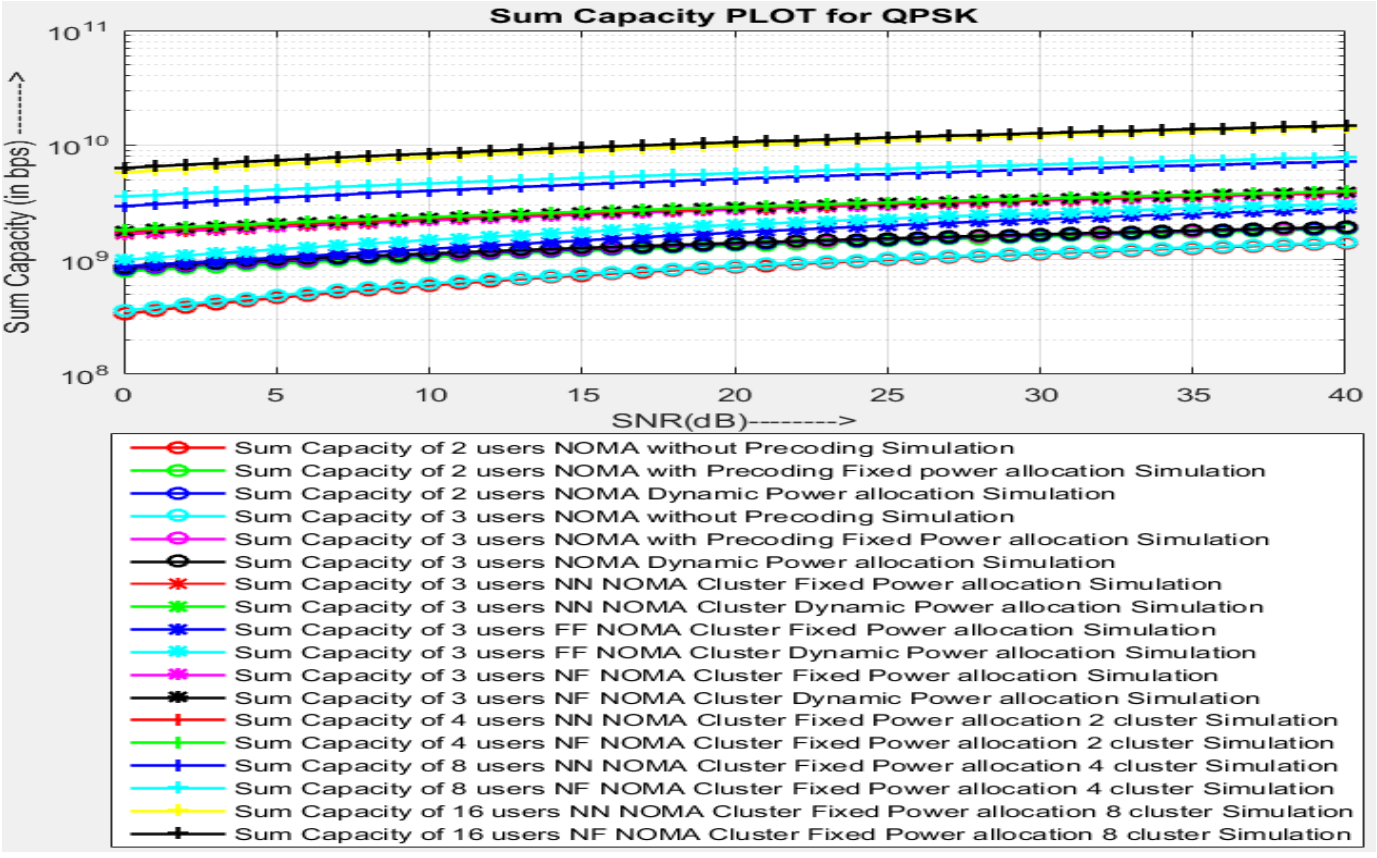


Fig 6.74: Comparison between Sum Capacity performed by Simulation of different users PD-NOMA with and without Clustering for QPSK modulation

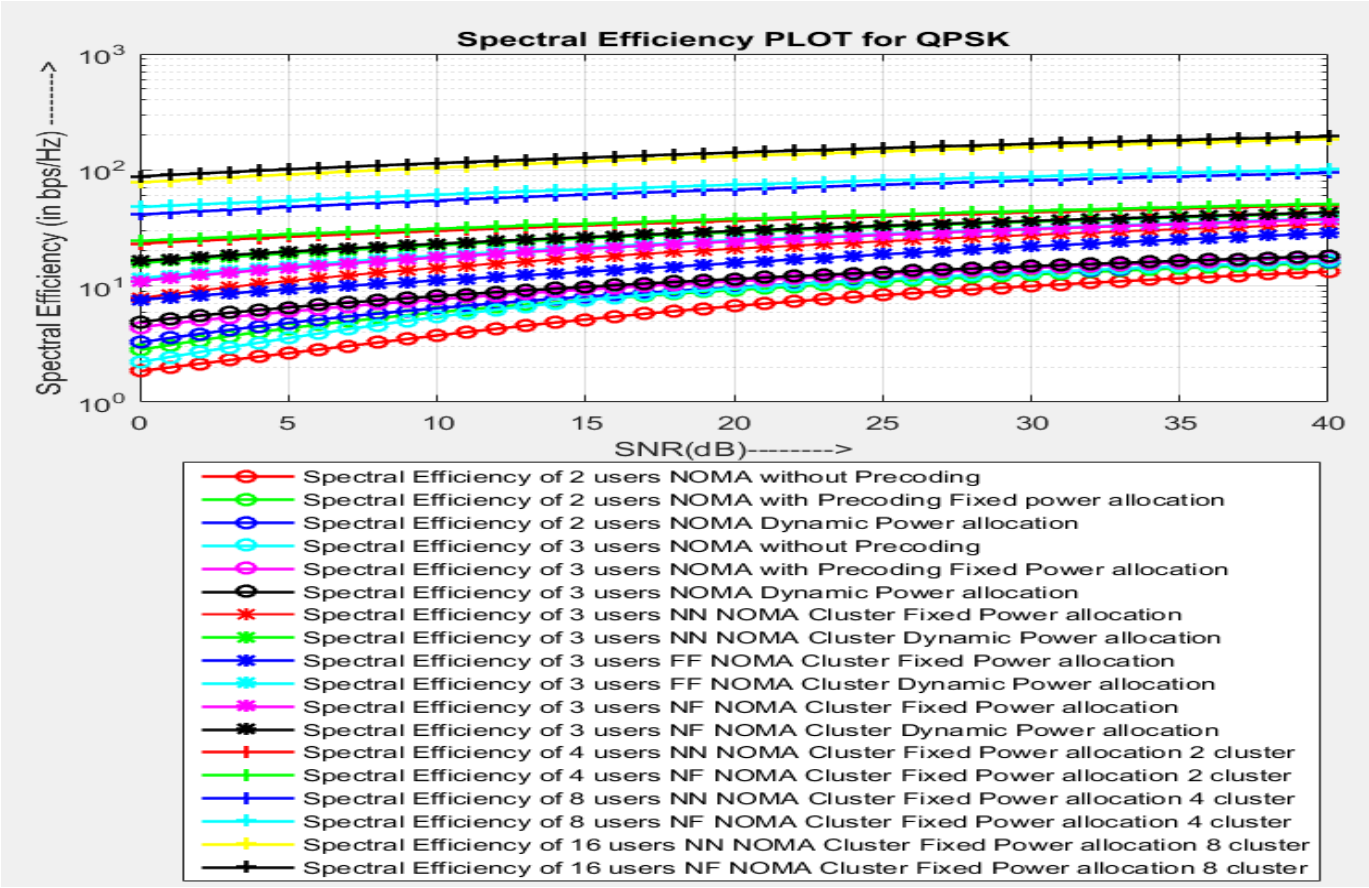


Fig 6.75: Comparison between Spectral Efficiency performed by Simulation and WARP V3 board of different users PD-NOMA with and without Clustering for QPSK modulation

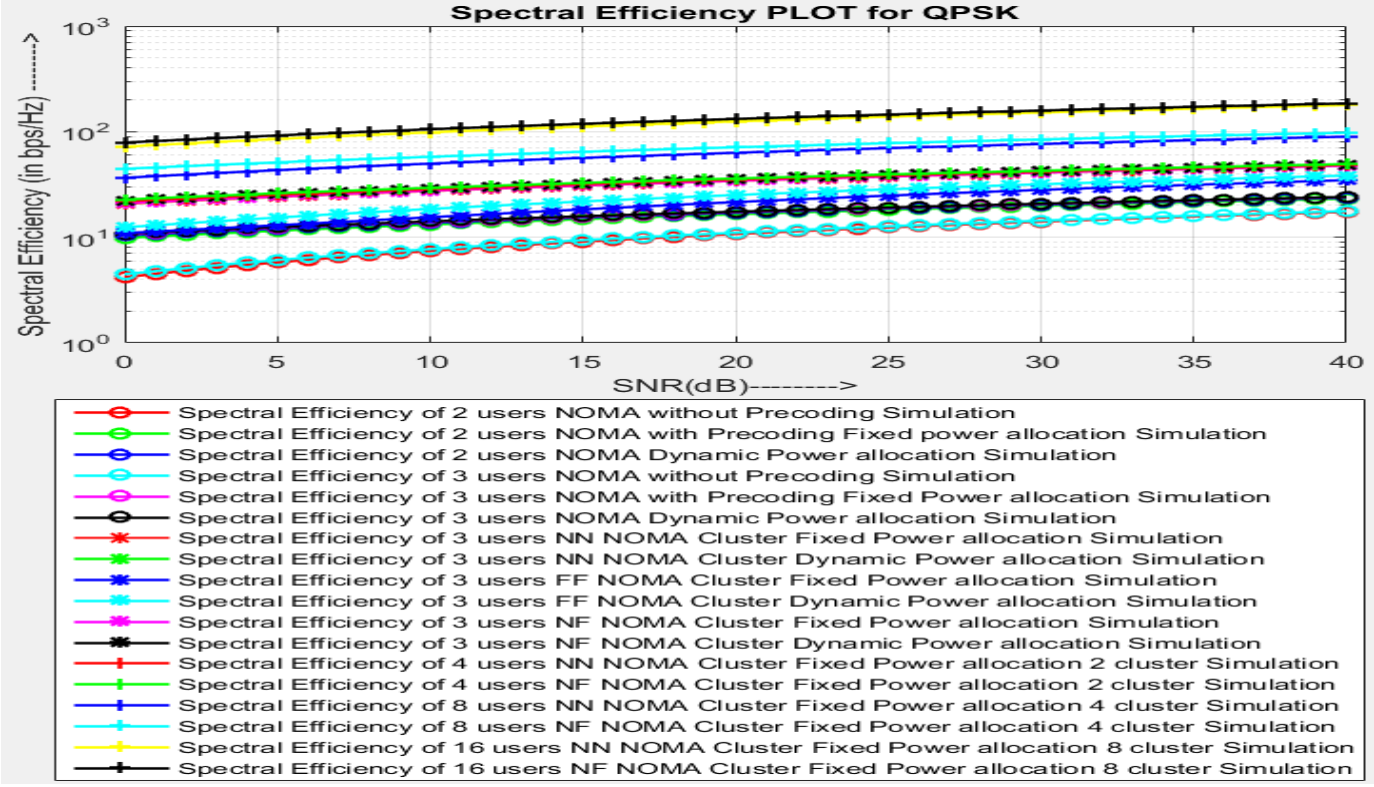


Fig 6.76: Comparison between Spectral Efficiency performed by Simulation of PD-NOMA different users PD-NOMA with and without Clustering for QPSK modulation

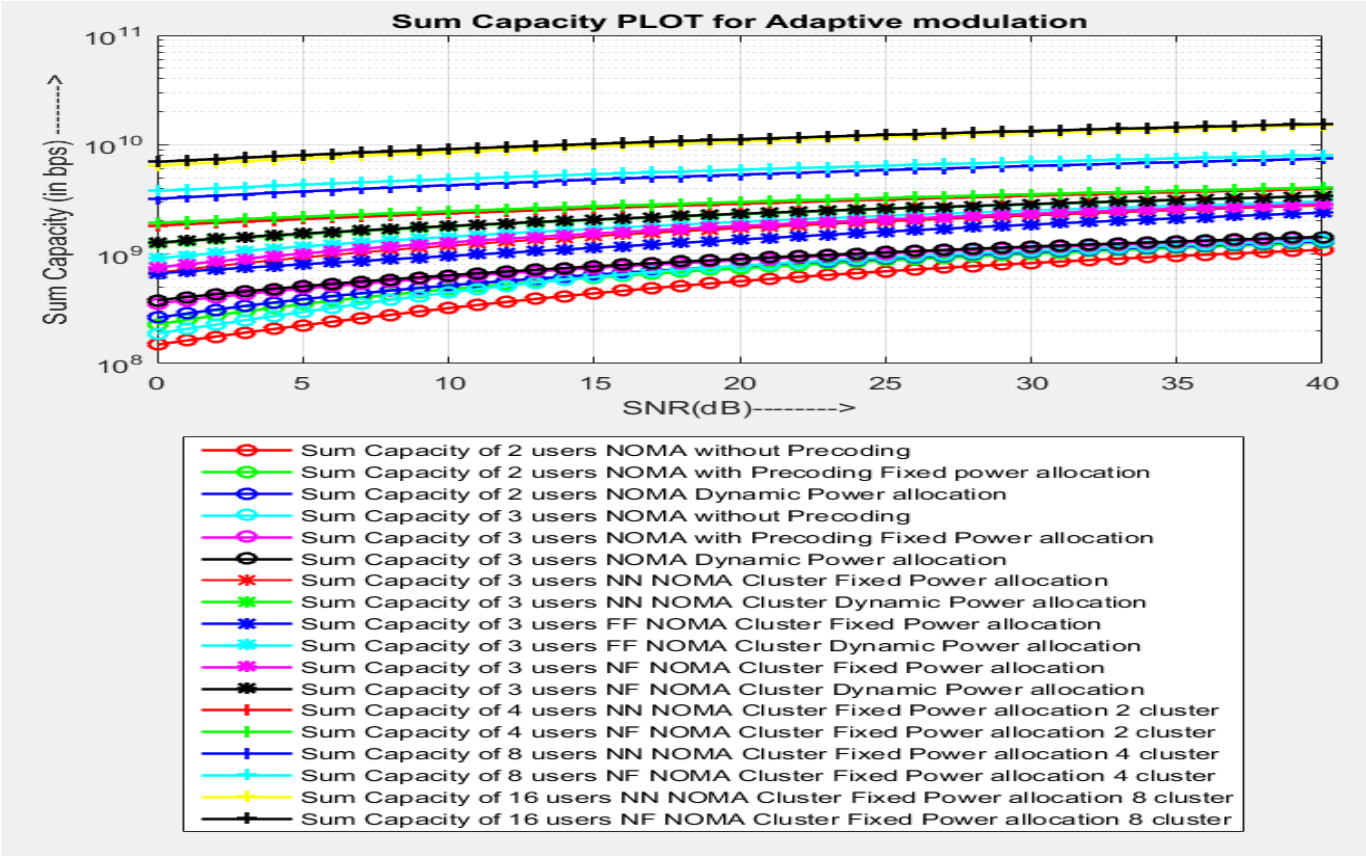


Fig 6.77: Comparison between Sum Capacity performed by Simulation and WARP V3 board of different users PD-NOMA with and without Clustering for Adaptive modulation

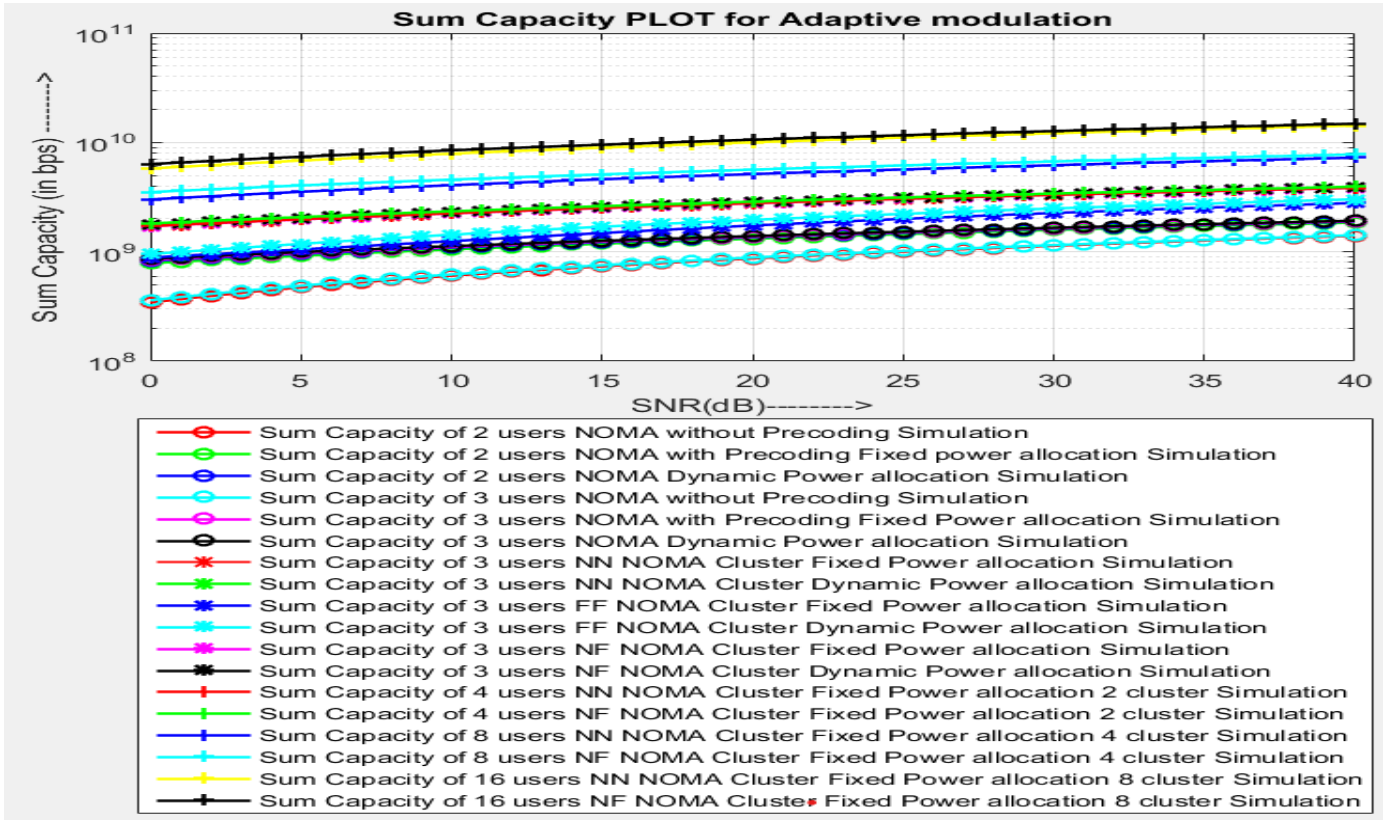


Fig 6.78: Comparison between Sum Capacity performed by Simulation of different users PD-NOMA with and without Clustering for Adaptive modulation

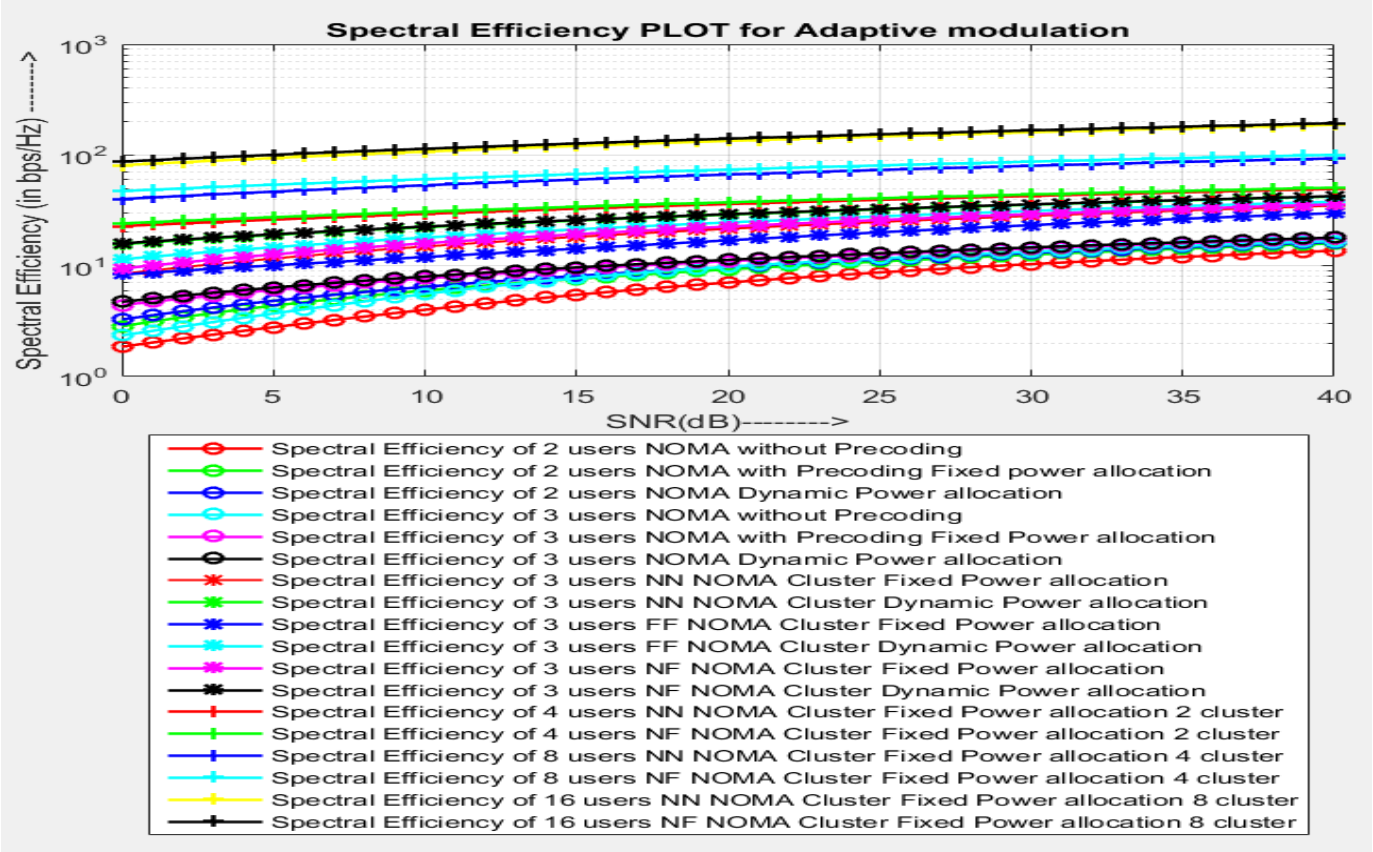


Fig 6.79: Comparison between Spectral Efficiency performed by Simulation and WARP V3 board of different users PD-NOMA with and without Clustering for Adaptive modulation

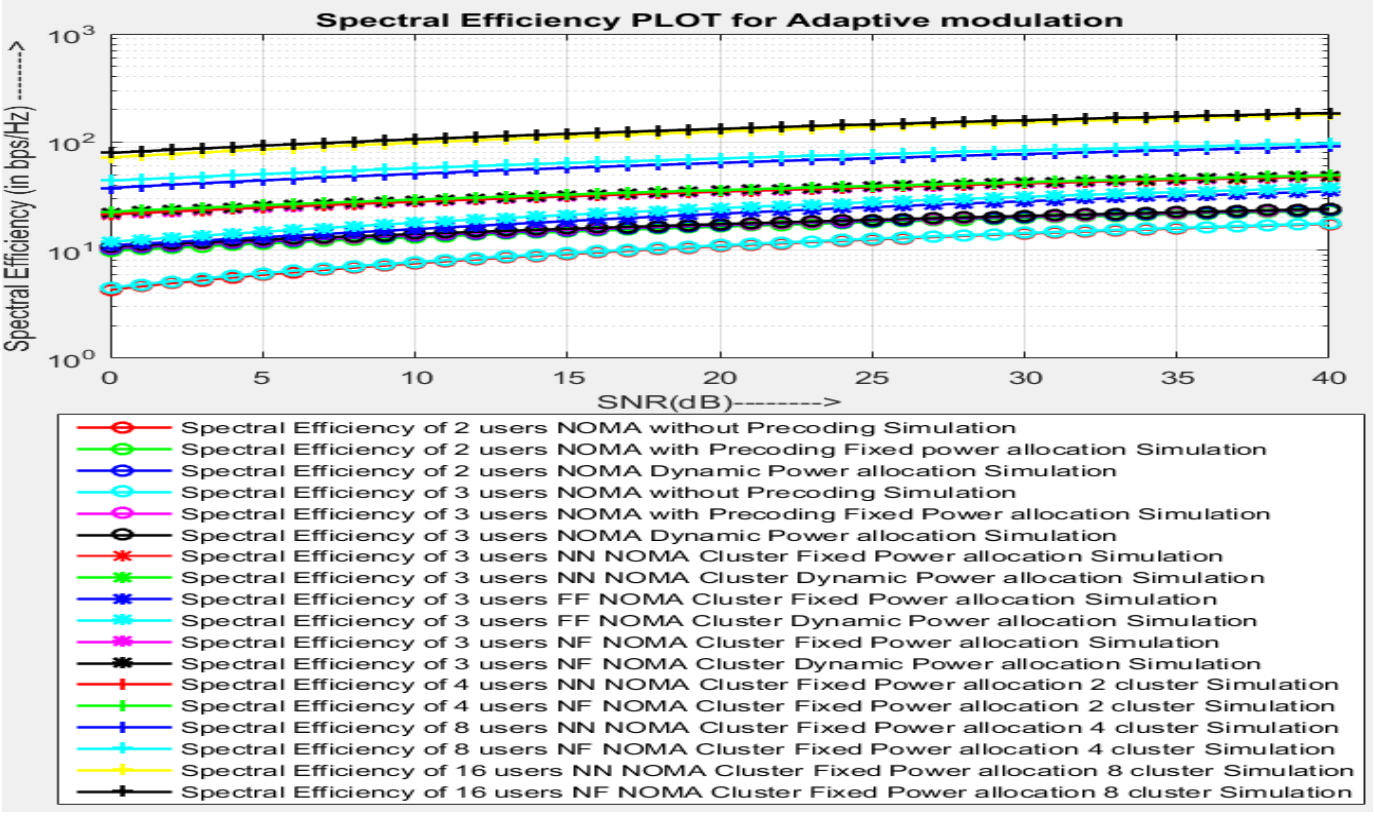


Fig 6.80: Comparison between Spectral Efficiency performed by Simulation of different users PD-NOMA with and without Clustering for Adaptive modulation

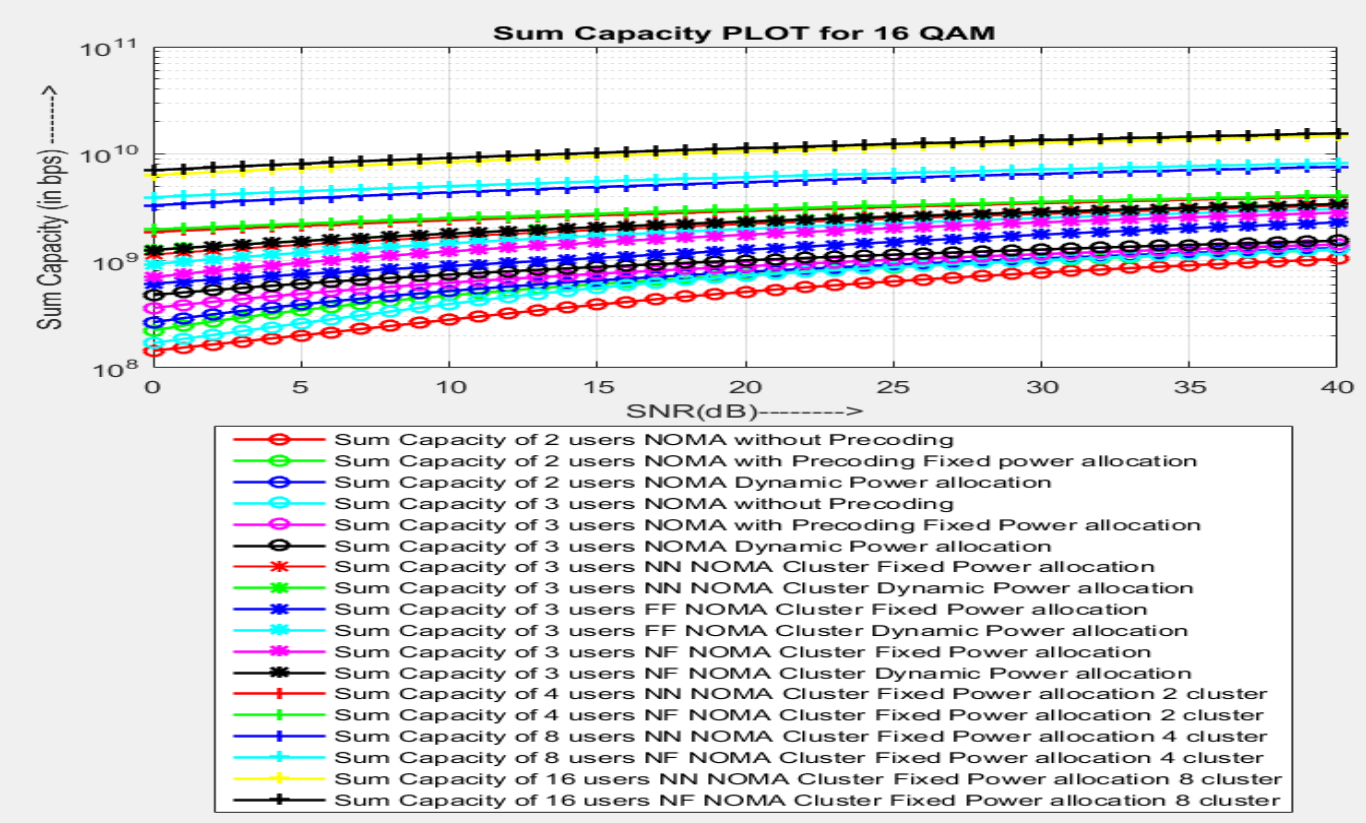


Fig 6.81: Comparison between Sum Capacity performed by Simulation and WARP V3 board of different users PD-NOMA with and without Clustering for 16 QAM modulation

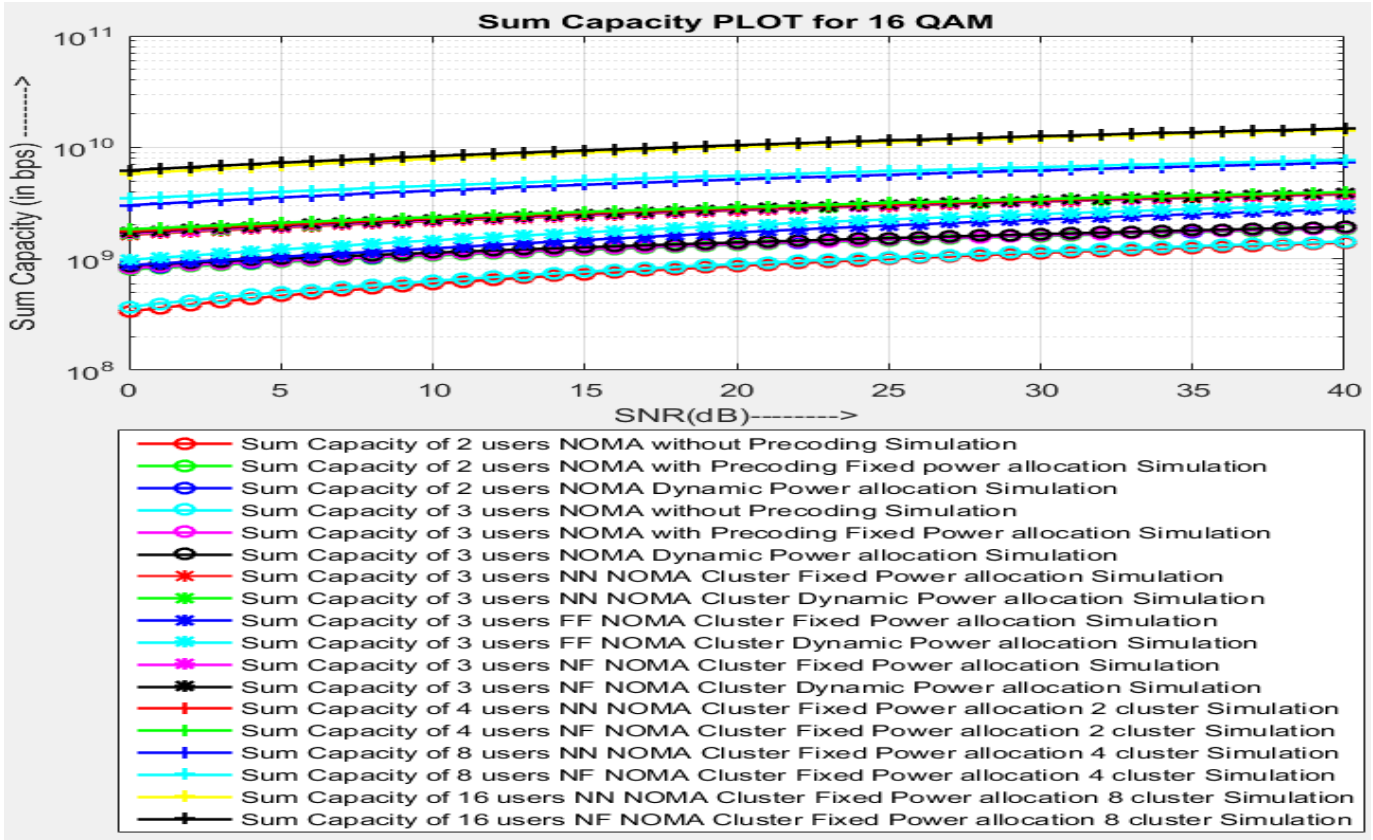


Fig 6.82: Comparison between Sum Capacity performed by Simulation of different users PD-NOMA with and without Clustering for 16 QAM modulation

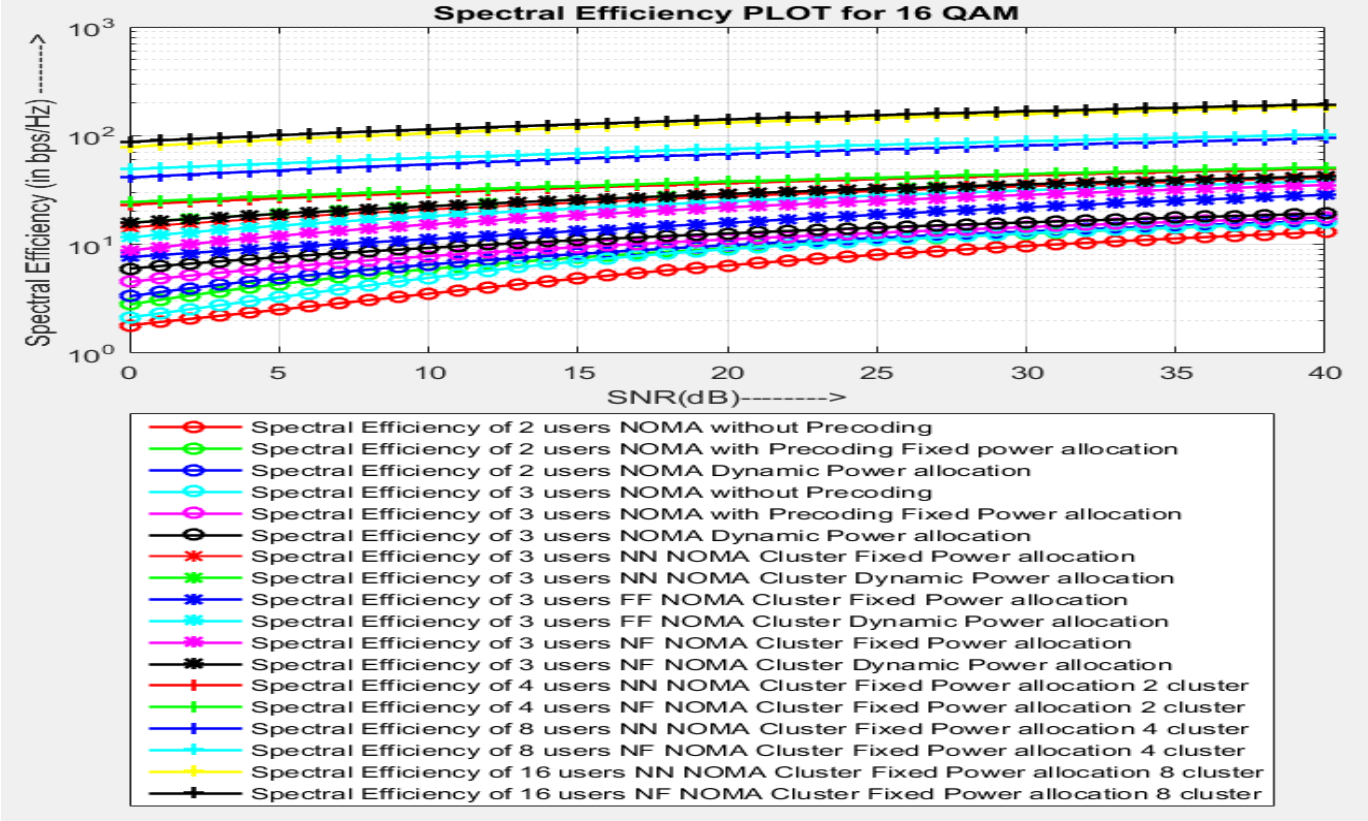


Fig 6.83: Comparison between Spectral Efficiency performed by Simulation and WARP V3 board of different users PD-NOMA with and without Clustering for 16 QAM modulation

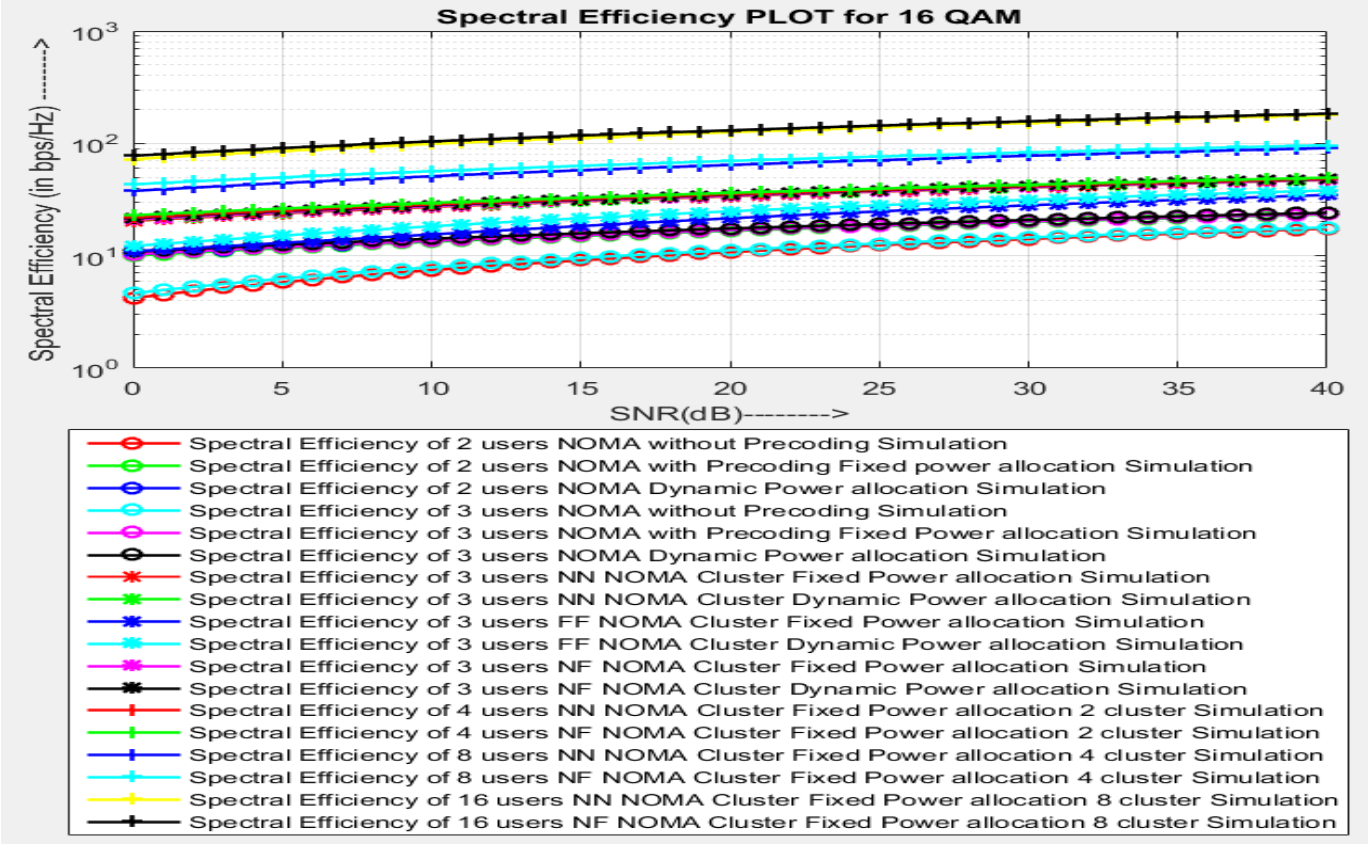


Fig 6.84: Comparison between Spectral Efficiency performed by Simulation of different users PD-NOMA with and without Clustering for 16 QAM modulation

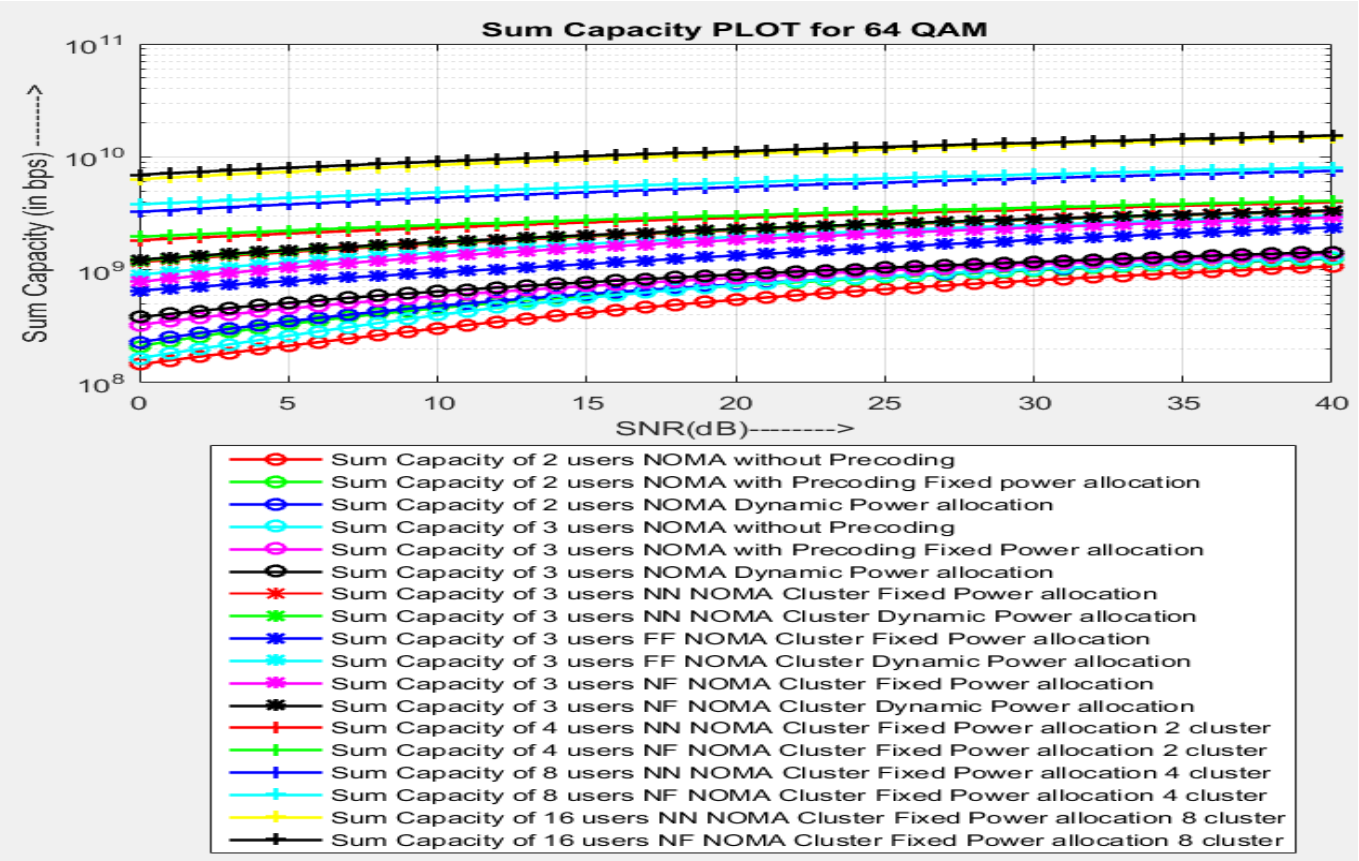


Fig 6.85: Comparison between Sum Capacity performed by Simulation and WARP V3 board of different users PD-NOMA with and without Clustering for 64 QAM modulation

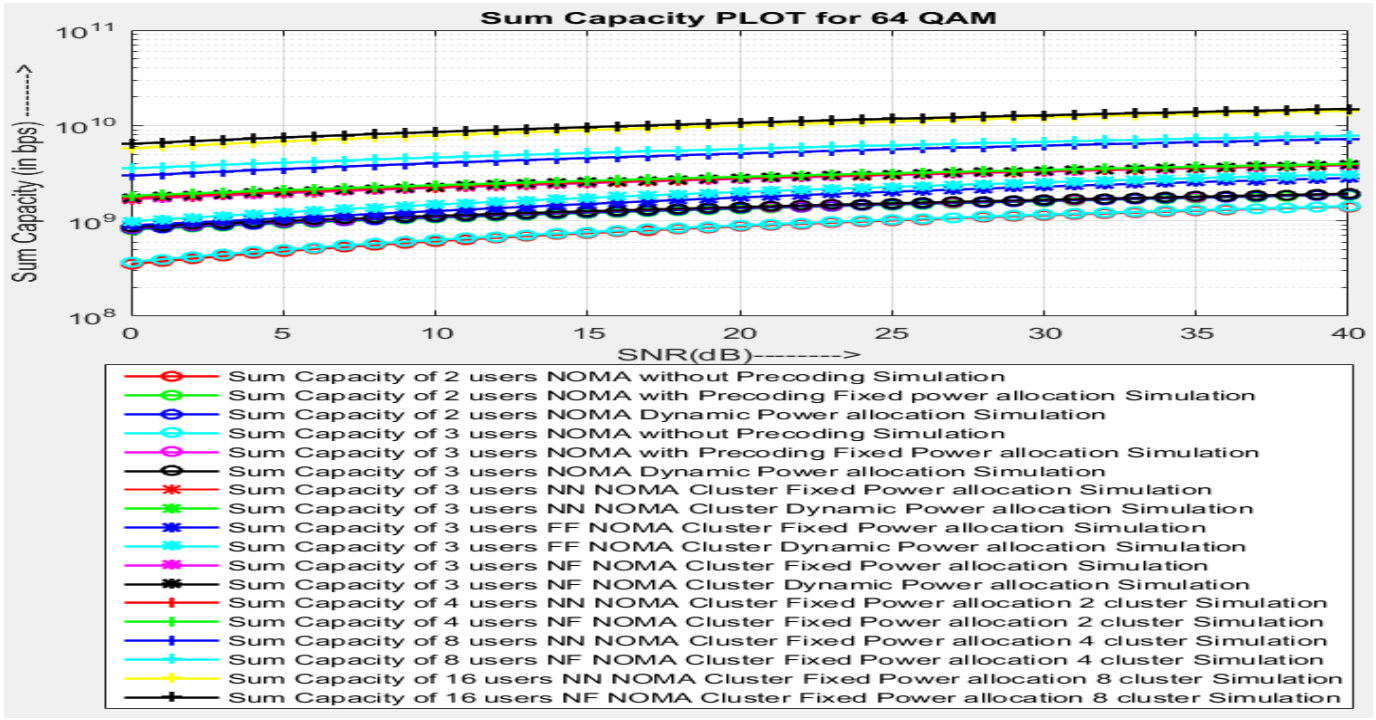


Fig 6.86: Comparison between Sum Capacity performed by Simulation of different users PD-NOMA with and without Clustering for 64 QAM modulation

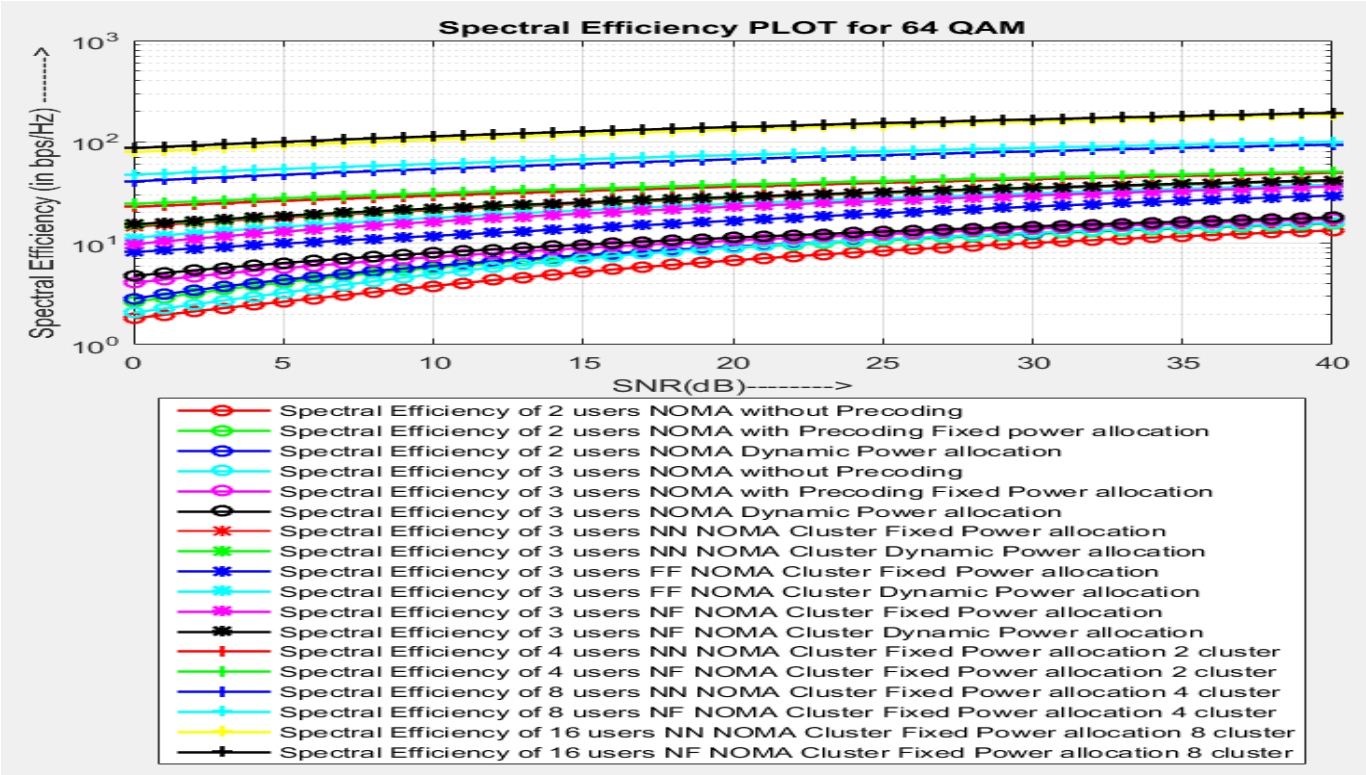


Fig 6.87: Comparison between Spectral Efficiency performed by Simulation and WARP V3 board of different users PD-NOMA with and without Clustering for 64 QAM modulation

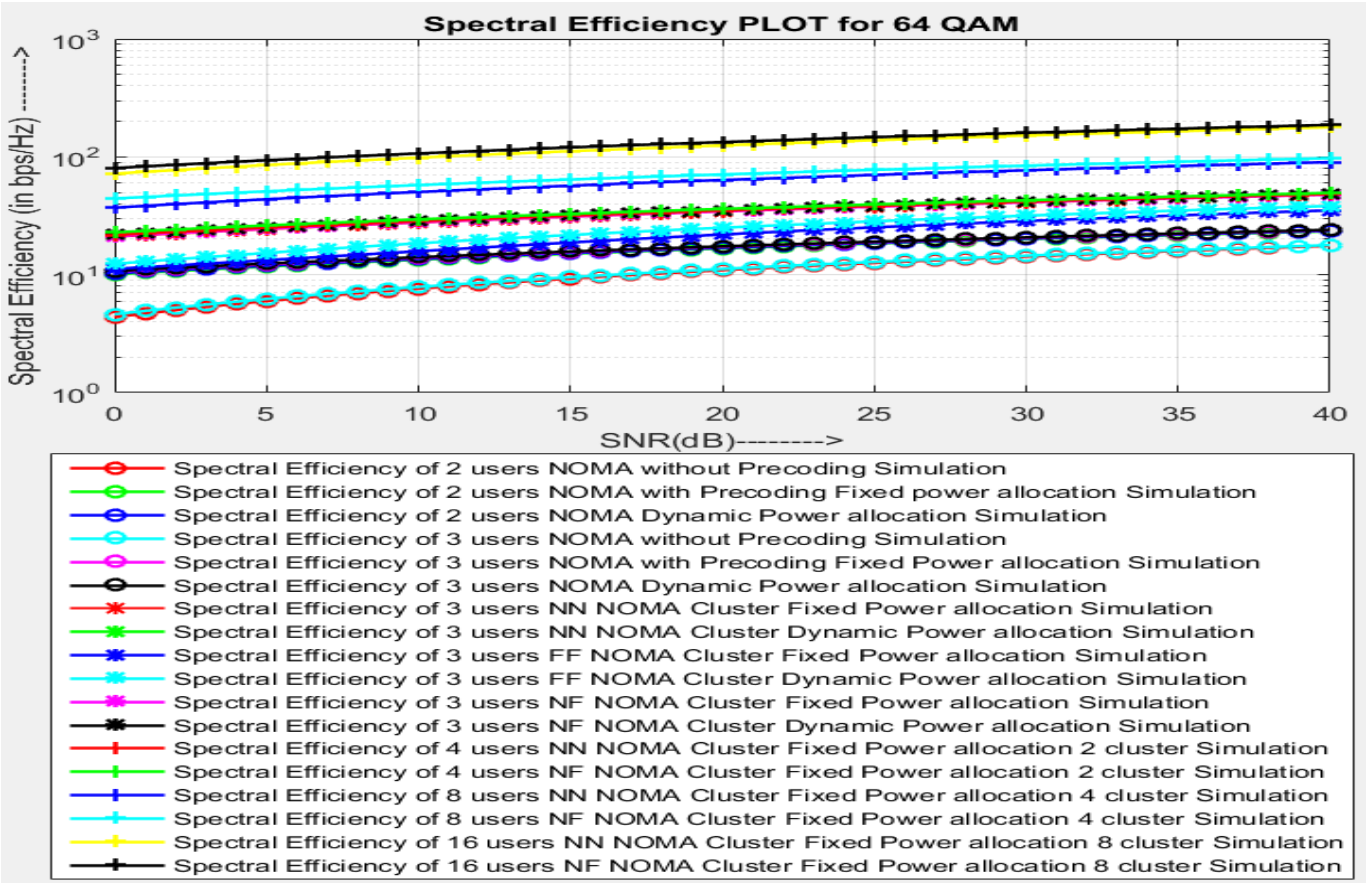


Fig 6.88: Comparison between Spectral Efficiency performed by Simulation of different users PD-NOMA with and without Clustering for 64 QAM modulation

Fig 6.69, Fig 6.73, Fig 6.77, Fig 6.81, and Fig 6.85 represent the comparison of Sum Capacity of different users Downlink-PD-NOMA system with and without clustering in the presence and absence of SVD Precoding for 2 different power allocation schemes (FPA and Dynamic Power Allocation) using different modulation techniques. Here due to hardware constraint we can perform up to 3 users NOMA with and without clustering system using WARP V3 board. 4, 8 and 16 users clustering system we have performed by MATLAB simulation. Here from these graphs we can see that as the number of users increases, Sum Capacity of the system also increases. It is observed that in all modulation schemes 16 users NF Cluster system with SVD precoding provides the highest Sum Capacity. This is because Sum Capacity increases as the number of users of the system increases. Clustering technique along with SVD precoding scheme reduces amount of interference of the system. NF Clustering provides least amount of interference among all these 3 clustering techniques.

Fig 6.70, Fig 6.74, Fig 6.78, Fig 6.82, and Fig 6.86 represent the comparison of Sum Capacity of different users Downlink-PD-NOMA system with and without clustering in the presence and absence of SVD Precoding for 2 different power allocation schemes (FPA and Dynamic Power Allocation) using different modulation schemes. Here we have performed all the system by MATLAB simulation. Here from these graphs we can see that as the number of users increases, Sum Capacity of the system also increases. It is observed that in all modulation schemes 16 users NF Cluster system with SVD precoding provides the highest Sum Capacity. Here, we can see that, when experiments are performed in a MATLAB simulation, the NOMA and NOMA clustering system with up to three users offers a higher Sum Capacity. This is due to the fact that experiments performed by WARP board are conducted in real time, which means that there is greater chance of interference.

Fig 6.71, Fig 6.75, Fig 6.79, Fig 6.83, and Fig 6.87 represent the comparison of Spectral Efficiency of different users Downlink-PD-NOMA system with and without clustering in the presence and absence of SVD Precoding for 2 different power allocation schemes (FPA and Dynamic Power Allocation) using different modulation schemes. Here due to hardware constraint we can perform up to 3 users NOMA with and without clustering system using WARP V3 board. 4, 8 and 16 users clustering system we have performed by MATLAB simulation. Here from these graphs we can see that as the number of users increases, Spectral Efficiency of the system also increases. It is observed that in all modulation schemes 16 users NF Clustering system with SVD precoding provides the highest Spectral Efficiency. This is because Spectral Efficiency is directly related to the Sum Capacity of the system and 16 users NF Clustering system with SVD precoding provides the highest Sum Capacity.

Fig 6.72, Fig 6.76, Fig 6.80, Fig 6.84, and Fig 6.88 represent the comparison of Spectral Efficiency of different users Downlink-PD-NOMA system with and without clustering in the presence and absence of SVD Precoding for 2 different power allocation schemes (FPA and Dynamic Power Allocation) using different modulation schemes. Here we have performed all the system by MATLAB simulation. Here from these graphs we can see that as the number of users increases, Spectral Efficiency of the system also increases. It is observed that in all modulation schemes 16 users NF Cluster system with SVD precoding provides the highest Spectral Efficiency. This is because 16 users NF Clustering with SVD precoding provides highest Sum Capacity.

Simulation based experiment provides least amount of total Interference compared to Hardware based experiment. This is because Hardware based experiment is a real time experiment and it suffers from more amount of interference. So, the Sum Capacity and Spectral Efficiency is more in case of simulation-based experiment compared to Hardware based experiment.

Summary of the chapter:

This chapter presents a thorough analysis of the performances of various users' downlink PD-NOMA systems with downlink PD-NOMA Clustering systems for various Power Allocation strategies and modulation techniques, with respect to Sum Capacity, Spectral Efficiency, Energy Efficiency, and Total Amount of Interference. Both Fixed Power Allocation (FPA) and Dynamic Power Allocation techniques are used for power allocation. We have also compared the performance of the system performed by WARP V3 hardware (Hardware based experiment) and MATLAB simulation (Simulation based experiment).

Chapter-7

Conclusion and Future Scope:

7.1 Conclusion:

Throughout this thesis, we have studied the performance of different downlink PD-NOMA systems (SIMO NOMA and MIMO NOMA) using a transceiver board named WARP V3 in 2.4 GHz band and MATLAB simulation. We have performed the experiments for different numbers of users, with and without precoding, for different power allocation schemes and different modulation techniques. The parameters that we have calculated to analyze the performance of the systems are Sum Capacity, Spectral Efficiency, Energy Efficiency, and total amount of Interference. For experimental analysis we have also observed the Constellation diagram of NOMA system with and without precoding, for different power allocation strategies and different modulation techniques. But as the number of users increases in NOMA system, it faces some challenges that NOMA Clustering aims to address. We have analyzed the performance of PD-NOMA Clustering system and compared the performance with the performance of PD-NOMA system. From the output results we can observe that NOMA Clustering with Precoding and Dynamic power allocation scheme provides more Sum Capacity, Spectral Efficiency, and Energy Efficiency and less amount of Interference compared to NOMA system. We have performed up to 3 users PD-NOMA and PD-NOMA Clustering system by both WARP V3 hardware (hardware-based experiment) and MATLAB simulation (simulation-based experiment) and compared their performances. We observe that simulation-based experiments perform better than hardware-based experiments, i.e, simulation-based experiments provide more Sum Capacity, and Spectral Efficiency than Hardware based experiments. This is because Hardware based experiment is a real time experiment and it suffers from more amount of interference than simulation-based experiments. Through simulation-based experiments, we observe that the Sum Capacity of the system increases with the increase in number of users and Out of all the Downlink PD-NOMA and PD-NOMA Clustering systems that we have performed, 16-user NF Clustering system with SVD precoding offers the best performance. We have also validated these observations through hardware-based experiments.

7.2 Future Scope:

- **Beyond 5G and 6G Networks:** NOMA is expected to continue playing a vital role in the development of next-generation wireless communication systems. As demand for higher data rates, lower latency, and massive connectivity increases, NOMA's ability to efficiently allocate resources and accommodate multiple users simultaneously will be crucial for meeting these requirements.
- **Interference management and Spectrum sharing:** NOMA techniques can help to mitigate interference and improve spectrum efficiency in coexisting wireless systems, such as heterogeneous networks (HetNets) and shared spectrum environments. NOMA clustering can enable coordinated resource allocation and interference management strategies, fostering efficient spectrum sharing among multiple operators, technologies, or services while ensuring quality of service (QoS) guarantees for users.
- **Interaction with other Techniques:** The interaction of NOMA with other wireless communication techniques like Multiple Input Multiple Output (MIMO), Beamforming, and Millimeter-Wave (mmWave) technologies can lead to even higher gains in throughput, and efficiency.
- **IoT and Massive connectivity:** With the proliferation of IoT devices and the need for massive connectivity, NOMA offers a promising solution for efficiently handling the transmissions of a large number of devices. NOMA clustering systems can group IoT devices with similar communication requirements, enabling better utilization of resources and accommodating the diverse connectivity needs of IoT applications across various sectors, including smart cities, healthcare, agriculture, and industrial IoT.
- **Machine Learning and Optimization:** Future research in NOMA and NOMA clustering may leverage machine learning (ML) and optimization techniques to further enhance system performance and adaptability. ML algorithms can be employed for intelligent user clustering, adaptive resource allocation, predictive channel estimation, and interference prediction, leading to self-optimizing and self-configuring NOMA systems capable of autonomously adapting to changing network conditions and user dynamics.
- **Disaster Management:** In disaster scenarios, NOMA can enable rapid and efficient communication for rescue operations by supporting a large number of devices with different QoS requirements.
- **Security and Privacy:** Future research in NOMA may also focus on enhancing security and privacy mechanisms to address potential vulnerabilities associated with simultaneous

transmission of multiple users' data within the same resource block. Techniques such as secure user grouping and encryption can help protect users' data and ensure privacy in NOMA-enabled networks.

In conclusion, the future of NOMA and NOMA clustering systems is characterized by their potential to address the evolving needs of wireless communication networks, including higher capacity, lower latency, massive connectivity, and energy efficiency. Continued research and innovation in NOMA technology are expected to unlock new opportunities for enhancing the performance, efficiency, and scalability of future wireless networks across various applications and deployment scenarios.

References

[1] Al-mamun, B. A., Biswas, S., Bellal, H., & Saibba, B. (2017). Past, Present and Future of Mobile Wireless Communication Past. *IOSR J. Electron. Commun. Eng*, *12*(5), 55-58.

[2] Nair, A., Gupta, G., & Srinivas, K. (2018). Review on Multiple Access Techniques Used in Mobile Telecommunication Generations. *Int. Res. J. Eng. Techno I.*, *5*(10), 350-354.

[3] A. F. M. S. Shah, A. N. Qasim, M. A. Karabulut, H. Ilhan and M. B. Islam, "Survey and Performance Evaluation of Multiple Access Schemes for Next-Generation Wireless Communication Systems," in *IEEE Access*, vol. 9, pp. 113428-113442, 2021, doi: 10.1109/ACCESS.2021.3104509.

[4] https://www.researchgate.net/publication/349348812/figure/fig1/AS:991889025150976@1613496180993/Fig-31-Frequency-Division-Multiple-Access-FDMA.ppm

[5] Miao, G., Zander, J., Sung, K. W., & Slimane, S. B. (2016). *Fundamentals of mobile data networks*. Cambridge University Press.

[6] https://www.researchgate.net/publication/349348812/figure/fig2/AS:991889029341184@1613496181049/Fig-32-Time-Division-Multiple-Access-TDMA.jpg

[7] Chen, H. H. (2007). *The next generation CDMA technologies*. John Wiley & Sons.

[8] https://phdessay.com/wp-content/uploads/aaimagestoreessays/1497428.005.png

[9] Christopher Cox, "Orthogonal Frequency Division Multiple Access," in *An Introduction to LTE: LTE, LTE-Advanced, SAE, VoLTE and 4G Mobile Communications*, Wiley, 2014, pp.67-85, doi: 10.1002/9781118818046.ch4.

[10] https://media.geeksforgeeks.org/wp-content/uploads/20220627133057/OFDM.png

[11] https://i0.wp.com/yubanet.com/wp-content/uploads/2022/02/file-20220218-49929-6p63vs.png?fit=1000%2C497&ssl=1

[12] T. Kebede, Y. Wondie, J. Steinbrunn, H. B. Kassa and K. T. Kornegay, "Multi-Carrier Waveforms and Multiple Access Strategies in Wireless Networks: Performance, Applications, and Challenges," in *IEEE Access*, vol. 10, pp. 21120-21140, 2022, doi: 10.1109/ACCESS.2022.3151360.

[13] Misra, I. S. (2013). *Wireless communications and networks: 3G and beyond*. McGraw Hill Education (India) Pvt Ltd.

[14] Rappaport, T.S. *Wireless Communications: Principles and Practice*; Prentice Hall: Hoboken, NJ, USA, 2002; Volume 2.

[15] L. Dai, B. Wang, Y. Yuan, S. Han, I. Chih-lin and Z. Wang, "Non-orthogonal multiple access for 5G: solutions, challenges, opportunities, and future research trends," in *IEEE*

Communications Magazine, vol. 53, no. 9, pp. 74-81, September 2015, doi: 10.1109/MCOM.2015.7263349.

[16] B. Patnaik, A. Agarwal, S. Mali, G. Misra and K. Agarwal, "A Review on Non-Orthogonal Multiple Access Technique for Emerging 5G Networks and Beyond," *2020 International Conference on Smart Electronics and Communication (ICOSEC)*, Trichy, India, 2020, pp. 698-703, doi: 10.1109/ICOSEC49089.2020.9215412.

[17] A. Khairat and I. A. Ali, "Performance Analysis of OMA and NOMA Access Techniques," *2022 39th National Radio Science Conference (NRSC)*, Cairo, Egypt, 2022, pp. 131-140, doi: 10.1109/NRSC57219.2022.9971343.

[18] S. M. R. Islam, N. Avazov, O. A. Dobre and K. -s. Kwak, "Power-Domain Non-Orthogonal Multiple Access (NOMA) in 5G Systems: Potentials and Challenges," in *IEEE Communications Surveys & Tutorials*, vol. 19, no. 2, pp. 721-742, Secondquarter 2017, doi: 10.1109/COMST.2016.2621116.

[19] P. V. Reddy *et al*., "Analytical Review on OMA vs. NOMA and Challenges Implementing NOMA," *2021 2nd International Conference on Smart Electronics and Communication (ICOSEC)*, Trichy, India, 2021, pp. 552-556, doi: 10.1109/ICOSEC51865.2021.9591629.

[20] M. Kokilavani, R. Siddharth, S. Mohamed Riyaz, P. Ramesh, S. Ezhilarasi and P. T. V. Bhuvaneswari, "Downlink Performance Analysis of 5G PD-NOMA System," 2022 IEEE Global Conference on Computing, Power and Communication Technologies (GlobConPT), New Delhi, India, 2022, pp. 1-6, doi: 10.1109/GlobConPT57482.2022.9938331.

[21] V. O. Kazachkov and N. A. Soldatenkova, "Bit Error Rate Performance of Power Domain Non-Orthogonal Multiple Access Systems," 2021 Systems of Signals Generating and Processing in the Field of on Board Communications, Moscow, Russia, 2021, pp. 1-5, doi: 10.1109/IEEECONF51389.2021.9416041.

[22] A. A. Khansa, X. Chen, G. Gui and H. Sari, "A BER Analysis of NOMA on Rician Fading Channels," *2020 IEEE Latin-American Conference on Communications (LATINCOM)*, Santo Domingo, Dominican Republic, 2020, pp. 1-6, doi: 10.1109/LATINCOM50620.2020.9282306.

[23] M. Aldababsa, C. Göztepe, G. K. Kurt and O. Kucur, "Bit Error Rate for NOMA Network," in *IEEE Communications Letters*, vol. 24, no. 6, pp. 1188-1191, June 2020, doi: 10.1109/LCOMM.2020.2981024.

[24] B. Pavithra and P. Chakraborty, "Performance Analysis of Bit Error Rate, Capacity and Outage Probability using Power Domain Non-Orthogonal Multiple Access (PD-NOMA) and Orthogonal Multiple Access (OMA) with Far/Near User," *2022 6th International Conference*

on Intelligent Computing and Control Systems (ICICCS), Madurai, India, 2022, pp. 166-170, doi: 10.1109/ICICCS53718.2022.9788438.

[25] S. K. Saraswat and D. Singh, "Analysis of Optimization of Rate in Power Domain NOMA Schemes for MIMO," 2020 International Conference on Power Electronics & IoT Applications in Renewable Energy and its Control (PARC), Mathura, India, 2020, pp. 481-484, doi: 10.1109/PARC49193.2020.236660.

[26] S. Ismail, F. D'Andreagiovanni, H. Lakhlef and Y. Imine, "Recent Advances on 5G Resource Allocation Problem using PD-NOMA," *2020 International Symposium on Networks, Computers and Communications (ISNCC)*, Montreal, QC, Canada, 2020, pp. 1-7, doi: 10.1109/ISNCC49221.2020.9297208.

[27] M. Hassan, M. Singh and K. Hamid, "Survey on NOMA and Spectrum Sharing Techniques in 5G," *2021 IEEE International Conference on Smart Information Systems and Technologies (SIST)*, Nur-Sultan, Kazakhstan, 2021, pp. 1-4, doi: 10.1109/SIST50301.2021.9465962.

[28] R. Chandrasekhar, R. Navya, P. K. Kumari, K. Kausal, V. Bharathi and P. Singh, "Performance Evaluation of MIMO-NOMA for the Next Generation Wireless Communications," *2021 3rd International Conference on Signal Processing and Communication (ICPSC)*, Coimbatore, India, 2021, pp. 631-636, doi: 10.1109/ICSPC51351.2021.9451780.

[29] S. Srivastava, P. P. Dash and S. Kumar, "Decisive Analysis of Fixed Power Allocation Coefficients in a PD-NOMA Network," *2022 IEEE 4th International Conference on Cybernetics, Cognition and Machine Learning Applications (ICCCMLA)*, Goa, India, 2022, pp. 1-6, doi: 10.1109/ICCCMLA56841.2022.9989217.

[30] A. Chauhan and A. Jaiswal, "Power Allocation Constraint and Error Rate Analysis for Multi-User PD-NOMA System Employing M–Ary PSK," in *IEEE Communications Letters*, vol. 27, no. 5, pp. 1452-1456, May 2023, doi: 10.1109/LCOMM.2023.3253857.

[31] M. Raju, M. V. Surya Prasad, H. V. Reddy, L. P. Kodari and C. Rohith, "Exploring the Superior Performance of NOMA: A Comparative Study of Wireless Communication Techniques," *2023 Third International Conference on Secure Cyber Computing and Communication (ICSCCC)*, Jalandhar, India, 2023, pp. 252-256, doi: 10.1109/ICSCCC58608.2023.10176387.

[32] M. B. Dadi and B. C. Rehaimi, "Performance of downlink MIMO-NOMA system in 5G Networks," *2023 IEEE International Workshop on Mechatronic Systems Supervision (IW_MSS)*, Hammamet, Tunisia, 2023, pp. 1-4, doi: 10.1109/IW_MSS59200.2023.10368947.

[33] Jongmok Kim, Jeongwan Koh, J. Kang, Kwangeog Lee and J. Kang, "Design of user clustering and precoding for downlink non-orthogonal multiple access (NOMA)," *MILCOM 2015 - 2015*

IEEE Military Communications Conference, Tampa, FL, USA, 2015, pp. 1170-1175, doi: 10.1109/MILCOM.2015.7357604.

[34] M. S. Ali, H. Tabassum and E. Hossain, "Dynamic User Clustering and Power Allocation for Uplink and Downlink Non-Orthogonal Multiple Access (NOMA) Systems," in *IEEE Access*, vol. 4, pp. 6325-6343, 2016, doi: 10.1109/ACCESS.2016.2604821.

[35] Z. Ding, P. Fan and H. V. Poor, "Impact of User Pairing on 5G Nonorthogonal Multiple-Access Downlink Transmissions," in *IEEE Transactions on Vehicular Technology*, vol. 65, no. 8, pp. 6010-6023, Aug. 2016, doi: 10.1109/TVT.2015.2480766.

[36] X. Zhang, J. Wang, J. Wang and J. Song, "A Novel User Pairing in Downlink Non-Orthogonal Multiple Access," *2018 IEEE International Symposium on Broadband Multimedia Systems and Broadcasting (BMSB)*, Valencia, Spain, 2018, pp. 1-5, doi: 10.1109/BMSB.2018.8436709.

[37] H. You, Z. Pan, N. Liu and X. You, "User Clustering Scheme for Downlink Hybrid NOMA Systems Based on Genetic Algorithm," in *IEEE Access*, vol. 8, pp. 129461-129468, 2020, doi: 10.1109/ACCESS.2020.3009018.

[38] L. Zhu, J. Zhang, Z. Xiao, X. Cao and D. O. Wu, "Optimal User Pairing for Downlink Non-Orthogonal Multiple Access (NOMA)," in *IEEE Wireless Communications Letters*, vol. 8, no. 2, pp. 328-331, April 2019, doi: 10.1109/LWC.2018.2853741.

[39] Chen, R.; Shu, F.; Lei, K.; Wang, J.; Zhang, L. User Clustering and Power Allocation for Energy Efficiency Maximization in Downlink Non-Orthogonal Multiple Access Systems. *Appl. Sci.* 2021, *11*, 716. https://doi.org/10.3390/app11020716.

[40] J. Ren, Z. Wang, M. Xu, F. Fang and Z. Ding, "Unsupervised User Clustering in Non-orthogonal Multiple Access," *ICASSP 2019 - 2019 IEEE International Conference on Acoustics, Speech and Signal Processing (ICASSP)*, Brighton, UK, 2019, pp. 3332-3336, doi: 10.1109/ICASSP.2019.8682205.

[41] T. V. Tai, N. T. Xuan Uyen and D. L. Khoa, "Optimal User Clustering and Power Allocation in NOMA Systems," *2022 International Conference on Advanced Technologies for Communications (ATC)*, Ha Noi, Vietnam, 2022, pp. 350-355, doi: 10.1109/ATC55345.2022.9943029.

[42] N. S. Mouni, P. R. M., A. Kumar, P. K. Upadhyay and M. Magarini, "Adaptive Multi-User Clustering and Power Allocation for Hybrid OMA-NOMA System with Imperfect SIC," *2024 16th International Conference on COMmunication Systems & NETworkS (COMSNETS)*, Bengaluru, India, 2024, pp. 747-751, doi: 10.1109/COMSNETS59351.2024.10426961.

[43] Z. Sun and Y. Jing, "Average Power Analysis and User Clustering Design for MISO-NOMA Systems," 2020 IEEE 21st International Workshop on Signal Processing Advances in Wireless

Communications (SPAWC), Atlanta, GA, USA, 2020, pp. 1-5, doi: 10.1109/SPAWC48557.2020.9154316.

[44] S. Chakraborti, S. R. Chatterjee and M. Chakraborty, "Power Distribution in Clustered NOMA," *2022 IEEE 9th Uttar Pradesh Section International Conference on Electrical, Electronics and Computer Engineering (UPCON)*, Prayagraj, India, 2022, pp. 1-5, doi: 10.1109/UPCON56432.2022.9986361.

[45] S. Rezwan, S. Shin and W. Choi, "Efficient User Clustering and Reinforcement Learning Based Power Allocation for NOMA Systems," *2020 International Conference on Information and Communication Technology Convergence (ICTC)*, Jeju, Korea (South), 2020, pp. 143-147, doi: 10.1109/ICTC49870.2020.9289376.

[46] F. Saggese, M. Moretti and A. Abrardo, "A Quasi-Optimal Clustering Algorithm for MIMO-NOMA Downlink Systems," in IEEE Wireless Communications Letters, vol. 9, no. 2, pp. 152-156, Feb. 2020, doi: 10.1109/LWC.2019.2946548.

[47] S. Ali, E. Hossain and D. I. Kim, "Non-Orthogonal Multiple Access (NOMA) for Downlink Multiuser MIMO Systems: User Clustering, Beamforming, and Power Allocation," in *IEEE Access*, vol. 5, pp. 565-577, 2017, doi: 10.1109/ACCESS.2016.2646183.

[48] S. Liu, C. Zhang and G. Lyu, "User selection and power schedule for downlink non-orthogonal multiple access (NOMA) system," *2015 IEEE International Conference on Communication Workshop (ICCW)*, London, UK, 2015, pp. 2561-2565, doi: 10.1109/ICCW.2015.7247563.

[49] J. Guo, X. Wang, J. Yang, J. Zheng and B. Zhao, "User Pairing and Power Allocation for Downlink Non-Orthogonal Multiple Access," 2016 IEEE Globecom Workshops (GC Wkshps), Washington, DC, USA, 2016, pp. 1-6, doi: 10.1109/GLOCOMW.2016.7849074.

[50] M. Zeng, A. Yadav, O. A. Dobre, G. I. Tsiropoulos and H. V. Poor, "On the Sum Rate of MIMO-NOMA and MIMO-OMA Systems," in *IEEE Wireless Communications Letters*, vol. 6, no. 4, pp. 534-537, Aug. 2017, doi: 10.1109/LWC.2017.2712149.

[51] W. Liang, Z. Ding, Y. Li and L. Song, "User Pairing for Downlink Non-Orthogonal Multiple Access Networks Using Matching Algorithm," in *IEEE Transactions on Communications*, vol. 65, no. 12, pp. 5319-5332, Dec. 2017, doi: 10.1109/TCOMM.2017.2744640.

[52] A. Mahmoudi, B. Abolhassani, S. M. Razavizadeh and H. H. Nguyen, "User Clustering and Resource Allocation in Hybrid NOMA-OMA Systems Under Nakagami-m Fading," in *IEEE Access*, vol. 10, pp. 38709-38728, 2022, doi: 10.1109/ACCESS.2022.3165756.

[53] Elsaraf, Z., Khan, F., & Ahmed, Q. (2018). Performance analysis of code-domain NOMA in 5G communication systems. *Proceedings of the 2018 ELEKTRO, Mikulov, Czech Republic*, 21-23.

[54] https://d3i71xaburhd42.cloudfront.net/e5f3d429fc9a99de2d0098983bc64e964040e3b6/2-Figure1-1.png

[55] I. Budhiraja *et al*., "A Systematic Review on NOMA Variants for 5G and Beyond," in *IEEE Access*, vol. 9, pp. 85573-85644, 2021, doi: 10.1109/ACCESS.2021.3081601.

[56] https://www.researchgate.net/publication/355410089/figure/fig1/AS:1145677107208192@1650162116191/Block-diagram-of-a-basic-NOMA-structure.png

[57] https://www.researchgate.net/publication/328280600/figure/fig4/AS:681843179397120@1539575490843/Resource-allocation-in-code-domain-NOMA-Colours-represent-different-users-which-are-more.png

[58] Anwar A, Seet B-C, Hasan MA, Li XJ. A Survey on Application of Non-Orthogonal Multiple Access to Different Wireless Networks. *Electronics*. 2019; 8(11):1355. https://doi.org/10.3390/electronics8111355

[59] https://www.researchgate.net/publication/337298297/figure/fig2/AS:825852426199041@1573909970521/Transmitter-implementing-superposition-coding-SC.png

[60] K. R. Patel and S. Dasrao Deshmukh, "2S (Superposition Coding, Successive Interference Cancellation) Operations in NOMA Technology for 5G Networks: Review and Implementation," *2023 IEEE 8th International Conference for Convergence in Technology (I2CT)*, Lonavla, India, 2023, pp. 1-6, doi: 10.1109/I2CT57861.2023.10126268.

[61] https://d3i71xaburhd42.cloudfront.net/de13552fa38655f98409c7684181a85e7c4452bc/1-Figure1-1.png

[62] https://encrypted-tbn0.gstatic.com/images?q=tbn:ANd9GcQp-RC4MVKQcMs745KBhdKhma4mkwComBQ5xpw7l76-wg&s

[63] Shehab, W. A., & Al-qudah, Z. (2017). Singular value decomposition: Principles and applications in multiple input multiple output communication system. *Int. J. Comput. Networks Commun*, *9*(1), 13-21.

[64] A. Kassir, R. A. Dziyauddin, H. M. Kaidi and M. A. Mohd Izhar, "Power Domain Non Orthogonal Multiple Access: A Review," *2018 2nd International Conference on Telematics and Future Generation Networks (TAFGEN)*, Kuching, Malaysia, 2018, pp. 66-71, doi: 10.1109/TAFGEN.2018.8580477.

[65] R. Sirait and G. Wibisono, "Capacity Analysis of Non-Orthogonal Multiple Access (NOMA) Network over Rayleigh Fading Channel with Dynamic Power Allocation and Imperfect SIC," *2021 4th International Seminar on Research of Information Technology and Intelligent Systems (ISRITI)*, Yogyakarta, Indonesia, 2021, pp. 7-11, doi: 10.1109/ISRITI54043.2021.9702840.

[66] D. Ni, L. Hao, Q. T. Tran and X. Qian, "Power Allocation for Downlink NOMA Heterogeneous Networks," in *IEEE Access*, vol. 6, pp. 26742-26752, 2018, doi: 10.1109/ACCESS.2018.2835568.

[67] Alghasmari, W. F., & Nassef, L. (2020). Power allocation evaluation for downlink non-orthogonal multiple access (NOMA). *IJACSA) International Journal of Advanced Computer Science and Applications*, *11*(4).

[68] Channi, H. K. (2016). A comparative study of various digital modulation techniques. *International Journal in IT and Engineering*, *4*(03).

[69] Barnela, M., & Kumar, D. S. (2014). Digital modulation schemes employed in wireless communication: A literature review. *International Journal of Wired and Wireless Communications*, *2*(2), 15-21.

[70] https://drmoazzam.com/wp-content/uploads/2016/04/BPSK_modulator.png

[71] https://media.geeksforgeeks.org/wp-content/uploads/20230924143610/WhatsApp-Image-2023-08-29-at-125537-PM.webp

[72] https://drmoazzam.com/wp-content/uploads/2016/04/BPSK_receiver.png

[73] Bhandari, A. (2019). SIMULATION OF SIGNAL CONSTELLATIONS OF BPSK, QPSK AND QAM AND THEIR ANALYSIS.

[74] https://www.tutorialspoint.com/digital_communication/images/qpsk_modulator.jpg

[75] https://www.researchgate.net/publication/343452908/figure/fig4/AS:921314432917504@1596669886560/MATLAB-simulation-output-of-a-coherent-QPSK-modulator-Note-i-i-s-2i-i-b1.png

[76] https://www.tutorialspoint.com/digital_communication/images/qpsk_demodulator.jpg

[77] Srivastava, S., Dash, P. P., & Kumar, S. (2020). Analysis of NOMA: In Capacity Domain. In *International Symposium on 5G & Beyond for Rural Upliftment* (pp. 28-38).

[78] Zuo, Y., Zhu, X., Jiang, Y., Wei, Z., Zeng, H., & Wang, T. (2018, August). Energy efficiency and spectral efficiency tradeoff for multicarrier NOMA systems with user fairness. In *2018 IEEE/CIC international conference on communications in China (ICCC)* (pp. 666-670). IEEE.

[79] N. Glei and R. Belgacem Chibani, "Power Allocation for Energy-Efficient Downlink NOMA Systems," *2019 19th International Conference on Sciences and Techniques of Automatic Control and Computer Engineering (STA)*, Sousse, Tunisia, 2019, pp. 611-613, doi: 10.1109/STA.2019.8717240.

[80] Combs, A. Application Note AN-005: Understanding Constellation Diagrams and How They Are Used.

[81] https://aerospaceresearch.net/wp-content/uploads/2018/07/const.png

[82] https://warpproject.org/trac/wiki/HardwareUsersGuides/WARPv3

[83] https://warpproject.org/trac/wiki/GettingStarted/WARPv3/Hardware

[84] https://warpproject.org/trac/wiki/WARPLab

[85] https://warpproject.org/trac/wiki/WARPLab/Examples/OFDM